2011-12-12

Damage Tolerance of Unidirectional Basalt/Epoxy Composites In Co-Cured Aramid Sleeves

Devin Nelson Allen
Brigham Young University - Provo

Damage Tolerance of Unidirectional Basalt/Epoxy Composites

In Co-Cured Aramid Sleeves

Devin Nelson Allen

A thesis submitted to the faculty of
Brigham Young University
in partial fulfillment of the requirements for the degree of

Master of Science

David W. Jensen, Chair
Richard J. Balling
Fernando S. Fonseca

Department of Civil & Environmental Engineering

Brigham Young University

December 2011

ABSTRACT

Damge Tolerance of Unidirectional Basalt/Epoxy Composites
In Co-Cured Aramid Sleeves

Devin Nelson Allen
Department of Civil & Environmental Engineering, BYU
Master of Science

Unidirectional basalt fiber rods consolidated with an aramid sleeve were measured for compression strength after impact at various energy levels and compared to undamaged control specimens. These structural elements represent local members of open three-dimensional composite lattice structures (e.g., based on isogrid or IsoTruss® technologies) that are continuously fabricated using advanced three-dimensional braiding techniques. The unidirectional core specimens, nominally 8 mm (5/16") and 11 mm (7/16") in diameter, were manufactured using bi-directional braided sleeves or unidirectional spiral sleeves with full or partial (approximately half) coverage of the core fibers. The 51 mm (2") specimens were shorter than the critical buckling length, ensuring the formation of kink bands, typical of strength-controlled compression failure of unidirectional composites. The test results indicate an approximate decrease in the average undamaged compression strength of approximately 1/3 and 2/3 when impacted with 5 J (3.7 ft-lbs) and 10 J (7.4 ft-lbs) for the 8 mm (5/16") diameter specimens and 10 J (7.4 ft-lbs.) and 20 J (14.8 ft-lbs.) for the 11 mm (7/16") diameter specimens, respectively. The aramid sleeves improved the damage tolerance of the composite members, with the amount of coverage having the greatest effect; full coverage exhibiting up to 45% greater strength than partial coverage. Braided sleeves improved compression strength after impact by up to 23% over spiral sleeves, but generally had little effect on damage tolerance. Larger diameter specimens tend to be more resistant to damage than those specimens of a smaller diameter. The compressive material properties for undamaged basalt composites are also presented with the average compressive strength being 800 MPa (116 ksi).

Keywords: basalt composites, damage tolerance, IsoTruss, compression strength after impact, unidirectional, Kevlar sleeves

ACKNOWLEDGMENTS

My first thanks are for Dr. David W. Jensen, and his continuing patience and persistence with me while performing this research. There were countless occasions that he spent extra time going over concepts, writing techniques and making sure I knew which direction to take the research.

Additionally thanks are needed for Novatek who graciously funded and supported this research from the beginning. Craig Garvin, Mark Jensen and Aaron Howcraft were a great technical support team when faced with manufacturing dilemmas.

My peers at CASC also deserve warm thanks for the countless hours spent preparing tables, setting specimens, sanding specimens and taking pictures of them. Without their help it would have taken an additional year to complete this research. It was an honor to work with them and I have received many great friendships as a result.

I also need to thank my friends and family, that although were not directly participating in the research, were always there offering me the emotional support that I needed. The encouragement I needed was always there when I was going through difficult times or when there simply were not enough hours in the day.

TABLE OF CONTENTS

LIST OF TABLES

LIST OF FIGURES

1 INTRODUCTION

The IsoTruss® technology offers a highly efficient composite structure; however, the IsoTruss, like all advanced composite structures, is susceptible to damage. The purpose of this research is to quantify the effect of a consolidating sleeve (necessary in the production of the IsoTruss) on the compression strength after impact (CSAI) of unidirectional transversely isotropic composites.

1.1 Overview of Composite IsoTruss Structures

The use of composites is not new; early civilizations noticed that straw mixed with mud provided much stronger structures than either substrate alone. Generally speaking composites, as was demonstrated with adobe centuries ago, are the combining of two materials into an integral composite with properties superior to the individual components alone. Material science has surpassed the era of adobe bricks, and now advanced fiber-reinforced polymer material composites represent the latest composite technology by combining fibers (e.g., carbon, glass and basalt) with a polymer matrix (resin). These composites provide strong, stiff and, lightweight alternatives to the more traditionally used structural materials. According to Agarwal, et al., [1] "fiber-reinforced polymer matrix composites are the most widely used fiber composites," with 4 billion lbs. being shipped domestically in 2004. The advanced composites

industry is substantial and the use of advanced composites continues to grow as the limits of engineering are pushed.

More structurally efficient uses of advanced composites are being developed, one of which is the IsoTruss® [2] (Figure 1.1). Unlike typical composites with fiber-reinforced transversely isotropic layers in several orientations, the IsoTruss is comprised of straight unidirectional transversely-isotropic fibers. Transversely isotropic materials (Figure 1.2) are symmetric in three planes, with straight, continuous, unidirectional fibers parallel to the loaded axis embedded in a matrix. In IsoTruss structure's the fibers in the members are consolidated into a cylindrical rod, using an aramid sleeve wrapped around the circumference of the members. These members, encased in the consolidating sleeves, make up the longitudinal members and the helicals. This configuration, longitudinal members joined by a helical lattice structure, effectively reduces the buckling length of the individual axial-load-carrying longitudinal members. Apart from increasing the local and global stiffness of the structure, the helical members also resist any applied torsional loads. The specifics on IsoTruss nomenclature and geometries are located in Scoresby [3] and McCune [4]. Kesler [5] and Winkel [6] have documented geometric equations that can be used for analysis.

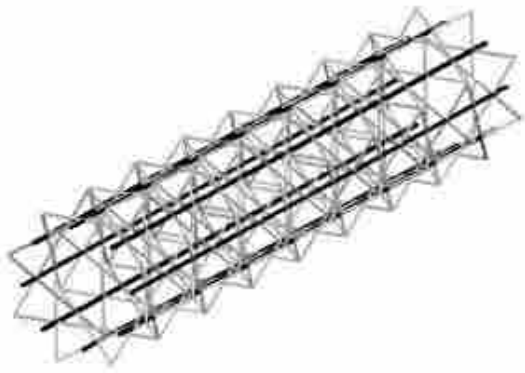

Figure 1.1: Typical IsoTruss Structure

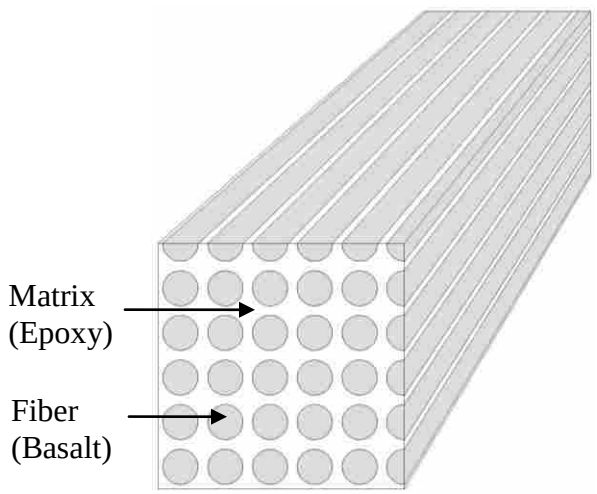

Figure 1.2: Transversely Isotropic Unidirectional Fiber-Reinforced Composite Material

Advanced composite materials are brittle, with their structural integrity jeopardized by even low impact energies. Although the IsoTruss does provide a more structurally efficient use of advanced composites, it is still susceptible to damage. This issue becomes important, for example, when utilizing the IsoTruss structure in the aerospace industry where debris strikes are common place, and when used in civil applications where a factor of safety against impact damage is needed.

One advantage of a 3-dimensional open lattice structure (e.g., IsoTruss or isogrid) is that it allows visual inspection of damaged members. Areas of extreme damage in composites are easily identified enabling an appropriate repair or replacement. Low-velocity impact damage however can still go unnoticed and cause a reduction in structural integrity.

During manufacture of IsoTruss structures an aramid sleeve is tension wound around the members acting as an effective consolidator of the unidirectional core fibers and has been shown to create a transverse stress that confines the core fibers and effectively increases the tensile capacity of the resin [7]. Apart from being an effective consolidator the sleeve can also have a beneficial effect on the damage tolerance of local IsoTruss members. Quantifying the influence

of a consolidating sleeve on the damage tolerance, particularly the compression strength after impact, of unidirectional basalt/epoxy composites is the focus of this research.

1.2 Related Studies

Advanced composites provide many ideal characteristics such as high strength and stiffness while remaining lightweight. These superior properties are degraded once impacted representing a major hurdle that has received much attention in the composites industry. In the following paragraphs current areas of research for improving damage tolerance of composites are presented. The discussion is followed by methods of analytical research being performed to predict the strength of the composite after being impacted. Current research methods for quantifying the improvement in damage tolerance are also presented followed by a study investigating unidirectional cylindrical composite rods.

Several methods have been investigated in hopes of reducing impact damage on composites through absorption or dissipation of impact energy. Wisnom [8] looked at using an aramid sleeve as a method for dispersing the impact energy to protect a unidirectional transversely isotropic core of carbon fiber. Wisnom's test differs from the current study in that the aramid in this study acts not only as the protective barrier but also as the sole means of fiber consolidation during curing, whereas the sleeve in Wisnom's study was applied after curing the core.

Jao [9] looked at using a thin rubber coating on the surface of composite plates. With the rubber coating, the high stress zones in the material were shown to spread out to a larger volume effectively increasing the damage resistance of the composite.

Duguay, et al., [10] investigated using nano-composite fillers at different weight percentages and diameter size. Smaller diameter fillers proved to be more effective at improving the impact properties of the composites. When a coupling agent was added to aid in particle dispersion, the impact properties deteriorated due to increased adhesion between the filler and the matrix.

Beard and Chang [11] studied the energy absorption of braided cylindrical tubes for use in automobiles. These hollow tubes were crushed longitudinally to the axis which differs from the current research being impacted transversely to the axis. Fiber architecture was shown to significantly affect the energy absorption of the tubes. The architecture, or type of sleeve, used in the current research could potentially alter the impact properties.

Hamada, et al., [12] treated composite tubes with an amino-siline showing improved energy absorption during a crushing test.

Cwik, et al., [13] performed high-velocity impact test on carbon fiber plates. Several non-conventional layup configurations were studied including combinations of cured, partially cured and uncured carbon fiber fabric with and without spacers between the layers. Partially cured carbon fiber plates showed a doubling of impact resistance over a cured plate. Adding spacers between the plies showed similar results with a decrease in material usage. Plates made of Dyneema® were used as the benchmark, and exhibited superior impact resistance over the carbon fiber panels.

Zammit, et al., [14] showed that pre-loading causes more impact damage if the level of pre-tensioning is high compared to the tensile strength of the material or if the impactor is sharp, thus inducing more damage. The specimens in the current test are not preloaded during testing although they will be when in service.

Kang and Lee [15] have shown that residual strength after impact is a decreasing function of incident impact energy. Applying this function to a 2-parameter Weibull distribution the authors were able to closely predict residual compression strength based on the impact energy. This modeling was applied to a plate and it is unknown whether these results apply to unidirectional cylindrical rods. Kong, et al., [16] performed an analysis where the region of impact was modeled as an equivalent hole and as a soft inclusion. The predicted damage model was developed using a simple non-linear approximation method (Rayleigh-Ritz method) applied to the Soutis-Fleck model. The model based on the equivalent hole was within 10% of experimental results while the soft inclusion model over predicted strength by approximately 40%.

Compression strength after impact is a widely accepted and practiced testing procedure. This test is typically used on composite plates and has been discussed by many researchers [17-21]. Although not related directly to unidirectional cylindrical members specifically, the articles provide good insight for general CSAI procedures and parameters. A drop-weight impact machine similar to the one employed in the current research was common among the test processes described. The impact energies in these articles ranged from 2.5 J (1.85 ft-lbs.) to 20 J (14.8 ft-lbs.), representing low-velocity impacts. High velocity impact tests [22], representing impact events such as a bird strike on the blades of a turbofan engine [23], are also commonly done, but is beyond the scope of this research.

The global response to impact on a complete IsoTruss structure is very different than that occurring at a local member level as in this study. The end conditions differ when impacting a complete IsoTruss rather than a specimen representing only a local IsoTruss member. A complete IsoTruss structure will deflect more, allowing more energy dissipation. A single

element, as addressed in this research, behaves more like a fixed-fixed connection with little deflection occurring at impact. Carroll [24] performed analytical research showing that boundary conditions greatly affect the impact response of IsoTruss structures.

Scoresby [3] looked at both radial and longitudinal impact on complete IsoTruss structures. Rather than looking at the effect of the sleeves on damage pertained to the total energy absorption potential of the IsoTruss.

Several methods have been used to quantify the amount of damage caused by impact. Lee, et al., [16] used x-ray technology to establish the damaged area. Ultra-sonic imaging, an industry standard, can also be used to assess damage. Others, such as Cwik, et al., [13] and Woo, et al., [22] established comparisons based on the velocity of the projectile rather than evaluating the damaged area. Due to the current lack of proper imaging capabilities available for this research, impact energy, rather than a measurement of the actual damaged area, was used for the standard of comparison. The geometry, or bluntness of the striking head plays a direct role in damage formation during impact [25] which encourages measuring the damage area for comparison. For this research however, the striking head remained constant.

Soutis [26] studied the compressive strength of pultruded unidirectional carbon/epoxy members. Although the members were not impacted, Soutis provides good insight on the problems that can occur when loading unidirectional composite fiber members in compression, such as the importance of introducing the load uniformly into the specimen and having proper specimen alignment. The recommendations found in this article were helpful in improving the quality of this research.

These studies provide the basis for the current research. No data or studies have been found that quantify the effect of a consolidating sleeve on the damage tolerance of unidirectional basalt/epoxy composites, thus justifying the need for the current research.

1.3 Motivation and Scope of Work

A braided, rather than the traditional spiral sleeve employed in IsoTruss manufacture, could potentially increase the damage tolerance of the structure. Creating an intricate braid complicates manufacturing by requiring a larger machine capable of incorporating additional bobbins of sleeve material. Using complete (full) sleeve coverage rather than partial coverage provides more protection to the core fibers at the cost of additional time and material. Ideally, the cost and time of manufacturing IsoTruss structures would be minimized. In this research the damage tolerance of specimens differing in their sleeve type (bi-directional braid or unidirectional spiral) and the nominal amount of coverage provided by the sleeve (partial or full) were quantified to address the following questions:

1. Can braided and spiral sleeves produced by the latest machine properly consolidate continuously-manufactured unidirectional basalt composites?
2. How much more damage tolerant is a braided sleeve than a spiral sleeve?
3. How much more damage tolerant is full coverage than partial coverage?
4. Do the results from question 2 and 3 scale to different diameter members?
5. What is the relationship between impact energy and compression strength after impact of unidirectional composites with a consolidating sleeve?

For this research, specimens were manufactured with a basalt/epoxy core with diameters of 8 mm (5/16”) and 11 mm (7/16”). The specimens were 51 mm (2”) long for the primary

testing and 76 mm (3”) long for the preliminary testing. Both bi-directional braids and unidirectional spirals providing both full and half coverage sleeves were made from an aramid (Kevlar®) tow. Five specimens at each configuration were tested after being impacted at one of two energy levels independently; undamaged specimens acted as a control.

1.4 Thesis Overview

Chapter Two provides an overview of the experiment and defines the variables investigated in this research. Chapter Three outlines the process for specimen manufacturing, and final preparation for testing. Chapter Four provides the results for the preliminary testing performed on the 76 mm (3”) long specimens. Chapter Five provides the primary test results for the 51 mm (2”) long specimens. These specimens were tested because the 76 mm (3”) long specimens showed a mixture of strength- and buckling-controlled failure. Shorter specimens limited the failure to strength only. Chapters Six and Seven compare the test results and Chapter Eight summarizes the final conclusions and recommendations.

2 EXPERIMENTAL OVERVIEW

This chapter provides a brief overview of the testing procedure and a detailed description of the materials used and the variables considered in the testing, which are presented in a test matrix. The process of defining the variables is also explained.

2.1 General Overview of Experiment

The basic method for testing was based on a common composites test, Compression Strength After Impact (CSAI) [8][17-19]. The theory behind this test is that impact, at a particular energy level, inflicts damage indicative of a real world occurrence. This impact could be caused by a tool, which is dropped during installation of the structure, or the strike from a foreign object after installation. After impact, the specimens are loaded axially until failure. From this process a correlation can be made between impact energy and specimen residual compression strength.

2.2 Experimental Variables

Ultimately there are hundreds of variables that can be considered in testing. These could be secondary variables, that are minimized or fixed for consistency of testing, or variables that are the focus of the research. In this section both those variables that change from test to test and those that remain fixed are presented and defined.

2.2.1 Specimen Geometry

The specimen diameter was based on the 136 tows of basalt available at the time of manufacture. Larger and smaller core diameters were of interest. An additional thirty spools were created, for a total of 166 tows, to make a core diameter of 11 mm (7/16”). An 8 mm (5/16”) diameter core was chosen for the smaller geometry, representing approximately one-half the cross-sectional area of the larger samples. These specimens required a total of 86 tows.

The length of the specimens was based on the height of the extensometer that was used in testing and the predicted buckling length of the specimens. The length of the specimen was designed to be shorter than the critical length to ensure that a compression strength failure occurred, as opposed to a buckling failure. To determine the critical length, Euler’s buckling equation, as seen in Equation 2-1, was solved for critical length:

$$F = \frac{\pi^2 EI}{(KL)^2} \tag{2-1}$$

A load of 445 kN (100 kips) was assumed for F, and a K value of 0.75, which is between pinned-pinned and fixed-fixed connections, was used. The Young’s modulus, E, of 64.5 GPa (9.35×10^6 psi) was determined from preliminary basalt compression testing (Chapter 4), and the moment of inertia, I, was calculated form the cross-sectional area. This is a non-conservative estimate, and as such, the actual buckling length of the specimens should be well below this figure. From Euler’s Buckling formulas the critical length was calculated to be 80 mm (3.16”) for the 8 mm (5/16”) diameter specimens and 112 mm (4.43”) for the 11 mm (7/16”) inch specimens.

The specimens also need to be sufficiently long to ensure proper failure. Assuming a failure plane of 45° degrees, and in order to have sufficient length to avoid end condition effects,

the unsupported specimen length should generally be at least three times the diameter of the specimen. This limits the length of the 8 mm (5/16”) diameter specimens to be at least 24 mm (15/16”) and the 11 mm (7/16”) diameter specimens to be at least 33 mm (1-5/16”). One additional limiting factor is the height of the extensometer. The clearance needed for the extensometer was 35 mm (1-3/8”), plus 16 mm (5/8”) for a factor of safety, yielding a minimum length of 51 mm (2”). The end caps that were attached to the specimens to facilitate testing required an additional 38 mm (1-1/2”) of specimen length. This resulted in a total specimen length of 89 mm (3-1/2”) long.

Initially an unsupported length of 76 mm (3”) was used for the 8 mm (5/16”) diameter specimens. This length proved to be too close to the critical length, with some of the more damaged specimens having a buckling type failure mode rather than the desired compression strength failure. The results of the 76 mm (3”) unsupported lengths are presented as “preliminary data” while the 51 mm (2”) length specimens are presented as the “primary data.”

2.2.2 Materials

The materials used, and their tensile properties from the manufactures, are in Table 2.1 For the core, a basalt fiber produced by Kamenny Vek [27] pre-impregnated with epoxy was used to eliminate the need apply the epoxy during specimen manufacture. This method also ensured that all fibers were completely covered with epoxy. The epoxy, applied by TCR Composites [28], is commonly used in high pressure vessels and sporting goods. Refrigeration is not needed for this epoxy, since it has a long shelf life, which was beneficial for the length of time required to manufacture the test specimens.

For the sleeves, a dry aramid produced by DuPont, commonly known as Kelvar® [29], was used. Originally basalt and aramid were both going to be used, independently, for making the sleeves; however the basalt proved to be too difficult to work with for the sleeves. Due to friction and tight radii, the basalts fibers exhibited extensive fiber breakage and fraying. Eventually the entire tow of fiber was destroyed as shown in Figure 2.1. Basalt was eliminated as a sleeve material and all specimens were made with a dry aramid, due to its more favorable winding characteristics.

Table 2.1: Material Properties Provided by the Manufactures

Materials	**Basalt**	**Aramid**	**Epoxy**
Manufacture	Kamenny Vek	DuPont	TCR Composites
Type	BCF 13.2100	Kevlar 49- 7100 Denier	UF3330-100
Filament per Tow	4,400	4,700	-
Filament Diameter [μm(μin)]	13 (512)	12 (472)	-
Density [g/cm^3(oz/in^3)]	2.67 (1.54)	1.44 (0.83)	1.21 (0.70)
Tensile Strength [MPa(ksi)]	2800-3000 (406-435)	3000 (435)	69 (10)
Tensile Young's Modulus [GPa(10^6psi)]	84.7-89.6 (12.3-13.0)	112.3 (16.3)	2.8 (0.4)

Figure 2.1: Damage to Fibers Used for the Sleeve

2.2.3 Curing Temperatures

According to TCR composites, the UF3330-100 epoxy should cure at 154°C (310°F) for one hour, preceded by a temperature ramp up of 2.75°C (5°F) per minute, and followed by a cool down at the same rate. The curing time can be reduced in half with each 11° C (20°F) increase in curing temperature, as shown in Table 2.2. In order to find the optimal cure temperature and

reduce the time needed to cure the specimens a short study was done, with the complete report in Appendix A. Table 2.2 summarizes the results of this test. The compression strength is plotted against the cure temperature in Figure 2.2. In Figure 2.3, the Young's modulus is plotted against the cure temperature. Trend lines were added to both of these figures. Compression strength peaks when cured near 188°C (370°F). Compression Young's modulus remains fairly constant with an increasing cure temperature. From the standpoint of cure time practicality, and compression strength, a cure temperature 199°C (390°F) was chosen. At this temperature the cure time is reduced to 4 minutes, not including the ramp up and cool down periods.

Overall the difference in strength and Young's modulus, with increasing cure temperatures is negligible when taking into account one standard deviation error that is shown with error bars on the two plots. To reduce the amount of cure time for manufacturing specimens, however, a cure temperature of 199°C (390°F) was used.

Table 2.2: Summary of Cure Temperature Study

Configuration	Cure Temperature [°C(°F)]	Cure Time [min.]	Ultimate Compression Strength [MPa (ksi)]	Strain at Max Stress [10^3 με]	Compression Young's Modulus [GPa (10^6 psi)]
5BB43HNC310	154 (310)	60	675.4 (98.0)	11.5	67.5 (9.8)
5BA43HNC350	166 (330)	15	710.3 (103.0)	11.5	64.6 (9.4)
5BA43HNC370	177 (350)	8	597.7 (86.7)	10.4	59.8 (9.3)
5BB43HNC370	188 (370)	8	794.4 (115.2)	12.5	67.0 (9.7)
5BA43HNC390	199 (390)	4	675.4 (98.0)	11.5	67.5 (9.8)
5BA43HNC410	210 (410)	2	608.4 (88.2)	10.2	66.2 (9.6)

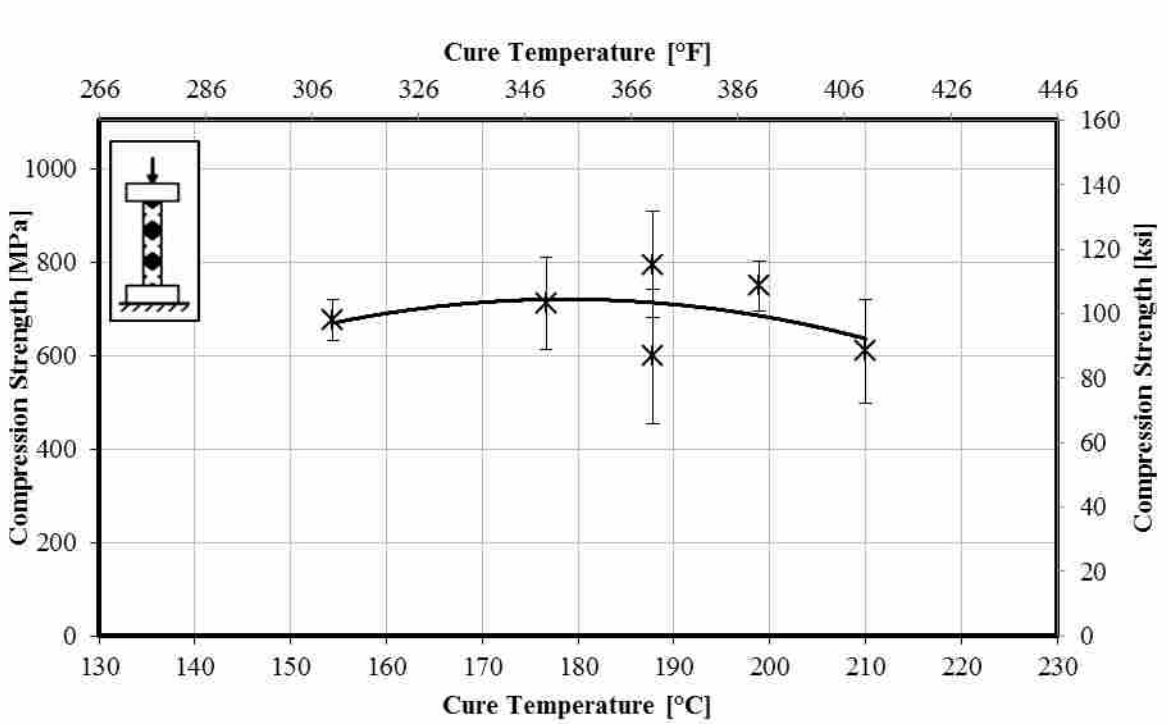

Figure 2.2: Compression Strength vs. Cure Temperature

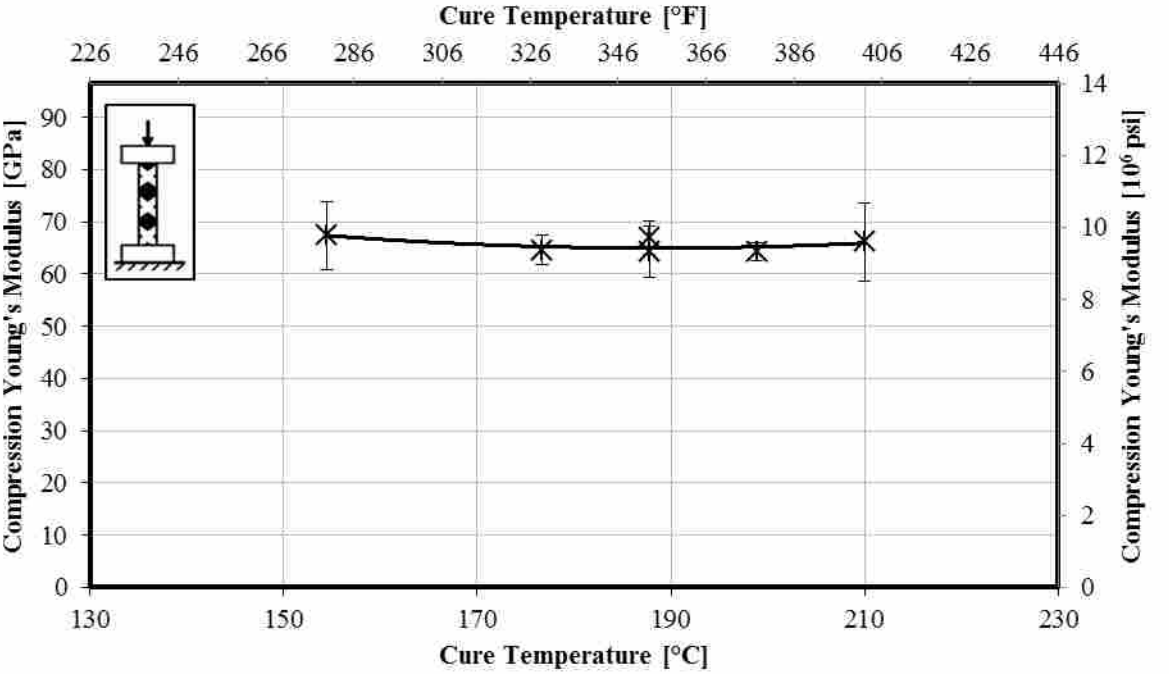

Figure 2.3: Compression Young's Modulus vs. Cure Temperature

2.2.4 Sleeve Patterns

Initially the hope was to study three types of sleeve coverage, but this was limited to two types based on the current programing limitations of the IsoTruss machine. The two types of sleeves were the unidirectional spiral wrap, and the bi-directional braid.

The unidirectional spiral path on the IsoTruss machine is shown in Figure 2.4, this path and how it works in conjunction with manufacturing is explained more in Sub-Section 3.1.1. This sleeve type requires two bobbins of sleeve material, circling in the same direction around the core material. The two tows of sleeve material never cross over each other. Both full and half coverage are possible, with typical manufactured specimens shown in Figure 2.5.

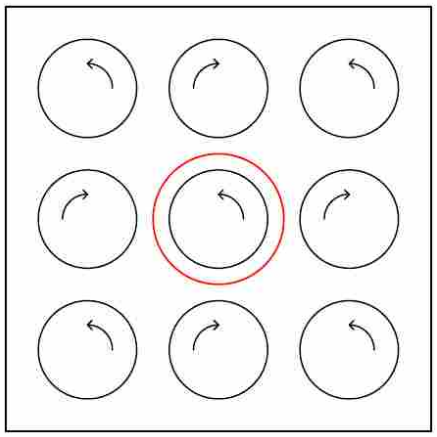

Figure 2.4: Unidirectional Spiral Sleeve Path on IsoTruss Machine Wall

The bi-directional braid path on the IsoTruss machine is shown in Figure 2.6. This sleeve type requires six bobbins of sleeve material. There are three bobbins on each of the two paths, with each path moving in opposing directions. In this manner a crisscrossing of tows occurs at each location where the two tow paths cross, as seen in Figure 2.6, creating a braid. The braid is not symmetric, with one side of the specimen differing in pattern from the other side. The braid is,

however, consistent along the length of the specimen. Both full and half coverage are possible, with typical manufactured specimens shown in Figure 2.7.

Figure 2.5: Spiral Sleeve: A) Full Coverage (Top); and, B) Half Coverage (Bottom)

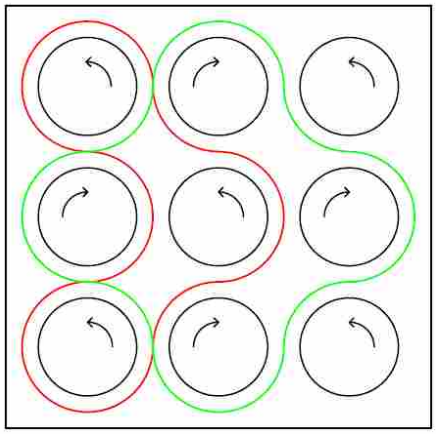

Figure 2.6: Bi-Directional Braid Sleeve Path on the IsoTruss Machine Wall

Figure 2.7: Braided Sleeve: A) Full Coverage (Top); and, B) Half Coverage (Bottom)

2.2.5 Test Matrix

A nominal 5 specimens for each configuration were tested. A summary of the test variables are shown in Table 2.3. A more detailed test matrix, including all configurations tested is found in Table 2.4. Overall there were approximately 60 specimens tested for each sub-group of specimens, making for a total of approximately 180 specimens tested.

Table 2.3: Summary of Test Variables

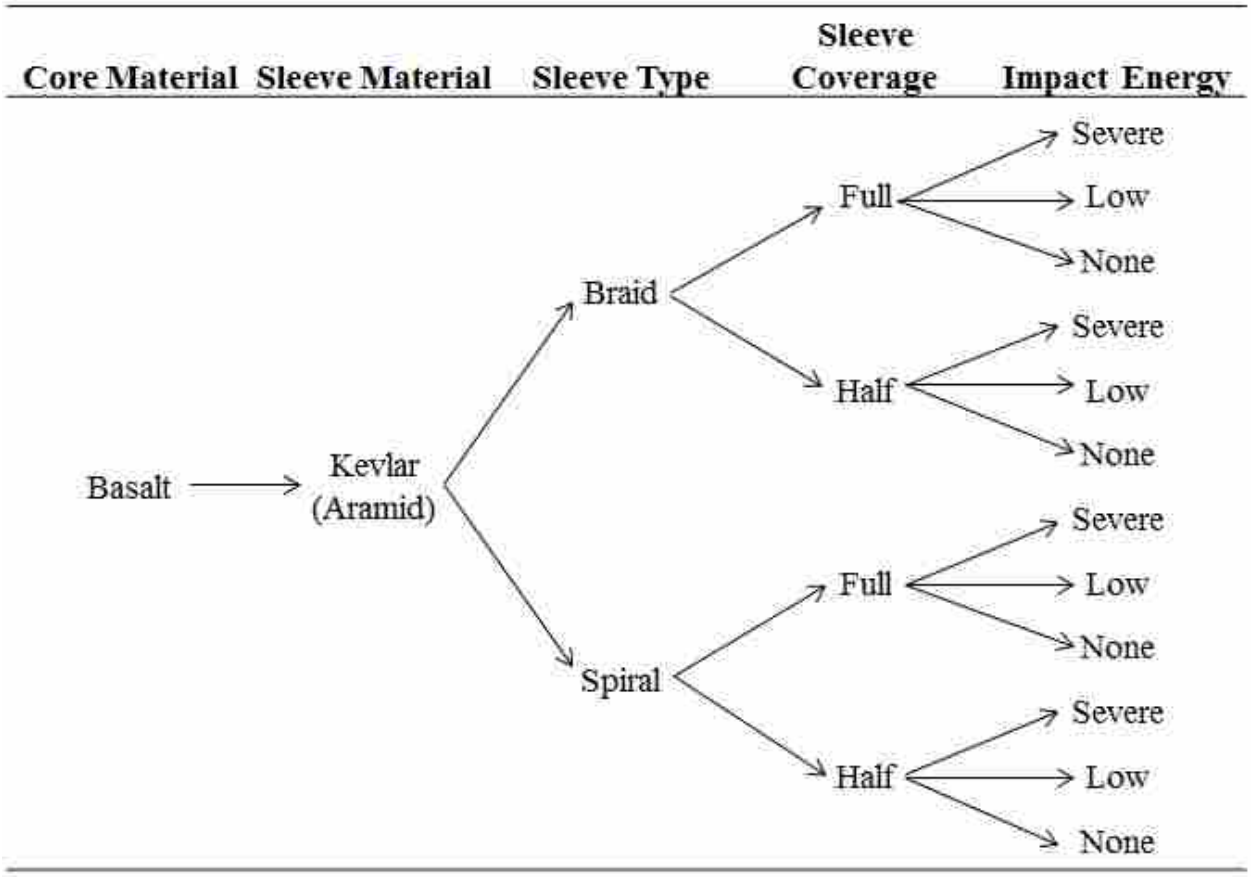

Table 2.4: Test Matrix Including all Specimen Configurations Divided into Sub-Groups

# of Specimens Tested	Core Material	Sleeve Material	Unsupported Length [mm(inch)]	Core Diameter [mm(inch)]	Sleeve Type	Sleeve Coverage	Impact Level
Group 1: Preliminary							
5	Basalt	Aramid	76 (3)	8 (5/16)	Braid	Full	Severe
5	Basalt	Aramid	76 (3)	8 (5/16)	Braid	Full	Low
5	Basalt	Aramid	76 (3)	8 (5/16)	Braid	Full	None
5	Basalt	Aramid	76 (3)	8 (5/16)	Braid	Half	Severe
5	Basalt	Aramid	76 (3)	8 (5/16)	Braid	Half	Low
5	Basalt	Aramid	76 (3)	8 (5/16)	Braid	Half	None
5	Basalt	Aramid	76 (3)	8 (5/16)	Spiral	Full	Severe
5	Basalt	Aramid	76 (3)	8 (5/16)	Spiral	Full	Low
5	Basalt	Aramid	76 (3)	8 (5/16)	Spiral	Full	None
5	Basalt	Aramid	76 (3)	8 (5/16)	Spiral	Half	Severe
5	Basalt	Aramid	76 (3)	8 (5/16)	Spiral	Half	Low
5	Basalt	Aramid	76 (3)	8 (5/16)	Spiral	Half	None
Group 2: 5/16” Diameter							
5	Basalt	Aramid	51 (2)	8 (5/16)	Braid	Full	Severe
5	Basalt	Aramid	51 (2)	8 (5/16)	Braid	Full	Low
5	Basalt	Aramid	51 (2)	8 (5/16)	Braid	Full	None
5	Basalt	Aramid	51 (2)	8 (5/16)	Braid	Half	Severe
5	Basalt	Aramid	51 (2)	8 (5/16)	Braid	Half	Low
5	Basalt	Aramid	51 (2)	8 (5/16)	Braid	Half	None
5	Basalt	Aramid	51 (2)	8 (5/16)	Spiral	Full	Severe
5	Basalt	Aramid	51 (2)	8 (5/16)	Spiral	Full	Low
5	Basalt	Aramid	51 (2)	8 (5/16)	Spiral	Full	None
5	Basalt	Aramid	51 (2)	8 (5/16)	Spiral	Half	Severe
5	Basalt	Aramid	51 (2)	8 (5/16)	Spiral	Half	Low
5	Basalt	Aramid	51 (2)	8 (5/16)	Spiral	Half	None
Group 3: 7/16” Diameter							
5	Basalt	Aramid	51 (2)	11 (7/16)	Braid	Full	Severe
5	Basalt	Aramid	51 (2)	11 (7/16)	Braid	Full	Low
5	Basalt	Aramid	51 (2)	11 (7/16)	Braid	Full	None
5	Basalt	Aramid	51 (2)	11 (7/16)	Braid	Half	Severe
5	Basalt	Aramid	51 (2)	11 (7/16)	Braid	Half	Low
5	Basalt	Aramid	51 (2)	11 (7/16)	Braid	Half	None
5	Basalt	Aramid	51 (2)	11 (7/16)	Spiral	Full	Severe
5	Basalt	Aramid	51 (2)	11 (7/16)	Spiral	Full	Low
5	Basalt	Aramid	51 (2)	11 (7/16)	Spiral	Full	None
5	Basalt	Aramid	51 (2)	11 (7/16)	Spiral	Half	Severe
5	Basalt	Aramid	51 (2)	11 (7/16)	Spiral	Half	Low
5	Basalt	Aramid	51 (2)	11 (7/16)	Spiral	Half	None

2.2.6 Specimen Notation

In order to facilitate testing and ensure proper recording of results, a coding system was developed to keep track of the specimens. The coding system allowed for unique identification of each specimen that was tested. The first character in the code represents the diameter of the specimen core, a “5” being used for 8 mm (5/16”) and a “7” being used for (7/16”) specimens. The next character was a “B” for the basalt core, followed by an “A” for the aramid sleeve. The next two characters specified the sleeve type, a “43” for the unsymmetric braid and “10” for the spiral sleeve. The “43” and “10” are representative of the number of lobes used to create the two paths followed by the bobbins on the IsoTruss machine. The next character is either an “F” for full coverage, or an “H” for half coverage. Next in line is an “S” for severe impact, an “L” for low impact, or an “N” for no-impact. The second to last character is a “C” for a compression or strength-controlled failure mode, as opposed to buckling. The final character is either a “2” or a “3” indicating whether the specimen is 51 mm (2”) or 76 mm (3”) long, respectively. The end of the code had a “- #” to indicate the individual specimen within that configuration (typically 1 through 5). Table 2.5 is a summary of the notations used to create the coding system, in order of how they appear in the identification code.

As an example, the specimen identification 5BA43FNC2-3 is an 8 mm (5/16”) basalt core, with an aramid braided sleeve, with full coverage, that is not impacted, tested for compression strength, and an unsupported length of 51 mm (2”). The “3” at the end indicates that it is the third specimen in this particular test configuration. This coding system proved to be quite successful, and helpful, in keeping test and data collection organized.

Table 2.5: Specimen Coding System Notation

Variable	Notation	Description
Core Diameter	**5**	*8mm (5/16")*
	7	*11 mm (7/16")*
Core Material	**B**	*Basalt*
Sleeve Material	**A**	*Aramid*
Sleeve Type	**10**	*Spiral*
	43	*Braid*
Sleeve Coverage	**H**	*Half*
	F	*Full*
Impact Level	**N**	*None*
	L	*Low*
	S	*Severe*
Failure Method	**C**	*Compression Strength*
Unsupported Length	**2**	*51 mm (2")*
	3	*76 mm (3")*

3 EXPERIMENTAL PROCEDURE

In this chapter the processes for manufacturing the specimens, preparing the specimens for testing, and testing the specimens are described. Also, several of the problems encountered while manufacturing and testing, and their resolutions, are presented in this chapter.

3.1 Specimen Manufacturing

The specimens were manufactured by BYU student researchers on a prototype automated continuous fabrication machine for IsoTruss structures located at Novatek Inc. facilities. They were manufactured during the period of September 2010 to June 2011. The conditions for manufacturing the composite specimens were less than ideal, with many possible sources of contamination coming from the machine shop adjacent to the IsoTruss machine and the large exterior overhead door nearby that was occasionally left open. Specimens were manufactured on the IsoTruss machine in runs of approximately 4.9 m (16’), which is the current length of the mandrel. The specimens were cured under tension while in line with the IsoTruss machine.

3.1.1 Automated IsoTruss® Manufacturing Proto-Type Machine

The IsoTruss machine was built with the purpose of creating an automated process for continuous production of IsoTruss beams [30][31]. Four key aspects of the IsoTruss machine are discussed: 1) the wall; 2) the bobbins; 3) the mandrel; and, 4) the fiber creel.

The wall is the main component of the IsoTruss machine, for creating the braided and spiral sleeves. When operating at full potential, the wall will also facilitate the manufacture of the helical members of the IsoTruss. Figure 3.1 is a picture of the wall as used for the production of specimens in this research. The bobbin tracks are clearly seen on the bottom portion of the wall as a series of interconnecting circles. At each node where the circular tracks touch, there is a pneumatic servo switch that allows a bobbin, carrying a tow of fiber, to either be passed onto another circular track or remain on the initial circular track. The paths followed by the bobbins were outlined previously in Figure 2.4 and Figure 2.6. The bobbins are carried along these tracks by a series of horn gears, as seen on the top portion of the machine, which are driven by gears on the backside of the machine. Each gear turns in an opposing direction to the gear at its side. The combination of the bobbin track, the horn gears and their opposing revolution allows for complex weaving patterns to be created as mentioned in Chapter 2.

Figure 3.1: Picture of the IsoTruss Wall

One of the bobbins is shown in Figure 3.2. The bobbins supply sleeve material to the manufacturing process, and allow the sleeve fibers to be moved in complex patterns around the IsoTruss wall. The sleeves consolidate the core fibers and simultaneously increase the damage tolerance of the composite structure. The bobbins have a specially designed base to fit into the track on the wall and driven by the horn gears. The ability of the bobbin to maintain tension while weaving is the key aspect. The distance from the bobbin to the core material being consolidated, is continuously changing. This continual change necessitates the ability of the bobbin to rewind, thus maintaining tension. Without constant tension, in this case 22.2-35.6 N (5-8 lbs.), sufficient consolidation would not occur.

Figure 3.2: IsoTruss Bobbin Loaded with Aramid Spool

The mandrel advances the fibers as the IsoTruss structure is being manufactured by pulling the core fibers and the sleeve fibers out at the rate of production specified. The mandrel is made of a hollow square steel section that is pushed through the center of the wall with a high

torque motor behind the wall, as seen in Figure 3.3. The ratio of the mandrel speed relative to the speed of the bobbins on the wall determines the sleeve coverage. An increased ratio decreases the coverage, while a decreased ratio will increase the percentage of core material covered by the sleeve.

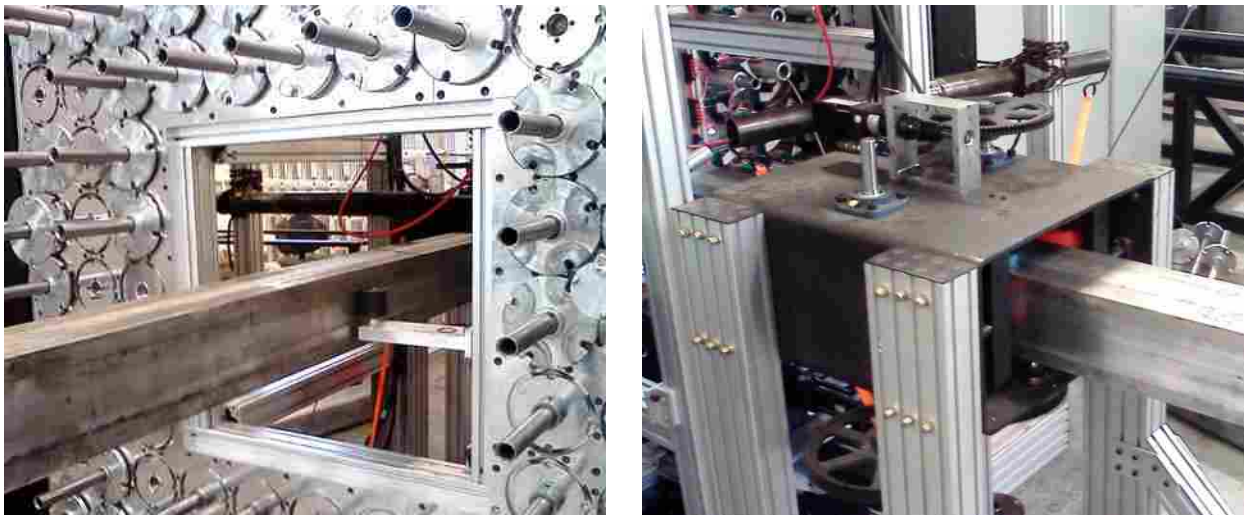

Figure 3.3: Views of the IsoTruss Machine: A) The Mandrel Passing Through Wall (Left); and, B) Motor for Pushing Mandrel (Right)

The final key piece of the IsoTruss machine is the fiber creel. The fiber creel sits behind the IsoTruss wall and holds the fibers that comprise the core of the specimens. The creel holds each individual spool of material on a tensioned roller. Each roller is under 13.3-22.2 N (3-5 lbs.) tension, which keeps the core fibers straight and parallel to each other while being consolidated by the sleeves. The fibers travel to the wall through a series of pulleys. Contamination of the fiber is minimized by a plastic cover attached to the creel structure as shown in Figure 3.4.

Figure 3.4: Fiber Creel Loaded with Basalt and Protected by Plastic Covering

A plan view schematic of how these four key components work together is shown in Figure 3.5. The core fiber begins at the fiber creel, and through a series of pulleys the fiber arrives at the IsoTruss wall where it travels through a hollow shaft at the center of the horn gears. To start the process, the fibers used to create the basalt core and aramid sleeve are attached to the mandrel. The mandrel pulls the fibers and advances the production of IsoTruss sections. The core fibers are consolidated by the aramid sleeve as they exit the hollow shaft. Photos showing the fiber traveling to the machine wall and the core fibers being consolidated by the sleeve are shown in Figures 3.6 and 3.7, respectively.

To evaluate the effectiveness of the IsoTruss machine in producing quality IsoTruss members fiber volume percentages were measured optically. The measurements were taken from various locations on one specimen of each configuration type. The average of these measurements was a fiber volume of 59% indicating good consolidation. A table presenting the

fiber volumes for the different configurations is provided in Appendix B, along with typical images used to obtain measurements.

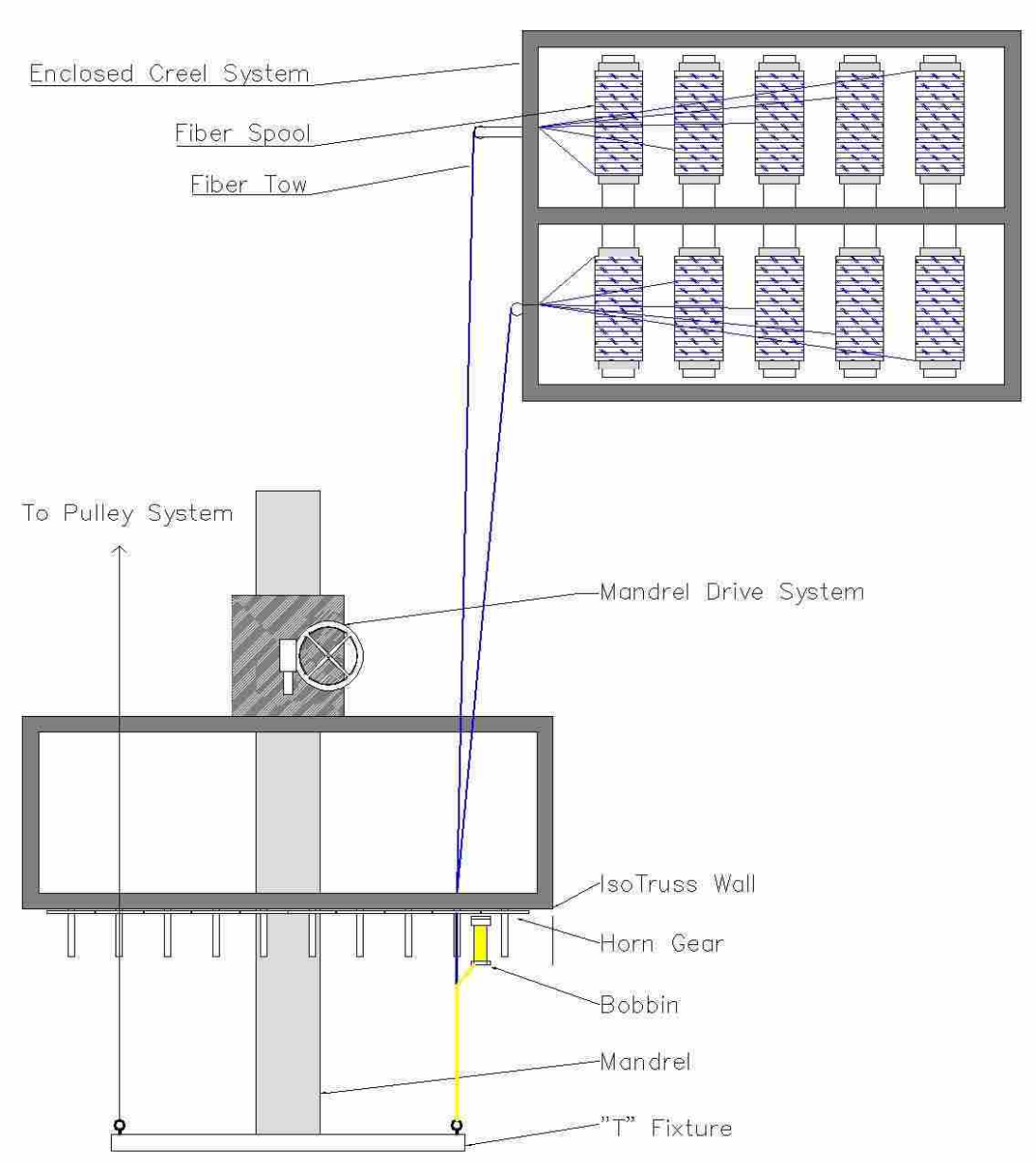

Figure 3.5: Plan View Schematic of the IsoTruss Machine and Creel System

Figure 3.6: Core Material Traveling from Fiber Creel to the Machine Wall

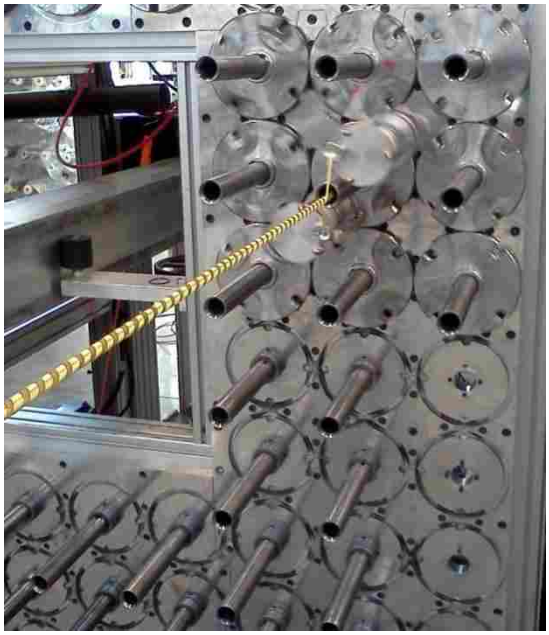

Figure 3.7: Core Material Being Consolidated by the Sleeve

3.1.2 Specimen Curing

The specimens were cured in two steps: 1) the initial in-line cure; and, 2) a post cure. The initial in-line cure was done in a SPX Lindberg Model 54977 curing oven shown in Figure

3.8. This oven is designed to close down on top of the mandrel, and allows the mandrel to extend out from both ends of the oven. The internal heating elements, and the thermocouples, which measure the temperature, were all rebuilt as part of this research. The oven temperature was controlled by a program written in RSView32 by Rockwell Software. Figure 3.9 shows the results of a short study that compared the internal temperature of the specimen, the actual ambient temperature of the oven, and the programmed cure cycle. The internal temperature was taken by inserting a thermocouple into the specimen during curing, located 280 mm (11") from the edge of the oven. The initial temperatures are slightly higher than room temperature due to a malfunction of the oven for this test. The solid line is the desired programmed cure cycle that should be followed. As seen, the average oven temperature follows the program very well, with only a slight overshot of the initial max temperature and a failure to reduce temperature at the proper rate. This lack of cooling is not a problem and will not affect the curing of the specimen. The internal temperature of the specimen lags behind the program as expected, as the core slowly increases in temperature. An exothermic reaction occurs and the internal temperature overshoots the maximum programmed temperature and the oven ambient temperature and then reduces in temperature quickly.

Figure 3.8: SPX Lindberg Model 54977 Curing Oven

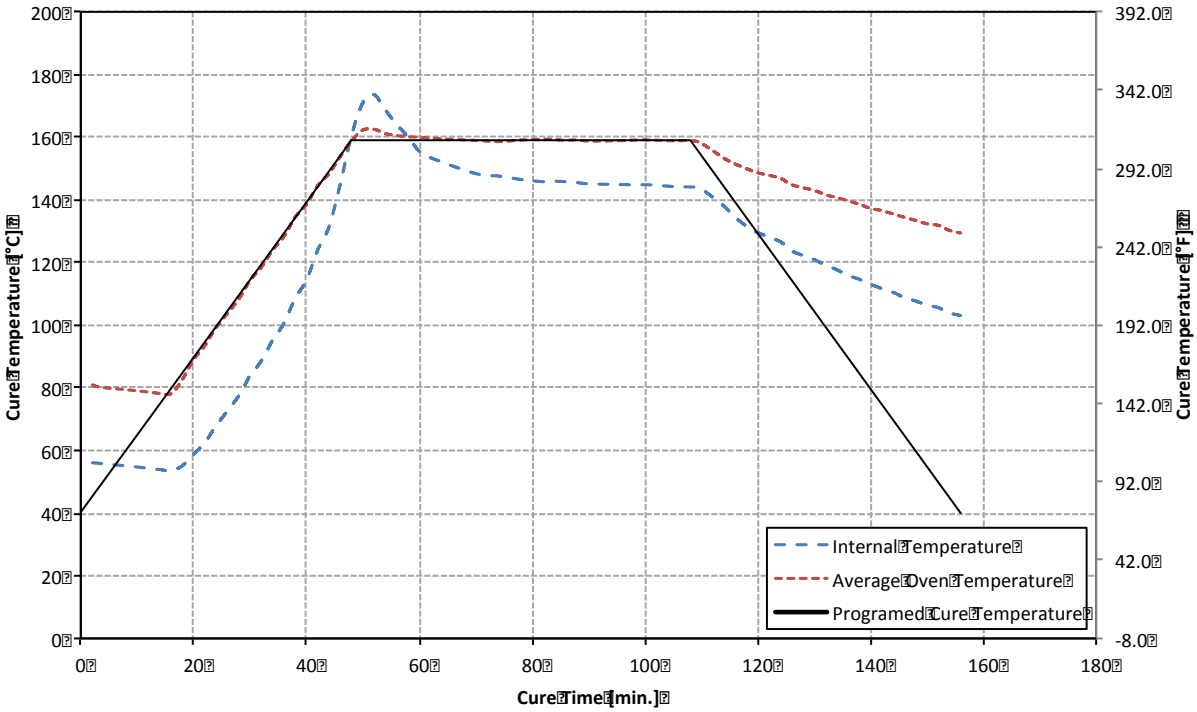

Figure 3.9: Internal Specimen Temperature vs. Programmed Curing Temperature

The specimens were post-cured at 177 °C (350 °F) for one hour in a NAPCO 630-7 oven. The specimens were not under tension during the post cure, since the initial cure solidified the members.

3.1.3 Problems Encountered with Specimen Manufacturing

Several problems were encountered while manufacturing the specimens related to the bobbins, the shafts in the IsoTruss wall, unsymmetrical forces on the mandrel and, the curing oven.

The initial bobbins had a rewind capability of 76 mm (3”). The design of the IsoTruss machine required much more rewind capability than that, due to the continually changing

distance of the bobbin from the core material. This resulted in an inconsistent tension on the sleeve, resulting in insufficient consolidation and inadequate part quality.

A new bobbin was developed that allowed 711 mm (28”) of fiber rewind capability, greatly surpassing the original rewind capability. Proper tension and fiber consolidation were achieved with the new bobbin design.

The IsoTruss wall uses shafts, running parallel to the core fibers, which connect the drive gears on the back of the IsoTruss wall to the horn gears on the front of the wall. These shafts incorporated a keyway running the length of the shaft. The sharp edges of the keyway broke down the needle bearings required to allow smooth rotation of the shafts. Each bearing failure caused the wall to seize requiring the bearing to be replaced. To avoid further problems, all shafts, except those needed to manufacture test specimens, were removed from the wall. New shafts with the keyways terminating outside of the bearings were manufactured after the completion of this research.

The 166 basalt fiber tows, each under 13.3-22.2 N (3-5 lbs.) tension, translates to about 2,200-3,700 N (500-830 lbs.) of compression force on the end of the mandrel. This is within the capacity of the high torque motor, but causes the segmented mandrel to be pulled off-axis in the direction of the loaded side during manufacture.

The core fibers are pulled through a shaft that is offset form the mandrel by 61 cm (24”). This offset results in a horizontal force on the shaft. (see Figure 3.10). This transverse force causes the machine to seize similar to a shaft/bearing failure. Fiber fraying was also caused by this horizontal force. To eliminate the transverse force a “T” fixture was attached to the end of the mandrel. This fixture allowed the fiber to be pulled out from the wall parallel to the shaft, without touching the shaft. This created a large eccentric load which was balanced by adding a

weighted pulley system to the opposing end of the "T" fixture. This is only a consequence of specimen manufacture and will not be an issue when manufacturing full IsoTruss structures.

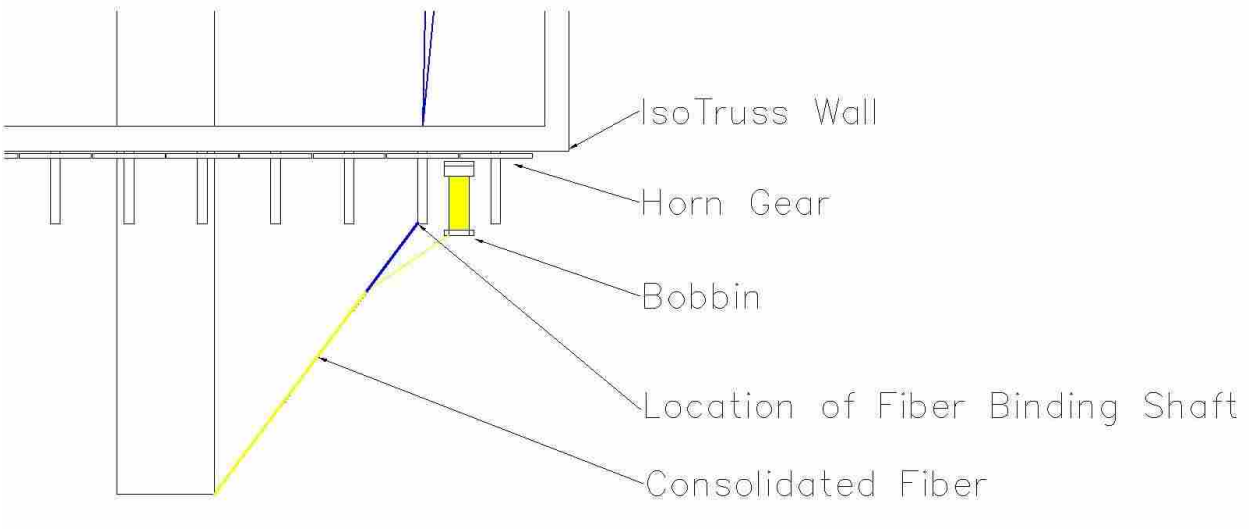

Figure 3.10: Fiber Causing IsoTruss Machine Shaft to Bind

The final significant problem encountered during manufacturing was the inconsistency of the SPX Lindberg Model 54977 curing oven. This oven was rebuilt for the purpose of this research but encountered many problems due to failures of the heating elements and thermocouples. To compensate for oven temperature variations, the specimens were post-cured as described in Sub-Section 3.1.2. The thermocouples, heating elements, and wiring were eventually replaced leading to a more reliable and consistent curing cycle.

3.2 Specimen Preparation

For consistent and reliable results a standard process was developed for preparing specimens. Error was caused by misalignment and/or poor quality end surfaces. Proper load introduction requires precise alignment in the test fixture and a flat and smooth surface on the

ends. Otherwise, the results could be unreliable [26]. The following sub-sections outline the exact method used to prepare the specimens for testing.

3.2.1 Specimen Cutting

Test materials were manufactured in approximately 4.9 m (16') lengths. The specimens were cut to their proper length with a diamond-coated cutting blade, using a Leco CM-10 cutoff machine, shown in Figure 3.11, was used. A fixture was made to hold the specimens in place and to ensure that the cut was perpendicular to the longitudinal axis of the specimens. Light pressure was used to lower the blade into the specimen, which kept the fragile blade from breaking, and reduced the coarseness of the blade marks on the specimen end surfaces.

Figure 3.11: Leco CM-10 Cutoff Machine

3.2.2 Initial Specimen Sanding

To ensure a flat and smooth end surface, perpendicular to the longitudinal axis of the specimen, each end surface was sanded. A specially-designed fixture was made to hold the

specimens perpendicular to the sanding surface, as shown in Figure 3.12. The v-notch receives the specimen to be sanded and holds the specimen vertically. The various clearance holes allow attachment of the fixture to the head of a Leco Spectrum System 2000 sander, as shown in Figure 3.13. A 600-grit sandpaper was used for initial sanding.

Figure 3.12: Specimen End Sanding Fixture

Figure 3.13: Specimen End Sanding Fixture Attached to the Spectrum System 2000 Sander

3.2.3 Specimen Setting in End Caps

Each end of the specimen was set in an end cap which fits into the specially designed compression testing receptacle. The end caps aided in vertical alignment and enabled quick specimen loading and unloading during testing, and reduced the occurrence of brooming or spalling failures at the ends. Each end cap has an outer diameter of 38.1 mm (1-1/2”), an inner diameter ranging from 12.4-15 mm (0.49”-0.59”) , and a height of 19.1 mm (3/4”). Figure 3.14 shows a specimen, with these end caps, ready for testing.

Figure 3.14: Typical Specimen Set in End Caps

The end caps are attached to the specimen with a 2-ton Loctite® 5-min instant mix epoxy. In order to align and center the specimen in the end caps, a setting fixture was designed and built (see Figure 3.15). The fixture was designed to be adjustable to handle specimens with different lengths and diameters. The alignment clamps were initially set using an alignment rod, the alignment rod was removed, and the end caps were placed in the base of the fixture. Specimens were clamped into the fixture and set in the end caps with epoxy. Note that due to gravity, epoxy could only be applied on one end at a time.

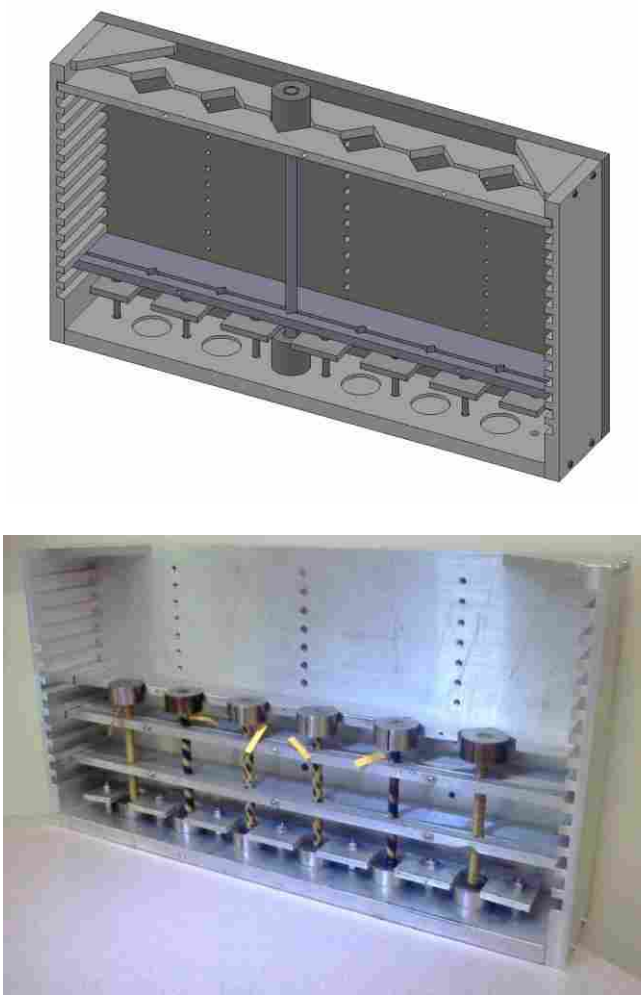

Figure 3.15: End Cap Setting Fixture: A) Computer Rendering (Top); and, B) Manufactured Fixture (Bottom)

3.2.4 Specimen Surface Preparation

A thin washer shaped spacer was placed between the end cap and the setting fixture base plate when setting the specimens in the end caps. This spacer allowed the specimen to extend past the end cap surface. The extended portion of the specimen was removed by sanding until the end of the specimen was flush with the end caps, using the Leco Spectrum System 2000 sander. The flush surface discourages end condition failures and ensures proper introduction of the load.

3.3 Specimen Measurements

Precise measurements of cross-sectional area, sleeve coverage, and specimen offset were taken using a digital microscope. These measurements were used in the reduction of data, to assess the quality of the testing and also to identify problems in the specimen preparation.

3.3.1 Microscope

The measurements were taken using an Olympus SZX12 digital microscope as shown in Figure 3.16. Pax-it® software, which controlled the digital aspect of the microscope, analyzes the different levels of material reflectivity and creates bounded areas for quantification.

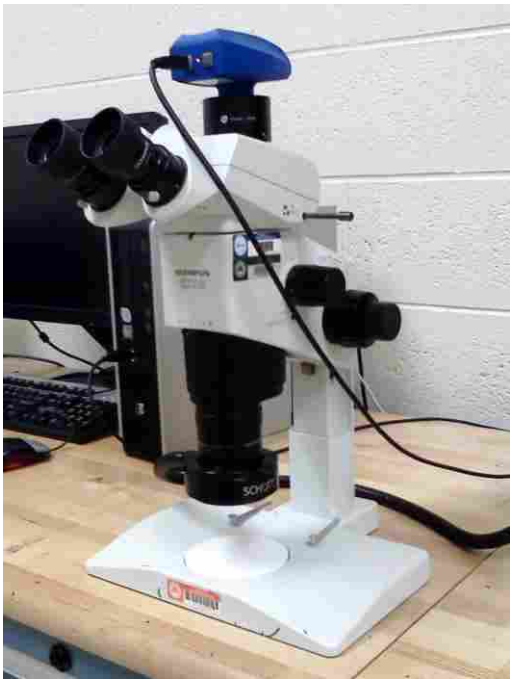

Figure 3.16: Olympus SZX12 Digital Microscope

3.3.2 Cross-Sectional Area Measurements

Pictures of both ends of each specimen were taken with a 7x zoom. These images were used to measure the cross-sectional area using the Pax-it software. An example of a cross-

sectional measurement is shown by the shaded area (green) in Figure 3.17. A single cross-sectional area was applied to each specimen based on an average of the measurements taken at the two ends. (see Appendix C).

Figure 3.17: Typical Specimen Cross-Sectional Area Measurement

3.3.3 Sleeve Coverage Measurements

To account for variations in sleeve coverage, the percentage of surface area covered by the sleeve was measured for each specimen. Pictures were taken on all four sides of each specimen. The Pax-it software was used to quantify the coverage on each side, with the four measurements averaged. The shaded portions (green) shown in Figure 3.18 represent the areas not covered by a sleeve. Since the specimen surface is curved, and the measurements were taken from a 2-D picture, there is a discrepancy from the true coverage. This method did, however, provide a standardized method for comparison. A table with the coverage of each specimen is in Appendix D.

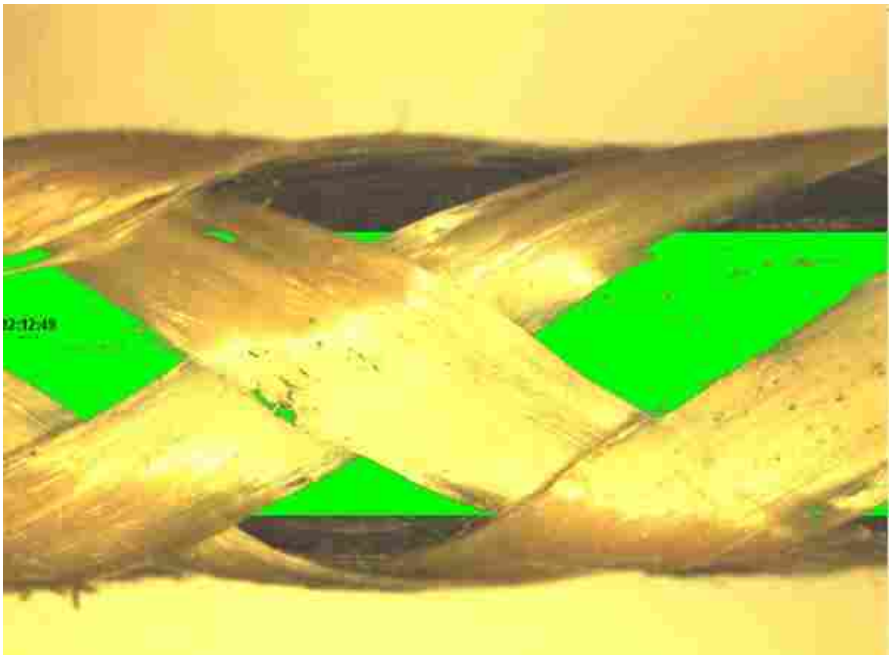

Figure 3.18: Typical Specimen Sleeve Coverage Determination

3.3.4 Axis Offset Measurements

To evaluate specimen alignment in each end cap, the x and y offsets of the longitudinal axis of the specimen from the center of the end caps were measured. A transparent overlay with a circle and cross-hairs was placed over the end cap, to identify the center as shown in Figure 3.19. Perpendicular diametric lines were drawn on the image using the Pax-it software to locate the center of the specimen. These measurements were used to determine the angle between the longitudinal axis of the specimen and the surface of the end caps. Plots showing how the compressive stress was affected by offset are in Figure 3.20 and Figure 3.21 for the 8 mm (5/16”) diameter 51 mm (2”) length, and the 11 mm (7/16”) diameter 51 mm (2”) length, respectively. The effects on stiffness are shown in Figure 3.22 and Figure 3.23. Note that offset measurements were not taken for the preliminary 76 mm (3”) specimens.

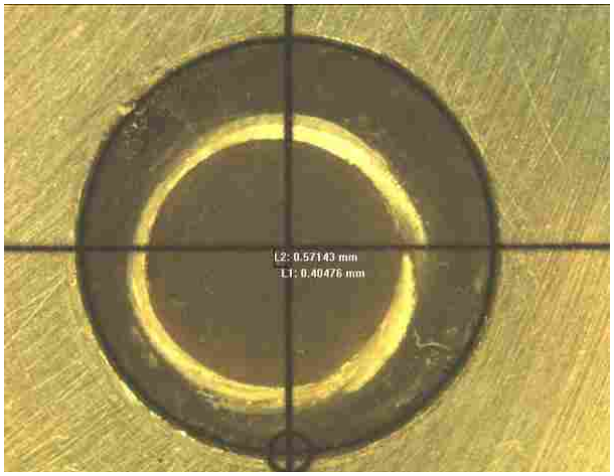

Figure 3.19: Typical Image Used to Determine of Specimen Offset

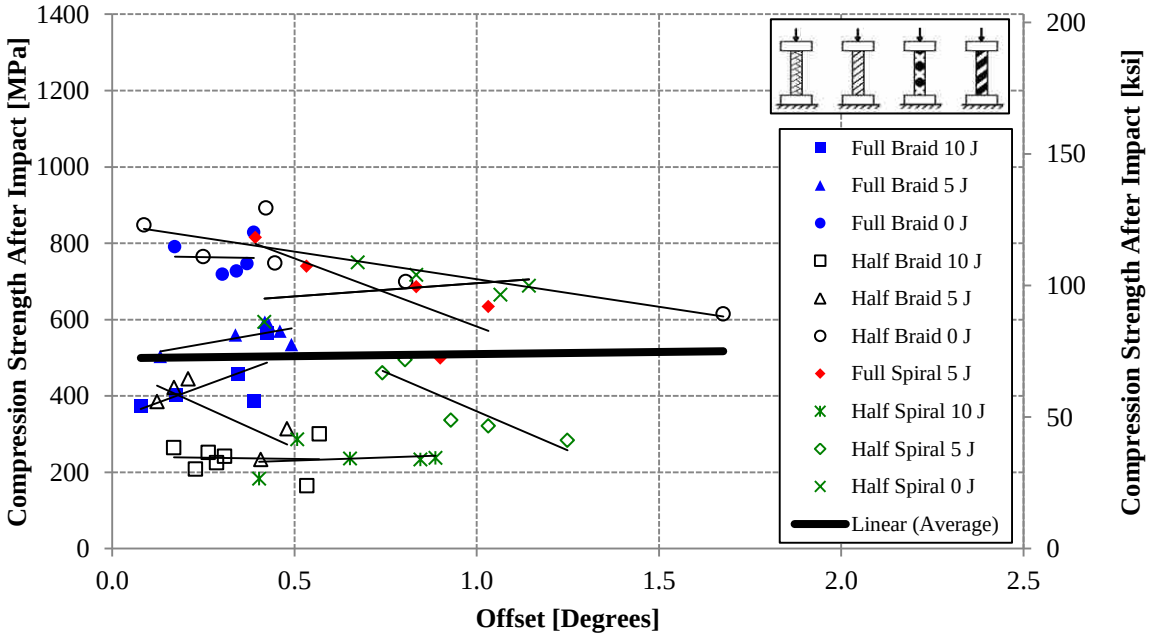

Figure 3.20: Compression Strength vs. Offset for 8 mm (5/16") Diameter, 51 mm (2") Length

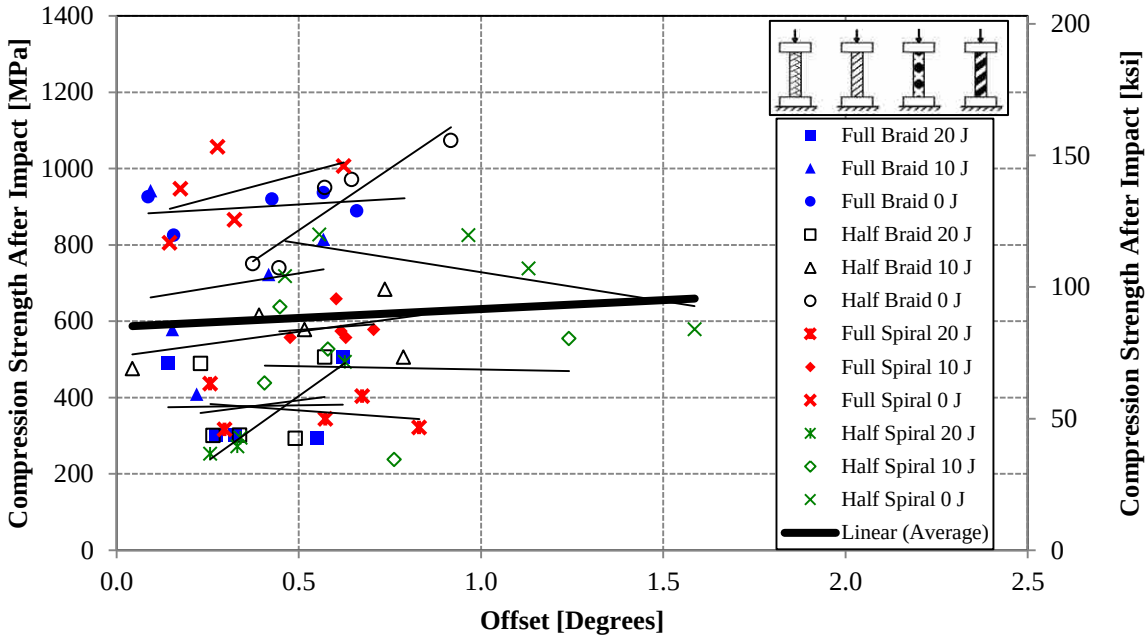

Figure 3.21: Compression Strength vs. Offset for 11 mm (7/16") Diameter, 51 mm (2") Length

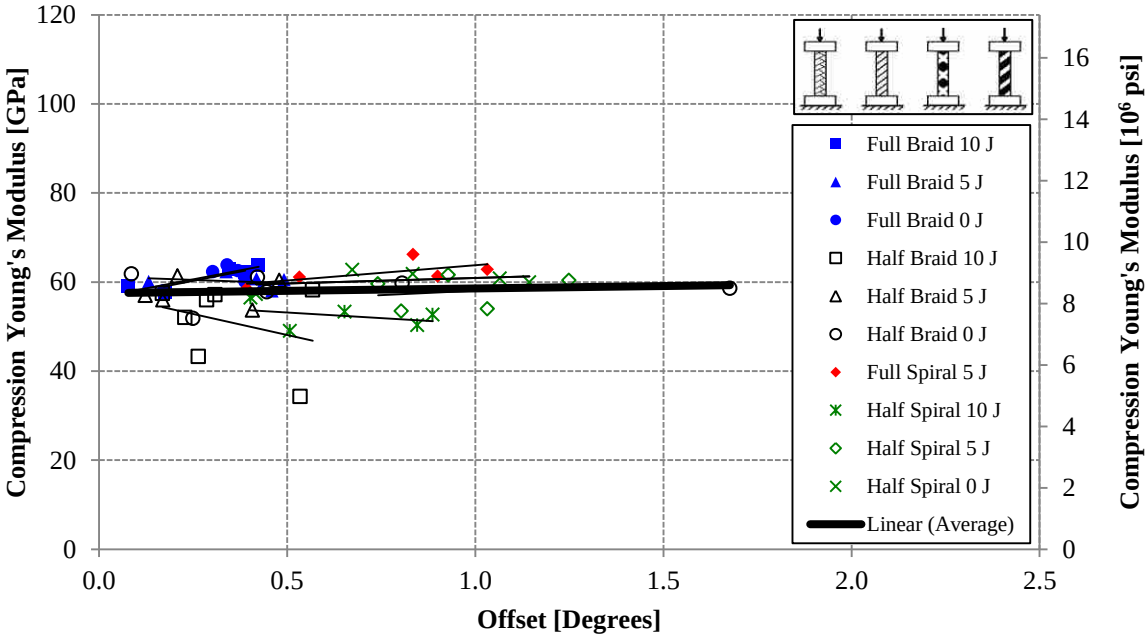

Figure 3.22: Compression Young's Modulus vs. Offset for 8 mm (5/16") Diameter, 51 mm (2") Length

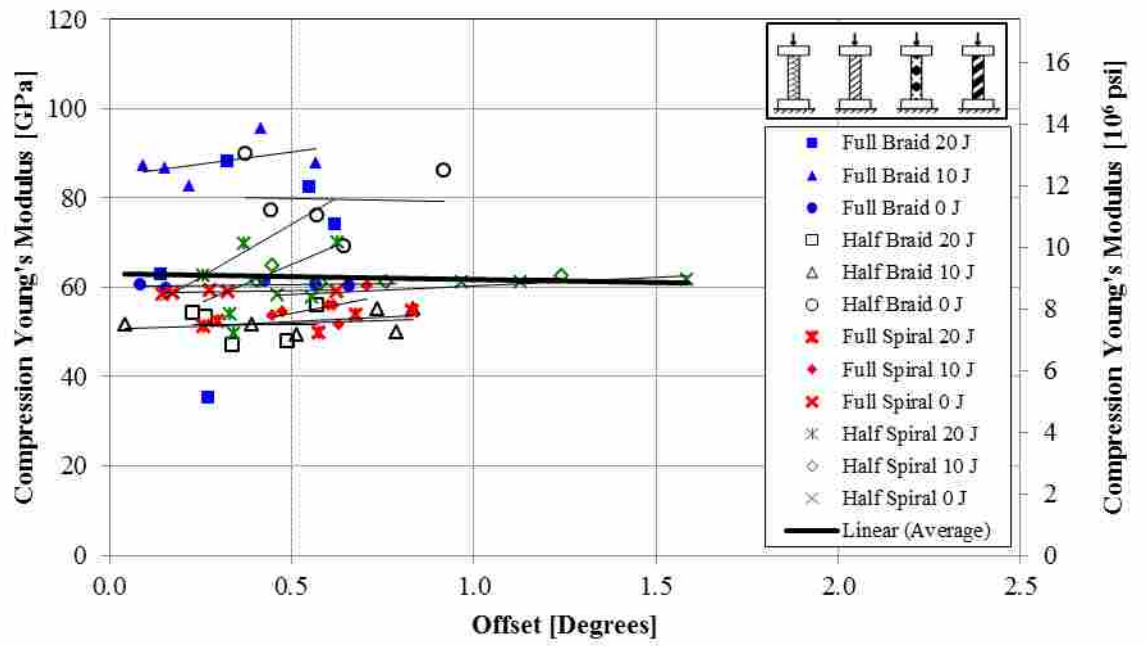

Figure 3.23: Compression Young's Modulus vs. Offset for 11 mm (7/16") Diameter, 51 mm (2") Length

Individual trend lines are included in Figures 3.20 through 3.23 for each specimen configuration. The bold lines represent the overall trends for all configurations in each figure. The shallow slopes of the overall trend lines confirm that there is little effect on the overall strength and stiffness of the specimens, particularly if the alignment is within 1° (in this research only a few specimens had angles greater than 1°). The largest offset (1.67°), did, in fact, indicate a reduction in compressive strength and stiffness with increasing offset. Thus, the alignment of the specimens in this research was within reasonable limits, ensuring the strength and stiffness were not severely degraded by the offset angle.

3.4 Specimen Impacting

A Dynatup® 8200 drop-weight impact machine (Figure 3.24) was used to impact the specimens. Typically, a spherical *tup*, striking head, is used for impact testing. This testing

employed a cylindrical tup, designed to limit the occurrence of a glancing blow. The cylindrical tup, shown in Figure 3.25, was oriented at a 90° angle to the longitudinal axis of the specimen during impact. A clamping fixture, Figure 3.26, was designed and built to hold the specimen by the end caps in place during impact. The fixture provides effectively fixed boundary conditions for the specimen. A picture of a typical specimen immediately prior to impact is shown in Figure 3.27.

Figure 3.24: Dynatup 8200 Drop Impact Machine

Figure 3.25: Cylindrical Tup Used to Impact Specimens

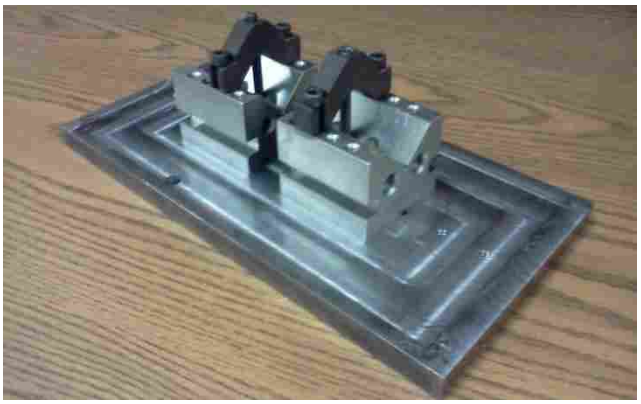

Figure 3.26: Clamp Used to Hold Specimens while Impacted

Figure 3.27: Photo of Specimen at Impact

The theory behind the drop-weight impact machine is that a specific weight and drop height create a specific amount of impact energy. The associated software calculates kinetic energy using Equation 3-1:

$$E = \frac{1}{2}mv^2 \tag{3-1}$$

where m is the mass of the tup and cross-head and v is the velocity just prior to impact. A more appropriate form of the kinetic energy equation facilitating instrument set up is given by Equation 3-2:

$$E = wd \tag{3-2}$$

where w is the weight of the tup and cross-head and d is the distance measured from the tip of the tup to the surface of the specimen. The various drop heights used for testing are in Table 3.1.

Table 3.1: Nominal Impact Energy Levels and Drop Heights Based on a Tup and Cross-Head Weight of 48.57 N [10.92 lbs.]

Impact Energy [J (ft-lbs.)]	Drop Height [cm (inches)]
5 (3.7)	10.4 (4.1)
10 (7.4)	20.6 (8.1)
20 (14.8)	41.4 (16.3)

Specimens were impacted at an energy level representing an approximate 1/3 and 2/3 reduction in strength compared to an undamaged specimen. Several preliminary tests were done at various impact energies to determine impact levels. Tests were performed on the half spiral specimens to verify the choice of 5 J (3.7 ft-lbs.) and 10 J (7.4 ft-lbs.) for the 8 mm (5/16") specimens, and 10 J (7.4 ft-lbs.) and 20 J (14.8 ft-lbs.) for the 11 mm (7/16") specimens. Figure 3.28 shows the approximate 1/3 and 2/3 reduction in strength for both specimen diameters.

3.5 Compression Testing

The specimens were loaded in axial compression to failure for evaluation of the residual compression strength. The 8 mm (5/16") diameter specimens were tested on an Instron Model 1321 compression machine with a 90 kN (20 kip) capacity (Figure 37). The 11 mm (7/16")

diameter specimens were tested in an MTS model 312.41 compression machine with a 489 kN (110 kip) capacity (Figure 3.29).

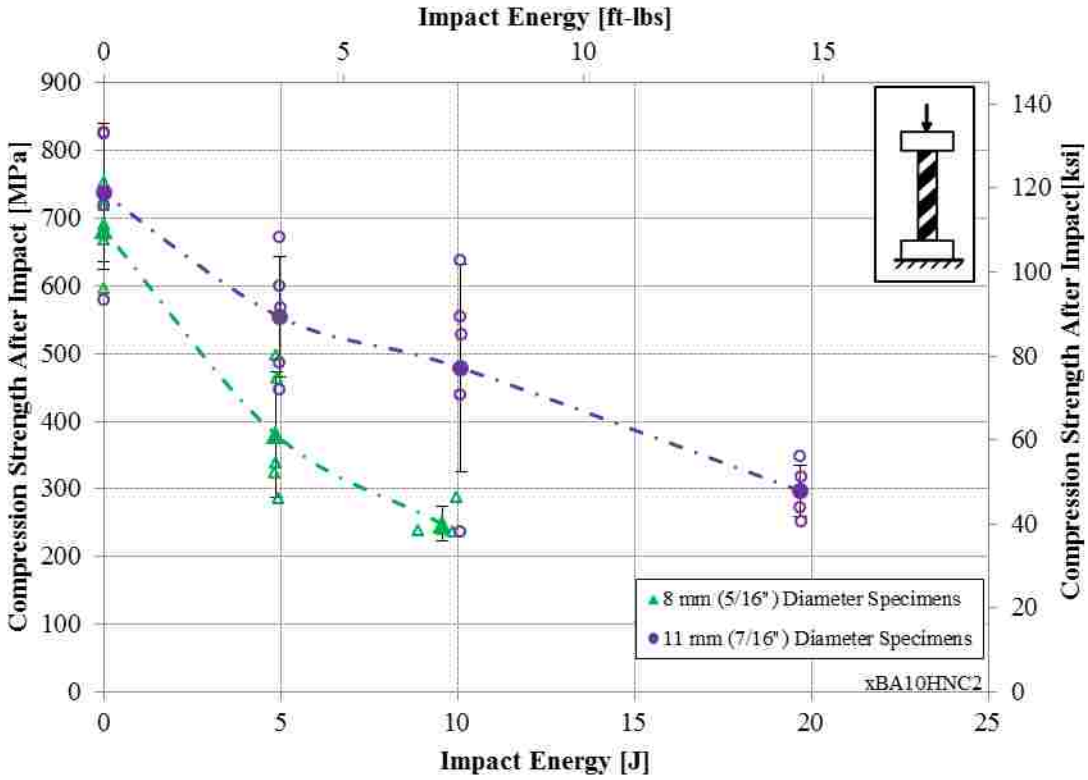

Figure 3.28: Impact Energy vs. Compression Strength for 8 mm (5/16”) and 11 mm (7/16”) Diameter Specimens

The specimens were aligned as shown in Figure 3.30. The specimen receptacles, Figure 3.31, allowed quick loading and alignment of specimens. The receptacles were hydraulically clamped in the testing machines by their stems. Tungsten carbide pucks were inserted between the specimens and the receptacles to maintain flat smooth test surfaces after repeated use of the receptacles.

Figure 3.29: Compression Machines: A) 90 kN (20 kip) Instron (left); and, B) 489 kN (110 kip) MTS

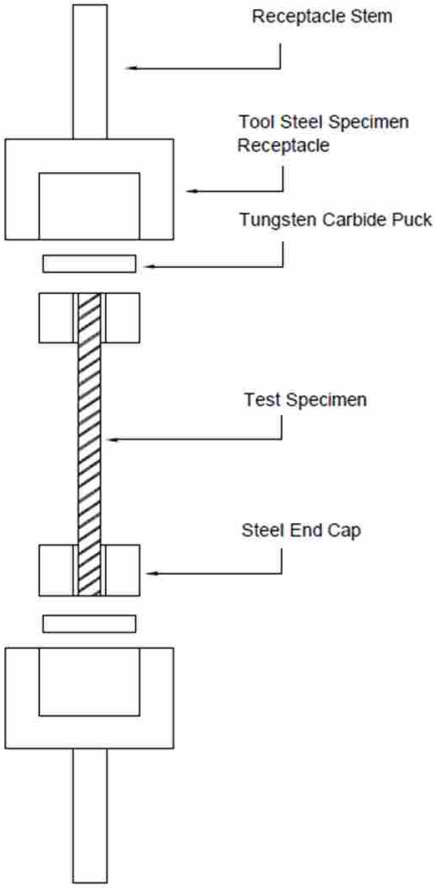

Figure 3.30: Configuration of Specimen for Compression Testing

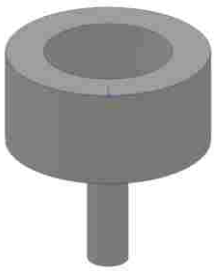

Figure 3.31: 3-D Rendering of Test Specimen Receptacle

Testing was stroke-controlled with a displacement rate of 1.27 mm/minute (0.05"/minute). The data was recorded by the WaveMatrix acquisition system on the Instron. Initially the displacement rate, load and extensometer data were collected. Due to inconsistencies in the extensometer strain data, the extensometer was abandoned after the preliminary testing. The machine displacement was ultimately used to infer the strain in the specimens. An empirical adjustment factor for machine strain was derived to separate the strain components attributable to the machine and test fixtures from the strain in the specimens. A study of the extensometer malfunctions including a presentation of how the strain adjustment factors were calculated is in Appendix E. The results for the 76 mm (3") specimens are based on machine strain and the extensometer strain. The results for the 51 mm (2") specimens are based on machine strain only, since the extensometer was not used.

3.6 Data Reduction and Chauvenet's Criterion

Stress-strain plots were developed for each specimen configuration consisting of one curve for each individual specimen and an average curve representing all specimens with that configuration. The average curve was obtained by determining stress values at uniform strain increments, typically between 0.00002 and 0.0001. This allowed the stress in all of the

specimens to be averaged at each strain increment. The average curve continues until strain data for only two individual specimens remained; with a dashed line connecting the end of the average curve to the average ultimate stress and the corresponding average strain value. Note that these values do not typically fall on the average curve since the various peaks do not occur at the same point. The curves were adjusted to have the linear portion go through the origin, with an additional dashed line near the origin demonstrating that adjustment. Strength, strain at ultimate stress, and Young's modulus are summarized in tables.

Occasionally an individual test gave abnormal results. To eliminate the skew caused by these outliers a very conservative data elimination criterion, Chauvenet's criterion, was applied. This criterion utilizes the ratio of the difference between an individual value and the data set mean to the standard deviation of the full data set. This ratio is compared to a set criterion, based on the number of specimens in the set, as shown in Table 3.2. Specimens with a ratio greater than the value listed are excluded and a new average and standard deviation are calculated for the remaining specimens. Additional specimens were prepared and tested to replace the excluded values.

Table 3.2: Values for Chauvenet's Criterion

Number of SpecimensTested	Chauvenet's Limit
3	1.38
4	1.54
5	1.65
6	1.73
7	1.80
10	1.96

4 PRELIMINARY TEST RESULTS

Test results based on specimens with a length of 76 mm (3") are provided in this chapter. These specimens failed in a mixture of strength- and buckling-controlled failure rather than the desired strength-controlled failure(Appendix F)[32]. Subsequent testing on 51 mm (2") long specimens exhibited strength controlled failure; those results are in Chapter 5.

4.1 5/16" Diameter Configuration Test Results for 3" Specimens

The test results in this section are based on 8 mm (5/16") diameter specimens with an unsupported length of 76 mm (3"). The data is presented in two ways: 1) based on extensometer strain; and, 2) based on the machine-strain. This shows the disparity between the results of the two methods, caused by the inconsistencies of the extensometer (Appendix E). Each configuration is presented (Full Braid, Half Braid, Full Spiral, Half Spiral) for No-impact, 5 J (3.7 ft-lbs.), and 10 J (7.4 ft-lbs.) of impact energy.

4.1.1 Full Braid No-impact (5BA43FNC3)

The full braid coverage no-impact specimen test results, based on extensometer strain, are presented here in the stress-strain plot in Figure 4.1 and summarized in Table 4.1. The average compression strength is 722.3 MPa (104.8 ksi), the corresponding strain is 13.83 mm/mm (in./in.), and the average Young's modulus is 69.5 GPa (10.08×10^6 psi).

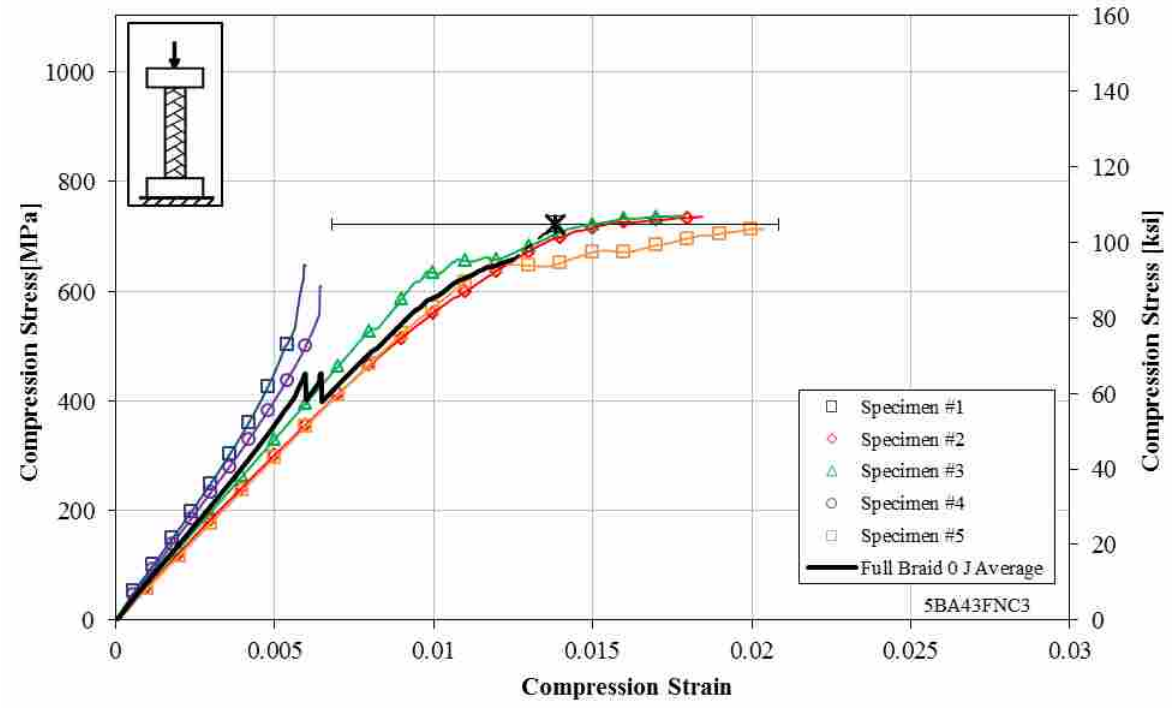

Figure 4.1: Stress-Strain Plot Based on Extensometer Strain for Full Braid, No-Impact Specimens, 8 mm (5/16") Diameter, 76 mm (3") Length, (5BA43FNC3)

Table 4.1: Summary Table Based on Extensometer Strain for Full Braid, No-Impact Specimens, 8 mm (5/16") Diameter, 76 mm (3") Length, (5BA43FNC3)

Specimen Number (5BA43FNC3)	Cross Sectional Area [mm^2 (in^2)]	Ultimate Compression Strength [MPa (ksi)]	Strain at Max Stress [10^3 με]	Compression Young's Modulus [GPa (10^6 psi)]
1	48.9 (0.076)	706.1 (102.4)	6.0	84.1 (12.2)
2	48.8 (0.076)	735.9 (106.7)	18.5	59.4 (8.6)
3	49.3 (0.076)	737.7 (107.0)	17.9	65.8 (9.5)
4	49.9 (0.077)	717.7 (104.1)	6.5	78.6 (11.4)
5	49.7 (0.077)	714.0 (103.6)	20.4	59.5 (8.6)
Average	49.3 (0.076)	722.3 (104.8)	13.8	69.5 (10.1)
Standard Deviation	0.50 (0.001)	13.9 (2.0)	7.0	11.3 (1.6)
	1.0%	1.9%	50.8%	16.3%

The full braid coverage no-impact specimen test results based on machine strain are presented in the stress-strain plot in Figure 4.2 and summarized in Table 4.2. The average

compression strength is 722.3 MPa (104.8 ksi), the corresponding strain is 12.4 mm/mm (in./in.), and the average Young's modulus is 64.1 GPa (9.3x10^6 psi).

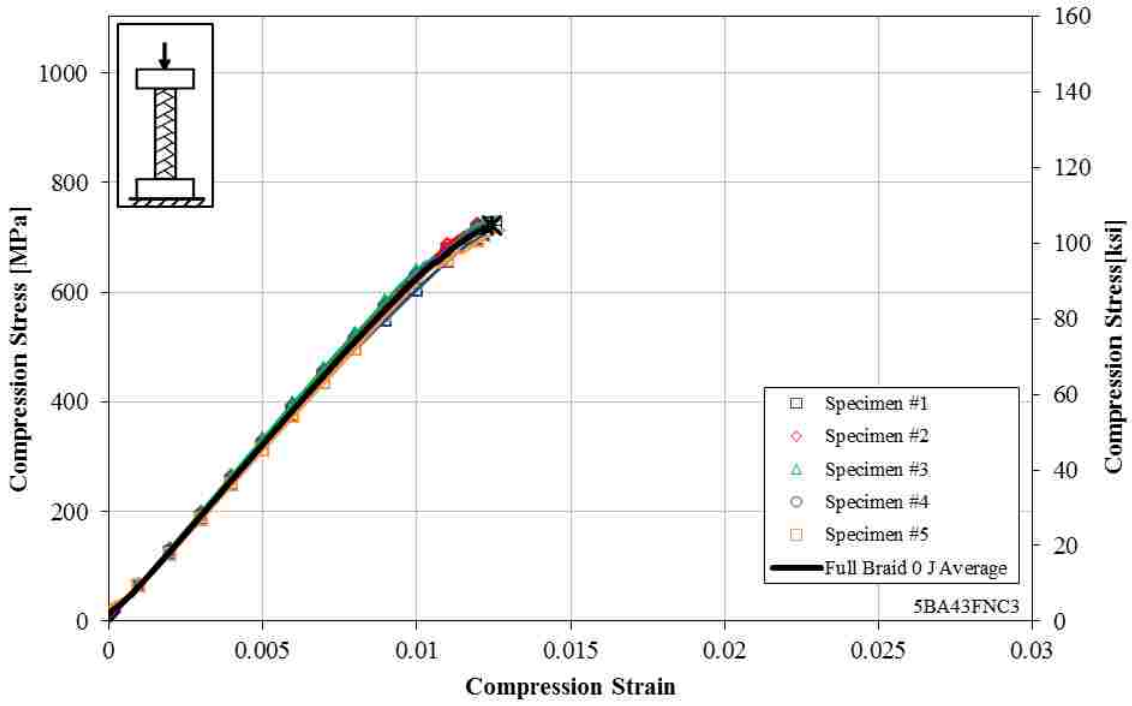

Figure 4.2: Stress-Strain Plot Based on Machine Strain for Full Braid, No-Impact Specimens, 8 mm (5/16") Diameter, 76 mm (3") Length, (5BA43FNC3)

Table 4.2: Summary Table Based On Machine Strain For Full Braid, No-Impact Specimen, 8 Mm (5/16") Diameter, 76 mm (3") Length, (5BA43FNC3)

Specimen Number (5BA43FNC3)	Cross Sectional Area [mm^2 (in^2)]	Ultimate Compression Strength [MPa (ksi)]	Strain at Max Stress [10^3 με]	Compression Young's Modulus [GPa (10^6 psi)]
1	48.9 (0.076)	706.1 (102.4)	12.2	62.0 (9.0)
2	48.8 (0.076)	735.9 (106.7)	12.6	65.6 (9.5)
3	49.3 (0.076)	737.7 (107.0)	12.7	66.6 (9.7)
4	49.9 (0.077)	717.7 (104.1)	12.0	64.8 (9.4)
5	49.7 (0.077)	714.0 (103.6)	12.7	61.3 (8.9)
Average	49.3 (0.076)	722.3 (104.8)	12.4	64.1 (9.3)
Standard	0.50 (0.001)	13.9 (2.0)	0.32	2.3 (0.3)
Deviation	1.0%	1.9%	2.6%	3.6%

4.1.2 Full Braid 5 J Impact (5BA43FLC3)

The full braid coverage 5 J (3.7 ft-lbs.) impact specimen test results based on extensometer strain are presented in the stress-strain plot in Figure 4.3 and summarized in Table 4.3. The average compression strength is 489.9 MPa (71.0 ksi), the corresponding strain is 8.73 mm/mm (in./in.), and the average Young's modulus is 55.06 GPa (8.07×10^6 psi). Specimen 5 was eliminated based on Chauvenet's envelope for compression Young's modulus, but was not eliminated when based on machine strain.

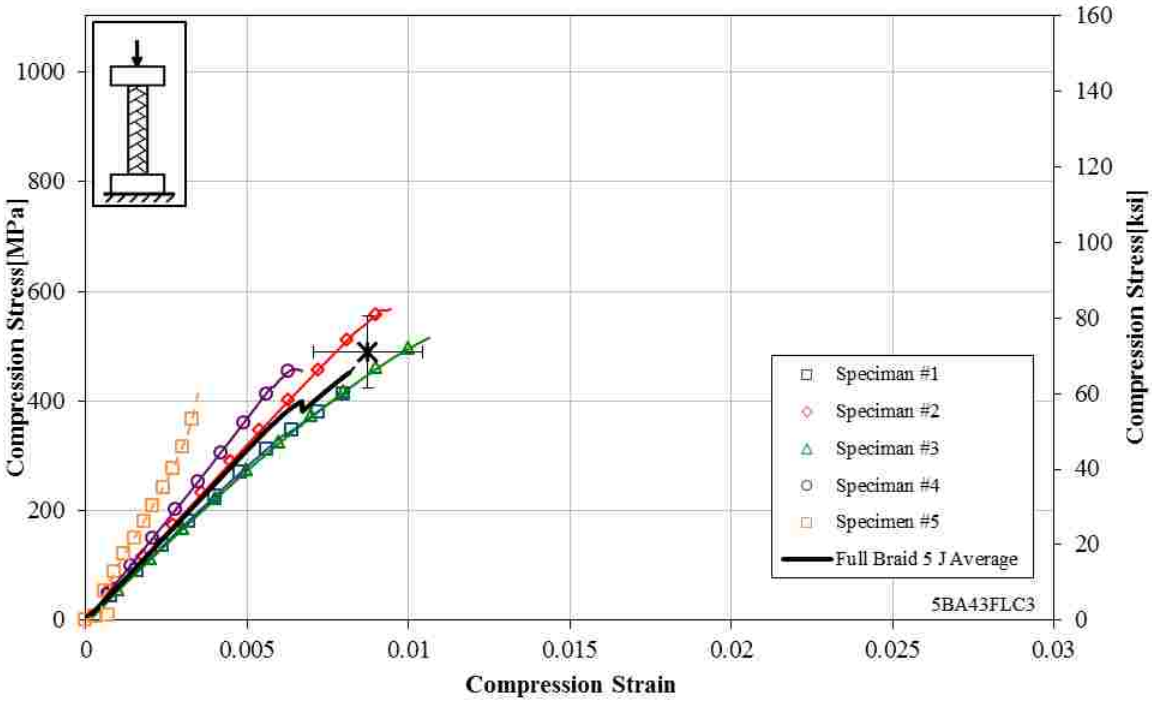

Figure 4.3: Stress-Strain Plot Based on Extensometer Strain for Full Braid, 5 J (3.7 ft-lbs.) Impact Specimens, 8 mm (5/16") Diameter, 76 mm (3") Length, (5BA43FLC3)

The full braid coverage 5 J (3.7 ft-lbs.) impact specimen test results, based on machine strain, are presented in the stress-strain plot shown in Figure 4.4 and summarized in Table 4.4. The average compression strength is 489.9 MPa (71.0 ksi), the corresponding strain is 8.2 mm/mm (in./in.), and the average Young's modulus is 59.8 GPa (8.68×10^6 psi).

Table 4.3: Summary Table Based on Extensometer Strain for Full Braid, 5 J (3.7 ft-lbs.) Impact Specimens, 8 mm (5/16") Diameter, 76 mm (3") Length, (5BA43FLC3)

Specimen Number (5BA43FLC3)	Cross Sectional Area [mm^2 (in^2)]	Ultimate Compression Strength [MPa (ksi)]	Strain at Max Stress [10^3 με]	Compression Young's Modulus [GPa (10^6 psi)]
1	49.2 (0.076)	417.6 (60.6)	8.2	55.6 (8.1)
2	49.5 (0.077)	568.0 (82.4)	9.4	64.3 (9.3)
3	49.5 (0.077)	515.2 (74.7)	10.6	54.1 (7.8)
4	49.5 (0.077)	458.6 (66.5)	6.7	73.3 (10.6)
5	48.7 (0.076)	445.7 (64.6)	3.5	105.1 (15.2)*
Average	49.2 (0.076)	489.9 (71.0)	8.7	61.8 (8.68)
Standard Deviation	0.35 (0.001)	65.7 (9.5)	1.7	8.9 (0.45)
	0.7%	8.3%	20%	14.4%

* *Specimen did not pass Chauvenet's Criterion, not included in averages.*

4.1.3 Full Braid 10 J Impact (5BA43FSC3)

The full braid coverage, 10 J (7.4 ft-lbs.) impact specimen test results, based on extensometer strain, are presented in the stress-strain plot shown in Figure 4.5 and summarized in Table 4.5. The average compression strength is 300.4 MPa (43.6 ksi), the corresponding strain is 11.77 mm/mm (in./in.), and the average Young's modulus is 50.0 GPa (7.26×10^6 psi). Specimen 2 was eliminated based on Chauvenet's envelope for compression Young's modulus, but it was not rejected when based on adjusted machine displacement.

The full braid coverage 10 J (7.4 ft-lbs.) impact specimen test results, based on machine strain, are presented in the stress-strain plot shown in Figure 4.6 and summarized in Table 4.6. The average compression strength was 301.0 MPa (43.7 ksi), the corresponding strain is 5.99 mm/mm (in./in.), and the average Young's modulus is 53.7 GPa (7.79×10^6 psi).

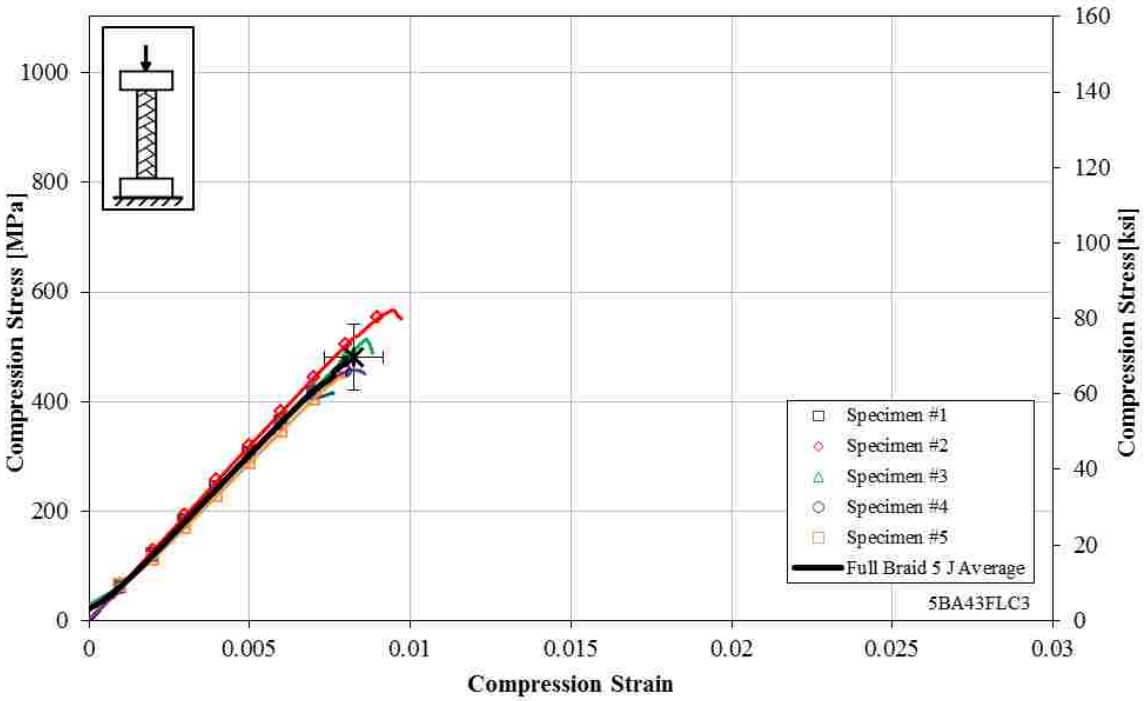

Figure 4.4: Stress-Strain Plot Based on Machine Strain for Full Braid, 5 J (3.7 ft-lbs.) Impact Specimens, 8 mm (5/16") Diameter, 76 mm (3") Length, (5BA43FLC3)

Table 4.4: Summary Table Based on Machine Strain for Full Braid, 5 J (3.7 ft-lbs.) Impact Specimens, 8 mm (5/16") Diameter, 76 mm (3") Length, (5BA43FLC3)

Specimen Number (5BA43FLC3)	Cross Sectional Area [mm^2 (in^2)]	Ultimate Compression Strength [MPa (ksi)]	Strain at Max Stress [10^3 με]	Compression Young's Modulus [GPa (10^6 psi)]
1	49.0 (0.076)	417.6 (60.6)	7.0	60.9 (8.8)
2	49.7 (0.077)	568.0 (82.4)	9.4	63.9 (9.3)
3	49.7 (0.077)	515.2 (74.7)	8.6	59.1 (8.6)
4	49.7 (0.077)	458.6 (66.5)	8.1	59.9 (8.7)
5	48.4 (0.075)	445.7 (64.6)	7.9	55.3 (8.0)
Average	49.0 (0.076)	481.0 (69.8)	8.2	59.8 (8.2)
Standard Deviation	0.6 (0.001)	60.2 (8.7)	0.8	3.1 (0.9)
	1.3%	12.5%	9.8%	5.2%

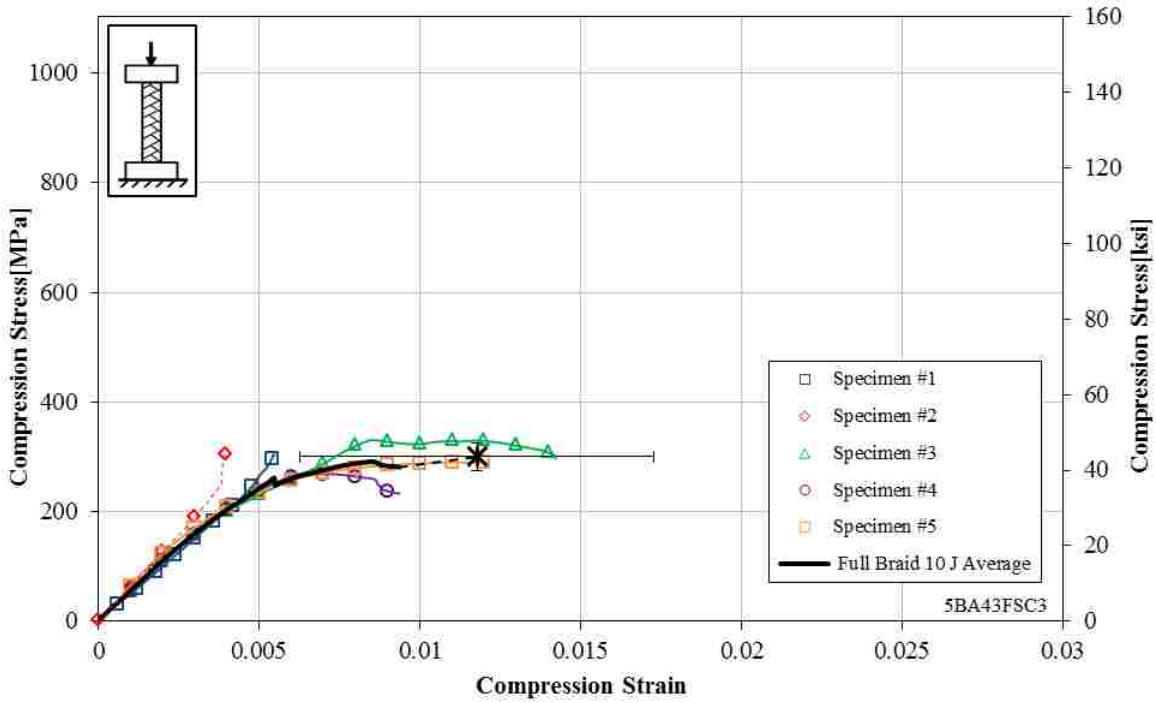

Figure 4.5: Stress-Strain Plot Based on Extensometer Strain for Full Braid, 10 J (7.4 ft-lbs.) Impact Specimens, 8 mm (5/16") Diameter, 76 mm (3") Length, (5BA43FSC3)

Table 4.5: Summary Table Based on Extensometer Strain for Full Braid, 10 J (7.4 ft-lbs.) Impact Specimens, 8 mm (5/16") Diameter, 76 mm (3") Length, (5BA43FSC3)

Specimen Number (5BA43FSC3)	Cross Sectional Area [mm^2 (in^2)]	Ultimate Compression Strength [MPa (ksi)]	Strain at Max Stress [10^3 με]	Compression Young's Modulus [GPa (10^6 psi)]
1	49.0 (0.076)	309.0 (44.8)	5.5	50.8 (7.4)
2	49.4 (0.077)	303.4 (44.0)	4.0	63.6 (9.2)*
3	49.2 (0.076)	331.3 (48.0)	14.2	49.0 (7.1)
4	49.4 (0.077)	270.7 (39.3)	9.4	50.1 (7.3)
5	49.1 (0.076)	290.5 (42.1)	18.0	50.2 (7.3)
Average	49.2 (0.076)	300.4 (43.6)	11.8	50.0 (7.3)
Standard Deviation	0.16 (0.000)	25.9 (3.8)	5.5	0.7 (0.1)
	0.3%	8.6%	46.8%	1.5%

* *Specimen did not pass Chauvenet's Criterion, not included in averages.*

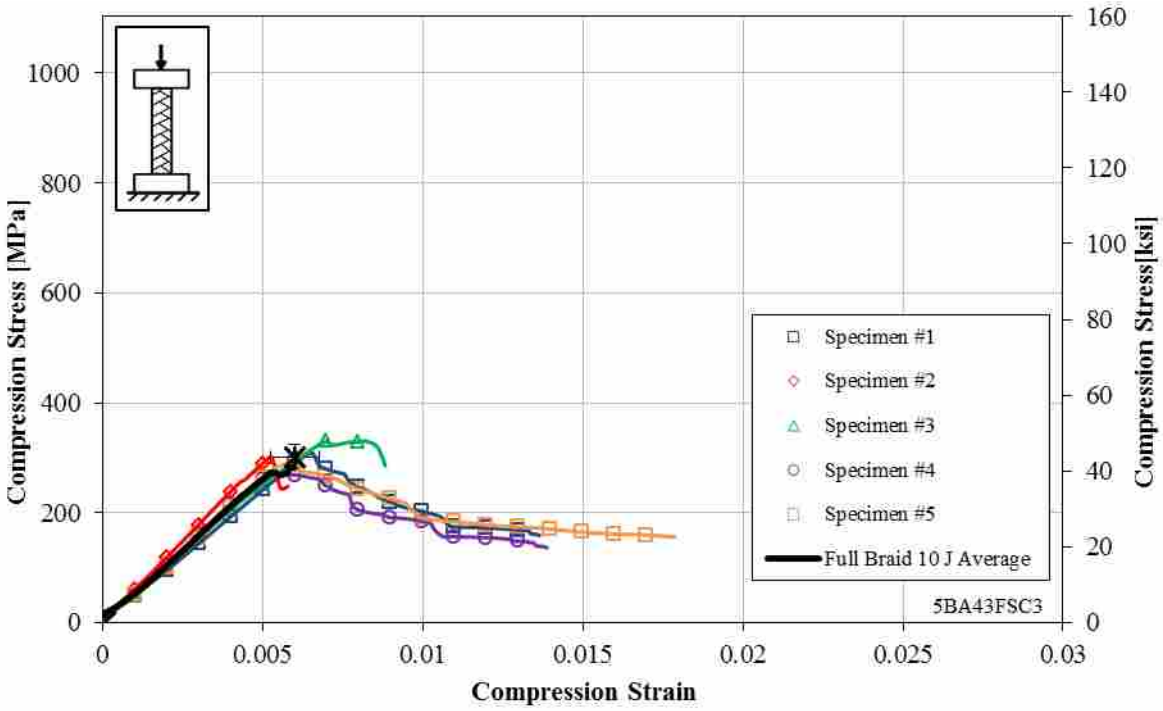

Figure 4.6: Stress-Strain Plot Based on Machine Strain for Full Braid, 10 J (7.4 ft-lbs.) Impact Specimens, 8 mm (5/16") Diameter, 76 mm (3") Length, (5BA43FSC3)

Table 4.6: Summary Table Based on Machine Strain for Full Braid, 10 J (7.4 ft-lbs.) Impact Specimens, 8 mm (5/16") Diameter, 76 mm (3") Length, (5BA43FSC3)

Specimen Number (5BA43FSC3)	Cross Sectional Area [mm^2 (in^2)]	Ultimate Compression Strength [MPa (ksi)]	Strain at Max Stress [10^3 με]	Compression Young's Modulus [GPa (10^6 psi)]
1	49.0 (0.076)	309.0 (44.8)	6.5	47.9 (7.0)
2	49.4 (0.077)	303.4 (44.0)	5.3	58.7 (8.5)
3	49.2 (0.076)	331.3 (48.0)	7.0	54.1 (7.8)
4	49.4 (0.077)	270.7 (39.3)	5.4	55.2 (8.0)
5	49.1 (0.076)	290.5 (42.1)	5.8	52.8 (7.7)
Average	49.2 (0.076)	301.0 (43.7)	6.0	53.7 (7.8)
Standard Deviation	0.16 (0.000)	22.5 (3.3)	0.8	3.9 (0.6)
	0.3%	7.5%	12.7%	7.3%

4.1.4 Half Braid No-impact (5BA43HNC3)

The half braid coverage, no-impact specimen test results, based on extensometer strain, are presented in the stress-strain plot shown in Figure 4.7 and summarized in Table 4.7. The

average compression strength is 744.1 MPa (107.9 ksi), the corresponding strain is 12.70 mm/mm (in./in.), and the average Young's modulus is 64.4 GPa (9.34×10^6 psi). This testing occurred while the manufacturing process was still under development. The proposed full and half coverage braid specimens ended up having approximately half sleeve coverage. Therefore, these two sets of results were combined, resulting in a total of 12 specimens. Specimens 7 through 12 use the nominal cross-sectional area because precise cross-sectional area measurement techniques had not yet been developed. Specimen 12 was eliminated based on Chauvenet's envelope for compression strength and Young's modulus.

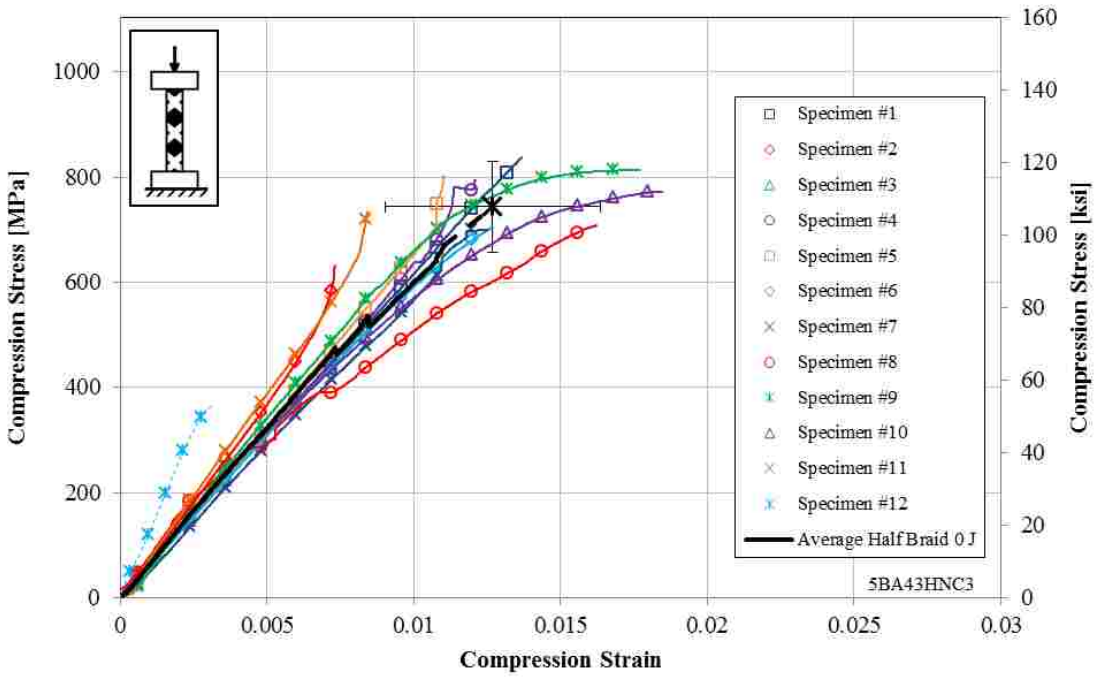

Figure 4.7: Stress-Strain Plot Based on Extensometer Strain for Half Braid, No-Impact Specimens, 8 mm (5/16") Diameter, 76 mm (3") Length, (5BA43HNC3)

Table 4.7: Summary Table Based on Extensometer Strain for Half Braid, No-Impact Specimens, 8 mm (5/16") Diameter, 76 mm (3") Length, (5BA43HNC3)

Specimen Number (5BA43HNC3)	Cross Sectional Area [mm^2 (in^2)]	Ultimate Compression Strength [MPa (ksi)]	Strain at Max Stress [10^3 με]	Compression Young's Modulus [GPa (10^6 psi)]
1	50.3 (0.078)	837.2 (121.4)	13.7	62.5 (9.1)
2	51.0 (0.079)	652.1 (94.6)	7.3	73.1 (10.6)
3	49.9 (0.077)	562.2 (81.5)	9.3	61.7 (9.0)
4	51.2 (0.079)	821.7 (119.2)	12.1	62.4 (9.1)
5	50.2 (0.078)	842.1 (122.1)	11.1	62.6 (9.1)
6	50.9 (0.079)	705.8 (102.4)	12.7	61.8 (9.0)
7	50.1 (0.078)	700.4 (101.6)	12.5	59.9 (8.7)
8	50.1 (0.078)	707.5 (102.6)	16.2	52.5 (7.6)
9	50.1 (0.078)	813.3 (118.0)	17.7	71.7 (10.4)
10	50.1 (0.078)	772.3 (112.0)	18.5	61.2 (8.9)
11	50.1 (0.078)	761.6 (110.5)	8.5	78.7 (11.4)
12	50.1 (0.078)	365.9 (53.1)*	3.1	127.1 (18.4)*
Average	50.6 (0.078)	744.1 (107.9)	12.7	64.4 (9.3)
Standard Deviation	0.57 (0.001)	87.5 (12.7)	3.7	7.3 (1.1)
	1.1%	11.8%	29.1%	11.8%

* *Specimen did not pass Chauvenet's Criterion, not included in averages.*

The half braid coverage no-impact specimen test results, based on machine strain, are presented in the stress-strain plot shown in Figure 4.8 and summarized in Table 4.8. The average compression strength was 744.1 MPa (107.9 ksi), the corresponding strain is 11.66 mm/mm (in./in.), and the average Young's modulus is 68.1 GPa (9.9x106 psi). Specimen 12 was eliminated based on Chauvenet's envelope for compression strength and strain at maximum stress.

4.1.5 Half Braid 5 J Impact (5BA43HLC3)

The half braid coverage, 5 J (3.7 ft-lbs.) impact specimen test results, based on extensometer strain, are presented in the stress-strain plot shown in Figure 4.9 and summarized in Table 4.9. The average compression strength is 546.5 Mpa (79.3 ksi), the corresponding strain

is 11.24 mm/mm (in./in.), and the average Young's modulus is 61.4 GPa ($8.9x10^6$ psi). This testing was done while the process of manufacturing specimens was still being mastared. The proposed full and half coverage braid specimens ended up having approximately half sleeve coverage. Therefore, these two sets of results were combined, resulting in a total of 12 specimens. Specimens 7 through 12 use the nominal cross-sectional area because precise cross-sectional area measurement techniques had not yet been developed. Specimen 2 was eliminated based on Chauvenet's envelope for compression strength and Specimen 7 was eliminated based on compression Young's modulus.

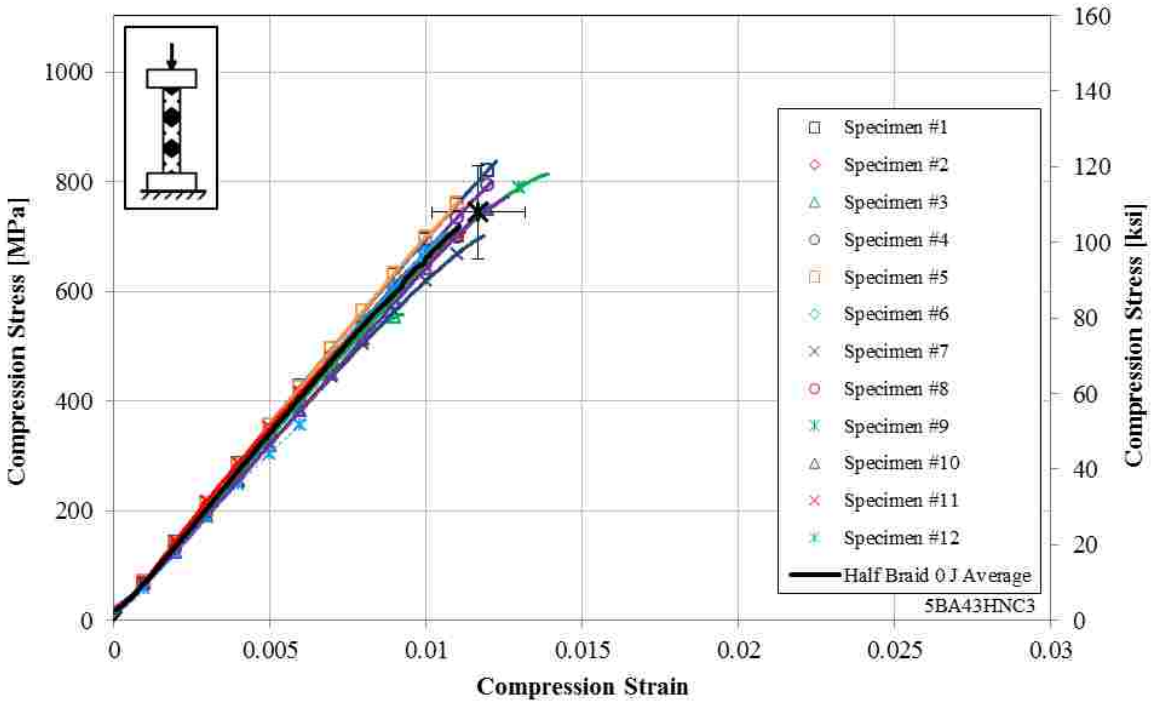

Figure 4.8: Stress-Strain Plot Based on Machine Strain for Half Braid, No-Impact Specimens, 8 mm (5/16") Diameter, 76 mm (3") Length, (5BA43HNC3)

Table 4.8: Summary Table Based on Machine Strain for Half Braid, No-Impact Specimens, 8 mm (5/16") Diameter, 76 mm (3") Length, (5BA43HNC3)

Specimen Number (5BA43HNC3)	Cross Sectional Area [mm^2 (in^2)]	Ultimate Compression Strength [MPa (ksi)]	Strain at Max Stress [10^3 με]	Compression Young's Modulus [GPa (10^6 psi)]
1	50.3 (0.078)	837.2 (121.4)	12.2	71.3 (10.3)
2	51.0 (0.079)	652.1 (94.6)	9.8	68.9 (10.0)
3	49.9 (0.077)	570.8 (82.8)	8.6	69.5 (10.1)
4	51.2 (0.079)	821.7 (119.2)	12.6	69.1 (10.0)
5	50.2 (0.078)	842.1 (122.1)	12.3	70.7 (10.3)
6	50.9 (0.079)	705.8 (102.4)	10.8	68.3 (9.9)
7	50.1 (0.078)	700.4 (101.6)	11.8	63.5 (9.2)
8	50.1 (0.078)	707.5 (102.6)	11.2	65.0 (9.4)
9	50.1 (0.078)	813.3 (118.0)	13.9	66.2 (9.6)
10	50.1 (0.078)	772.3 (112.0)	12.6	62.5 (9.1)
11	50.1 (0.078)	761.6 (110.5)	12.5	74.4 (10.8)
12	50.1 (0.078)	365.9 (53.1)*	6.2*	64.2 (9.3)
Average	50.6 (0.078)	744.1 (107.9)	11.7	68.1 (9.9)
Standard Deviation	0.57 (0.001)	85.7 (12.4)	1.5	3.6 (0.5)
	1.1%	11.5%	12.8%	5.1%

* *Specimen did not pass Chauvenet's Criterion, not included in averages.*

The half braid coverage 5 J (3.7 ft-lbs.) impact specimen test results, based on machine strain, are presented in the stress-strain plot shown in Figure 4.10 and summarized in Table 4.10. The average compression strength was 532.5 MPa (77.3 ksi), the corresponding strain is 8.76 mm/mm (in./in.), and the average Young's modulus is 67.2 GPa (9.8x106 psi). Specimen 2 was eliminated based on Chauvenet's envelope for compression strength and Specimen 11 based on strain at maximum stress and Young's modulus.

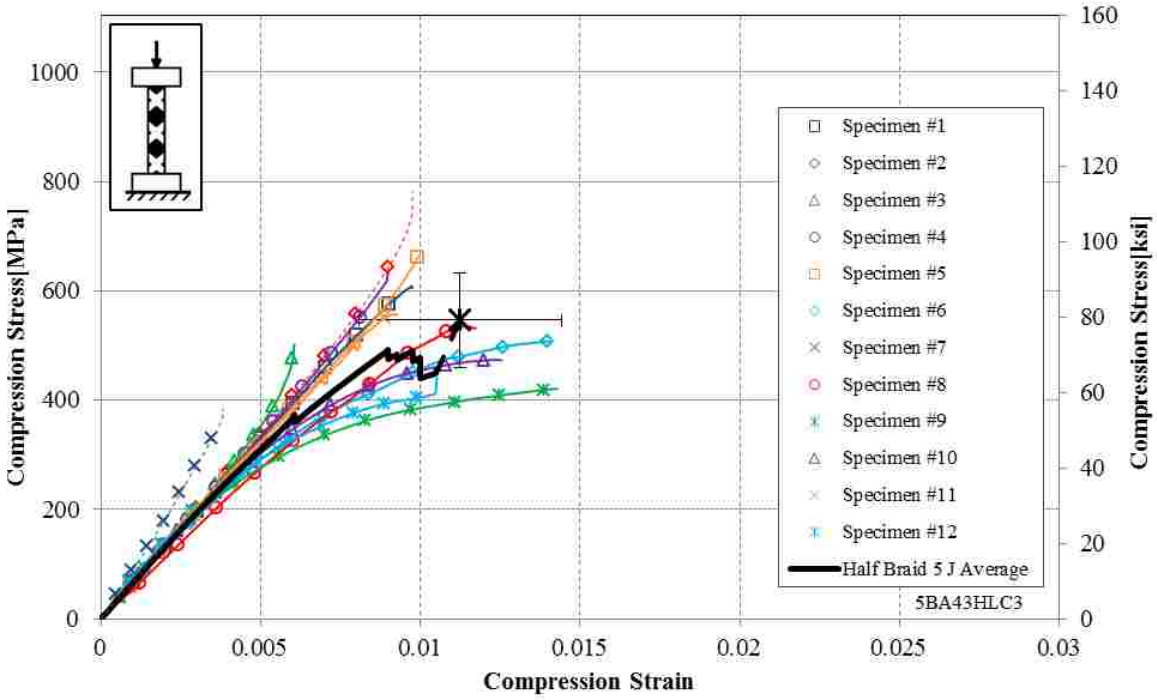

Figure 4.9: Stress-Strain Plot Based on Extensometer Strain for Half Braid, 5 J (3.7 ft-lbs.) Impact Specimen, 8 mm (5/16") Diameter, 76 mm (3") Length, (5BA43HLC3)

Table 4.9: Summary Table Based on Extensometer Strain for Full Braid, 5 J (3.7 ft-lbs.) Impact Specimens, 8 mm (5/16") Diameter, 76 mm (3") Length, (5BA43HLC3)

Specimen Number (5BA43HLC3)	Cross Sectional Area [mm^2 (in^2)]	Ultimate Compression Strength [MPa (ksi)]	Strain at Max Stress [10^3 με]	Compression Young's Modulus [GPa (10^6 psi)]
1	49.7 (0.077)	632.4 (91.7)	9.8	64.7 (9.4)
2	49.9 (0.077)	817.8 (118.6)*	9.8	67.1 (9.7)
3	49.7 (0.077)	558.8 (81.0)	6.1	68.5 (9.9)
4	50.0 (0.077)	662.7 (96.1)	9.0	66.6 (9.7)
5	50.8 (0.079)	665.5 (96.5)	10.0	65.2 (9.5)
6	49.9 (0.077)	508.4 (73.7)	14.1	57.9 (8.4)
7	50.1 (0.078)	422.5 (61.3)	3.9	95.3 (13.8)*
8	50.1 (0.078)	535.3 (77.6)	16.9	55.7 (8.1)
9	50.1 (0.078)	421.3 (61.1)	14.3	53.2 (7.7)
10	50.1 (0.078)	474.3 (68.8)	12.6	61.5 (8.9)
11	50.1 (0.078)	559.2 (81.1)	9.3	64.3 (9.3)
12	50.1 (0.078)	446.8 (64.8)	10.6	56.1 (8.1)
Average	50.1 (0.078)	546.5 (79.3)	11.2	61.4 (8.9)
Standard Deviation	0.44 (0.001)	86.7 (12.6)	3.2	5.3 (0.8)
	0.9%	15.9%	28.6%	9.0%

* *Specimen did not pass Chauvenet's Criterion, not included in averages.*

4.1.6 Half Braid 10 J Impact (5BA43HSC3)

The half braid coverage, 10 J (7.4 ft-lbs.) impact specimen test results, based on extensometer strain, are presented in a stress-strain plot shown in Figure 4.11 and summarized in Table 4.11. The average compression strength is 232.5 MPa (33.7 ksi), the corresponding strain is 10.5 mm/mm (in./in.), and the average Young's modulus is 53.3 GPa ($7.7x10^6$ psi). This testing occurred while the manufacturing process was still under development. The proposed full and half coverage braid specimens ended up having approximately half sleeve coverage. Therefore, these two sets of results were combined, resulting in a total of 12 specimens. Specimens 7 through 12 use the nominal cross-sectional area because precise cross-sectional area measurement techniques had not yet been developed. Specimen 2 was eliminated based on Chauvenet's envelope for strain at maximum stress, and Specimen 8 was not included for ultimate compression strength.

The half braid coverage 10 J (7.4 ft-lbs.) impact specimen test results, based on machine strain, are presented in the stress-strain plot shown in Figure 4.12 and summarized in Table 4.12. The average compression strength was 238.0 MPa (34.5 ksi), the corresponding strain is 5.81 mm/mm (in./in.), and the average Young's modulus is 54.4 GPa ($7.9x10^6$ psi). Specimen 3 was eliminated based on Chauvenet's envelope for compression Young's modulus, and Specimen 8 was rejected based on compression strength.

4.1.7 Full Spiral No-impact (5BA10FNC3)

The full spiral coverage, no-impact specimen test results, based on extensometer strain, are presented here in the stress-strain plot shown in Figure 4.13 and summarized in Table 4.13. The average compression strength is 731.6 MPa (106.1 ksi), the corresponding strain is 13.72

mm/mm (in./in.), and the average Young's modulus is 61.3 GPa ($8.9x10^6$ psi). Specimen 3 was eliminated based on Chauvenet's envelope for compression strength, and Specimen 6 was not included for Young's modulus.

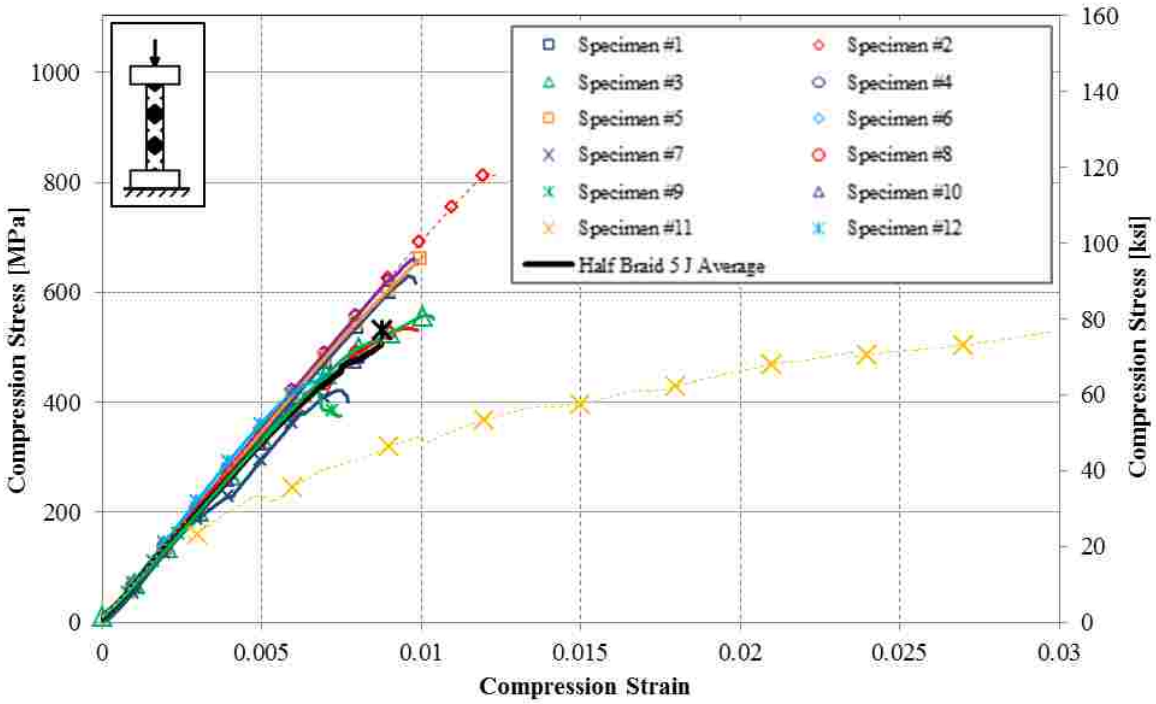

Figure 4.10: Stress-Strain Plot Based on Machine Strain for Half Braid, 5 J (3.7 ft-lbs.) Impact Specimens, 8 mm (5/16") Diameter, 76 mm (3") Length, (5BA43HLC3)

The full spiral coverage no-impact specimen test results, based on machine strain, are presented in the stress-strain plot shown in Figure 4.14 and summarized in Table 4.14. The average compression strength was 708.2 MPa (102.7 ksi), the corresponding strain is 12.65 mm/mm (in./in.), and the average Young's modulus is 63.3 GPa (9.2x106 psi). Specimen 3 was eliminated based on Chauvenet's envelope for strength and the corresponding strain.

Table 4.10: Summary Table Based on Machine Strain for Full Braid, 5 J (3.7 ft-lbs.) Impact Specimens, 8 mm (5/16") Diameter, 76 mm (3") Length, (5BA43HLC3)

Specimen Number (5BA43HLC3)	Cross Sectional Area [mm^2 (in^2)]	Ultimate Compression Strength [MPa (ksi)]	Strain at Max Stress [10^3 με]	Compression Young's Modulus [GPa (10^6 psi)]
1	49.7 (0.077)	632.4 (91.7)	9.6	67.8 (9.8)
2	49.9 (0.077)	817.8 (118.6)*	12.1	69.8 (10.1)
3	49.7 (0.077)	558.8 (81.0)	10.1	66.3 (9.6)
4	50.0 (0.077)	662.7 (96.1)	9.8	70.4 (10.2)
5	50.8 (0.079)	665.5 (96.5)	10.0	69.3 (10.1)
6	49.9 (0.077)	508.4 (73.7)	8.4	66.2 (9.6)
7	50.1 (0.078)	422.5 (61.3)	7.5	62.9 (9.1)
8	50.1 (0.078)	535.3 (77.6)	9.5	71.1 (10.3)
9	50.1 (0.078)	421.3 (61.1)	7.5	63.1 (9.2)
10	50.1 (0.078)	474.3 (68.8)	8.1	60.8 (8.8)
11	50.1 (0.078)	559.2 (81.1)	33.6*	38.2 (5.5)*
12	50.1 (0.078)	446.8 (64.8)	7.1	74.4 (10.8)
Average	50.1 (0.078)	532.8 (77.3)	8.8	67.2 (9.8)
Standard Deviation	0.44 (0.001)	94.9 (13.8)	1.2	4.2 (0.6)
	0.9%	17.8%	13.5%	6.3%

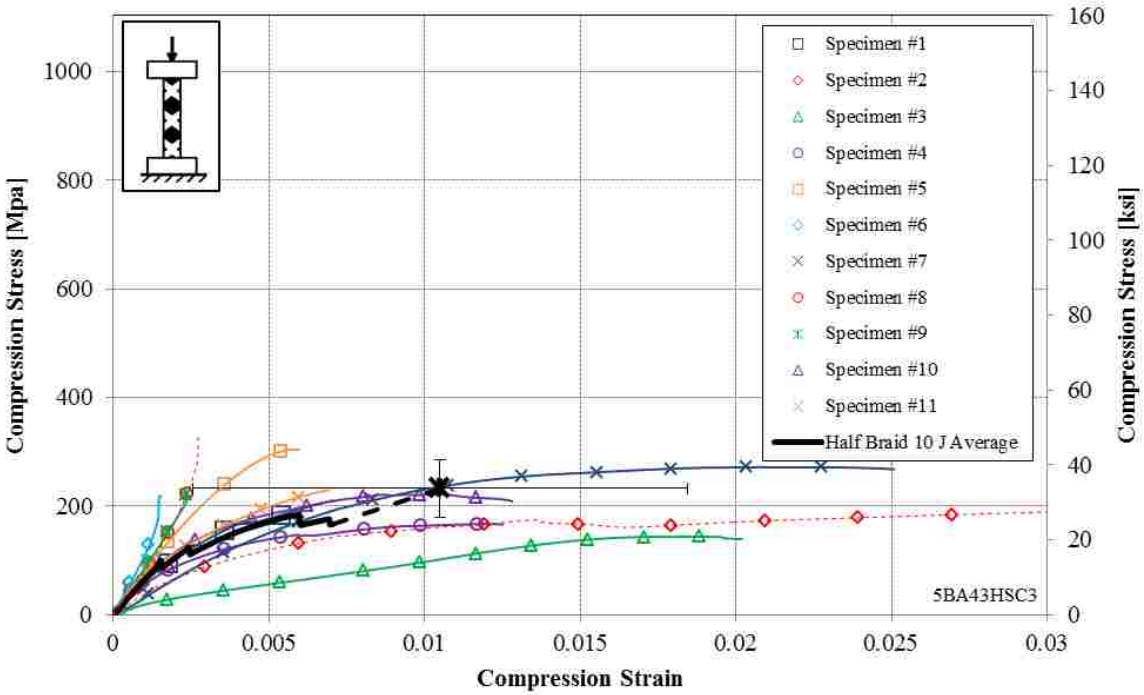

Figure 4.11: Stress-Strain Plot Based on Extensometer Strain for Half Braid, 10 J (7.4 ft-lbs.) Impact Specimens, 8 mm (5/16") Diameter, 76 mm (3") Length, (5BA43HSC3)

Table 4.11: Summary Table Based on Extensometer Strain for Half Braid, 10 J (7.4 ft-lbs.) Impact Specimen, 8 mm (5/16") Diameter, 76 mm (3") Length, (5BA43HSC3)

Specimen Number (5BA43HSC3)	Cross Sectional Area [mm^2 (in^2)]	Ultimate Compression Strength [MPa (ksi)]	Strain at Max Stress [10^3 με]	Compression Young's Modulus [GPa (10^6 psi)]
1	53.2 (0.082)	210.6 (30.5)	7.0	43.0 (6.2)
2	54.2 (0.084)	193.2 (28.0)	40.3*	19.4 (2.8)
3	53.4 (0.083)	143.9 (20.9)	20.2	8.4 (1.2)
4	53.2 (0.083)	167.4 (24.3)	12.5	26.3 (3.8)
5	52.7 (0.082)	304.2 (44.1)	6.0	74.6 (10.8)
6	50.1 (0.078)	262.7 (38.1)	1.5	111.2 (16.1)
7	49.0 (0.076)	271.9 (39.4)	25.1	31.6 (4.6)
8	49.4 (0.077)	383.8 (55.7)*	2.8	86.9 (12.6)
9	49.2 (0.076)	279.7 (40.6)	2.4	87.2 (12.7)
10	49.4 (0.077)	222.2 (32.2)	12.8	52.2 (7.6)
11	48.7 (0.075)	229.9 (33.3)	6.9	45.0 (6.5)
Average	51.2 (0.079)	232.5 (33.7)	10.5	53.3 (7.7)
Standard Deviation	2.27 (0.004)	53.1 (7.7)	8.0	32.3 (4.7)
	4.4%	22.8%	75.8%	60.6%

* *Specimen did not pass Chauvenet's Criterion, not included in averages.*

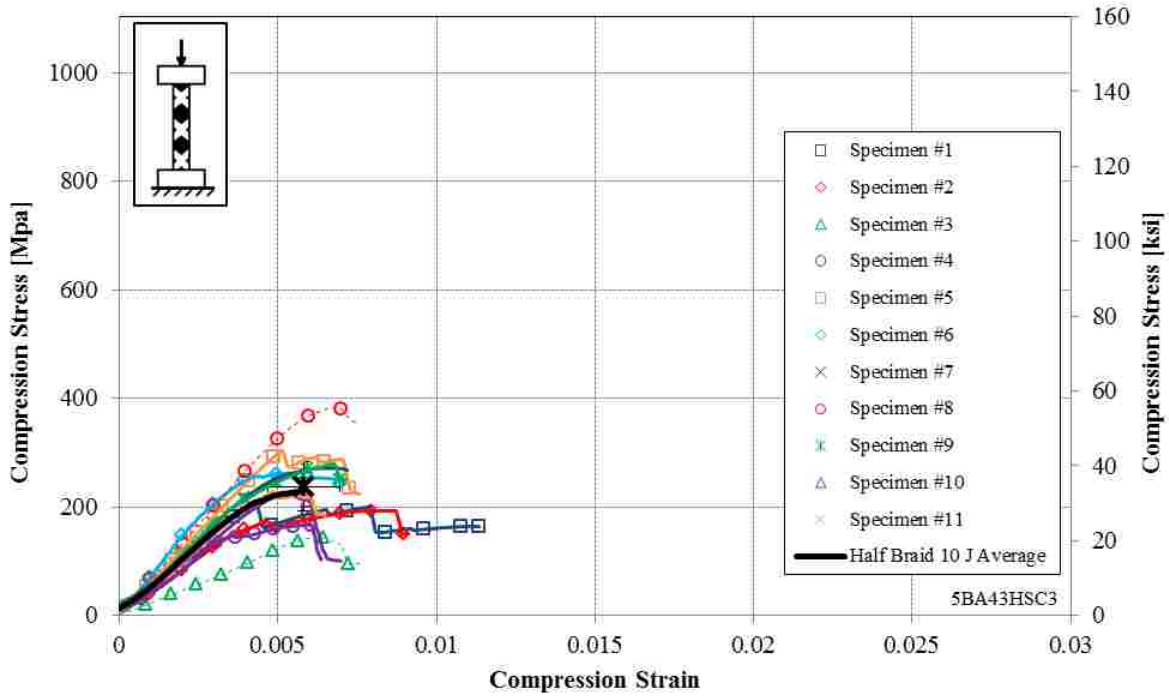

Figure 4.12: Stress-Strain Plot Based on Machine Strain for Half Braid, 10 J (7.4 ft-lbs.) Impact Specimens, 8 mm (5/16") Diameter, 76 mm (3") Length, (5BA43HSC3)

Table 4.12: Summary Table Based on Machine Strain for Half Braid, 10 J (7.4 ft-lbs.) Impact Specimens, 8 mm (5/16") Diameter, 76 mm (3") Length, (5BA43HSC3)

Specimen Number (5BA43HSC3)	Cross Sectional Area [mm^2 (in^2)]	Ultimate Compression Strength [MPa (ksi)]	Strain at Max Stress [10^3 με]	Compression Young's Modulus [GPa (10^6 psi)]
1	53.2 (0.082)	210.6 (30.5)	4.3	47.5 (6.9)
2	54.2 (0.084)	193.2 (28.0)	8.0	43.5 (6.3)
3	53.4 (0.083)	143.9 (20.9)	6.4	24.8 (3.6)*
4	53.2 (0.083)	167.4 (24.3)	6.0	48.6 (7.1)
5	52.7 (0.082)	304.2 (44.1)	5.1	58.8 (8.5)
6	50.1 (0.078)	262.7 (38.1)	5.4	74.0 (10.7)
7	49.0 (0.076)	271.9 (39.4)	6.4	57.0 (8.3)
8	49.4 (0.077)	383.8 (55.7)*	6.9	67.1 (9.7)
9	49.2 (0.076)	279.7 (40.6)	6.8	58.4 (8.5)
10	49.4 (0.077)	222.2 (32.2)	5.5	50.8 (7.4)
11	48.7 (0.075)	229.9 (33.3)	4.9	50.9 (7.4)
Average	51.2 (0.079)	238.0 (34.5)	5.8	54.4 (7.9)
Standard Deviation	2.27 (0.004)	44.6 (6.5)	1.1	9.0 (1.3)
	4.4%	18.8%	19.3%	16.6%

* *Specimen did not pass Chauvenet's Criterion, not included in averages.*

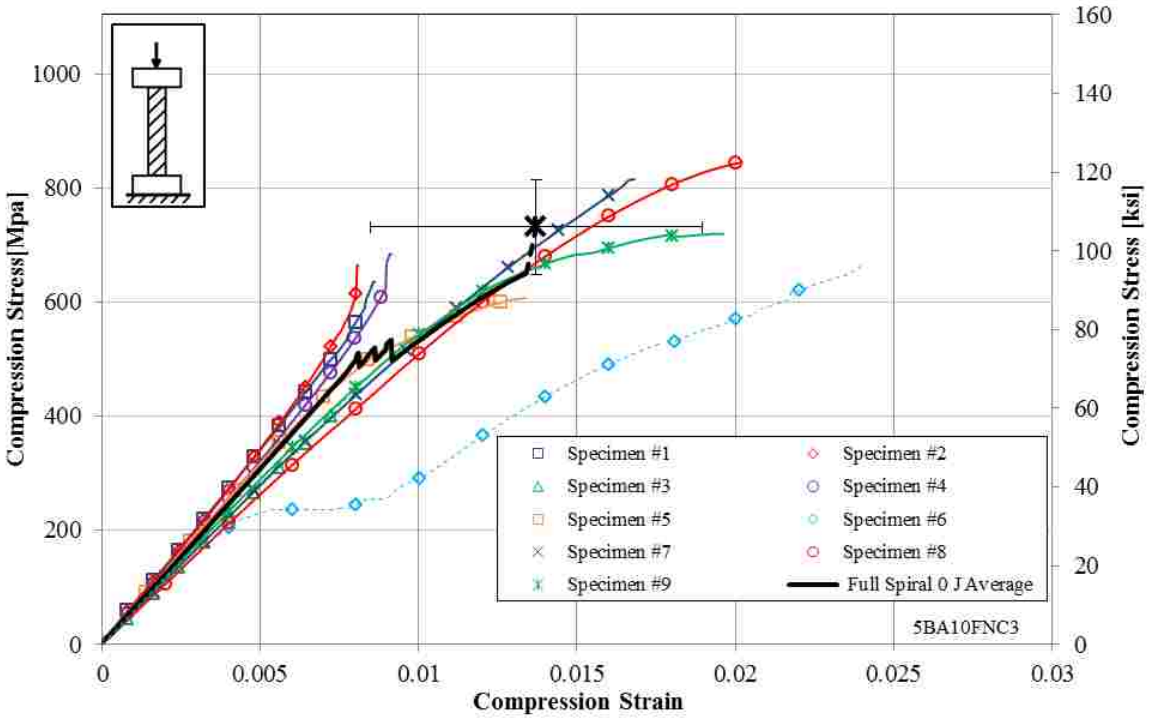

Figure 4.13: Stress-Strain Plot Based on Extensometer Strain for Full Spiral, No-Impact Specimens, 8 mm (5/16") Diameter, 76 mm (3") Length, (5BA10FNC3)

Table 4.13: Summary Table Based on Extensometer Strain for Full Spiral, No-Impact Specimen, 8 mm (5/16") Diameter, 76 mm (3") Length, (5BA10FNC3)

Specimen Number (5BA43FNC3)	Cross Sectional Area [mm^2 (in^2)]	Ultimate Compression Strength [MPa (ksi)]	Strain at Max Stress [10^3 με]	Compression Young's Modulus [GPa (10^6 psi)]
1	52.2 (0.081)	660.5 (95.8)	8.6	67.7 (9.8)
2	52.6 (0.082)	713.9 (103.5)	8.1	68.4 (9.9)
3	52.4 (0.081)	451.4 (65.5)*	8.0	54.9 (8.0)
4	52.6 (0.082)	760.6 (110.3)	9.1	64.6 (9.4)
5	50.6 (0.078)	606.8 (88.0)	13.5	63.3 (9.2)
6	51.0 (0.079)	681.2 (98.8)	24.0	34.1 (5.0)*
7	50.6 (0.078)	814.8 (118.2)	16.8	55.6 (8.1)
8	50.2 (0.078)	845.0 (122.6)	20.2	52.1 (7.6)
9	50.4 (0.078)	719.6 (104.4)	19.6	57.5 (8.3)
Average	50.6 (0.078)	731.6 (106.1)	13.7	61.3 (8.9)
Standard Deviation	0.31 (0.000)	83.4 (12.1)	5.3	6.3 (0.9)
	0.6%	11.4%	38.3%	10.3%

* *Specimen did not pass Chauvenet's Criterion, not included in averages.*

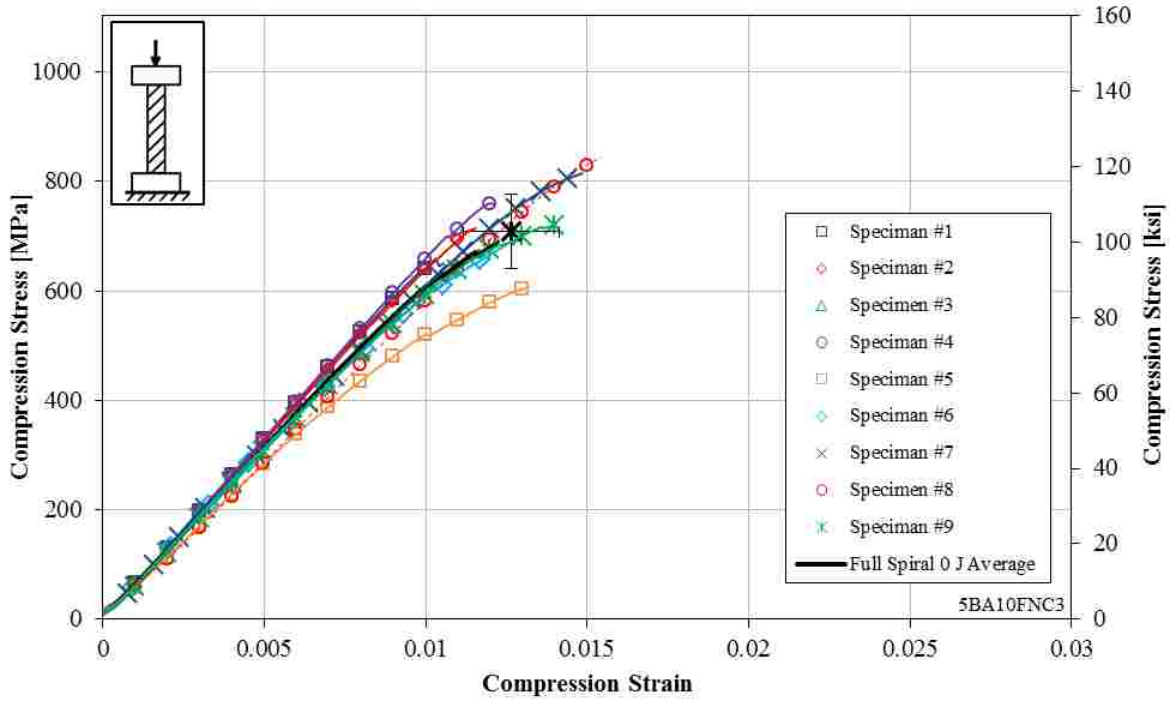

Figure 4.14: Stress-Strain Plot Based on Machine Strain for Full Spiral No-Impact Specimens, 8 mm (5/16") Diameter, 76 mm (3") Length, (5BA10FNC3)

Table 4.14: Summary Table Based on Machine Strain for Full Spiral No-Impact Specimens, 8 mm (5/16") Diameter, 76 mm (3") Length, (5BA10FNC3)

Specimen Number (5BA10FNC3)	Cross Sectional Area [mm^2 (in^2)]	Ultimate Compression Strength [MPa (ksi)]	Strain at Max Stress [10^3 με]	Compression Young's Modulus [GPa (10^6 psi)]
1	52.2 (0.081)	660.5 (95.8)	10.54	66.4 (9.63)
2	52.6 (0.082)	713.9 (103.5)	11.51	64.4 (9.33)
3	52.4 (0.081)	451.4 (65.5)*	7.3*	64.2 (9.3)
4	52.6 (0.082)	760.6 (110.3)	12.0	65.0 (9.4)
5	50.6 (0.078)	606.8 (88.0)	13.2	57.2 (8.3)
6	51.0 (0.079)	681.2 (98.8)	12.4	63.6 (9.2)
7	50.6 (0.078)	814.8 (118.2)	14.9	64.0 (9.3)
8	50.2 (0.078)	845.0 (122.6)	15.5	54.3 (7.9)*
9	50.4 (0.078)	719.6 (104.4)	14.0	62.6 (9.1)
Average	50.6 (0.078)	708.2 (102.7)	12.7	63.3 (9.2)
Standard Deviation	0.31 (0.000)	67.8 (9.8)	1.5	2.9 (0.4)
	0.6%	9.6%	11.7%	4.6%

* *Specimen did not pass Chauvenet's Criterion, not included in averages.*

4.1.8 Full Spiral 5 J Impact (5BA10FLC3)

The full spiral coverage, 5 J (3.7 ft-lbs.) impact specimen test results, based on extensometer strain, are presented in the stress-strain plot shown in Figure 4.15 and summarized in Table 4.15. The average strength is 529.8 MPa (76.8 ksi), the corresponding strain is 8.67 mm/mm (in./in.), and the average Young's modulus is 64.8 GPa ($9.4x10^6$ psi). Specimen 3 was eliminated based on Chauvenet's envelope for strength and the corresponding strain. The results based on machine strain are in Table 4.16.

4.1.9 Full Spiral 10 J Impact (5BA10FSC3)

The full spiral coverage, 10 J (7.4 ft-lbs.) impact specimen test results, based on extensometer strain, are presented in the stress-strain plot shown in Figure 4.17 and summarized in Table 4.17. The average compression strength is 334.4 MPa (48.5 ksi), the corresponding strain is 12.07 mm/mm (in./in.), and the average Young's modulus is 55.1 GPa ($8.0 x10^6$ psi).

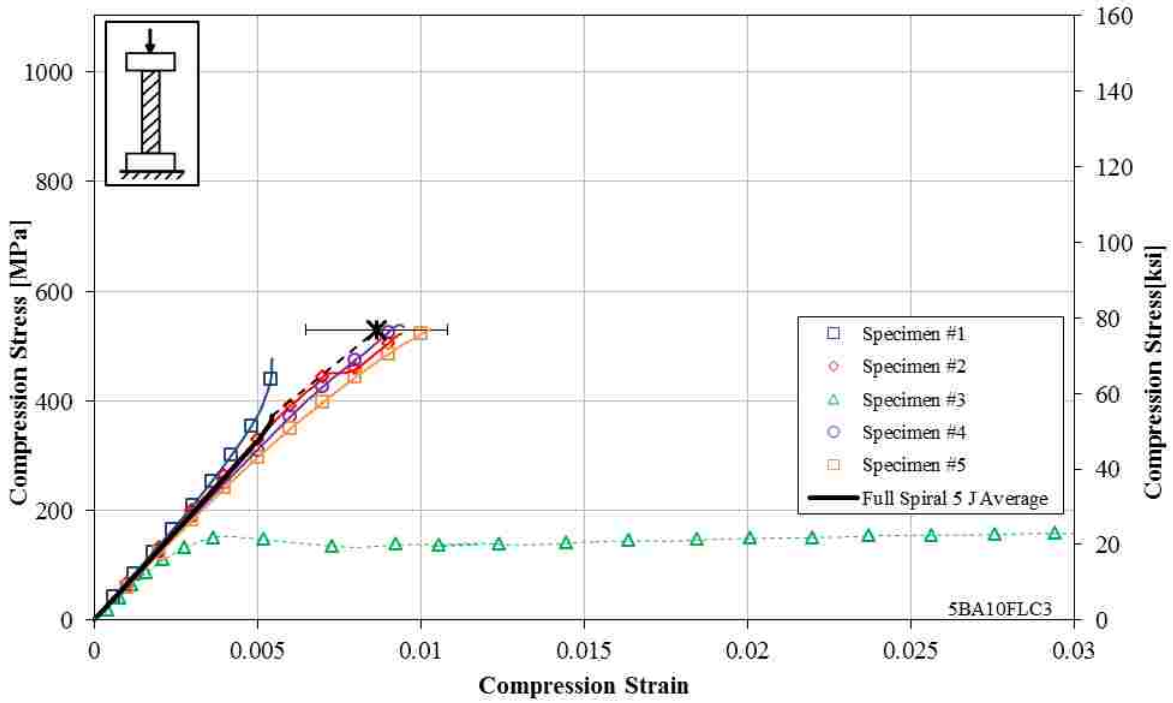

Figure 4.15: Stress-Strain Plot Based on Extensometer Strain for Full Spiral, 5 J (3.7 ft-lbs.) Impact Specimens, 8 mm (5/16") Diameter, 76 mm (3") Length, (5BA10FLC3)

Table 4.15: Summary Table Based on Extensometer Strain for Full Spiral, 5 J (3.7 ft-lbs.) Impact Specimens, 8 mm (5/16") Diameter, 76 mm (3") Length, (5BA10FLC3)

Specimen Number (5BA10FLC3)	Cross Sectional Area [mm^2 (in^2)]	Ultimate Compression Strength [MPa (ksi)]	Strain at Max Stress [10^3 με]	Compression Young's Modulus [GPa (10^6 psi)]
1	51.8 (0.080)	526.3 (76.3)	5.5	70.1 (10.2)
2	51.1 (0.079)	522.9 (75.8)	9.4	66.5 (9.6)
3	50.9 (0.079)	159.4 (23.1)*	30.3*	58.8 (8.5)
4	52.2 (0.081)	539.3 (78.2)	9.5	62.4 (9.1)
5	51.8 (0.080)	530.6 (77.0)	10.3	60.0 (8.7)
Average	51.6 (0.080)	529.8 (76.8)	8.7	64.8 (9.4)
Standard Deviation	0.55 (0.001)	7.1 (1.0)	2.2	4.4 (0.6)
	1.1%	1.3%	25.0%	6.9%

* *Specimen did not pass Chauvenet's Criterion, not included in averages.*

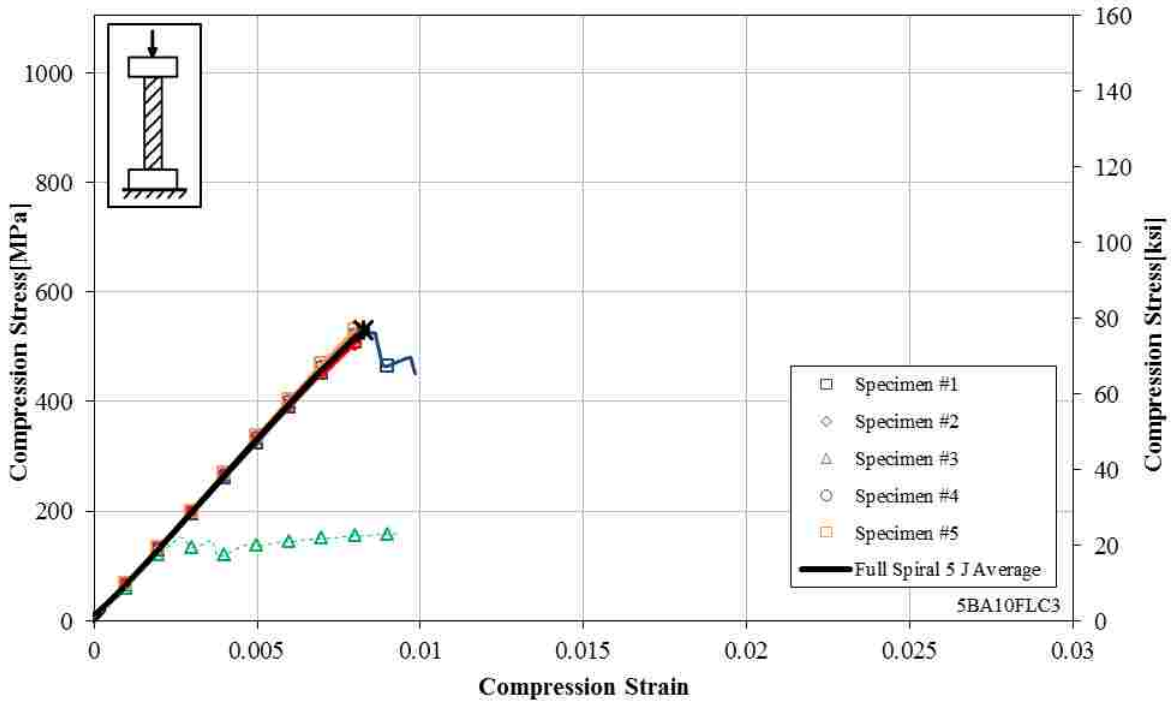

Figure 4.16: Stress-Strain Plot Based on Machine Strain for Full Spiral 5 J (3.7 ft-lbs.) Impact Specimens, 8 mm (5/16") Diameter, 76 mm (3") Length, (5BA10FLC3)

Table 4.16: Summary Table Based on Machine Strain for Full Spiral 5 J (3.7 ft-lbs.) Impact Specimen, 8 mm (5/16") Diameter, 76 mm (3") Length, (5BA10FLC3)

Specimen Number (5BA10FLC3)	Cross Sectional Area [mm^2 (in^2)]	Ultimate Compression Strength [MPa (ksi)]	Strain at Max Stress [10^3 με]	Compression Young's Modulus [GPa (10^6 psi)]
1	51.8 (0.080)	526.3 (76.3)	8.4	65.1 (9.4)
2	51.1 (0.079)	522.9 (75.8)	8.3	66.0 (9.6)
3	50.9 (0.079)	159.4 (23.1)*	9.3*	61.0 (8.9)
4	52.2 (0.081)	539.3 (78.2)	8.3	66.2 (9.6)
5	51.8 (0.080)	530.6 (77.0)	8.0	66.4 (9.6)
Average	51.6 (0.080)	529.8 (76.8)	8.3	65.9 (9.6)
Standard Deviation	0.55 (0.001)	7.1 (1.0)	0.2	0.6 (0.1)
	1.1%	1.3%	2.2%	0.9%

* *Specimen did not pass Chauvenet's Criterion, not included in averages.*

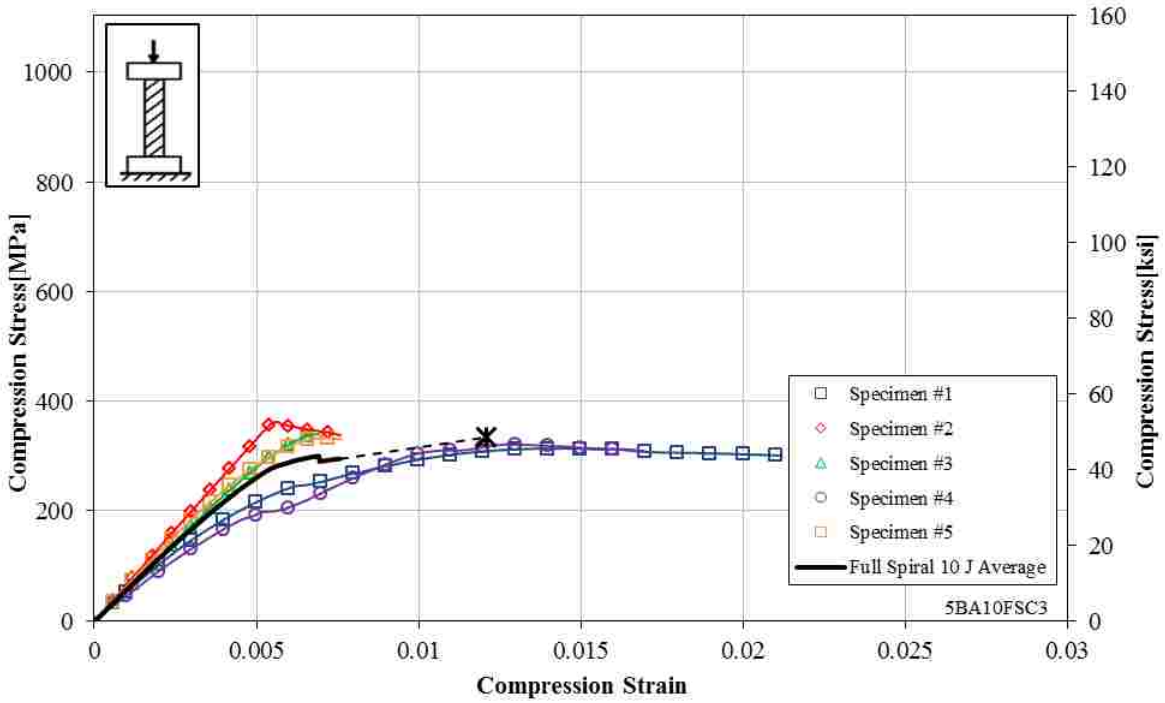

Figure 4.17: Stress-Strain Plot Based on Extensometer Strain for Full Spiral, 10 J (7.4 ft-lbs.) Impact Specimen, 8 mm (5/16") Diameter, 76 mm (3") Length, (5BA10FSC3)

Table 4.17: Summary Table Based on Extensometer Strain for Full Spiral, 10 J (7.4 ft-lbs.) Impact Specimens, 8 mm (5/16") Diameter, 76 mm (3") Length, (5BA10FSC3)

Specimen Number (5BA10FSC3)	Cross Sectional Area [mm^2 (in^2)]	Ultimate Compression Strength [MPa (ksi)]	Strain at Max Stress [10^3 με]	Compression Young's Modulus [GPa (10^6 psi)]
1	51.2 (0.079)	314.1 (45.5)	21.25	46.3 (6.7)
2	52.0 (0.081)	363.0 (52.7)	7.58	67.3 (9.8)
3	51.6 (0.080)	340.2 (49.3)	6.93	59.2 (8.6)
4	51.3 (0.080)	321.4 (46.6)	16.95	40.7 (5.9)
5	52.1 (0.081)	333.1 (48.3)	7.62	61.8 (9.0)
Average	51.6 (0.080)	334.4 (48.5)	12.07	55.1 (8.0)
Standard Deviation	0.40 (0.001)	19.0 (2.7)	6.60	11.1 (1.6)
	0.8%	5.7%	54.7%	20.2%

* *Specimen did not pass Chauvenet's Criterion, not included in averages.*

The full spiral coverage 10 J (7.4 ft-lbs.) impact specimen test results, based on machine strain, are presented in the stress-strain plot shown in Figure 4.18 and summarized in Table 4.18.

The average compression strength is 327.2 MPa (47.5 ksi), the corresponding strain is 6.43 mm/mm (in./in.), and the average Young's modulus is 55.9 GPa ($8.1x10^6$ psi). Specimen 2 was eliminated based on Chauvenet's envelope for strain at maximum stress.

4.1.10 Half Spiral No-impact (5BA10HNC3)

The half spiral coverage, no-impact specimen test results, based on extensometer strain, are presented in the stress-strain plot shown in Figure 4.19 and summarized in Table 4.19. The average strength is 647.5 MPa (93.9 ksi), the corresponding strain is 10.73 mm/mm (in./in.), and the average Young's modulus is 60.3 GPa ($8.8x10^6$ psi). Specimen 2 was eliminated based on Chauvenet's envelope for strain at maximum stress.

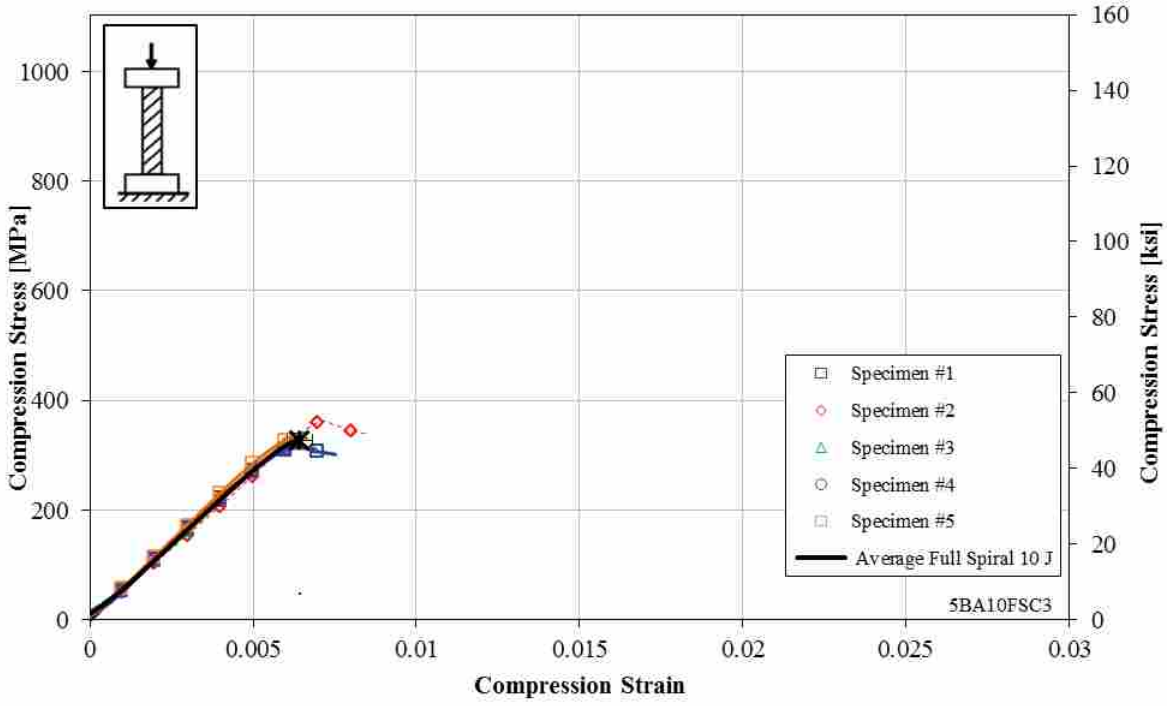

Figure 4.18: Stress-Strain Plot Based on Machine Strain for Full Spiral 10 J (7.4 ft-lbs.) Impact Specimen, 8 mm (5/16") Diameter, 76 mm (3") Length, (5BA10FSC3)

Table 4.18: Summary Table Based on Machine Strain for Full Spiral 10 J (7.4 ft-lbs.) Impact Specimens, 8 mm (5/16") Diameter, 76 mm (3") Length, (5BA10FSC3)

Specimen Number (5BA10FSC3)	Cross Sectional Area [mm^2 (in^2)]	Ultimate Compression Strength [MPa (ksi)]	Strain at Max Stress [10^3 με]	Compression Young's Modulus [GPa (10^6 psi)]
1	51.2 (0.079)	314.1 (45.5)	6.5	56.5 (8.2)
2	52.0 (0.081)	363.0 (52.7)	7.3*	51.5 (7.5)
3	51.6 (0.080)	340.2 (49.3)	6.6	54.2 (7.9)
4	51.3 (0.080)	321.4 (46.6)	6.3	55.1 (8.0)
5	52.1 (0.081)	333.1 (48.3)	6.4	57.9 (8.4)
Average	51.6 (0.080)	327.2 (47.5)	6.4	55.9 (8.1)
Standard Deviation	0.40 (0.001)	11.7 (1.7)	0.4	1.6 (0.2)
	0.8%	3.6%	6.0%	2.9%

* *Specimen did not pass Chauvenet's Criterion, not included in averages.*

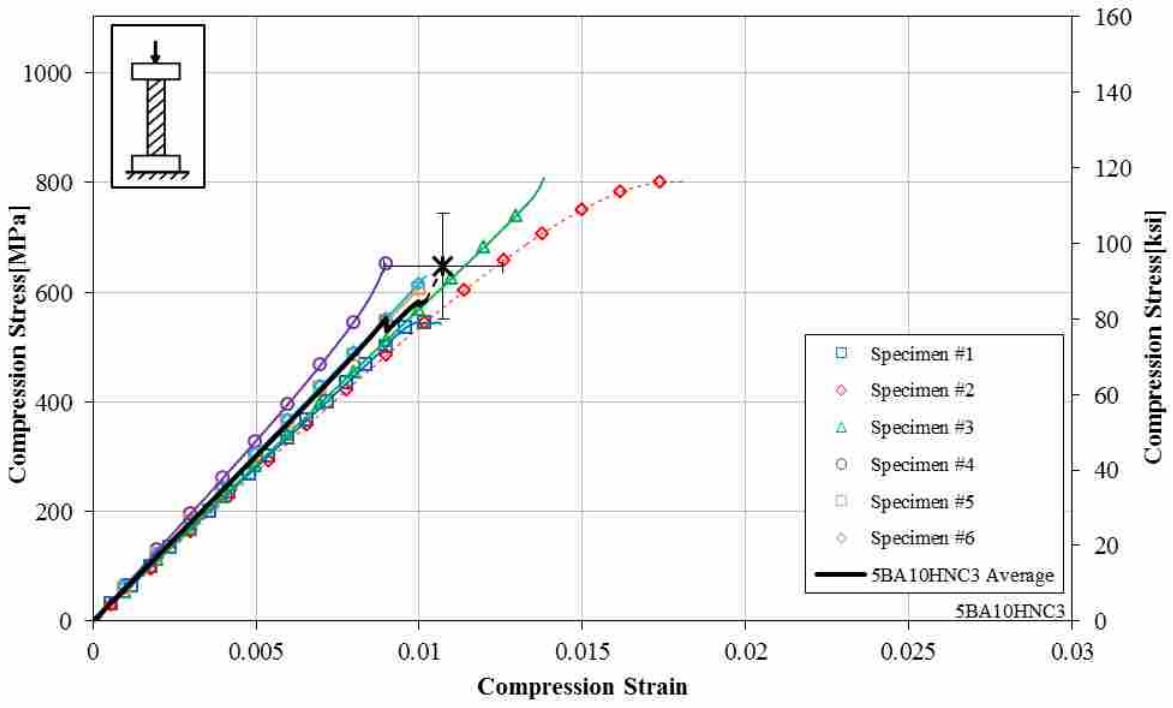

Figure 4.19: Stress-Strain Plot Based on Extensometer Strain for Half Spiral, No-Impact Specimens, 8 mm (5/16") Diameter, 76 mm (3") Length, (5BA10HNC3)

Table 4.19: Summary Table Based on Extensometer Strain for Half Spiral, No-Impact Specimens, 8 mm (5/16") Diameter, 76 mm (3") Length, (5BA10HNC3)

Specimen Number (5BA10HNC3)	Cross Sectional Area [mm^2 (in^2)]	Ultimate Compression Strength [MPa (ksi)]	Strain at Max Stress [10^3 με]	Compression Young's Modulus [GPa (10^6 psi)]
1	56.2 (0.087)	545.3 (79.1)	10.7	55.9 (8.1)
2	56.8 (0.088)	801.5 (116.2)	18.2*	54.4 (7.9)
3	55.3 (0.086)	806.5 (117.0)	13.8	57.3 (8.3)
4	52.7 (0.082)	651.8 (94.5)	9.0	66.3 (9.6)
5	52.5 (0.081)	604.2 (87.6)	10.0	61.1 (8.9)
6	52.5 (0.081)	629.5 (91.3)	10.2	61.1 (8.9)
Average	54.0 (0.084)	647.5 (93.9)	10.7	60.3 (8.8)
Standard Deviation	1.98 (0.003)	97.4 (14.1)	1.8	4.0 (0.6)
	3.7%	15.0%	17.1%	6.7%

* *Specimen did not pass Chauvenet's Criterion, not included in averages.*

The half spiral coverage no-impact specimen test results, based on machine strain, are presented in the stress-strain plot shown in Figure 4.20 and summarized in Table 4.20. The average strength is 673.1 MPa (97.6 ksi), the corresponding strain is 11.35 mm/mm (in./in.), and the average Young's modulus is 61.2 GPa ($8.9x10^6$ psi).

4.1.11 Half Spiral 5 J Impact (5BA10HLC3)

The half spiral coverage, 5 J (3.7 ft-lbs.) impact specimen test results, based on extensometer strain, are presented in the stress-strain plot shown in Figure 4.21 and summarized in Table 4.21. The average compression strength is 411.9 MPa (59.7 ksi), the corresponding strain is 8.68 mm/mm (in./in.), and the average Young's modulus is 55.6 GPa ($8.1x10^6$ psi).

The half spiral coverage 5 J (3.7 ft-lbs.) impact specimen test results, based on machine strain, are presented in the stress-strain plot shown in Figure 4.22 and in summary Table 4.22. The average compression strength is 411.9 MPa (59.7 ksi), the corresponding strain is 6.86 mm/mm (in./in.), and the average Young's modulus is 63.3 GPa ($9.2x10^6$ psi).

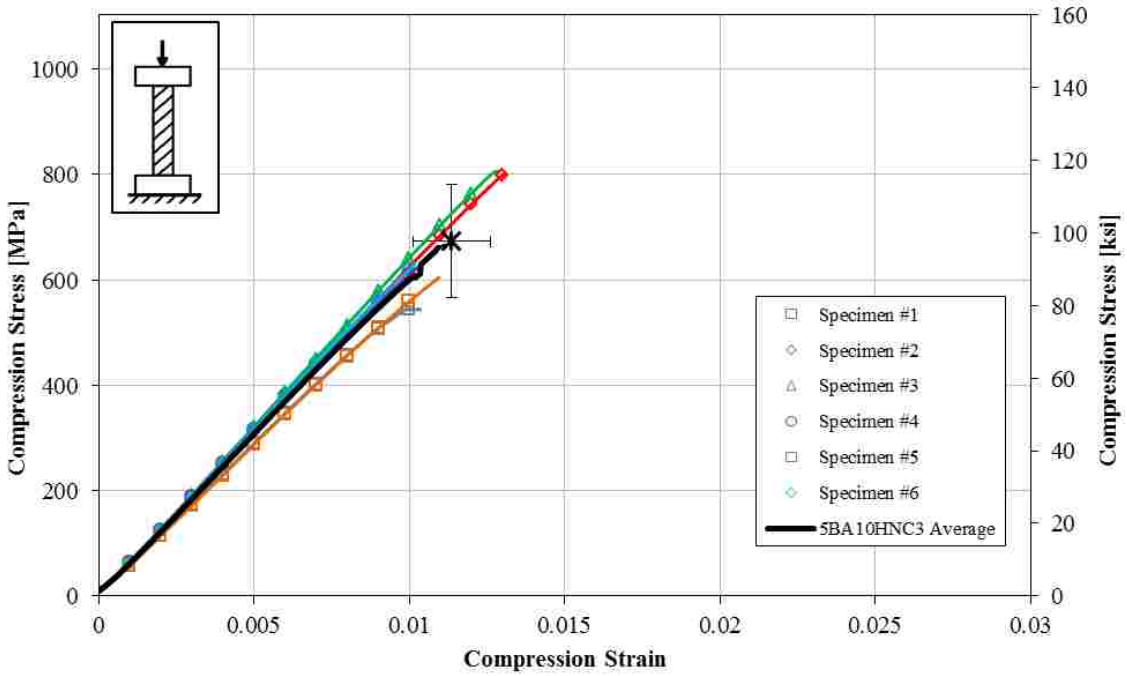

Figure 4.20: Stress-Strain Plot Based on Machine Strain for Half Spiral No-Impact Specimens, 8 mm (5/16") Diameter, 76 mm (3") Length, (5BA10HNC3)

Table 4.20: Summary Table Based on Machine Strain for Half Spiral No-Impact Specimens, 8 mm (5/16") Diameter, 76 mm (3") Length, (5BA10HNC3)

Specimen Number (5BA10HNC3)	Cross Sectional Area [mm^2 (in^2)]	Ultimate Compression Strength [MPa (ksi)]	Strain at Max Stress [10^3 με]	Compression Young's Modulus [GPa (10^6 psi)]
1	56.2 (0.087)	545.3 (79.1)	10.3	58.0 (8.4)
2	56.8 (0.088)	801.5 (116.2)	13.1	62.6 (9.1)
3	55.3 (0.086)	806.5 (117.0)	12.8	63.5 (9.2)
4	52.7 (0.082)	651.8 (94.5)	10.8	63.0 (9.1)
5	52.5 (0.081)	604.2 (87.6)	10.9	57.3 (8.3)
6	52.5 (0.081)	629.5 (91.3)	10.2	62.7 (9.1)
Average	54.0 (0.084)	673.1 (97.6)	11.4	61.2 (8.9)
Standard Deviation	1.98 (0.003)	107.4 (15.6)	1.2	2.8 (0.4)
	3.7%	16.0%	11.0%	4.5%

* *Specimen did not pass Chauvenet's Criterion, not included in averages.*

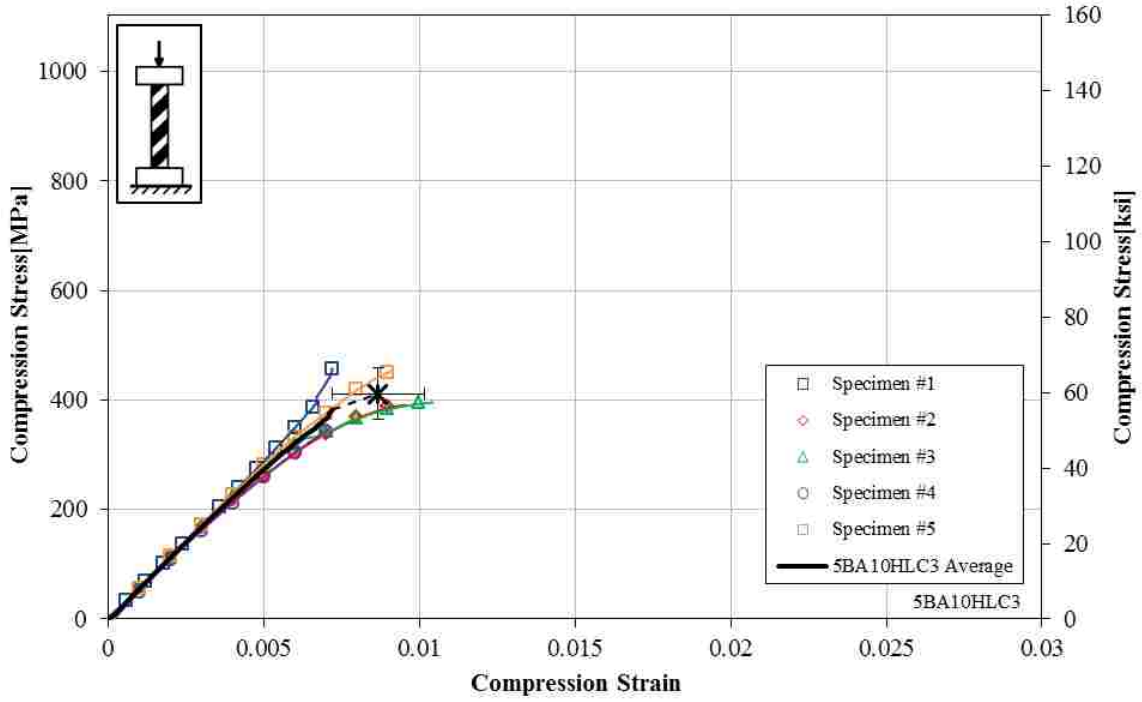

Figure 4.21: Stress-Strain Plot Based on Extensometer Strain for Half Spiral, 5 J (3.7 ft-lbs.) Impact Specimens, 8 mm (5/16") Diameter, 76 mm (3") Length, (5BA10HLC3)

Table 4.21: Summary Table Based on Extensometer Strain for Half Spiral, 5 J (3.7 ft-lbs.) Impact Specimens, 8 mm (5/16") Diameter, 76 mm (3") Length, (5BA10HLC3)

Specimen Number (5BA10HLC3)	Cross Sectional Area [mm^2 (in^2)]	Ultimate Compression Strength [MPa (ksi)]	Strain at Max Stress [10^3 με]	Compression Young's Modulus [GPa (10^6 psi)]
1	57.9 (0.090)	467.2 (67.8)	7.2	57.1 (8.3)
2	56.2 (0.087)	391.2 (56.7)	9.5	53.3 (7.7)
3	55.5 (0.086)	396.0 (57.4)	10.4	56.2 (8.2)
4	55.5 (0.086)	351.8 (51.0)	7.1	53.7 (7.8)
5	55.3 (0.086)	453.3 (65.7)	9.1	57.5 (8.3)
Average	56.1 (0.087)	411.9 (59.7)	8.7	55.6 (8.1)
Standard Deviation	1.08 (0.002)	47.6 (6.9)	1.5	1.9 (0.3)
	1.9%	11.6%	17.0%	3.5%

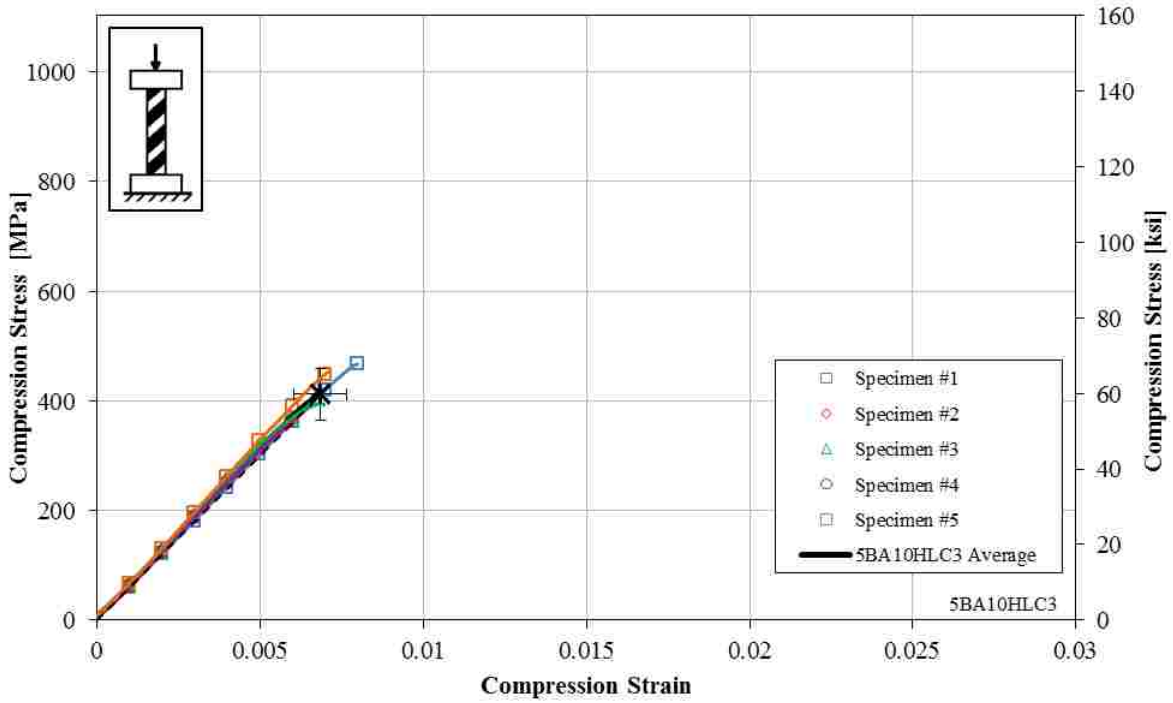

Figure 4.22: Stress-Strain Plot Based on Machine Strain for Half Spiral, 5 J (3.7 ft-lbs.) Impact Specimen, 8 mm (5/16") Diameter, 76 mm (3") Length, (5BA10HLC3)

Table 4.22: Summary Table Based on Machine Strain for Half Spiral, 5 J (3.7 ft-lbs.) Impact Specimen, 8 mm (5/16") Diameter, 76 mm (3") Length, (5BA10HLC3)

Specimen Number (5BA10HLC3)	Cross Sectional Area [mm^2 (in^2)]	Ultimate Compression Strength [MPa (ksi)]	Strain at Max Stress [10^3 με]	Compression Young's Modulus [GPa (10^6 psi)]
1	57.9 (0.090)	467.2 (67.8)	8.0	60.7 (8.8)
2	56.2 (0.087)	391.2 (56.7)	6.6	62.8 (9.1)
3	55.5 (0.086)	396.0 (57.4)	6.9	64.3 (9.3)
4	55.5 (0.086)	351.8 (51.0)	5.8	63.2 (9.2)
5	55.3 (0.086)	453.3 (65.7)	7.1	65.6 (9.5)
Average	56.1 (0.087)	411.9 (59.7)	6.9	63.3 (9.2)
Standard Deviation	1.08 (0.002)	47.6 (6.9)	0.8	1.8 (0.3)
	1.9%	11.6%	11.7%	2.9%

4.1.12 Half Spiral 10 J Impact (5BA10HSC3)

The half spiral coverage, 10 J (7.4 ft-lbs.) impact specimen test results, based on extensometer strain, are presented in the stress-strain plot shown in Figure 4.23 and summarized

in Table 4.23. The average strength is 232.2 MPa (33.7 ksi), the corresponding strain is 8.03 mm/mm (in./in.), and the average Young's modulus is 47.9 GPa (7.0x106 psi).

The half spiral coverage 10 J (7.4 ft-lbs.) impact specimen test results, based on machine strain, are presented in the stress-strain plot shown in Figure 4.24 and summarized in Table 4.24. The average compression strength is 234.2 MPa (34.0 ksi), the corresponding strain is 5.61 mm/mm (in./in.), and the average Young's modulus is 49.9 GPa (7.2x106 psi). Specimen 2 was eliminated based on Chauvenet's envelope for Young's modulus.

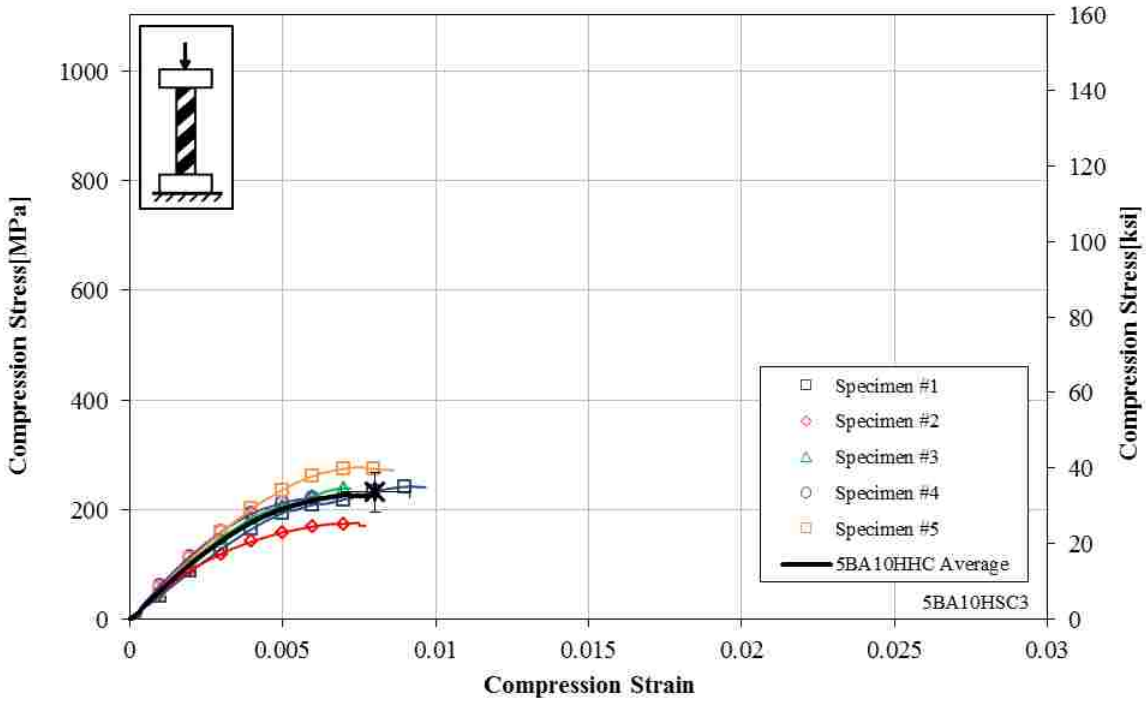

Figure 4.23: Stress-Strain Plot Based on Extensometer Strain for Half Spiral, 10 J (7.4 ft-lbs.) Impact Specimen, 8 mm (5/16") Diameter, 76 mm (3") Length, (5BA10HSC3)

Table 4.23: Summary Table Based on Extensometer Strain for Half Spiral, 10 J (7.4 ft-lbs.) Impact Specimens, 8 mm (5/16") Diameter, 76 mm (3") Length, (5BA10HSC3)

Specimen Number (5BA10HLC3)	Cross Sectional Area [mm^2 (in^2)]	Ultimate Compression Strength [MPa (ksi)]	Strain at Max Stress [10^3 με]	Compression Young's Modulus [GPa (10^6 psi)]
1	57.9 (0.090)	242.5 (35.2)	9.7	42.9 (6.2)
2	58.6 (0.091)	176.5 (25.6)	7.7	36.2 (5.3)
3	56.7 (0.088)	240.0 (34.8)	7.2	50.6 (7.3)
4	56.4 (0.087)	224.0 (32.5)	6.9	55.7 (8.1)
5	56.6 (0.088)	277.8 (40.3)	8.6	54.3 (7.9)
Average	57.3 (0.089)	232.2 (33.7)	8.0	47.9 (7.0)
Standard Deviation	0.95 (0.001)	36.8 (5.3)	1.1	8.2 (1.2)
	1.7%	15.8%	14.0%	17.2%

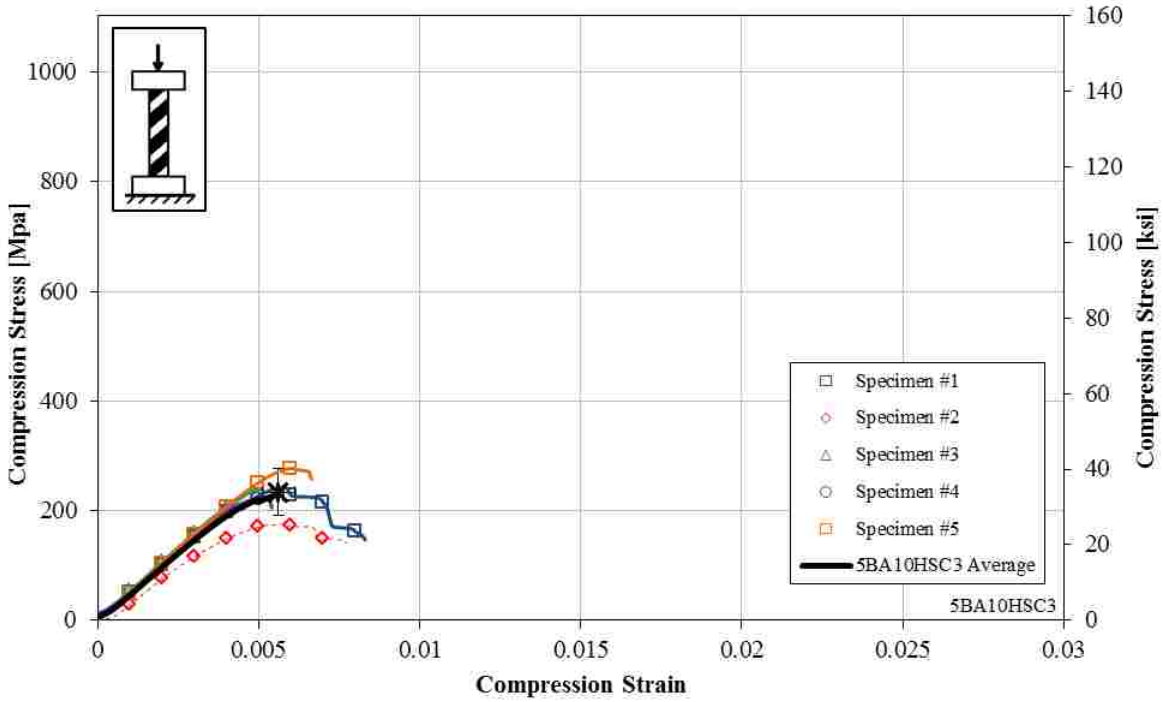

Figure 4.24: Stress-Strain Plot Based on Machine Strain for Half Spiral, 10 J (7.4 ft-lbs.) Impact Specimens, 8 mm (5/16") Diameter, 76 mm (3") Length, (5BA10HSC3)

Table 4.24: Summary Table Based on Machine Strain for Half Spiral, 10 J (7.4 ft-lbs.) Impact Specimens, 8 mm (5/16") Diameter, 76 mm (3") Length, (5BA10HSC3)

Specimen Number (5BA10HLC3)	Cross Sectional Area [mm^2 (in^2)]	Ultimate Compression Strength [MPa (ksi)]	Strain at Max Stress [10^3 με]	Compression Young's Modulus [GPa (10^6 psi)]
1	57.9 (0.090)	242.5 (35.2)	5.7	50.9 (7.4)
2	58.6 (0.091)	176.5 (25.6)	5.8	41.4 (6.0)*
3	56.7 (0.088)	240.0 (34.8)	4.9	53.1 (7.7)
4	56.4 (0.087)	224.0 (32.5)	5.3	52.6 (7.6)
5	56.6 (0.088)	277.8 (40.3)	6.1	54.2 (7.9)
Average	57.3 (0.089)	234.2 (34.0)	5.6	49.9 (7.2)
Standard Deviation	0.95 (0.001)	42.1 (6.1)	0.5	5.8 (0.8)
	1.7%	18.0%	8.8%	11.7%

* *Specimen did not pass Chauvenet's Criterion, not included in averages.*

4.2 5/16" Diameter Configuration Averages for 3" Specimens

This section summarizes the averaged results of the 8 mm (5/16") diameter specimens with a 76 mm (3") length, based on machine strain only. Plots with the average curves for the different configurations (Full Braid, Half Braid, Full Spiral, Half Spiral) are shown, followed by plots with the different impact energy levels (No-Impact, 5 J (3.7 ft-lbs.), and 10 J (7.4 ft-lbs.)), the different sleeve coverage amounts (Full, Half) and the different sleeves types (Braid and Spiral). Additional figures based on extensometer strain are provided in Appendix G.

All average curves for preliminary testing are in Figure 4.25. Three loose groupings of curves can be seen, each group indicative of one of the three impact energy levels. Note that the initial Young's moduli are similar for all configurations.

4.2.1 Full Braid

The average curves for the full braid sleeves are in Figure 4.26. As expected, the specimens that were not impacted had the greatest strength at 722.3 MPa (104.8 ksi) with an

approximate 1/3 and 2/3 reduction in strength for 5 J (3.7 ft-lbs.) and 10 J (7.4 ft-lbs.) of impact energy, respectively.

4.2.2 Half Braid

All average curves for half coverage braided sleeves are in Figure 4.27. This plot shows the superior strength of an un-impacted specimen being 744.1 MPa (107.9 ksi), with a steady reduction in strength and strain with increased impact energy levels.

4.2.3 Full Spiral

The average stress-strain curves for all full coverage spiral sleeves are shown in Figure 4.28. The no-impact configuration reached an ultimate strength of 708.2 MPa (102.7 ksi) with an expected reduction in strength with increasing impact energy.

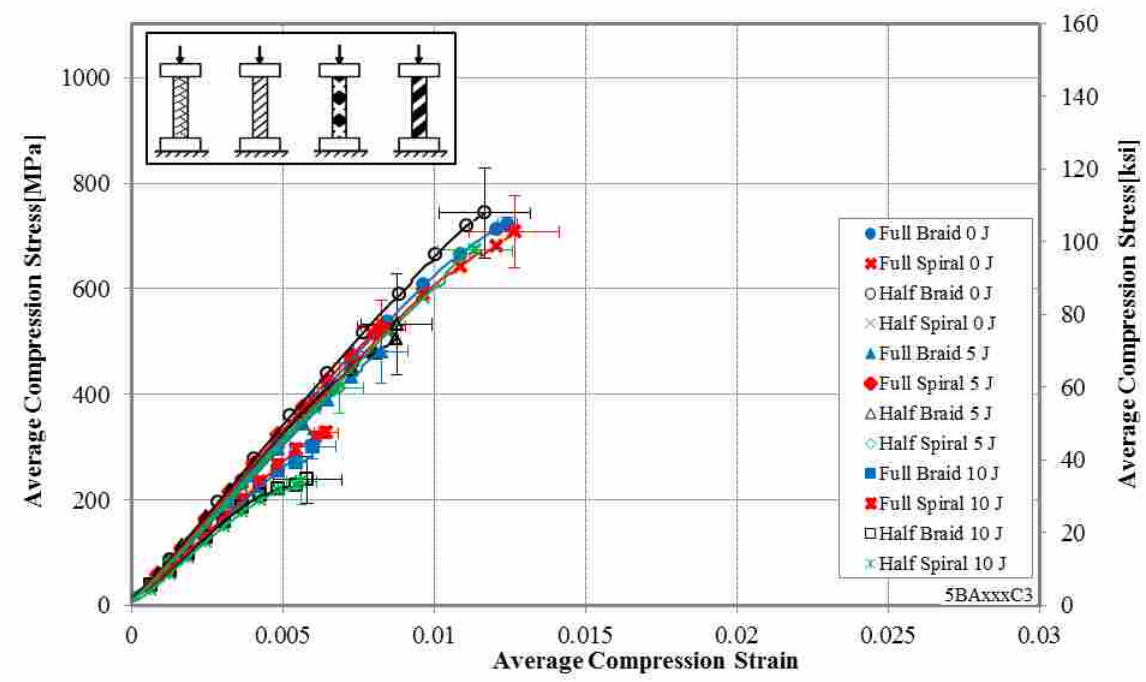

Figure 4.25: Average Stress-Strain Curves for all 8 mm (5/16") Diameter, 76 mm (3") Length Specimens

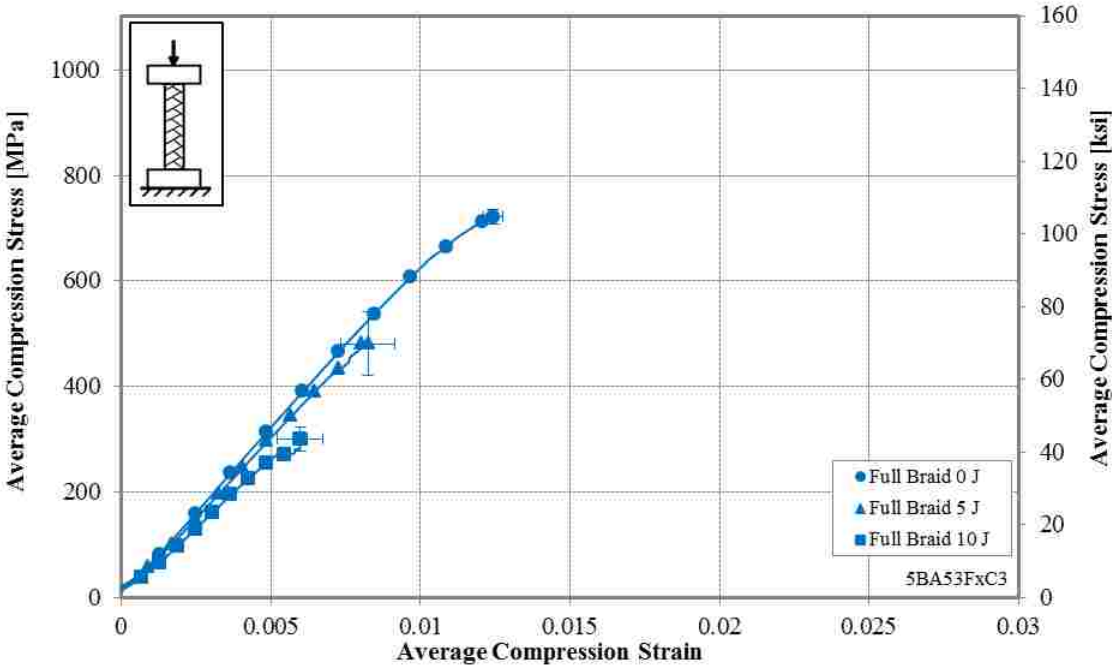

Figure 4.26: Average Stress-Strain Curves for all Full Braid, 8 mm (5/16") Diameter, 76 mm (3") Length Specimens

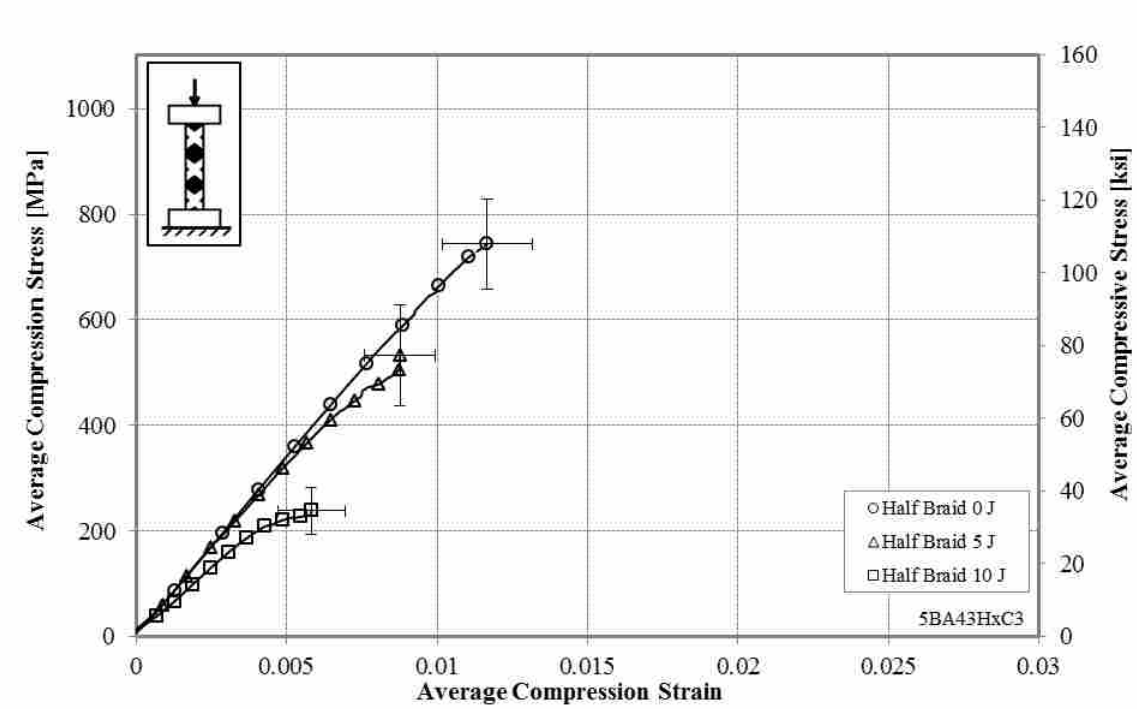

Figure 4.27: Average Stress-Strain Curves for all Half Braid, 8 mm (5/16") Diameter, 76 mm (3") Length Specimens

4.2.4 Half Spiral

The average curves for the half coverage spiral sleeve configurations are in Figure 4.29. The no-impact configuration average was 673.1 MPa (97.6 ksi) with the other specimens decreasing in strength with increasing impact energy.

4.2.5 No-impact

Average curves for all non-impacted specimens are in Figure 4.30. The differences in strength are not significant between the different sleeve configurations as expected according to Hansen [3]. All specimens have very similar slopes indicating that their stiffness is nearly the same.

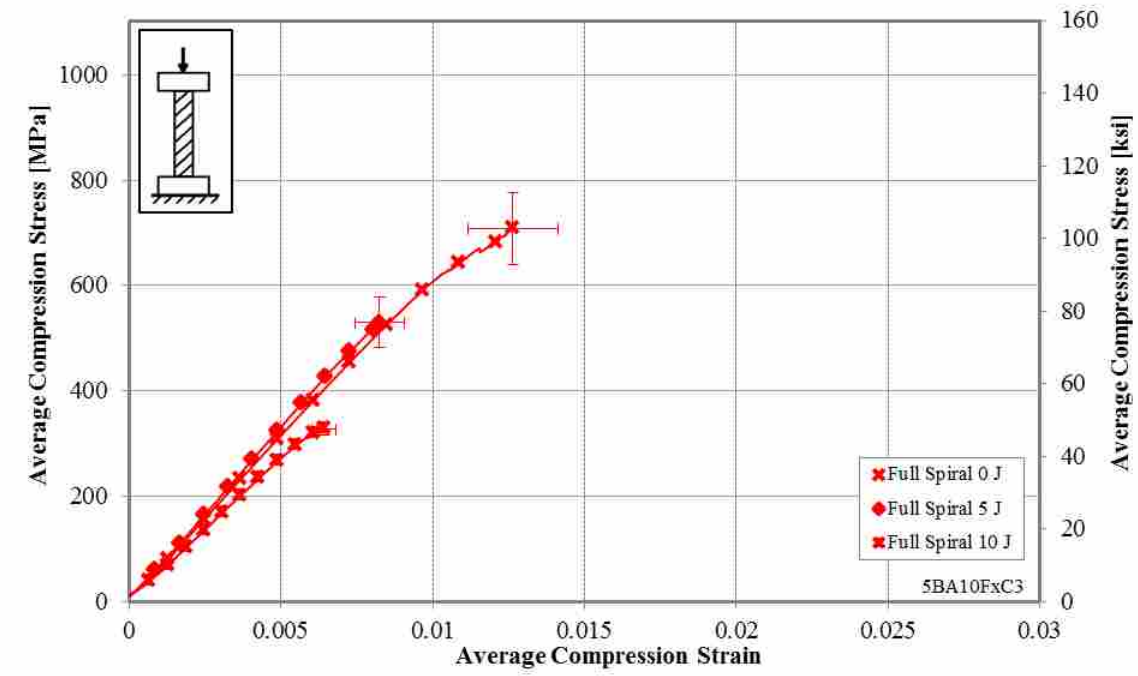

Figure 4.28: Average Stress-Strain Curves for all Full Spiral, 8 mm (5/16") Diameter, 76 mm (3") Length Specimens

4.2.6 5 J Impact

Average curves for specimens impacted with 5 J (3.7 ft-lbs.) are shown in Figure 4.31. There are no significant differences in strength besides the half coverage spiral which failed to achieve the same strength. All configurations have similar stiffness.

4.2.7 10 J Impact

Average curves for specimens impacted with 10 J (7.4 ft-lbs.) are shown in Figure 4.32. There is no significant difference between the full coverage braid and spiral and no significant difference between the half coverage braid and spiral sleeves. The full coverage specimens had greater strength than half coverage, suggesting sleeve coverage has more affect than sleeve type on the CSAI.

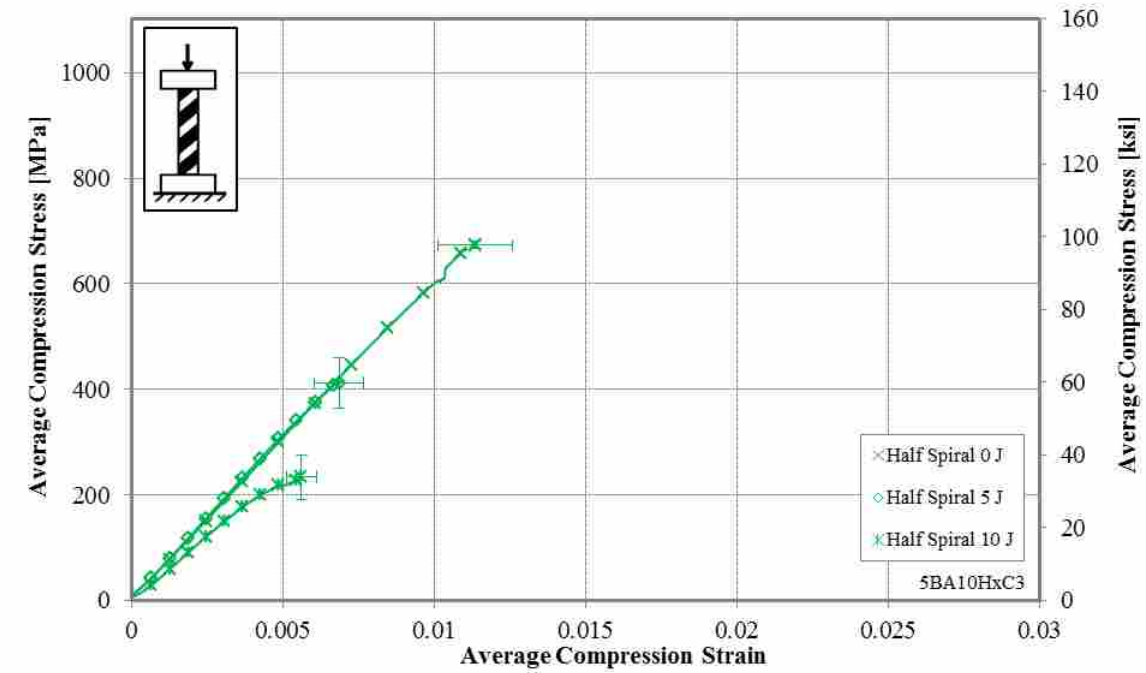

Figure 4.29: Average Stress-Strain Curves for all Half Spiral, 8 mm (5/16") Diameter, 76 mm (3") Length Specimens

4.2.8 Full Coverage

Average curves for all specimens with full sleeve coverage are in Figure 4.33. The three impact energy levels are clearly demonstrated, with no significant difference between a braid and a spiral sleeve.

4.2.9 Half Coverage

Average curves for all specimens with half sleeve coverage are in Figure 4.34. There is a significant difference in sleeve type when not impacted or impacted with 5 J (3.7 ft-bs). There is no significant difference in sleeve type when impacted with 10 J (7.4 ft-lbs.).

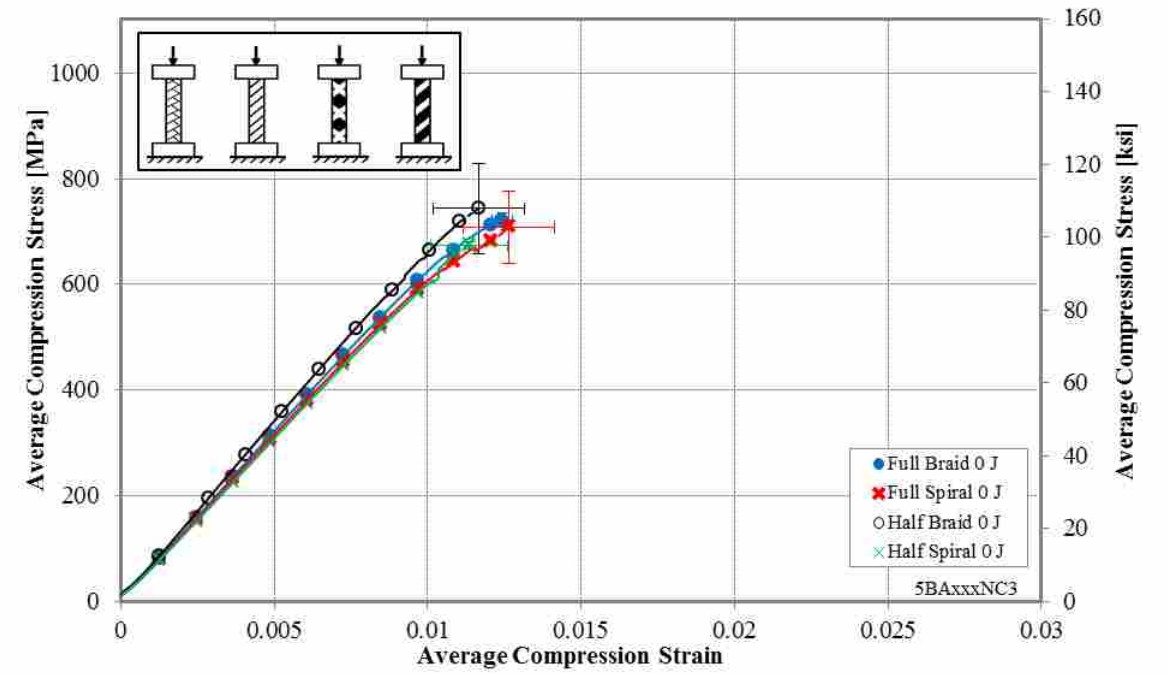

Figure 4.30: Average Stress-Strain Curves for all No-Impact, 8 mm (5/16") Diameter, 76 mm (3") Length Specimens

4.2.10 Braid Sleeve

Average curves for all specimens with a braided sleeve are in Figure 4.35. There is no significant difference in strength between a half and full coverage braid at no-impact and at 5 J (3.7 ft-lbs.) of impact. At 10 J (7.4 ft-lbs.) of impact energy, however, full coverage makes a significant difference in strength.

4.2.11 Spiral Sleeve

Average curves for all specimens with a spiral sleeve are in Figure 4.36. There is no significant difference in compression strength at no-impact. Once impacted the full coverage specimens have greater strength than the half coverage specimens.

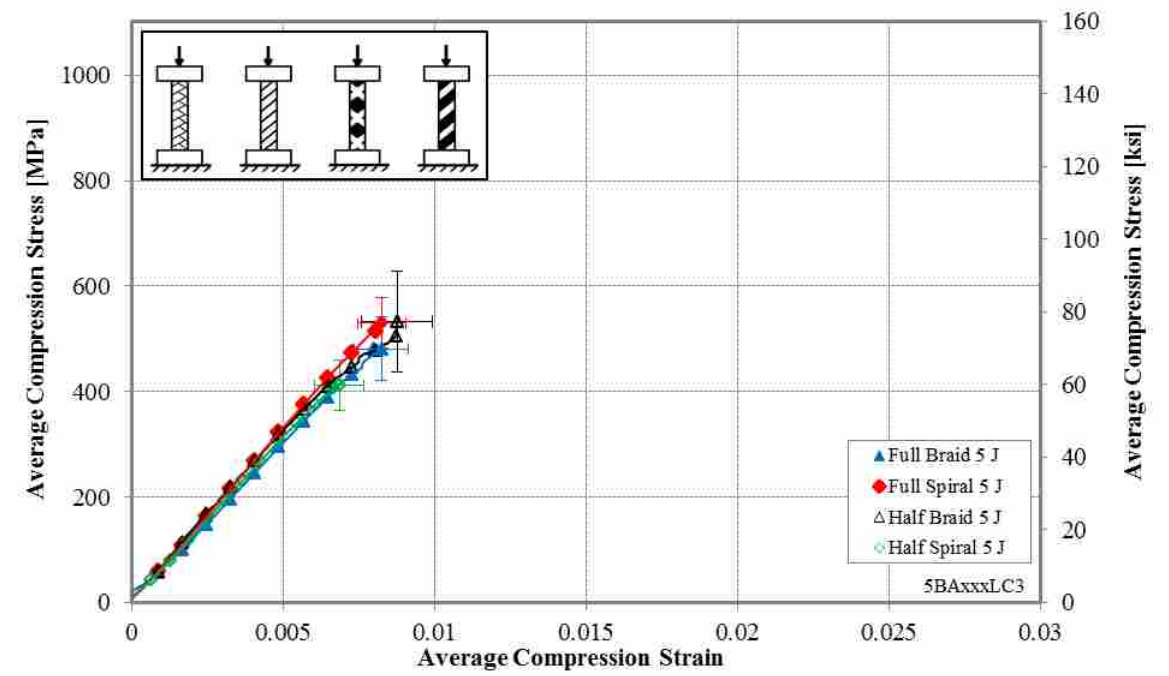

Figure 4.31: Average Stress-Strain Curves for all 5 J (3.7 Ft-lbs.) Impact, 8 mm (5/16") Diameter, 76 mm (3") Length Specimens

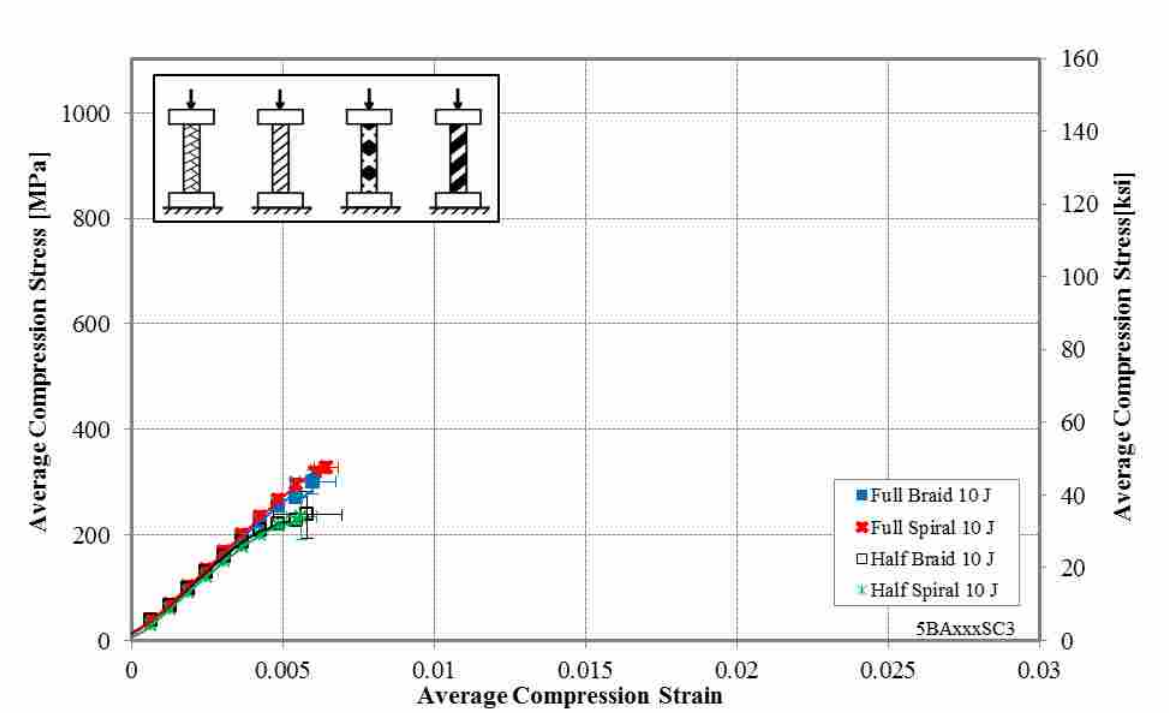

Figure 4.32: Average Stress-Strain Curves for all 10 J (7.4 Ft-lbs.) Impact, 8 mm (5/16") Diameter, 76 mm (3") Length Specimens

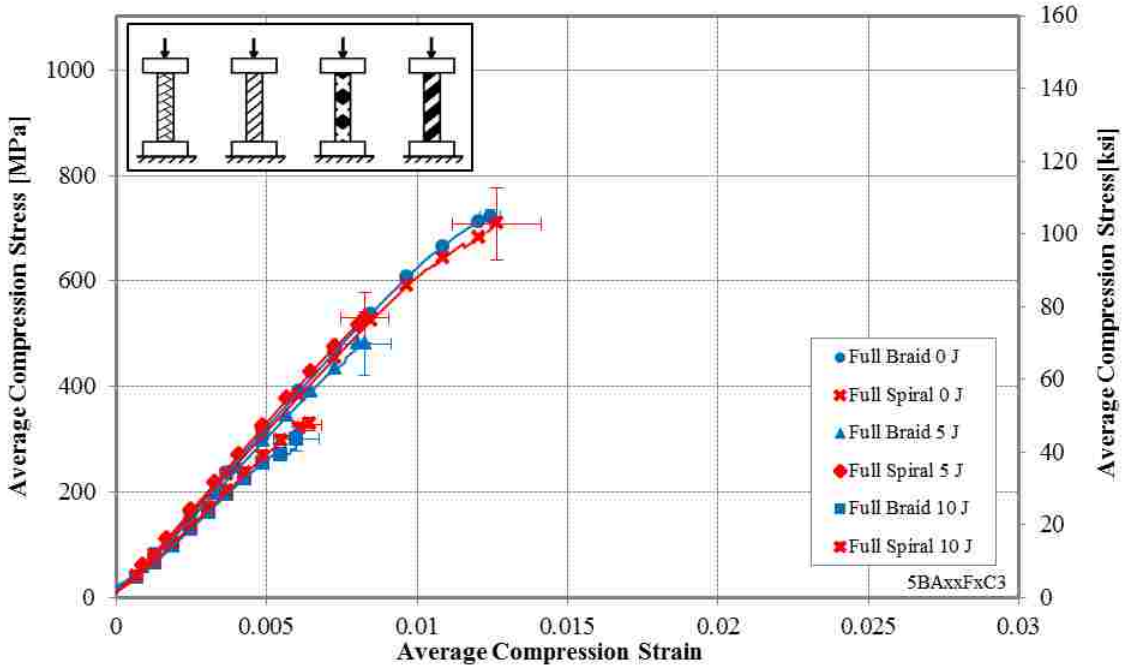

Figure 4.33: Average Stress-Strain Curves for all Full Coverage, 8 mm (5/16") Diameter, 76 mm (3") Length Specimens

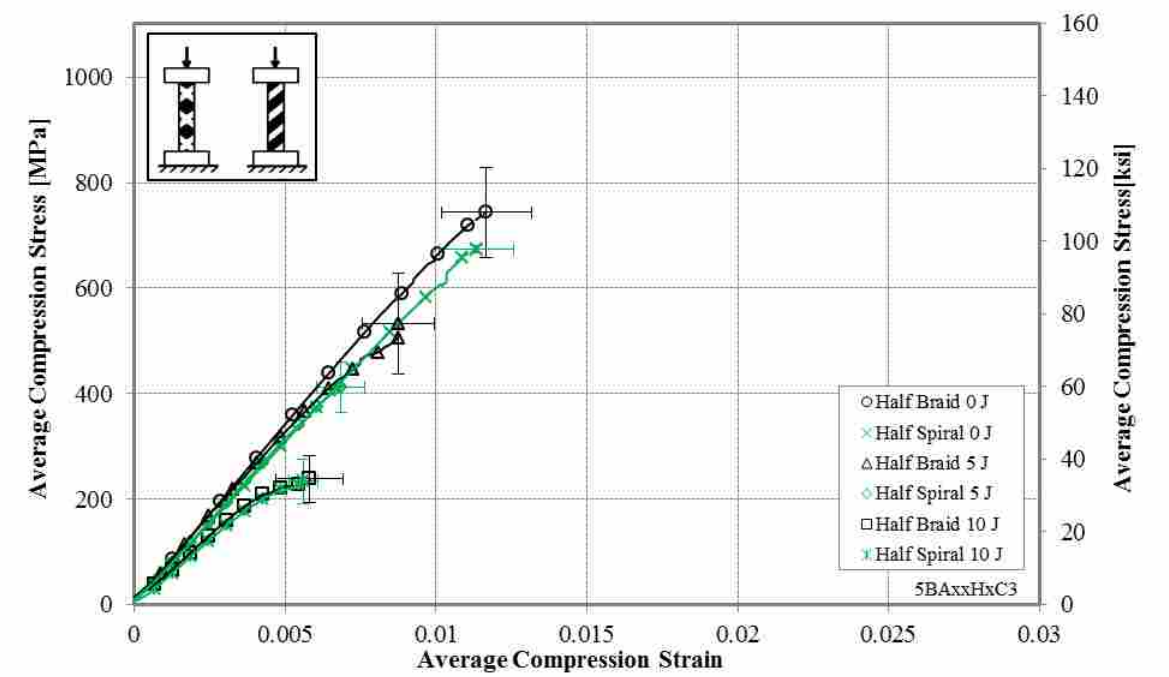

Figure 4.34: Average Stress-Strain Curves for all Half Coverage, 8 mm (5/16") Diameter, 76 mm (3") Length Specimens

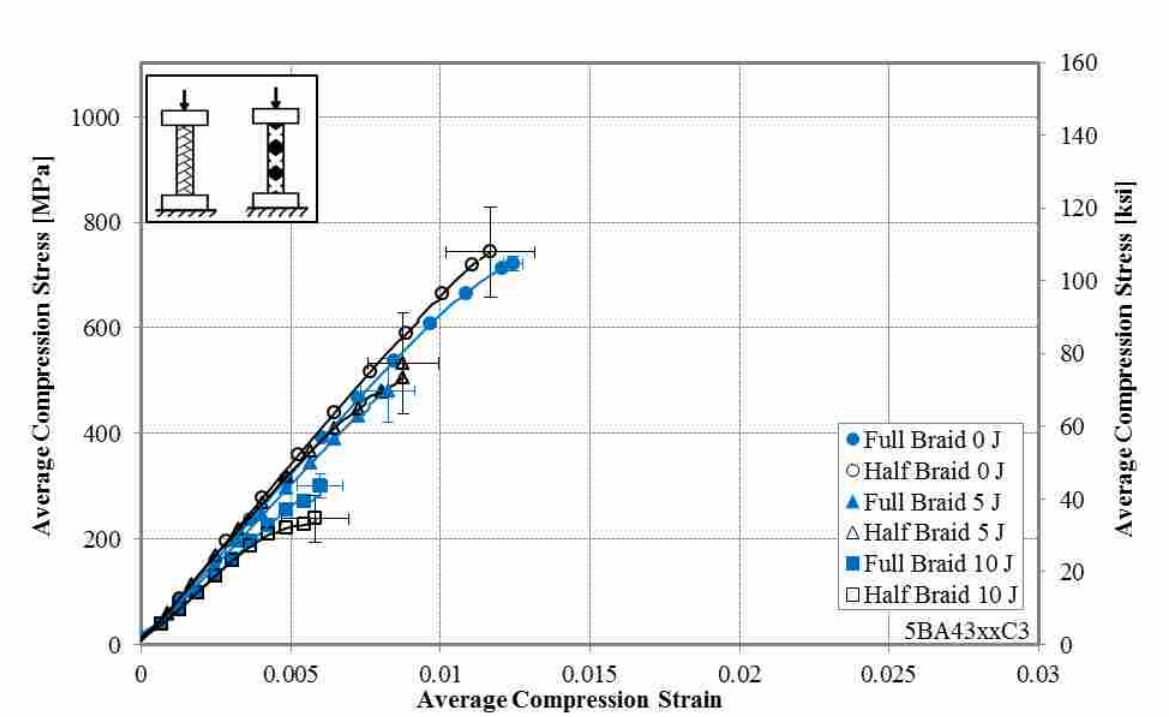

Figure 4.35: Configuration Average Stress-Strain Curves for all Braided Sleeves, 8 mm (5/16") Diameter, 76 mm (3") Length Specimens

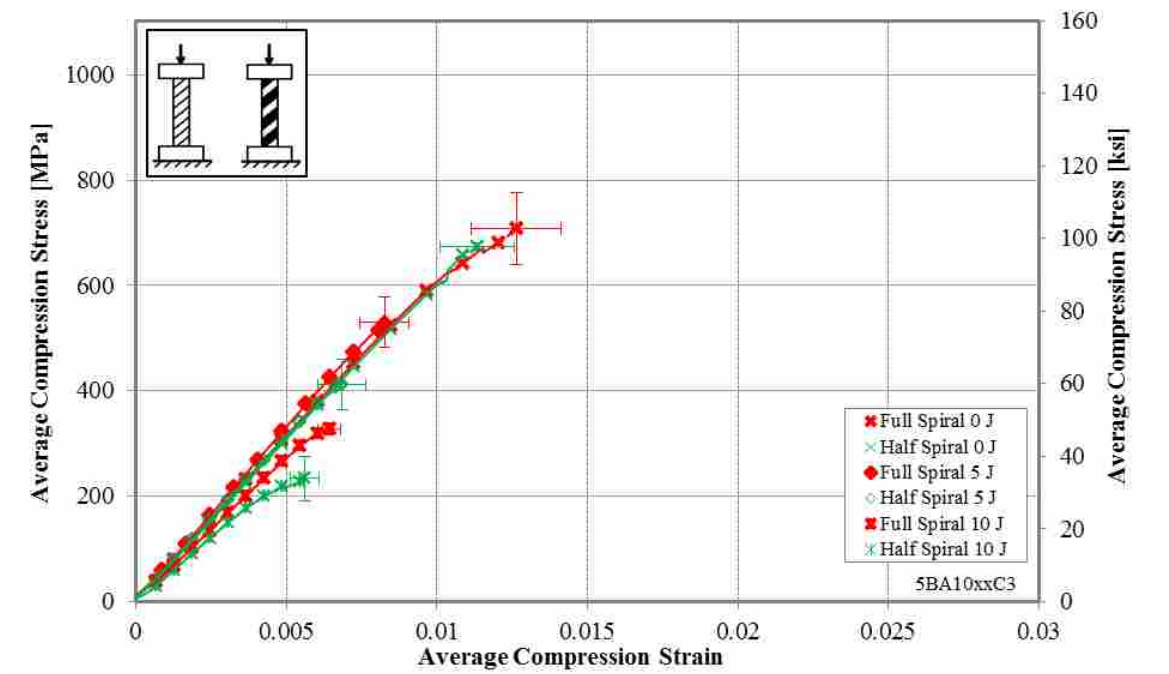

Figure 4.36: Average Stress-Strain Curves for all Spiral Sleeves, 8 mm (5/16") Diameter, 76 mm (3") Length Specimens

4.2.12 Configuration Averages Summary, 5/16" Diameter, 3" Length

Table 4.25 and Table 4.26 present the average compression strength for each configuration of the 8 mm (5/16") diameter, 76 mm (3") length specimens based on extensometer strain and machine strain, respectively. Although compression strength is independent of strain, the values in the two tables differ due to variation in the specimens that were eliminated by Chauvenet's criterion.

Table 4.25: Average Ultimate Compression Strength Based on Extensometer Strain, 8mm (5/16") Diameter, 76 mm (3") Length

Specimen Configuration & Impact Energy		Average Max [MPa (ksi)]	Standard Deviation	
			[MPa (ksi)]	[%]
Full Braid	**0 J**	722.3 (104.8)	13.9 (2.0)	2
	5 J	489.9 (71.0)	65.7 (9.5)	8
	10 J	300.4 (43.6)	25.9 (3.8)	9
Half Braid	**0 J**	744.1 (107.9)	87.5 (12.7)	12
	5 J	546.5 (79.3)	86.7 (12.6)	16
	10 J	232.5 (33.7)	53.1 (7.7)	23
Full Spiral	**0 J**	731.6 (106.1)	83.4 (12.1)	11
	5 J	529.8 (76.8)	7.1 (1.0)	1
	10 J	334.4 (48.5)	19.0 (2.7)	6
Half Spiral	**0 J**	647.5 (93.9)	97.4 (14.1)	15
	5 J	411.9 (59.7)	47.6 (6.9)	12
	10 J	232.2 (33.7)	36.8 (5.3)	16

Table 4.26: Average Ultimate Compression Strength Based on Machine Strain, 8mm (5/16") Diameter, 76 mm (3") Length

Specimen Configuration & Impact Energy		Average Max [MPa (ksi)]	Standard Deviation	
			[MPa (ksi)]	[%]
Full Braid	**0 J**	722.3 (104.8)	13.9 (2.0)	2
	5 J	481.0 (69.8)	60.2 (8.7)	13
	10 J	301.0 (43.7)	22.5 (3.3)	8
Half Braid	**0 J**	744.1 (107.9)	85.7 (12.4)	12
	5 J	532.8 (77.3)	94.9 (13.8)	18
	10 J	238.0 (34.5)	44.6 (6.5)	9
Full Spiral	**0 J**	708.2 (102.7)	67.8 (9.8)	10
	5 J	529.8 (76.8)	7.1 (1.0)	1
	10 J	327.2 (47.5)	11.7 (1.7)	4
Half Spiral	**0 J**	673.1 (97.6)	107.4 (15.6)	16
	5 J	411.9 (59.7)	47.6 (6.9)	12
	10 J	234.2 (34.0)	42.1 (6.1)	18

The average strain at maximum stress for each configuration of the 8 mm (5/16") diameter, 76 mm (3") length specimens based on extensometer strain and machine strain are presented in Table 4.27 and Table 4.28.

Table 4.27: Average Strain at Maximum Stress Based on Extensometer Strain, 8mm (5/16") Diameter, 76 mm (3") Length

Specimen Configuration & Impact Energy		Average Max [10^3 με]	Standard Deviation [10^3 με]	Standard Deviation [%]
Full Braid	**0 J**	13.8	7.0	51
	5 J	8.7	1.7	20
	10 J	11.8	5.5	47
Half Braid	**0 J**	12.7	3.7	29
	5 J	11.2	3.2	29
	10 J	10.5	8.0	76
Full Spiral	**0 J**	13.7	5.3	38
	5 J	8.7	2.2	25
	10 J	12.1	6.6	55
Half Spiral	**0 J**	10.7	1.8	17
	5 J	8.7	1.5	17
	10 J	8.0	1.1	14

Table 4.28: Average Strain at Maximum Stress Based on Machine Strain, 8mm (5/16") Diameter, 76 mm (3") Length

Specimen Configuration & Impact Energy		Average Max [10^3 με]	Standard Deviation [10^3 με]	Standard Deviation [%]
Full Braid	**0 J**	12.4	0.32	3
	5 J	8.2	0.8	10
	10 J	6.0	0.8	13
Half Braid	**0 J**	11.7	1.5	13
	5 J	8.8	1.2	14
	10 J	5.8	1.1	19
Full Spiral	**0 J**	12.7	1.5	12
	5 J	8.3	0.2	2
	10 J	6.4	0.4	6
Half Spiral	**0 J**	11.4	1.2	11
	5 J	6.9	0.8	12
	10 J	5.6	0.5	9

The average compression Young's modulus for each configuration of the 8 mm (5/16") diameter, 76 mm (3") length specimens based on extensometer strain and machine strain are presented in Table 4.29 and Table 4.30.

Table 4.29: Average Compression Young's Modulus Based on Extensometer Strain, 8mm (5/16") Diameter, 76 mm (3") Length

Specimen Configuration & Impact Energy		Average Max [GPa (10^6 psi)]	Standard Deviation	
			[GPa (10^6 psi)]	[%]
Full Braid	**0 J**	69.5 (10.1)	11.3 (1.6)	16
	5 J	61.8 (8.7)	8.9 (0.5)	14
	10 J	50.0 (7.3)	0.7 (0.1)	2
Half Braid	**0 J**	64.4 (9.3)	7.3 (1.1)	12
	5 J	61.4 (8.9)	5.3 (0.8)	9
	10 J	53.3 (7.7)	32.3 (4.7)	61
Full Spiral	**0 J**	61.3 (8.9)	6.3 (0.9)	10
	5 J	64.8 (9.4)	4.4 (0.6)	7
	10 J	55.1 (8.0)	11.1 (1.6)	20
Half Spiral	**0 J**	60.3 (8.8)	4.0 (0.6)	7
	5 J	55.6 (8.1)	1.9 (0.3)	4
	10 J	47.9 (7.0)	8.2 (1.2)	17

Table 4.30: Average Compression Young's Modulus Based on Machine Strain, 8mm (5/16") Diameter, 76 mm (3") Length

Specimen Configuration & Impact Energy		Average Max [GPa (10^6 psi)]	Standard Deviation	
			[GPa (10^6 psi)]	[%]
Full Braid	**0 J**	64.1 (9.3)	2.3 (0.3)	4
	5 J	59.8 (8.2)	3.1 (0.9)	5
	10 J	53.7 (7.8)	3.9 (0.6)	7
Half Braid	**0 J**	68.1 (9.9)	3.6 (0.5)	5
	5 J	67.2 (9.8)	4.2 (0.6)	6
	10 J	54.4 (7.9)	9.0 (1.3)	17
Full Spiral	**0 J**	63.3 (9.2)	2.9 (0.4)	5
	5 J	65.9 (9.6)	0.6 (0.1)	1
	10 J	55.9 (8.1)	1.6 (0.2)	3
Half Spiral	**0 J**	61.2 (8.9)	2.8 (0.4)	5
	5 J	63.3 (9.2)	1.8 (0.3)	3
	10 J	49.9 (7.2)	5.8 (0.8)	12

5 PRIMARY TEST RESULTS

Primary test results are presented in this chapter for the 8 mm (5/16”) [33] and the 11 mm (7/16”) specimens with a 51 mm (2”) length. These results are based on machine strain only, since extensometer data was not collected. Each test configuration is presented in a sub-section with a stress-strain plot and a summary table. The summary table includes the cross-sectional area of the specimen, the compression strength, the corresponding strain, and the Young’s modulus. A picture of each failed specimen, while loaded, is in Appendix F.

5.1 Test Results for the 5/16” Diameter 2” Length Specimens

The test results in this section are based on 8 mm (5/16”) diameter specimens with an unsupported length of 51 mm (2”). Each configuration is presented (Full Braid, Half Braid, Full Spiral, Half Spiral) for No-impact, 5 J (3.7 ft-lbs.), and 10 J (7.4 ft-lbs.) of impact energy.

5.1.1 Full Braid No-impact (5BA43FNC2)

The full braid coverage, no-impact specimen test results are presented in stress-strain curves in Figure 5.1 and summarized in Table 5.1. The average compression strength is 762.9 MPa (110.9 ksi), the corresponding strain is 13.66 mm/mm (in./in.), and the average Young’s modulus is 61.3 GPa (8.9×10^6 psi).

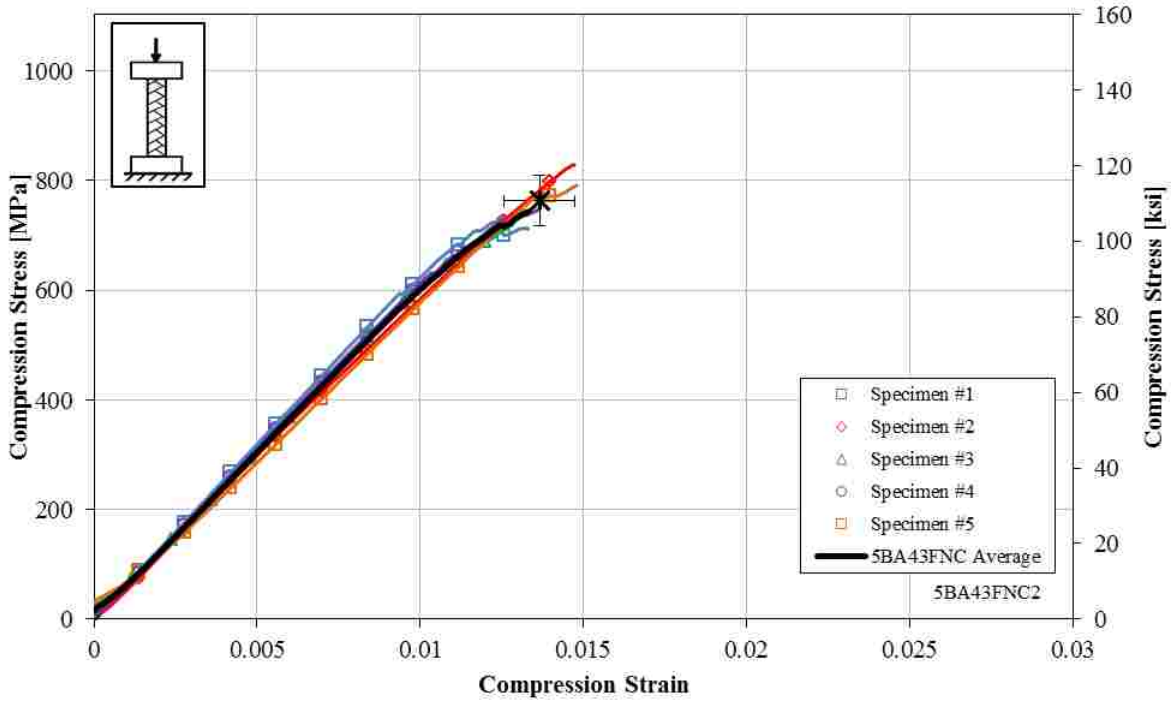

Figure 5.1: Stress-Strain Plot for Full Braid, No-Impact Specimen, 8 mm (5/16") Diameter, 51 mm (2") Length, (5BA43FNC2)

Table 5.1: Summary Table for Full Braid, No-Impact Specimen, 8 mm (5/16") Diameter, 51 mm (2") Length, (5BA43FNC2)

Specimen Number (5BA43FNC2)	Cross Sectional Area [mm^2 (in^2)]	Ultimate Compression Strength [MPa (ksi)]	Strain at Max Stress [10^3 με]	Compression Young's Modulus [GPa (10^6 psi)]
1	49.5 (0.077)	727.5 (105.5)	12.4	63.8 (9.3)
2	49.7 (0.077)	828.8 (120.2)	14.7	60.1 (8.7)
3	48.7 (0.076)	719.5 (104.3)	12.8	62.3 (9.0)
4	50.7 (0.079)	746.9 (108.3)	13.6	62.5 (9.1)
5	49.4 (0.077)	791.6 (114.8)	14.8	58.0 (8.4)
Average	49.6 (0.077)	762.9 (110.6)	13.7	61.3 (8.9)
Standard Deviation	0.72 (0.001)	46.3 (6.7)	1.1	2.3 (0.3)
	1.5%	6.1%	3.7%	7.9%

5.1.2 Full Braid 5 J Impact (5BA43FLC2)

The full braid coverage, 5 J (3.7 ft-lbs.) impact specimen test results are presented in the stress-strain plot shown in Figure 5.2 and summarized in Table 5.2. The average compression strength is 558.1 MPa (80.9 ksi), the corresponding strain is 10.23 mm/mm (in./in.), and the average Young's modulus is 60.1 GPa ($8.7x10^6$ psi).

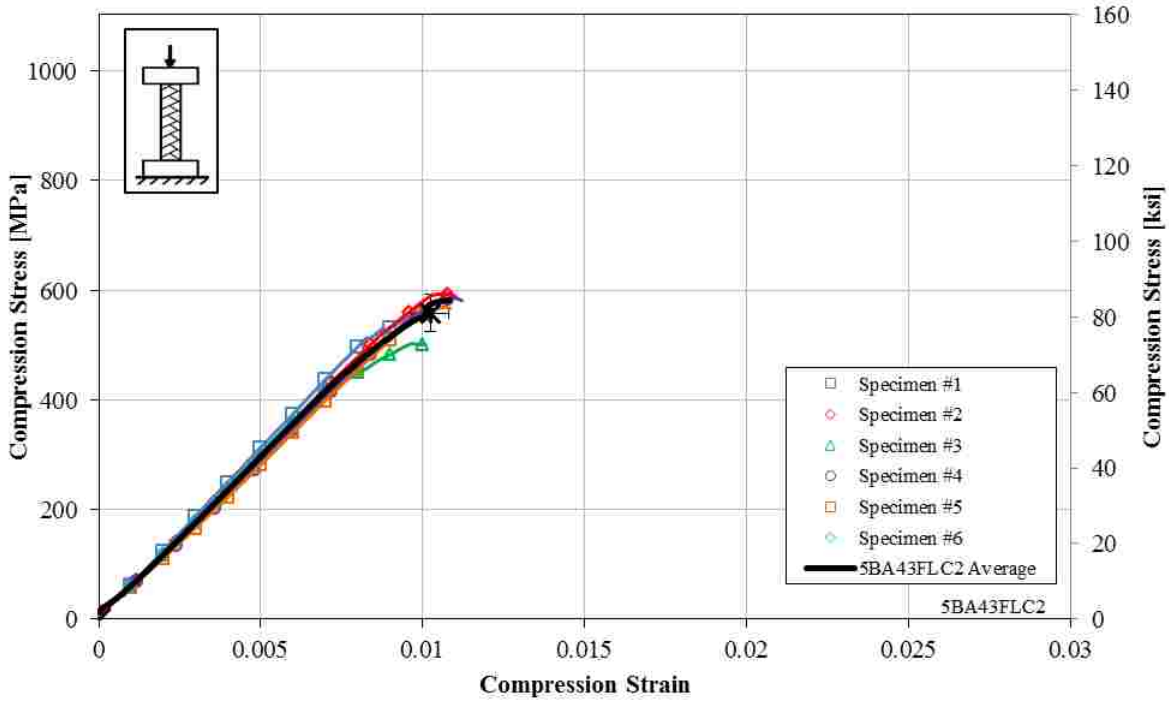

Figure 5.2: Stress-Strain Plot for Full Braid, 5 J (3.7 ft-lbs.) Impact Specimen, 8 mm (5/16") Diameter, 51 mm (2") Length, (5BA43FLC2)

5.1.3 Full Braid 10 J Impact (5BA43FSC2)

The full braid coverage, 10 J (7.4 ft-lbs.) impact specimen test results are presented in the stress-strain plot shown in Figure 5.3 and summarized in Table 5.3. The average compression strength is 437.1 MPa (63.4 ksi), the corresponding strain is 8.27 mm/mm (in./in.), and the average Young's modulus is 61.1 GPa ($8.9 x10^6$ psi).

Table 5.2: Summary Table for Full Braid, 5 J (3.7 ft-lbs.) Impact Specimen, 8 mm (5/16") Diameter, 51 mm (2") Length, (5BA43FLC2)

Specimen Number (5BA43FLC2)	Cross Sectional Area [mm^2 (in^2)]	Ultimate Compression Strength [MPa (ksi)]	Strain at Max Stress [10^3 με]	Compression Young's Modulus [GPa (10^6 psi)]
1	48.9 (0.076)	560.3 (81.3)	10.1	62.3 (9.0)
2	48.9 (0.076)	593.5 (86.1)	10.5	60.7 (8.8)
3	49.5 (0.077)	503.4 (73.0)	9.7	60.1 (8.7)
4	49.2 (0.076)	587.0 (85.1)	10.9	58.8 (8.5)
5	49.3 (0.076)	569.8 (82.6)	10.7	58.0 (8.4)
6	49.6 (0.077)	534.5 (77.5)	9.5	60.5 (8.8)
Average	49.2 (0.076)	558.1 (80.9)	10.2	60.1 (8.7)
Standard Deviation	0.28 (0.000)	34.0 (4.9)	0.6	1.5 (0.2)
	0.6%	6.1%	2.5%	5.6%

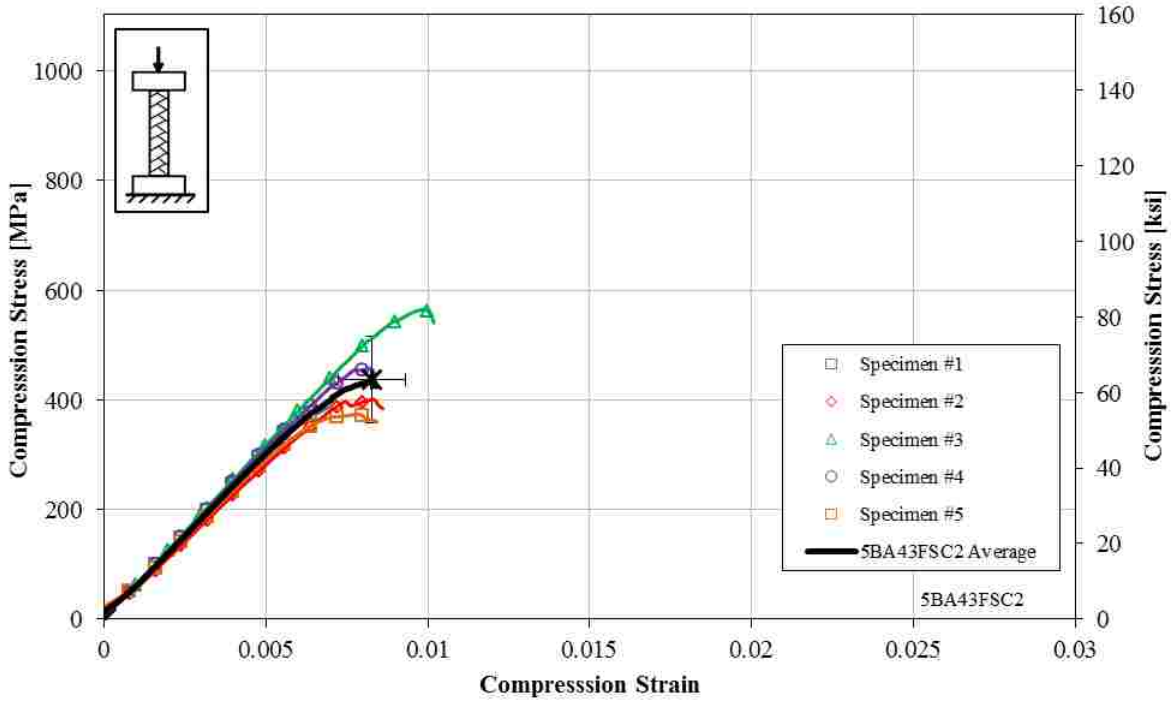

Figure 5.3: Stress-Strain Plot for Full Braid, 10 J (7.4 ft-lbs.) Impact Specimen, 8 mm (5/16") Diameter, 51 mm (2") Length, (5BA43FSC2)

Table 5.3: Summary Table for Full Braid, 10 J (7.4 ft-lbs.) Impact Specimen, 8 mm (5/16") Diameter, 51 mm (2") Length, (5BA43FSC2)

Specimen Number (5BA43FSC2)	Cross Sectional Area [mm^2 (in^2)]	Ultimate Compression Strength [MPa (ksi)]	Strain at Max Stress [10^3 με]	Compression Young's Modulus [GPa (10^6 psi)]
1	49.9 (0.077)	387.0 (56.1)	7.0	62.3 (9.0)
2	49.4 (0.077)	401.2 (58.2)	8.4	57.6 (8.4)
3	49.5 (0.077)	565.2 (82.0)	9.9	63.9 (9.3)
4	50.5 (0.078)	458.4 (66.5)	8.2	62.8 (9.1)
5	49.0 (0.076)	373.8 (54.2)	7.9	59.0 (8.6)
Average	49.7 (0.077)	437.1 (63.4)	8.3	61.1 (8.9)
Standard Deviation	0.58 (0.001)	78.5 (11.4)	1.0	2.7 (0.4)
	1.2%	18.0%	4.4%	12.6%

5.1.4 Half Braid No-impact (5BA43HNC2)

The full braid, no-impact results are shown in the stress-strain plot in Figure 5.4 and summarized in Table 5.4. The average compression strength is 761.1 MPa (110.4 ksi), the corresponding strain is 14.13 mm/mm (in./in.), and the average Young's modulus is 59.8 GPa ($8.7x10^6$ psi). Specimen 2 was eliminated based on Chauvenet's envelope for Young's modulus.

5.1.5 Half Braid 5 J Impact (5BA43HLC2)

The half braid coverage, 5 J (3.7 ft-lbs.) impact specimen test results are presented in the stress-strain plot shown in Figure 5.5 and summarized in Table 5.5. The average compression strength is 360.0 MPa (52.2 ksi), the corresponding strain is 7.00 mm/mm (in./in.), and the average Young's modulus is 57.7 GPa ($8.4x10^6$ psi).

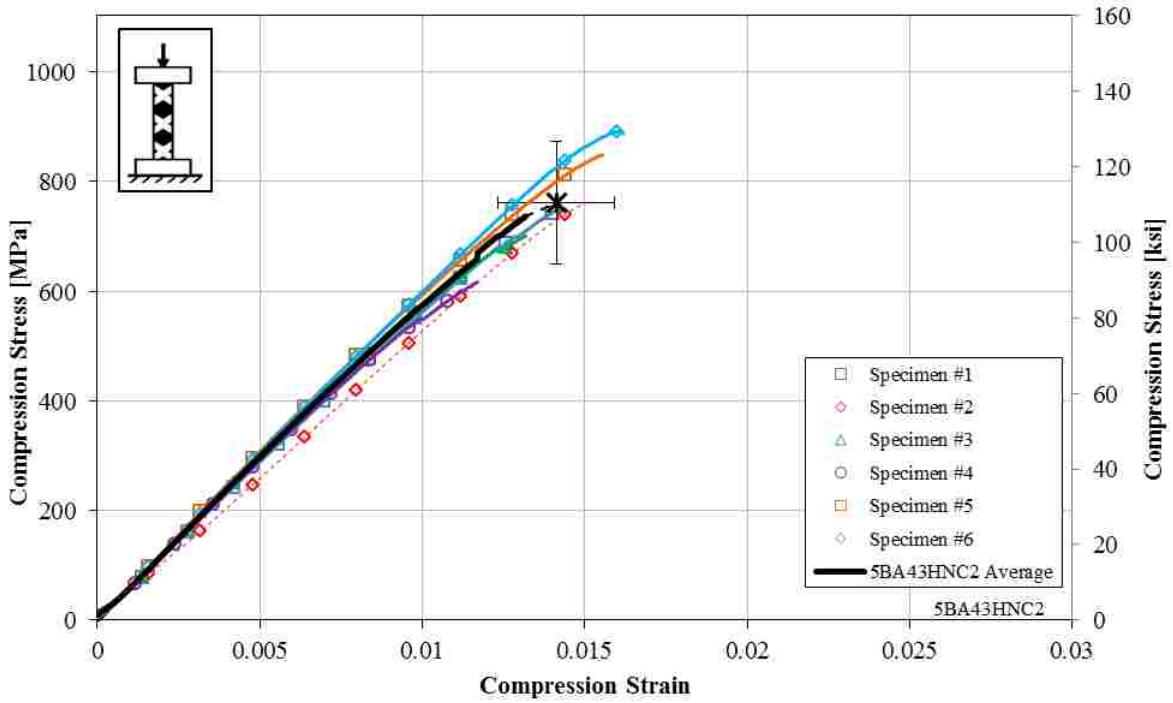

Figure 5.4: Stress-Strain Plot for Half Braid, No-Impact Specimen, 8 mm (5/16") Diameter, 51 mm (2") Length, (5BA43HNC2)

Table 5.4: Summary Table for Half Braid, No-Impact Specimen, 8 mm (5/16") Diameter, 51 mm (2") Length, (5BA43HNC2)

Specimen Number (5BA43HNC2)	Cross Sectional Area [mm^2 (in^2)]	Ultimate Compression Strength [MPa (ksi)]	Strain at Max Stress [10^3 με]	Compression Young's Modulus [GPa (10^6 psi)]
1	54.0 (0.084)	748.9 (108.6)	14.2	57.8 (8.4)
2	54.2 (0.084)	765.3 (111.0)	15.2	51.8 (7.5)*
3	54.4 (0.084)	700.3 (101.6)	13.2	59.7 (8.7)
4	55.0 (0.085)	615.6 (89.3)	11.7	58.6 (8.5)
5	55.4 (0.086)	848.5 (123.1)	15.5	61.8 (9.0)
6	53.7 (0.083)	892.4 (129.4)	16.1	61.1 (8.9)
Average	54.4 (0.084)	761.1 (110.4)	14.1	59.8 (8.7)
Standard Deviation	0.68 (0.001)	111.7 (16.2)	1.8	1.6 (0.2)
	1.2%	14.7%	2.8%	12.6%

* *Specimen did not pass Chauvenet's Criterion, not included in averages.*

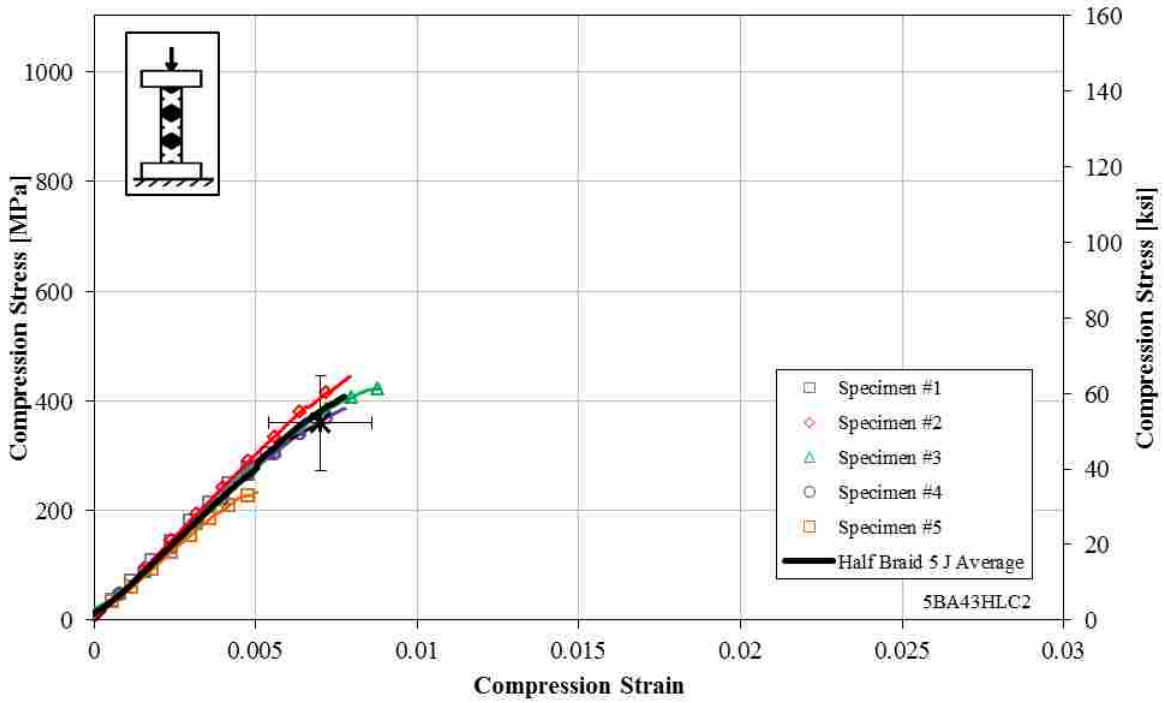

Figure 5.5: Stress-Strain Plot for Half Braid, 5 J (3.7 ft-lbs.) Impact Specimen, 8 mm (5/16") Diameter, 51 mm (2") Length, (5BA43HLC2)

Table 5.5: Summary Table for Half Braid, 5 J (3.7 ft-lbs.) Impact Specimen, 8 mm (5/16") Diameter, 51 mm (2") Length, (5BA43HLC2)

Specimen Number (5BA43HLC2)	Cross Sectional Area [mm^2 (in^2)]	Ultimate Compression Strength [MPa (ksi)]	Strain at Max Stress [10^3 με]	Compression Young's Modulus [GPa (10^6 psi)]
1	54.7 (0.085)	314.2 (45.6)	5.6	60.4 (8.8)
2	53.9 (0.084)	444.8 (64.5)	7.9	61.4 (8.9)
3	54.6 (0.085)	422.1 (61.2)	8.7	56.0 (8.1)
4	53.8 (0.083)	385.7 (55.9)	7.7	57.0 (8.3)
5	54.3 (0.084)	233.4 (33.8)	5.0	53.7 (7.8)
Average	54.3 (0.084)	360.0 (52.2)	7.0	57.7 (8.4)
Standard Deviation	0.42 (0.001)	86.4 (12.5)	1.6	3.2 (0.5)
	0.8%	24.0%	5.6%	22.7%

5.1.6 Half Braid 10 J Impact (5BA43HSC2)

The half braid coverage, 10 J (7.4 ft-lbs.) impact specimen test results are presented in the stress-strain plot shown in Figure 5.6 and summarized in Table 5.6. The average compression

strength is 249.0 MPa (36.1 ksi), the corresponding strain is 5.69 mm/mm (in./in.), and the average Young's modulus is 54.0 GPa ($7.8x10^6$ psi). Specimen 2 was eliminated based on Chauvenet's envelope for Young's modulus.

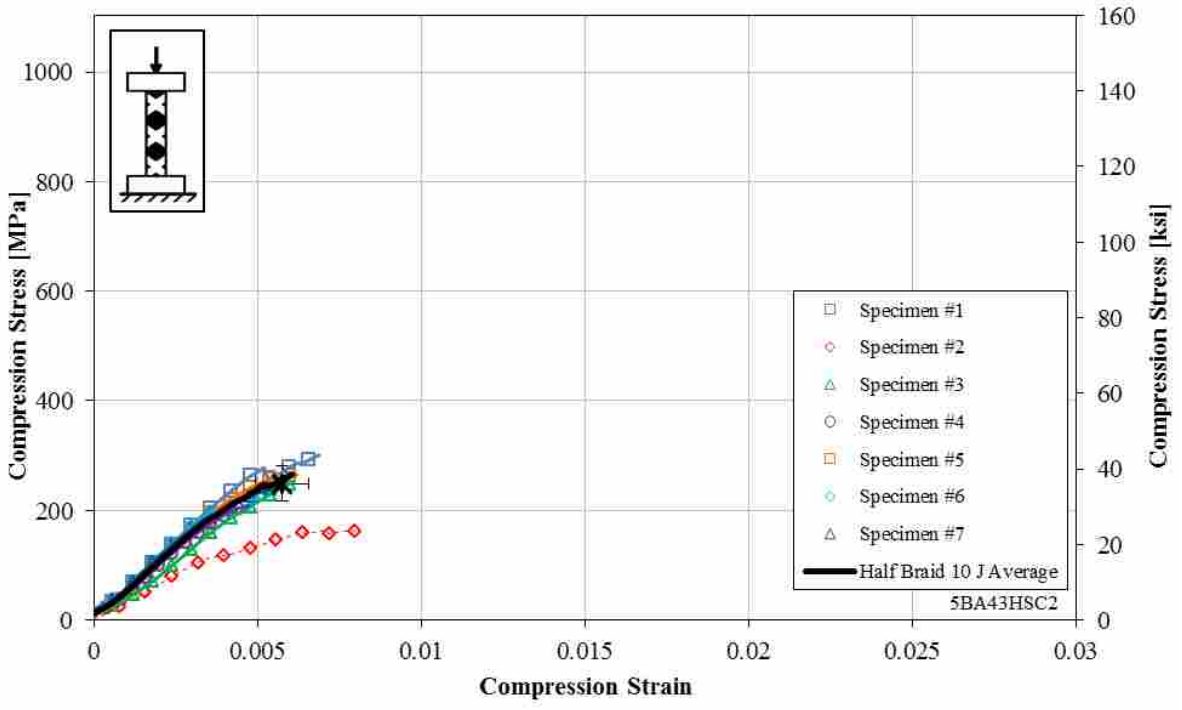

Figure 5.6: Stress-Strain Plot for Half Braid, 10 J (7.4 ft-lbs.) Impact Specimen, 8 mm (5/16") Diameter, 51 mm (2") Length, (5BA43HSC2)

5.1.7 Full Spiral No-impact (5BA10FNC2)

The full spiral coverage, no-impact specimen test results are presented in the stress-strain plot shown in Figure 5.7 and summarized in Table 5.7. The average compression strength is 723.4 MPa (104.9 ksi), the corresponding strain is 13.40 mm/mm (in./in.), and the average Young's modulus is 57.6 GPa ($8.3x10^6$ psi). Specimen 6 was eliminated based on Chauvenet's envelope for Young's modulus.

Table 5.6: Summary Table for Half Braid, 10 J (7.4 ft-lbs.) Impact Specimen, 8 mm (5/16") Diameter, 51 mm (2") Length, (5BA43HSC2)

Specimen Number (5BA43HSC2)	Cross Sectional Area [mm^2 (in^2)]	Ultimate Compression Strength [MPa (ksi)]	Strain at Max Stress [10^3 με]	Compression Young's Modulus [GPa (10^6 psi)]
1	54.4 (0.084)	301.0 (43.7)	6.9	58.2 (8.4)
2	58.4 (0.091)	165.2 (24.0)	7.1	34.3 (5.0)*
3	53.5 (0.083)	251.8 (36.5)	6.1	43.3 (6.3)
4	52.2 (0.081)	208.9 (30.3)	4.7	52.0 (7.5)
5	54.2 (0.084)	265.0 (38.4)	6.2	57.4 (8.3)
6	52.4 (0.081)	225.4 (32.7)	4.6	56.0 (8.1)
7	53.5 (0.083)	242.2 (35.1)	5.6	57.1 (8.3)
Average	54.1 (0.084)	249.0 (36.1)	5.7	54.0 (7.8)
Standard Deviation	0.83 (0.003)	32.2 (4.7)	0.9	5.7 (0.8)
	3.5%	12.9%	10.5%	15.6%

* *Specimen did not pass Chauvenet's Criterion, not included in averages.*

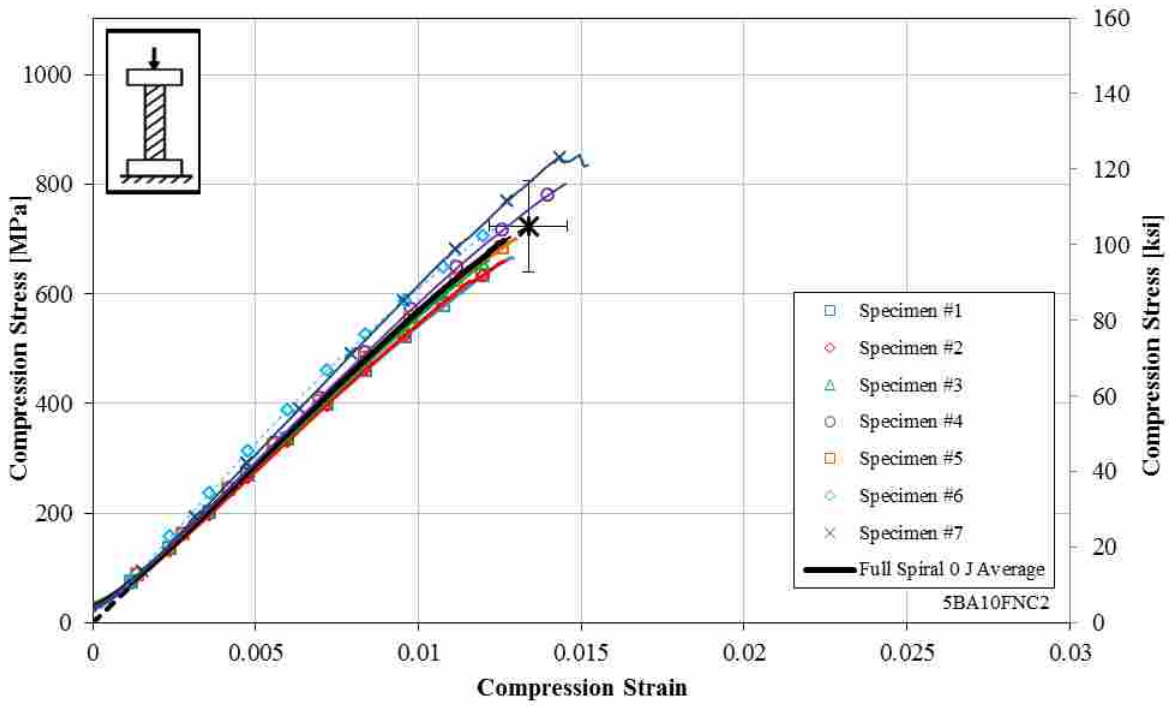

Figure 5.7: Stress-Strain Plot for Full Spiral, No-Impact Specimen, 8 mm (5/16") Diameter, 51 mm (2") Length, (5BA10FNC2)

Table 5.7: Summary Table for Full Spiral, No-Impact Specimen, 8 mm (5/16") Diameter, 51 mm (2") Length, (5BA10FNC2)

Specimen Number (5BA10FNC2)	Cross Sectional Area [mm^2 (in^2)]	Ultimate Compression Strength [MPa (ksi)]	Strain at Max Stress [10^3 με]	Compression Young's Modulus [GPa (10^6 psi)]
1	51.1 (0.079)	666.5 (96.7)	12.85	55.9 (8.1)
2	51.4 (0.080)	659.0 (95.6)	12.64	55.5 (8.1)
3	50.9 (0.079)	660.0 (95.7)	12.12	56.5 (8.2)
4	51.3 (0.079)	800.8 (116.1)	14.52	58.8 (8.5)
5	50.9 (0.079)	700.2 (101.6)	12.95	58.1 (8.4)
6	49.6 (0.077)	728.1 (105.6)	12.63	65.1 (9.4)*
7	49.0 (0.076)	853.6 (123.8)	15.20	60.5 (8.8)
Average	50.6 (0.078)	723.4 (104.9)	13.40	57.6 (8.3)
Standard Deviation	0.9 (0.001)	83.5 (12.11)	1.20	1.9 (0.3)
	1.8%	11.5%	8.9%	3.3%

* *Specimen did not pass Chauvenet's Criterion, not included in averages.*

5.1.8 Full Spiral 5 J Impact (5BA10FLC2)

The full spiral coverage, 5 J (3.7 ft-lbs.) impact specimen test results are presented in the stress-strain plot shown in Figure 5.8 and summarized in Table 5.8. The average compression strength is 675.2 MPa (97.93 ksi), the corresponding strain is 11.7 mm/mm (in./in.), and the average Young's modulus is 62.0 GPa (9.0 x10^6 psi).

5.1.9 Full Spiral 10 J Impact (5BA10FSC2)

The full spiral coverage, 10 J (7.4 ft-lbs.) impact specimen test results are presented in the stress-strain plot shown in Figure 5.9 and summarized in Table 5.9. The average compression strength is 395.0 MPa (57.3 ksi), the corresponding strain is 7.71 mm/mm (in./in.), and the average Young's modulus is 55.8 GPa (8.1 x10^6 psi).

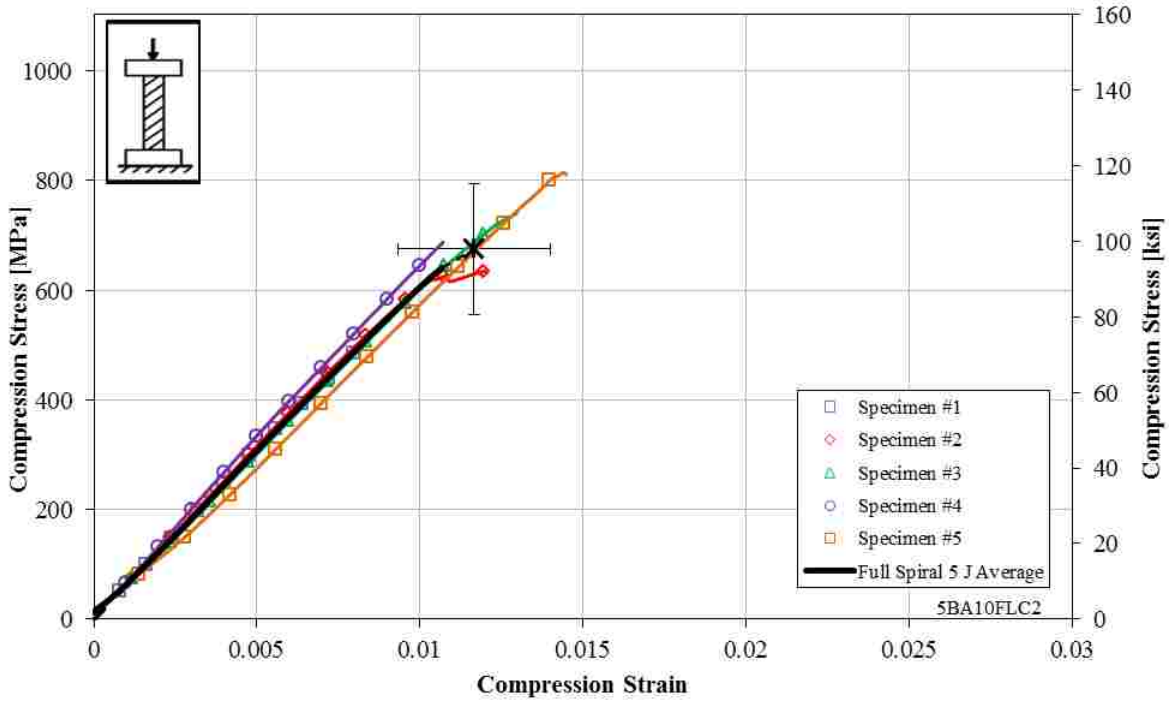

Figure 5.8: Stress-Strain Plot for Full Spiral, 5 J (3.7 ft-lbs.) Impact Specimen, 8 mm (5/16") Diameter, 51 mm (2") Length, (5BA10FLC2)

Table 5.8: Summary Table for Full Spiral, 5 J (3.7 Ft-lbs.) Impact Specimen, 8 mm (5/16") Diameter, 51 mm (2") Length, (5BA10FLC2)

Specimen Number (5BA10FLC2)	Cross Sectional Area [mm^2 (in^2)]	Ultimate Compression Strength [MPa (ksi)]	Strain at Max Stress [10^3 με]	Compression Young's Modulus [GPa (10^6 psi)]
1	50.7 (0.079)	499.1 (72.4)	8.3	61.3 (8.9)
2	50.7 (0.079)	634.7 (92.1)	12.0	62.8 (9.1)
3	50.5 (0.078)	739.9 (107.3)	13.0	61.1 (8.9)
4	50.5 (0.078)	686.8 (99.6)	10.7	66.2 (9.6)
5	51.3 (0.080)	815.8 (118.3)	14.40	58.5 (8.5)
Average	50.8 (0.079)	675.2 (97.93)	11.7	62.0 (9.0)
Standard Deviation	0.35 (0.001)	119.1 (17.28)	2.3	2.8 (0.4)
	0.7%	17.6%	20.0%	4.5%

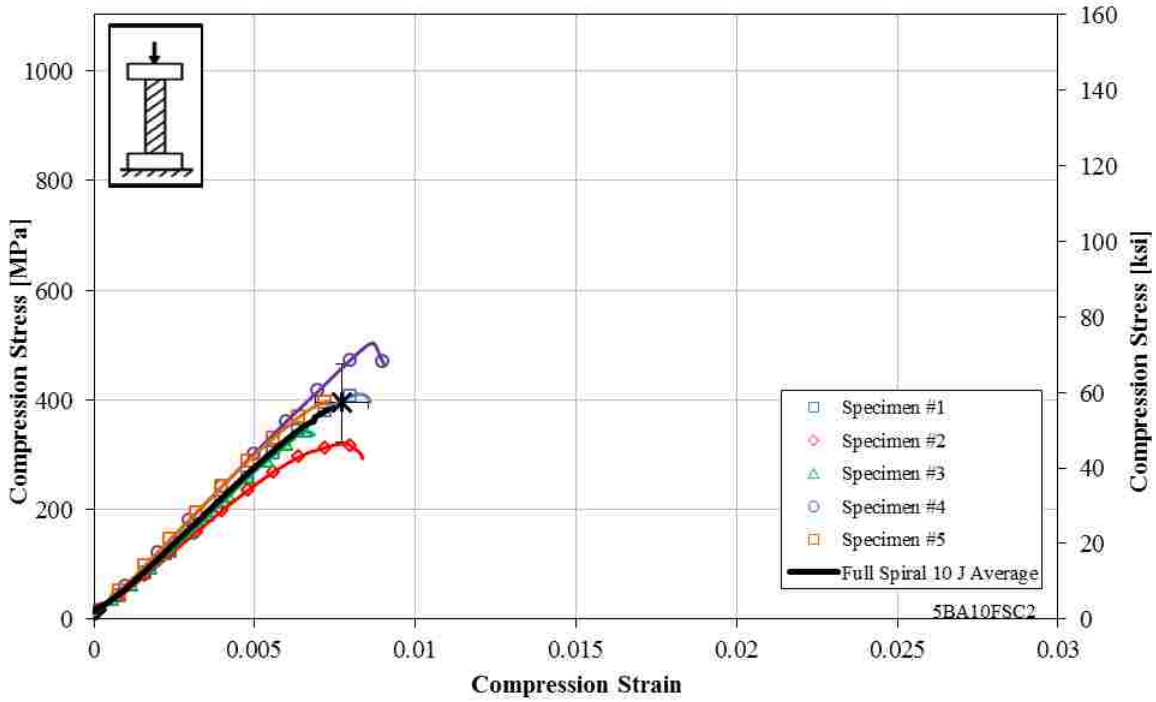

Figure 5.9: Stress-Strain Plot for Full Spiral, 10 J (7.4 ft-lbs.) Impact Specimen, 8 mm (5/16") Diameter, 51 mm (2") Length, (5BA10FSC2)

Table 5.9: Summary Table for Full Spiral, 10 J (7.4 Ft-lbs.) Impact Specimen, 8 mm (5/16") Diameter, 51 mm (2") Length, (5BA10FSC2)

Specimen Number (5BA10FSC2)	Cross Sectional Area [mm^2 (in^2)]	Ultimate Compression Strength [MPa (ksi)]	Strain at Max Stress [10^3 με]	Compression Young's Modulus [GPa (10^6 psi)]
1	50.7 (0.079)	410.4 (59.5)	8.3	53.6 (7.8)
2	51.7 (0.080)	320.7 (46.5)	7.8	49.9 (7.2)
3	51.0 (0.079)	342.7 (49.7)	6.6	53.2 (7.7)
4	51.5 (0.080)	504.0 (73.1)	8.7	61.1 (8.9)
5	50.7 (0.079)	396.9 (57.6)	7.2	61.3 (8.9)
Average	51.1 (0.079)	395.0 (57.3)	7.7	55.8 (8.1)
Standard Deviation	0.43 (0.001)	71.4 (10.4)	0.8	5.1 (0.7)
	0.8%	18.1%	10.7%	9.2%

5.1.10 Half Spiral No-impact (5BA10HNC2)

The half spiral coverage, no-impact specimen test results are presented in the stress-strain plot shown in Figure 5.10 and summarized in Table 5.10. The average compression strength is 683.5 MPa (99.1 ksi), the corresponding strain is 12.14 mm/mm (in./in.), and the average Young's modulus is 60.5 GPa ($8.8x10^6$ psi).

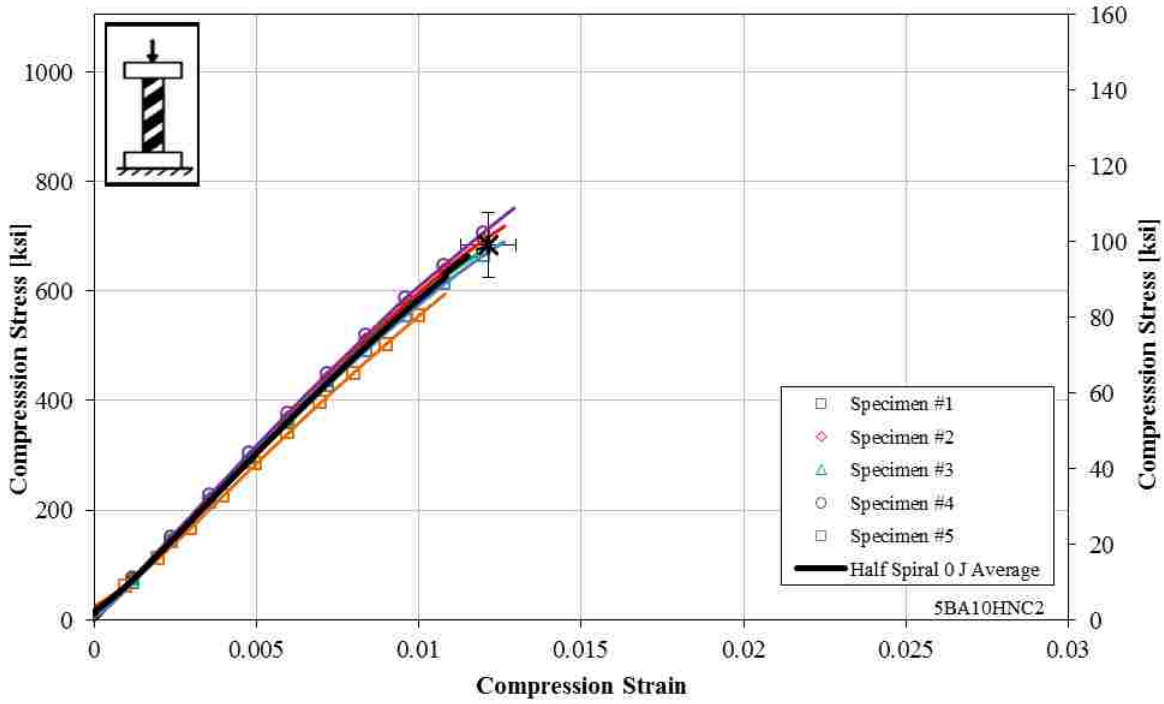

Figure 5.10: Stress-Strain Plot for Half Spiral, No-Impact Specimen, 8 mm (5/16") Diameter, 51 mm (2") Length, (5BA10HNC2)

5.1.11 Half Spiral 5 J Impact (5BA10HLC2)

The half spiral coverage, 5 J (3.7 ft-lbs.) impact specimen test results are presented in the stress-strain plot shown in Figure 5.11 and summarized in Table 5.11. The average compression strength is 379.7 MPa (55.1ksi), the corresponding strain is 7.30 mm/mm (in./in.), and the average Young's modulus is 57.8 GPa ($8.4x10^6$ psi).

Table 5.10: Summary Table for Half Spiral, No-Impact Specimen, 8 mm (5/16") Diameter, 51 mm (2") Length, (5BA10HNC2)

Specimen Number (5BA10HNC2)	Cross Sectional Area [mm^2 (in^2)]	Ultimate Compression Strength [MPa (ksi)]	Strain at Max Stress [10^3 με]	Compression Young's Modulus [GPa (10^6 psi)]
1	51.5 (0.080)	689.3 (100.0)	12.6	59.9 (8.7)
2	51.9 (0.080)	717.9 (104.1)	12.6	61.8 (9.0)
3	52.6 (0.082)	665.9 (96.6)	11.8	60.8 (8.8)
4	51.6 (0.080)	750.4 (108.8)	12.9	62.7 (9.1)
5	51.9 (0.081)	594.1 (86.2)	10.8	57.3 (8.3)
Average	51.9 0.080	683.5 (99.1)	12.1	60.5 (8.8)
Standard Deviation	0.42 0.001	59.1 (8.6)	0.9	2.1 (0.3)
	0.8%	8.7%	3.4%	7.1%

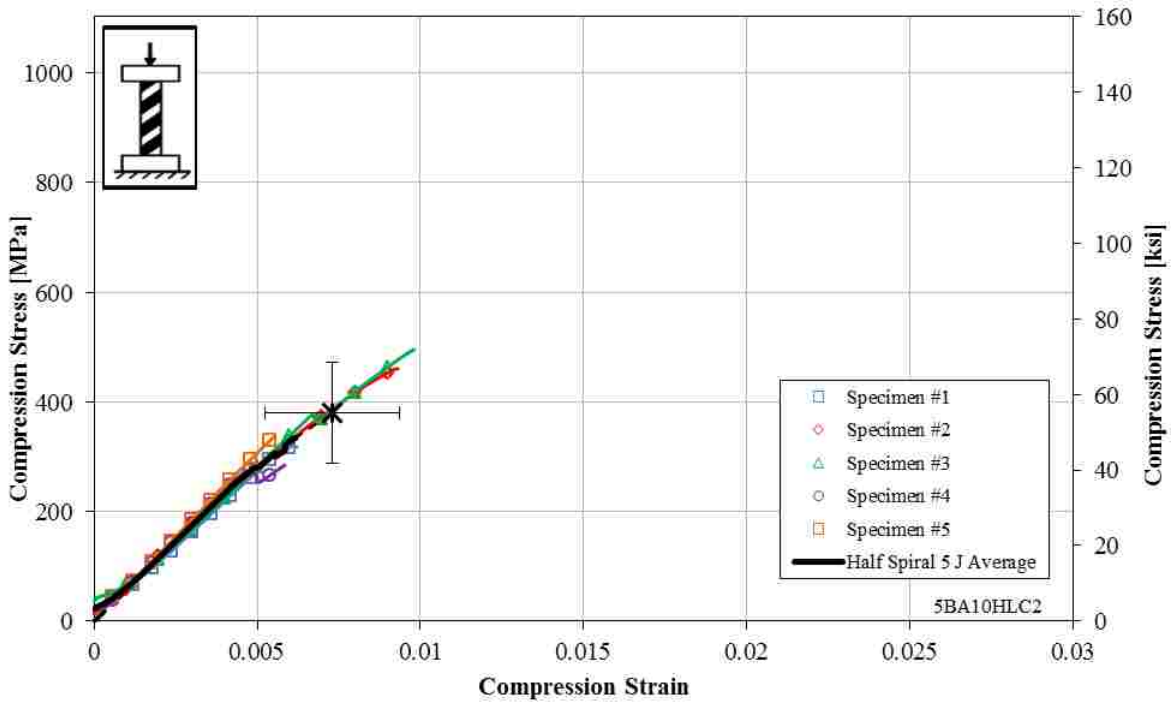

Figure 5.11: Stress-Strain Plot for Half Spiral, 5 J (3.7 ft-lbs.) Impact Specimen, 8 mm (5/16") Diameter, 51 mm (2") Length, (5BA10HLC2)

Table 5.11: Summary Table for Half Spiral, 5 J (3.7 ft-lbs.) Impact Specimen, 8 mm (5/16") Diameter, 51 mm (2") Length, (5BA10HLC2)

Specimen Number (5BA10HLC2)	Cross Sectional Area [mm^2 (in^2)]	Ultimate Compression Strength [MPa (ksi)]	Strain at Max Stress [10^3 με]	Compression Young's Modulus [GPa (10^6 psi)]
1	51.9 (0.081)	321.8 (46.7)	6.1	54.0 (7.8)
2	52.0 (0.081)	460.9 (66.8)	9.3	59.6 (8.6)
3	51.7 (0.080)	495.2 (71.8)	9.8	53.5 (7.8)
4	52.1 (0.081)	284.2 (41.2)	5.8	60.4 (8.8)
5	51.9 (0.080)	336.6 (48.8)	5.5	61.6 (8.9)
Average	51.9 (0.080)	379.7 (55.1)	7.3	57.8 (8.4)
Standard Deviation	0.13 (0.000)	92.5 (13.4)	2.1	3.8 (0.6)
	0.3%	24.4%	6.5%	28.2%

5.1.12 Half Spiral 10 J Impact (5BA10HSC2)

The full spiral coverage, 10 J (7.4 ft-lbs.) impact specimen test results are presented in the stress-strain plot shown in Figure 5.12 and summarized in Table 5.12. The average compression strength is 221.9 MPa (32.2 ksi), the corresponding strain is 5.50 mm/mm (in./in.), and the average Young's modulus is 52.3 GPa ($7.6x10^6$ psi). Specimen 6 was eliminated based on Chauvenet's envelope for Young's modulus.

5.1.13 Configuration Averages Summary, 7/16" Diameter, 2" Length

A summary of results for the 8 mm (5/16") diameter, 51 mm (2") length specimens are presented here. Table 5.13 presents the average compression strength, Table 5.14 presents the corresponding strain and Table 5.15 presents the average Young's modulus.

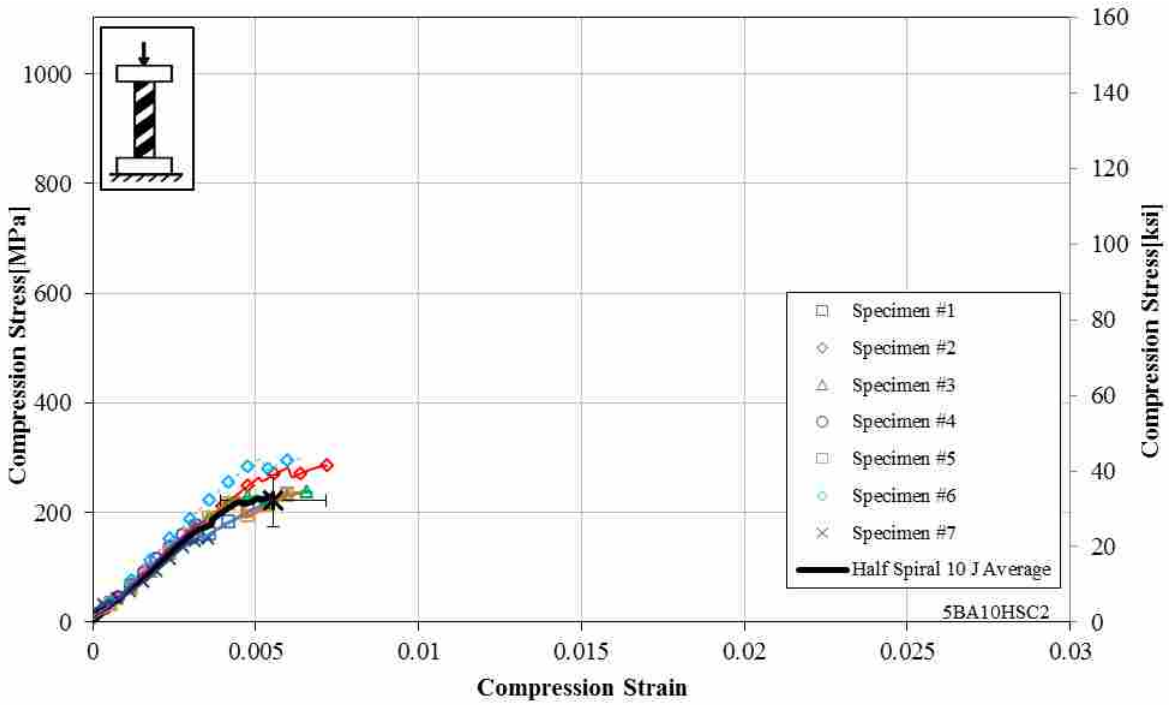

Figure 5.12: Stress-Strain Plot for Full Spiral, 10 J (7.4 ft-lbs.) Impact Specimen, 8 mm (5/16") Diameter, 51 mm (2") Length, (5BA10FSC2)

Table 5.12: Summary Table for Full Spiral, 10 J (7.4 ft-lbs.) Impact Specimen, 8 mm (5/16") Diameter, 51 mm (2") Length, (5BA10FSC2)

Specimen Number (5BA10FSC2)	Cross Sectional Area [mm^2 (in^2)]	Ultimate Compression Strength [MPa (ksi)]	Strain at Max Stress [10^3 με]	Compression Young's Modulus [GPa (10^6 psi)]
1	52.0 (0.081)	233.9 (33.9)	6.02	50.3 (7.3)
2	51.6 (0.080)	286.5 (41.5)	7.15	49.0 (7.1)
3	51.9 (0.080)	238.2 (34.6)	6.64	52.7 (7.7)
4	52.1 (0.081)	183.5 (26.6)	3.41	56.5 (8.2)
5	52.2 (0.081)	236.3 (34.3)	6.37	53.3 (7.7)
6	52.1 (0.081)	300.1 (43.5)	6.30	64.1 (9.3)*
7	52.3 (0.081)	153.1 (22.2)	3.6	52.1 (7.6)
Average	52.0 (0.081)	221.9 (32.2)	5.5	52.3 (7.6)
Standard Deviation	0.2 (0.000)	46.9 (6.8)	1.6	2.6 (0.4)
	0%	3.1%	29%	4.9%

* *Specimen did not pass Chauvenet's Criterion, not included in averages.*

Table 5.13: Average Compression Strength, 8 mm (5/16") Diameter, 51 mm (2") Length

Specimen Configuration & Impact Energy		Average Max [MPa (ksi)]	Standard Deviation [MPa (ksi)]	[%]
Full Braid	**0 J**	763 (111)	46.3 (6.71)	6
	5 J	558 (80.9)	34.0 (4.93)	6
	10 J	437 (63.4)	78.5 (11.4)	18
Half Braid	**0 J**	761 (110)	112 (16.2)	15
	5 J	360 (52.2)	86.4 (12.5)	24
	10 J	238 (34.6)	52.5 (7.61)	22
Full Spiral	**0 J**	723 (104.9)	83.5 (12.1)	12
	5 J	675 (97.9)	119 (17.3)	18
	10 J	395 (57.3)	71.4 (10.4)	18
Half Spiral	**0 J**	684 (99.1)	59.1 (8.58)	9
	5 J	380 (55.1)	92.5 (13.4)	24
	10 J	222 (32.2)	46.9 (6.8)	3

Table 5.14: Average Strain at Maximum Stress, 8 mm (5/16") Diameter, 51 mm (2") Length

Specimen Configuration & Impact Energy		Average Max [10^3 με]	Standard Deviation [10^3 με]	[%]
Full Braid	**0 J**	13.7	1.08	8
	5 J	10.2	0.57	6
	10 J	8.27	1.04	13
Half Braid	**0 J**	14.1	1.79	13
	5 J	7.00	1.59	23
	10 J	6.29	1.23	20
Full Spiral	**0 J**	13.4	1.20	9
	5 J	11.7	2.33	20
	10 J	7.71	0.83	11
Half Spiral	**0 J**	12.1	0.86	7
	5 J	7.30	2.06	28
	10 J	5.50	1.60	29

Table 5.15: Average Young's Modulus, 8 mm (5/16") Diameter, 51 mm (2") Length

Specimen Configuration & Impact Energy		Average Max [GPa (10^6 psi)]	Standard Deviation [GPa (10^6 psi)]	[%]
Full Braid	0 J	61.3 (8.89)	2.30 (0.33)	4
	5 J	60.1 (8.71)	1.51 (0.22)	3
	10 J	61.1 (8.87)	2.68 (0.39)	4
Half Braid	0 J	59.8 (8.67)	1.65 (0.24)	3
	5 J	57.7 (8.37)	3.21 (0.46)	6
	10 J	50.1 (7.27)	10.6 (1.53)	21
Full Spiral	0 J	57.6 (8.30)	1.90 (0.30)	3
	5 J	62.0 (8.99)	2.82 (0.41)	5
	10 J	55.8 (8.10)	5.13 (0.74)	9
Half Spiral	0 J	60.5 (8.77)	2.07 (0.30)	3
	5 J	57.8 (8.38)	3.78 (0.55)	7
	10 J	52.3 (7.59)	2.6 (0.38)	5

5.2 Test Results for the 7/16" Diameter 2" Length Specimens

The test results in this section are based on 11 mm (7/16") diameter specimens with an unsupported length of 51 mm (2"). Each configuration is presented (Full Braid, Half Braid, Full Spiral, Half Spiral) for No-impact, 10 J (7.4 ft-lbs.), and 20 J (14.8 ft-lbs.) of impact energy.

5.2.1 Full Braid No-impact (7BA43FNC2)

The full braid coverage, no-impact specimen test results are presented in the stress-strain plot shown in Figure 5.13 and in summary Table 5.16. The average compression strength is 899.5 MPa (130.5 ksi), the corresponding strain is 16.1 mm/mm (in./in.), and the average Young's modulus is 60.4 GPa (8.8×10^6 psi). Specimen 4 was eliminated based on Chauvenet's envelope for compression strain, and Young's modulus.

5.2.2 Full Braid 10 J Impact (7BA43FLC2)

The full braid coverage, 10 J (7.4 ft-lbs.) impact specimen test results are presented in the stress-strain plot shown in Figure 5.14 and summarized in Table 5.17. The average compression strength is 693.0 MPa (100.5 ksi), the corresponding strain is 12.5 mm/mm (in./in.), and the average Young's modulus is 58.6 GPa ($8.5x10^6$ psi).

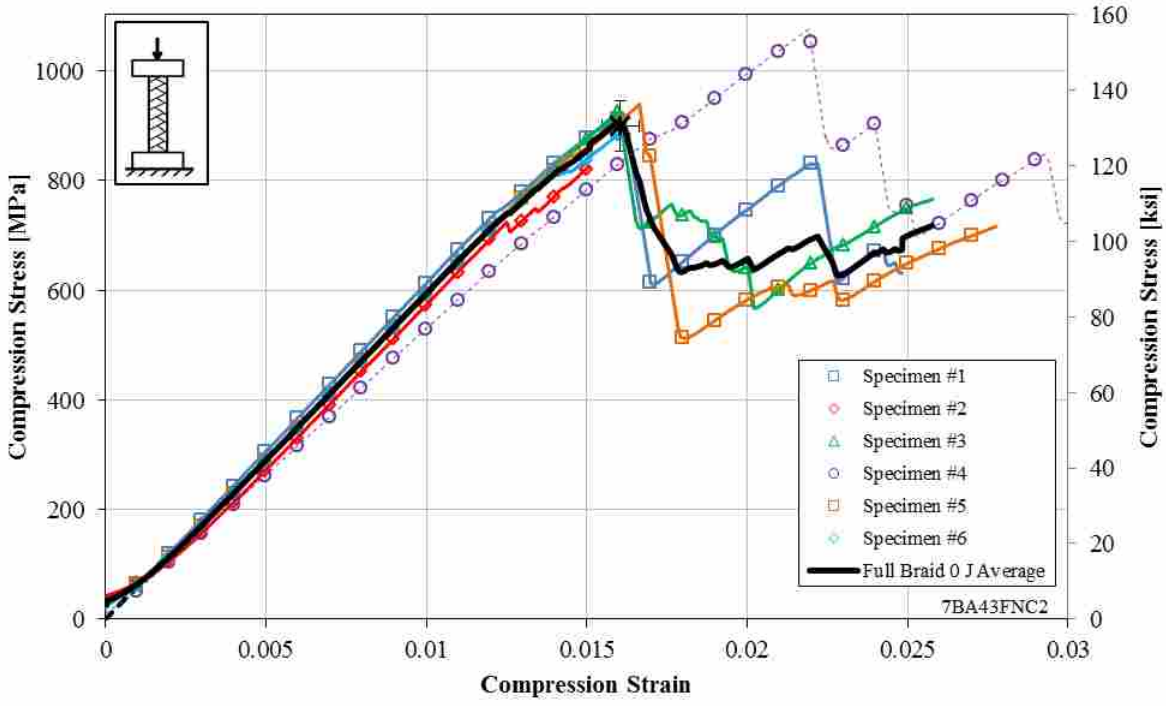

Figure 5.13: Stress-Strain Plot for Full Braid, No-Impact Specimen, 8 mm (5/16") Diameter, 51 mm (2") Length, (7BA43FNC2)

5.2.3 Full Braid 20 J Impact (7BA43FSC2)

The full braid coverage, 20 J (14.8 ft-lbs.) impact specimen test results are presented in the stress-strain plot shown in Figure 5.15 and summarized in Table 5.18. The average strength is 537.0 MPa (77.9 ksi), the corresponding strain is 10.2 mm/mm (in./in.), and the average Young's modulus is 51.2 GPa ($7.4x10^6$ psi).

Table 5.16: Summary Table for Full Braid, No-Impact Specimen, 8 mm (5/16") Diameter, 51 mm (2") Length, (7BA43FNC2)

Specimen Number (7BA43FNC2)	Cross Sectional Area [mm^2 (in^2)]	Ultimate Compression Strength [MPa (ksi)]	Strain at Max Stress [10^3 με]	Compression Young's Modulus [GPa (10^6 psi)]
1	94.1 (0.146)	919.9 (133.4)	16.1	61.5 (8.9)
2	94.4 (0.146)	825.4 (119.7)	15.1	59.6 (8.6)
3	94.3 (0.146)	925.7 (134.3)	16.2	60.5 (8.8)
4	95.8 (0.148)	1076.1 (156.1)*	21.9*	53.3 (7.7)*
5	93.5 (0.145)	937.2 (135.9)	16.6	60.5 (8.8)
6	94.5 (0.147)	889.2 (129.0)	16.3	60.3 (8.7)
Average	95.2 (0.148)	899.5 (130.5)	16.1	60.4 (8.8)
Standard Deviation	1.5 (0.002)	45.0 (6.5)	0.5	0.7 (0.1)
	1.5%	5.0%	3.1%	1.2%

* *Specimen did not pass Chauvenet's Criterion, not included in averages.*

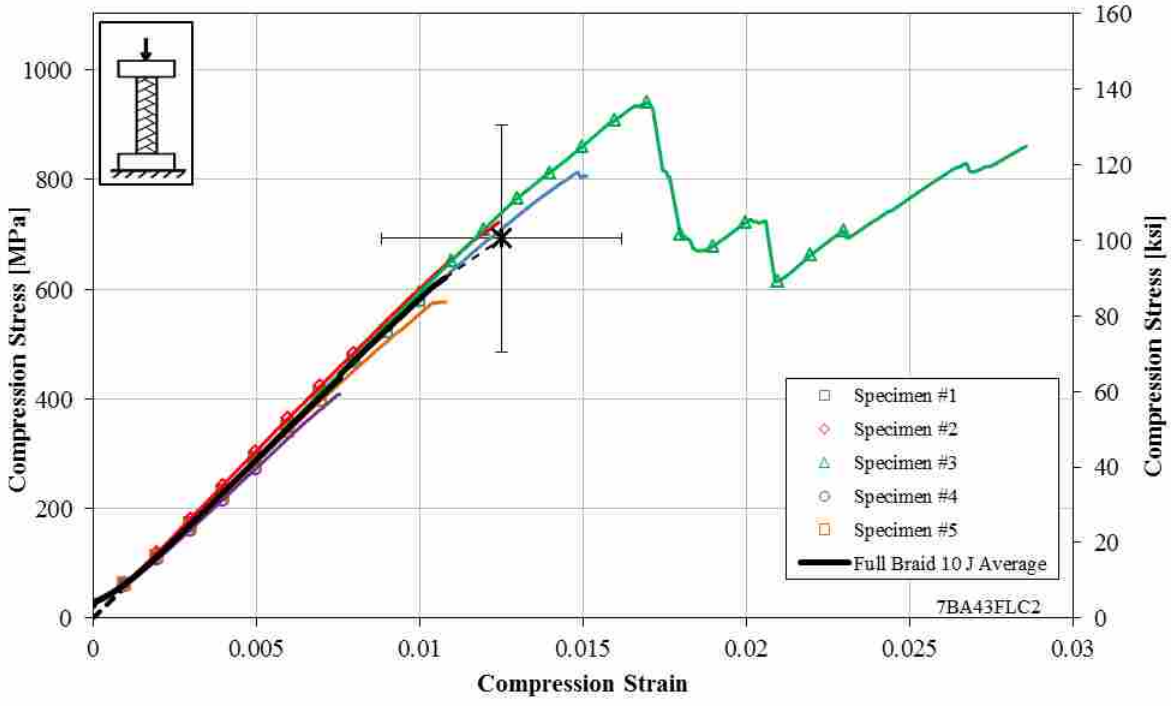

Figure 5.14: Stress-Strain Plot for Full Braid, 10 J (7.4 ft-lbs.) Impact Specimen, 8 mm (5/16") Diameter, 51 mm (2") Length, (7BA43FLC2)

Table 5.17: Summary Table for Full Braid, 10 J (7.4 ft-lbs.) Impact Specimen, 8 mm (5/16") Diameter, 51 mm (2") Length, (7BA43FLC2)

Specimen Number (7BA43FLC2)	Cross Sectional Area [mm^2 (in^2)]	Ultimate Compression Strength [MPa (ksi)]	Strain at Max Stress [10^3 με]	Compression Young's Modulus [GPa (10^6 psi)]
1	95.1 (0.148)	814.5 (118.1)	14.9	59.0 (8.6)
2	95.1 (0.148)	722.2 (104.7)	12.4	61.4 (8.9)
3	95.5 (0.148)	941.7 (136.6)	17.0	59.4 (8.6)
4	100.1 (0.155)	408.9 (59.3)	7.5	55.7 (8.1)
5	98.7 (0.153)	577.7 (83.8)	10.8	57.4 (8.3)
Average	96.9 (0.150)	693.0 (100.5)	12.5	58.6 (8.5)
Standard Deviation	2.3 (0.004)	207.0 (30.0)	3.7	2.1 (0.3)
	2.4%	29.9%	29.3%	3.6%

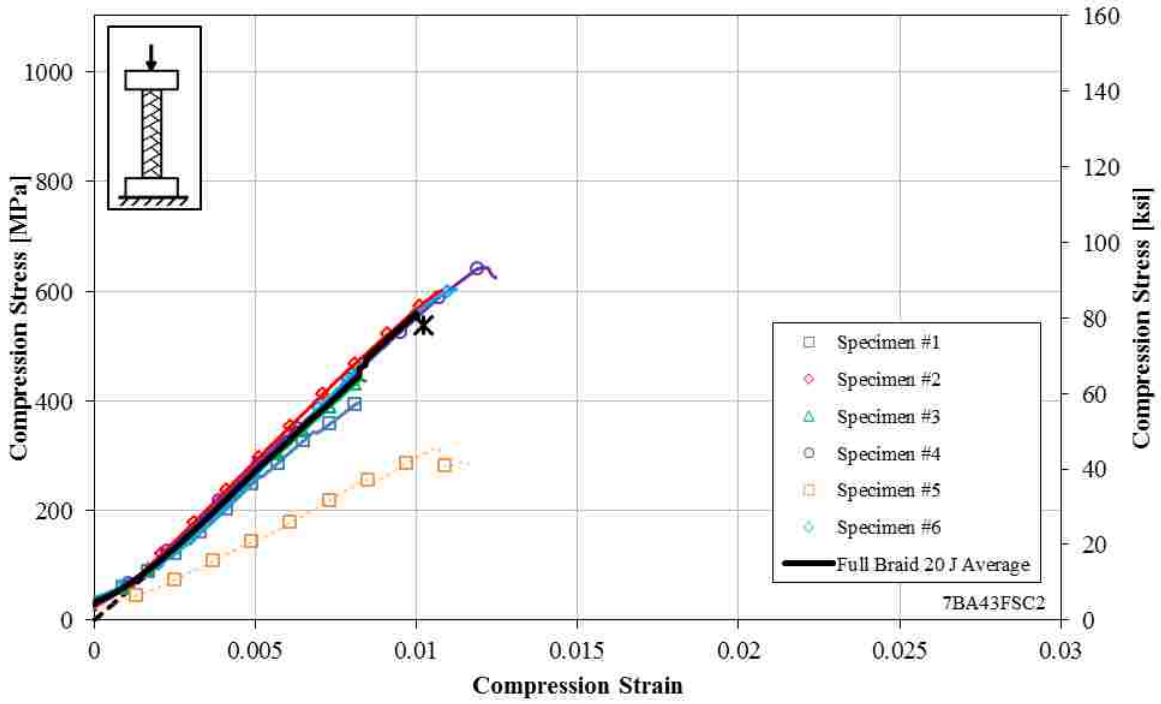

Figure 5.15: Stress-Strain Plot for Full Braid, 20 J (14.8 ft-lbs.) Impact Specimen, 8 mm (5/16") Diameter, 51 mm (2") Length, (7BA43FSC2)

Table 5.18: Summary Table for Full Braid, 20 J (14.8 ft-lbs.) Impact Specimen, 8 mm (5/16") Diameter, 51 mm (2") Length, (7BA43FSC2)

Specimen Number (7BA10FSC2)	Cross Sectional Area [mm^2 (in^2)]	Ultimate Compression Strength [MPa (ksi)]	Strain at Max Stress [10^3 με]	Compression Young's Modulus [GPa (10^6 psi)]
1	92.7 (0.144)	396.6 (57.5)	8.2	49.8 (7.2)
2	98.5 (0.153)	601.1 (87.2)	10.7	57.8 (8.3)
3	95.1 (0.147)	440.1 (63.8)	8.3	53.5 (7.8)
4	98.5 (0.153)	644.0 (93.4)	12.1	55.9 (8.11)
5	93.8 (0.145)	315.4 (45.7)	10.6	29.9 (4.3)*
6	94.0 (0.176)	603.8 (87.6)	11.2	46.9 (6.8)
Average	95.4 (0.148)	537.0 (77.9)	10.2	51.2 (7.4)
Standard Deviation	2.5 (0.004)	110.7 (16.1)	1.8	4.7 (0.7)
	2.8%	23.2%	19.4%	6.4%

5.2.4 Half Braid No-impact (7BA43HNC2)

The half braid coverage, no-impact specimen test results are presented in the stress-strain plot shown in Figure 5.16 and summarized in Table 5.19. The average compression strength is 897.1 MPa (130.1 ksi), the corresponding strain is 19.0 mm/mm (in./in.), and the average Young's modulus is 54.1 GPa ($7.8x10^6$ psi).

5.2.5 Half Braid 10 J Impact (7BA43HLC2)

The full braid coverage, 10 J (7.4 ft-lbs.) impact specimen test results are presented in the stress-strain plot shown in Figure 5.17 and summarized in Table 5.20. The average compression strength is 627.5 MPa (91.0 ksi), the corresponding strain is 13.8 mm/mm (in./in.), and the average Young's modulus is 51.5 GPa ($7.6x10^6$ psi). Specimen 1 was eliminated based on Chauvenet's envelope for compression strength and the corresponding strain.

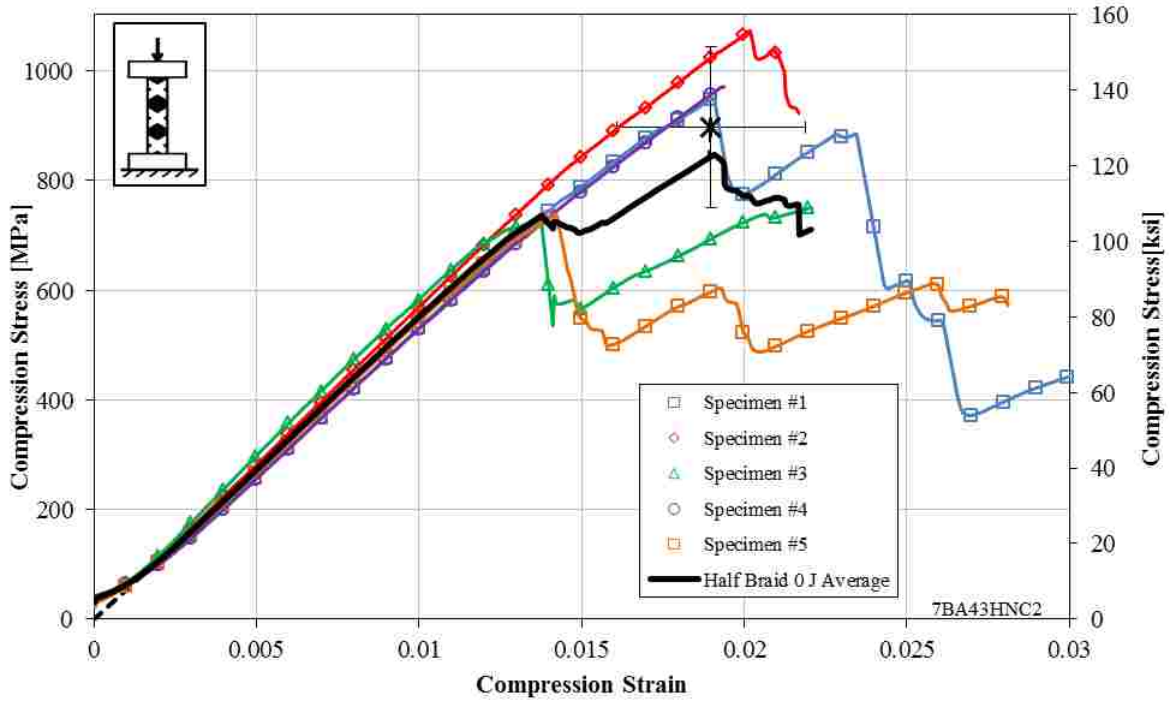

Figure 5.16: Stress-Strain Plot for Half Braid, No-Impact Specimen, 8 mm (5/16") Diameter, 51 mm (2") Length, (7BA43HNC2)

Table 5.19: Summary Table for Half Braid, No-Impact Specimen, 8 mm (5/16") Diameter, 51 mm (2") Length, (7BA43HNC2)

Specimen Number (7BA43HNC2)	Cross Sectional Area [mm^2 (in^2)]	Ultimate Compression Strength [MPa (ksi)]	Strain at Max Stress [10^3 με]	Compression Young's Modulus [GPa (10^6 psi)]
1	105.3 (0.163)	950.3 (137.8)	19.0	51.6 (7.5)
2	105.1 (0.163)	1073.1 (155.6)	20.2	56.1 (8.1)
3	101.2 (0.164)	751.0 (108.9)	22.0	59.1 (8.6)
4	105.8 (0.162)	971.0 (140.8)	19.4	50.5 (7.3)
5	104.8 (0.157)	739.9 (107.3)	14.2	52.8 (7.7)
Average	104.4 (0.162)	897.1 (130.1)	19.0	54.1 (7.8)
Standard	1.84 (0.003)	146.0 (21.2)	2.9	3.5 (0.5)
Deviation	1.8%	16.3%	15.3%	6.5%

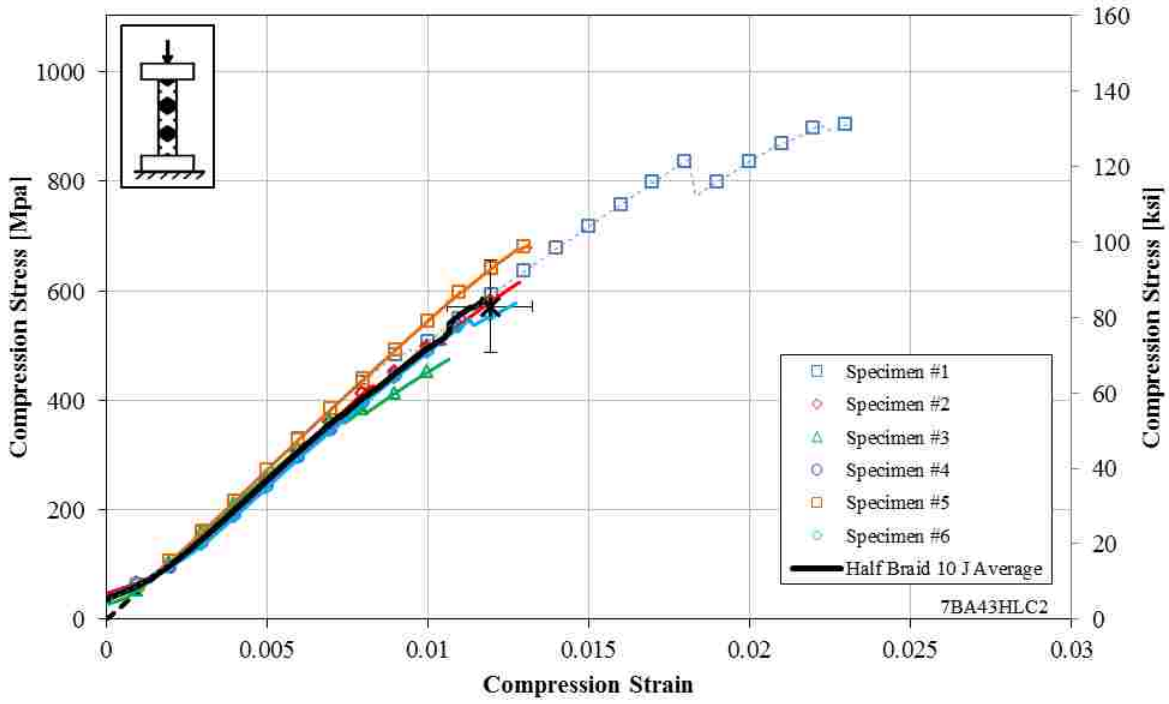

Figure 5.17: Stress-Strain Plot for Half Braid, 10 J (7.4 ft-lbs.) Impact Specimen, 8 mm (5/16") Diameter, 51 mm (2") Length, (7BA43HLC2)

Table 5.20: Summary Table for Half Braid, 10 J (7.4 ft-lbs.) Impact Specimen, 8 mm (5/16") Diameter, 51 mm (2") Length, (7BA43HLC2)

Specimen Number (7BA43HLC2)	Cross Sectional Area [mm^2 (in^2)]	Ultimate Compression Strength [MPa (ksi)]	Strain at Max Stress [10^3 με]	Compression Young's Modulus [GPa (10^6 psi)]
1	103.1 (0.160)	906.8 (131.5)*	23.1*	55.2 (8.0)
2	104.8 (0.162)	615.3 (89.2)	12.8	51.5 (7.5)
3	104.2 (0.162)	475.5 (69.0)	10.7	51.7 (7.5)
4	105.4 (0.163)	506.0 (73.4)	10.3	49.8 (7.2)
5	104.0 (0.161)	683.6 (99.1)	13.1	55.0 (8.0)
6	103.8 (0.161)	577.7 (83.8)	12.7	49.4 (7.2)
Average	104.2 (0.162)	627.5 (91.0)	13.8	51.5 (7.6)
Standard Deviation	0.8 (0.001)	156.0 (22.6)	4.7	2.2 (0.3)
	0.7%	24.8%	34.2%	4.3%

* *Specimen did not pass Chauvenet's Criterion.*

5.2.6 Half Braid 20 J Impact (7BA43HSC2)

The half braid coverage, 20 J (14.8 ft-lbs.) impact specimen test results are presented in the stress-strain plot shown in Figure 5.18 and summarized in Table 5.21. The average compression strength is 378.0 MPa (54.8 ksi), the corresponding strain is 8.7 mm/mm (in./in.), and the average Young's modulus is 51.7 GPa (7.5 x10^6 psi).

5.2.7 Full Spiral No-impact (7BA10FNC2)

The full spiral coverage, no-impact specimen test results are presented in the stress-strain plot shown in Figure 5.19 and summarized in Table 5.22. The average compression strength is 936.1 MPa (135.8 ksi), the corresponding strain is 17.38 mm/mm (in./in.), and the average Young's modulus is 58.9 GPa (8.6x10^6 psi).

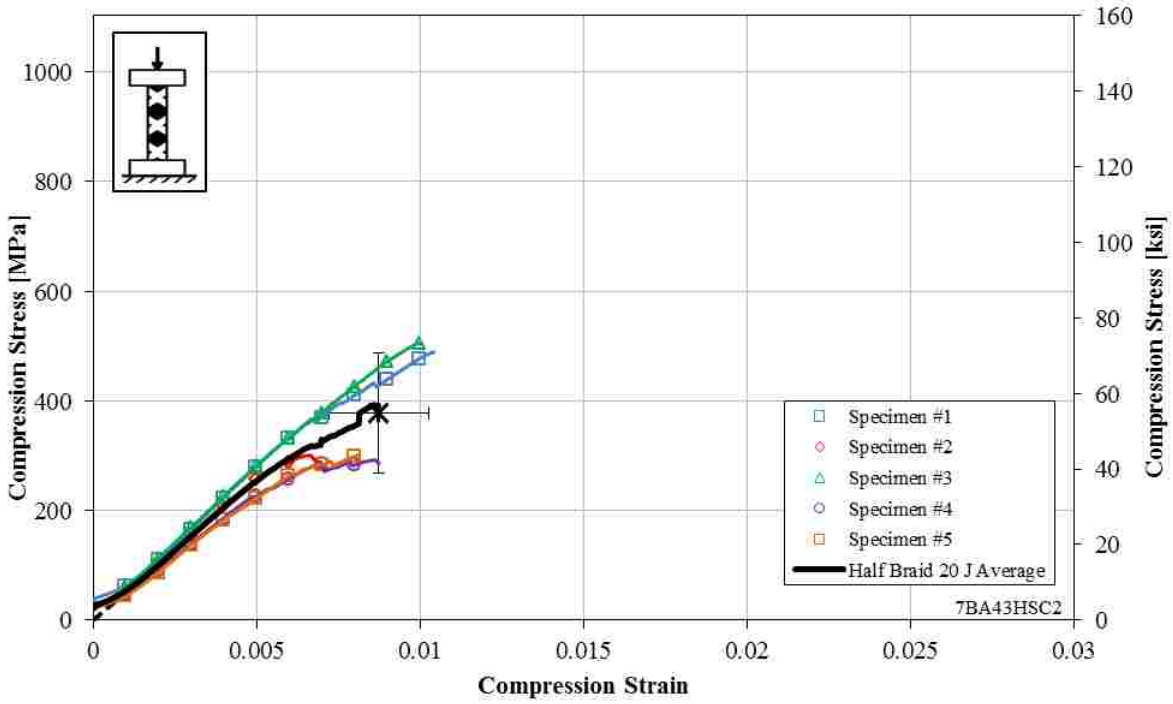

Figure 5.18: Stress-Strain Plot for Half Braid, 20 J (14.8 ft-lbs.) Impact Specimen, 8 mm (5/16") Diameter, 51 mm (2") Length, (7BA43HSC2)

Table 5.21: Summary Table for Half Braid, 20 J (14.8 ft-lbs.) Impact Specimen, 8 mm (5/16") Diameter, 51 mm (2") Length, (7BA43HSC2)

Specimen Number (7BA43HSC2)	Cross Sectional Area [mm^2 (in^2)]	Ultimate Compression Strength [MPa (ksi)]	Strain at Max Stress [10^3 με]	Compression Young's Modulus [GPa (10^6 psi)]
1	102.2 (0.158)	489.1 (70.9)	10.4	54.3 (7.9)
2	104.6 (0.162)	300.8 (43.6)	6.6	53.4 (7.8)
3	102.6 (0.159)	506.0 (73.4)	10.0	55.9 (8.1)
4	102.1 (0.158)	292.6 (42.4)	8.6	47.9 (7.0)
5	101.8 (0.158)	301.4 (43.7)	8.1	46.9 (6.8)
Average	102.7 (0.159)	378.0 (54.8)	8.7	51.7 (7.5)
Standard	1.116 (0.002)	109.4 (15.9)	1.5	4.0 (0.6)
Deviation	1.1%	28.9%	17.5%	7.8%

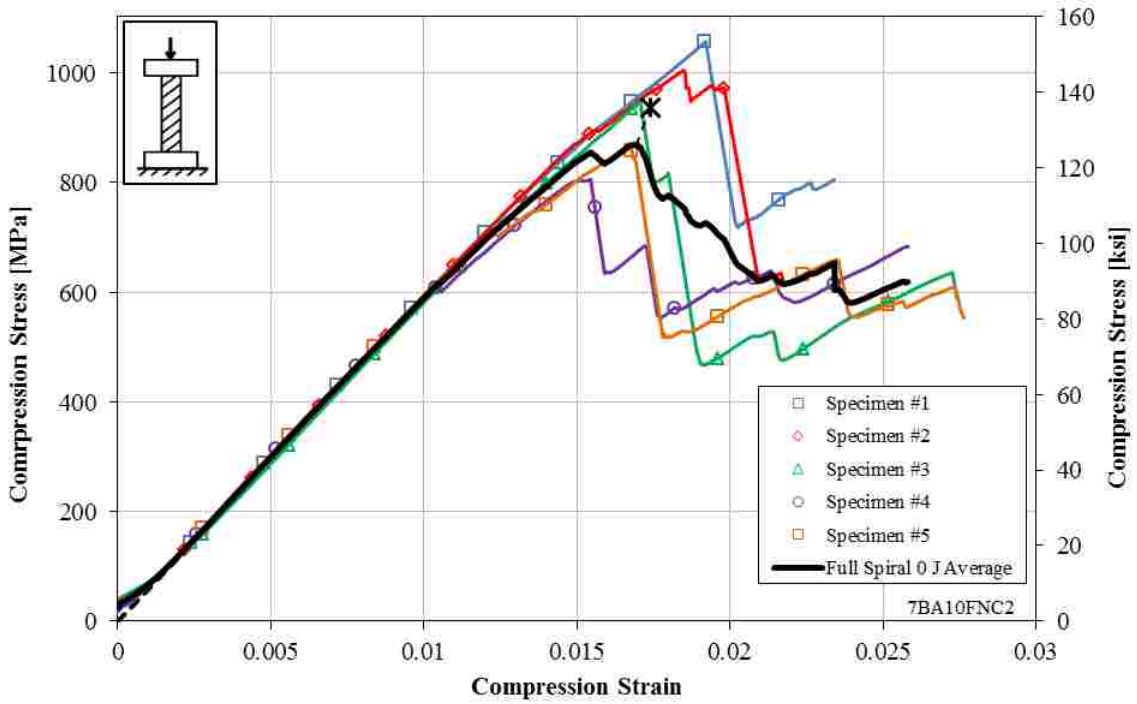

Figure 5.19: Stress-Strain Plot for Full Spiral, No-Impact Specimen, 8 mm (5/16") Diameter, 51 mm (2") Length, (7BA10FNC2)

Table 5.22: Summary Table for Full Spiral, No-Impact Specimen, 8 mm (5/16") Diameter, 51 mm (2") Length, (7BA10FNC2)

Specimen Number (7BA10FNC2)	Cross Sectional Area [mm^2 (in^2)]	Ultimate Compression Strength [MPa (ksi)]	Strain at Max Stress [10^3 με]	Compression Young's Modulus [GPa (10^6 psi)]
1	100.7 (0.156)	1056.3 (153.2)	19.18	59.3 (8.6)
2	99.2 (0.154)	1006.1 (145.9)	18.52	59.1 (8.6)
3	99.8 (0.155)	947.2 (137.4)	17.07	58.8 (8.5)
4	99.8 (0.155)	805.3 (116.8)	15.41	58.5 (8.5)
5	100.6 (0.156)	865.7 (125.6)	16.72	59.2 (8.6)
Average	100.0 (0.154)	936.1 (135.8)	17.38	58.9 (8.6)
Standard Deviation	0.97 (0.001)	101.9 (14.8)	1.50	0.3 (0.1)
	1.0%	10.8%	8.6%	0.6%

5.2.8 Full Spiral 10 J Impact (7BA10FLC2)

The full spiral coverage, 10 J (7.4 ft-lbs.) impact specimen test results are presented in the stress-strain plot shown in Figure 5.20 and summarized in Table 5.23. The average compression strength is 584.7 MPa (84.8 ksi), the corresponding strain is 11.9 mm/mm (in./in.), and the average Young's modulus is 55.6 GPa (8.1×10^6 psi). Specimen 4 was eliminated based on Chauvenet's envelope for strength.

5.2.9 Full Spiral 20 J Impact (7BA10FSC2)

The full spiral coverage, 20 J (14.8 ft-lbs.) impact specimen test results are presented in the stress-strain plot shown in Figure 5.21 and summarized in Table 5.24. The average compression strength is 364.5 MPa (52.9 ksi), the corresponding strain is 7.73 mm/mm (in./in.), and the average Young's modulus is 52.4 GPa (7.6×10^6 psi).

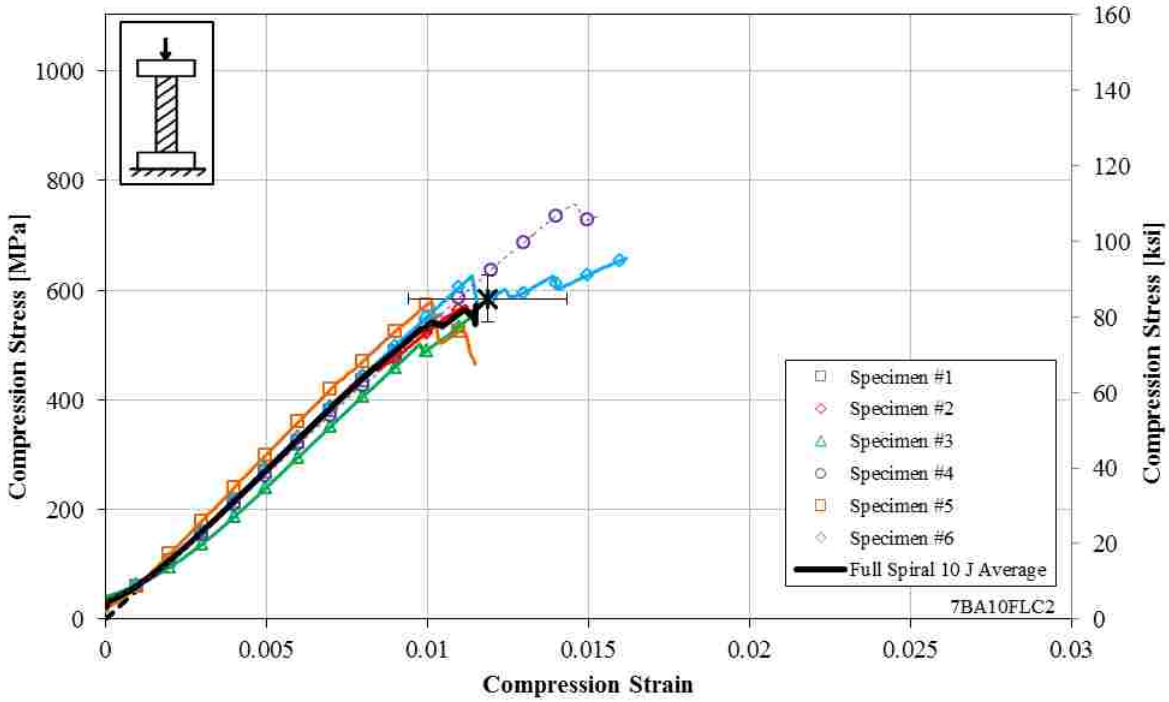

Figure 5.20: Stress-Strain Plot for Full Spiral, 10 J (7.4 ft-lbs.) Impact Specimen, 8 mm (5/16") Diameter, 51 mm (2") Length, (7BA10FLC2)

Table 5.23: Summary Table for Full Spiral, 10 J (7.4 ft-lbs.) Impact Specimen, 8 mm (5/16") Diameter, 51 mm (2") Length, (7BA10FLC2)

Specimen Number (7BA10FLC2)	Cross Sectional Area [mm^2 (in^2)]	Ultimate Compression Strength [MPa (ksi)]	Strain at Max Stress [10^3 με]	Compression Young's Modulus [GPa (10^6 psi)]
1	98.8 (0.153)	557.0 (80.8)	10.4	54.6 (7.9)
2	99.8 (0.155)	573.4 (83.2)	11.2	55.9 (8.1)
3	100.4 (0.156)	557.1 (80.8)	11.5	51.6 (7.5)
4	99.1 (0.154)	758.4 (109.9)*	14.6	53.7 (7.8)
5	96.1 (0.149)	577.8 (83.8)	10.1	60.1 (8.7)
6	100.6 (0.156)	658.3 (95.5)	16.2	55.9 (8.1)
Average	99.1 (0.154)	584.7 (84.8)	11.9	55.6 (8.1)
Standard Deviation	1.8 (0.003)	42.2 (6.1)	2.5	3.0 (0.4)
	1.9%	7.2%	20.8%	5.5%

**Specimen did not pass Chauvenet's Criterion, not included in averages.*

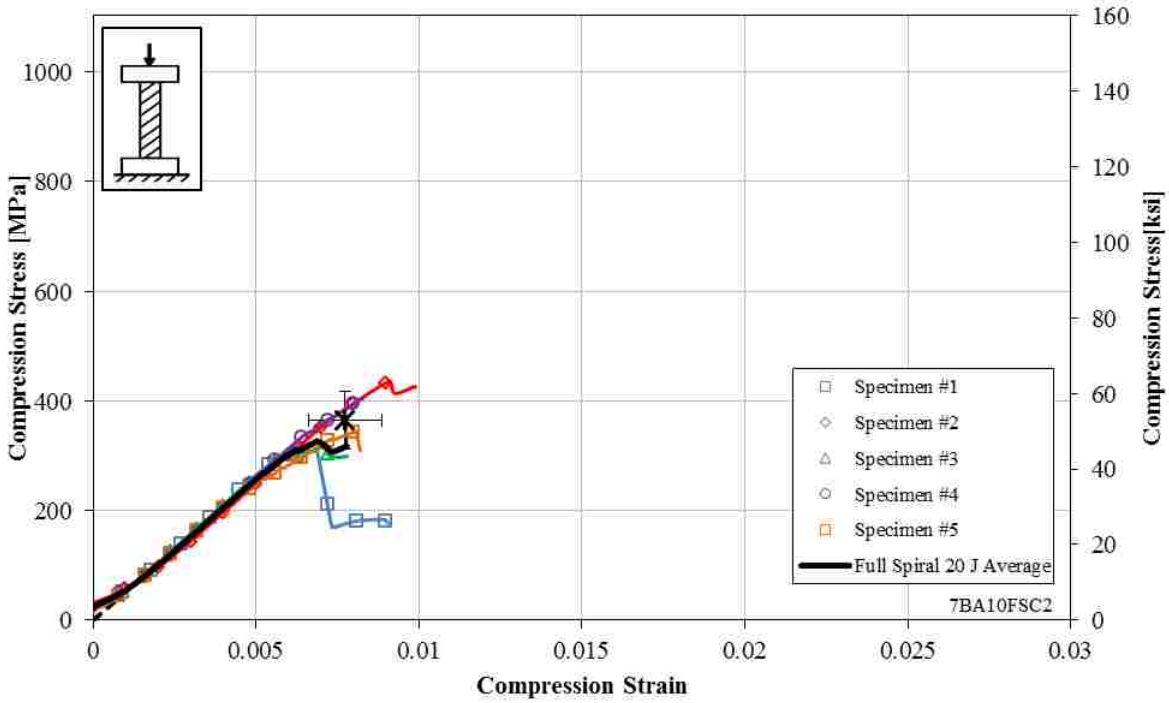

Figure 5.21: Stress-Strain Plot for Full Spiral, 20 J (14.8 ft-lbs.) Impact Specimen, 8 mm (5/16") Diameter, 51 mm (2") Length, (7BA10FSC2)

Table 5.24: Summary Table for Full Spiral, 20 J (14.8 ft-lbs.) Impact Specimen, 8 mm (5/16") Diameter, 51 mm (2") Length, (7BA10FSC2)

Specimen Number (7BA10FSC2)	Cross Sectional Area [mm^2 (in^2)]	Ultimate Compression Strength [MPa (ksi)]	Strain at Max Stress [10^3 με]	Compression Young's Modulus [GPa (10^6 psi)]
1	100.8 (0.156)	321.8 (46.7)	6.2	54.7 (7.9)
2	99.4 (0.154)	436.6 (63.3)	9.1	51.4 (7.5)
3	99.6 (0.154)	316.1 (45.8)	7.0	52.5 (7.6)
4	100.3 (0.156)	403.7 (58.5)	8.2	53.8 (7.8)
5	96.7 (0.150)	344.4 (49.9)	8.1	49.8 (7.2)
Average	99.4 (0.154)	364.5 (52.9)	7.7	52.4 (7.6)
Standard Deviation	1.61 (0.003)	53.1 (7.7)	1.1	1.9 (0.3)
	1.6%	14.6%	14.6%	3.7%

5.2.10 Half Spiral No-impact (7BA10HNC2)

The full spiral coverage, no-impact specimen test results are presented here in the stress-strain plot shown in Figure 5.22 and summarized in Table 5.25. The average compression

strength is 737.5 MPa (107.0 ksi), the corresponding strain is 13.2 mm/mm (in./in.), and the average Young's modulus is 60.0 GPa ($8.7x10^6$ psi).

5.2.11 Half Spiral 10 J Impact (7BA10HLC2)

The half spiral coverage, 10 J (7.4 ft-lbs.) impact specimen test results are presented in the stress-strain plot shown in Figure 5.23 and in summary Table 5.26. The average compression strength is 478.9 MPa (69.5 ksi), the corresponding strain is 9.1 mm/mm (in./in.), and the average Young's modulus is 62.2 GPa ($9.0x10^6$ psi).

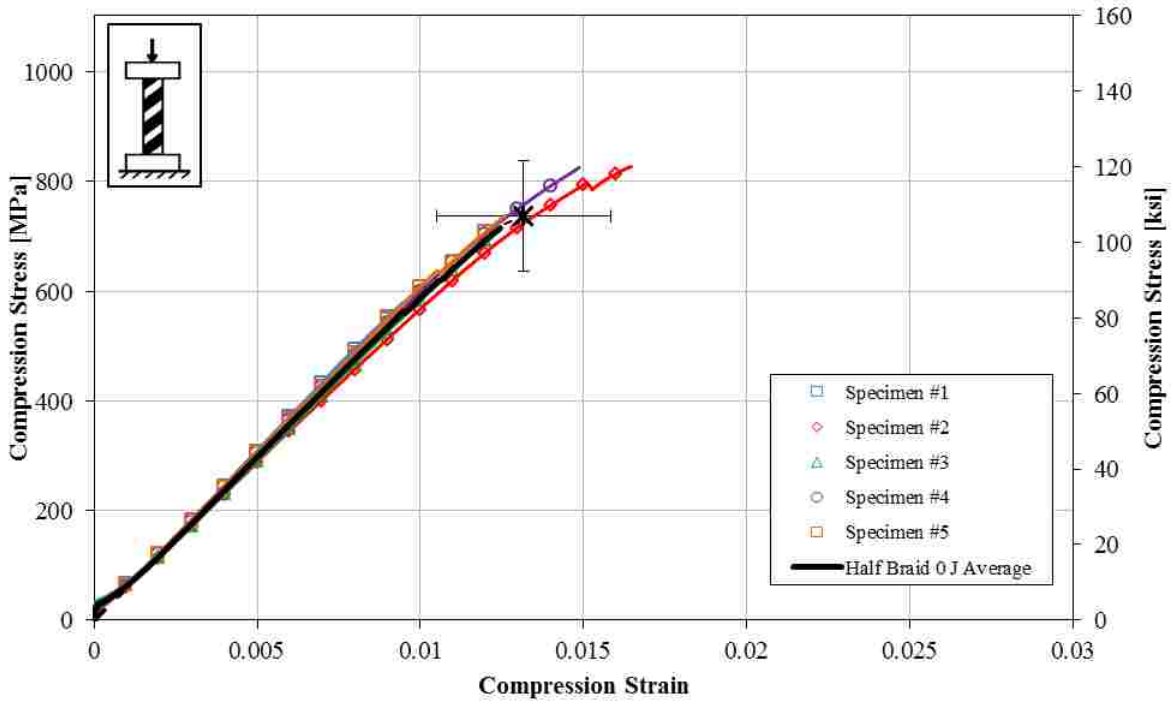

Figure 5.22: Stress-Strain Plot for Half Spiral, No-Impact Specimen, 8 mm (5/16") Diameter, 51 mm (2") Length, (7BA10HNC2)

Table 5.25: Summary Table for Half Spiral, No-Impact Specimen, 8 mm (5/16") Diameter, 51 mm (2") Length, (7BA10HNC2)

Specimen Number (7BA10HNC2)	Cross Sectional Area [mm^2 (in^2)]	Ultimate Compression Strength [MPa (ksi)]	Strain at Max Stress [10^3 με]	Compression Young's Modulus [GPa (10^6 psi)]
1	104.0 (0.161)	578.6 (83.9)	9.4	61.8 (9.0)
2	103.1 (0.160)	827.2 (120.0)	16.4	57.6 (8.4)
3	103.4 (0.160)	718.1 (104.2)	12.5	58.3 (8.5)
4	105.1 (0.163)	825.1 (119.7)	14.9	61.2 (8.9)
5	103.2 (0.160)	738.3 (107.1)	12.6	61.1 (8.9)
Average	103.8 (0.161)	737.5 (107.0)	13.2	60.0 (8.7)
Standard Deviation	0.8 (0.001)	101.6 (14.7)	2.7	1.9 (0.3)
	0.7%	13.7%	20.4%	3.2%

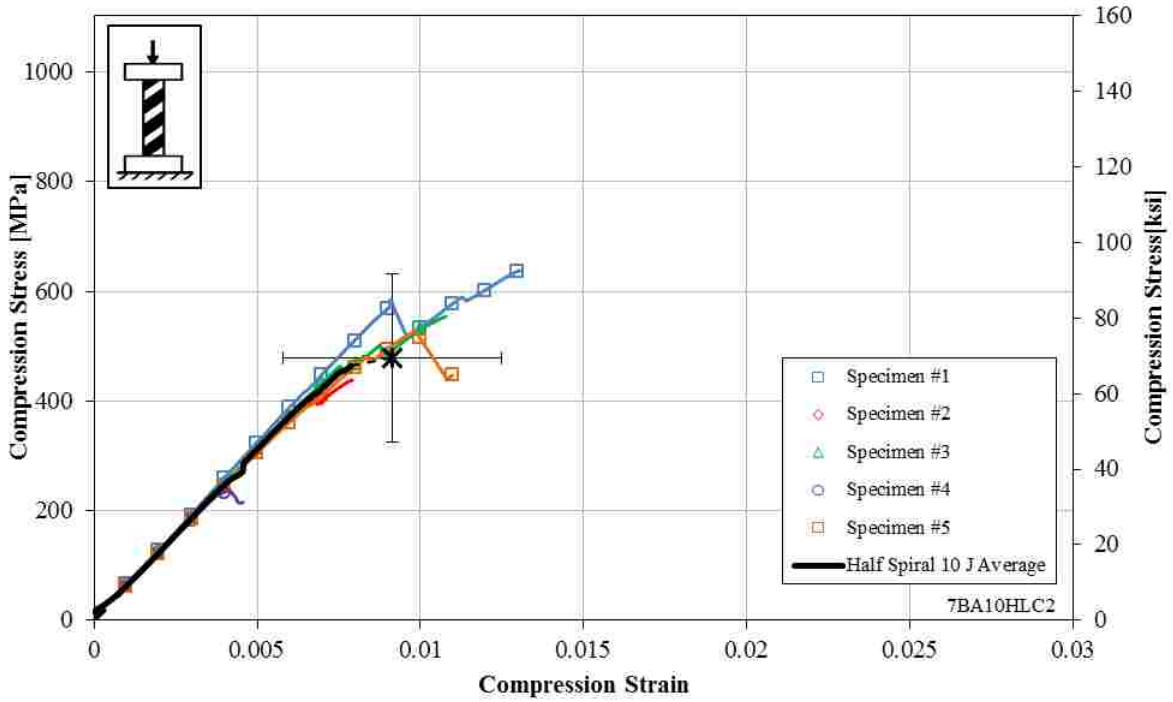

Figure 5.23: Stress-Strain Plot for Full Braid, 10 J (7.4 ft-lbs.) Impact Specimen, 8 mm (5/16") Diameter, 51 mm (2") Length, (7BA43FLC2)

Table 5.26: Summary Table for Full Braid, 10 J (7.4 ft-lbs.) Impact Specimen, 8 mm (5/16") Diameter, 51 mm (2") Length, (7BA43FLC2)

Specimen Number (7BA10HNC2)	Cross Sectional Area [mm^2 (in^2)]	Ultimate Compression Strength [MPa (ksi)]	Strain at Max Stress [10^3 με]	Compression Young's Modulus [GPa (10^6 psi)]
1	103.1 (0.160)	637.9 (92.5)	13.1	64.9 (9.4)
2	103.4 (0.160)	438.1 (63.5)	7.9	61.5 (8.9)
3	104.0 (0.161)	554.4 (80.4)	10.8	62.4 (9.0)
4	102.7 (0.159)	237.3 (34.4)	4.1	61.2 (8.9)
5	103.44 (0.160)	527.2 (76.5)	9.8	60.8 (8.8)
Average	103.3 (0.160)	478.9 (69.5)	9.1	62.2 (9.0)
Standard Deviation	0.5 (0.001)	152.7 (22.2)	3.4	1.6 (0.2)
	0.4%	31.8%	36.7%	2.6%

5.2.12 Half Spiral 20 J Impact (7BA10HSC2)

The half spiral coverage, 20 J (14.8 ft-lbs.) impact specimen test results are presented in the stress-strain plot shown in Figure 5.24 and summarized in Table 5.27. The average compression strength is 297.3 MPa (43.1 ksi), the corresponding strain is 5.0 mm/mm (in./in.), and the average Young's modulus is 63.3 GPa (9.2 x10^6 psi). Specimen 3 was eliminated based on Chauvenet's envelope for strength.

5.2.13 Test Results Summary

A summary of results for the 11 mm (7/16") diameter, 51 mm (2") length specimens are presented here. Table 5.28 presents the average strength, Table 5.29 presents the corresponding strain and Table 5.30 presents the average compression Young's modulus.

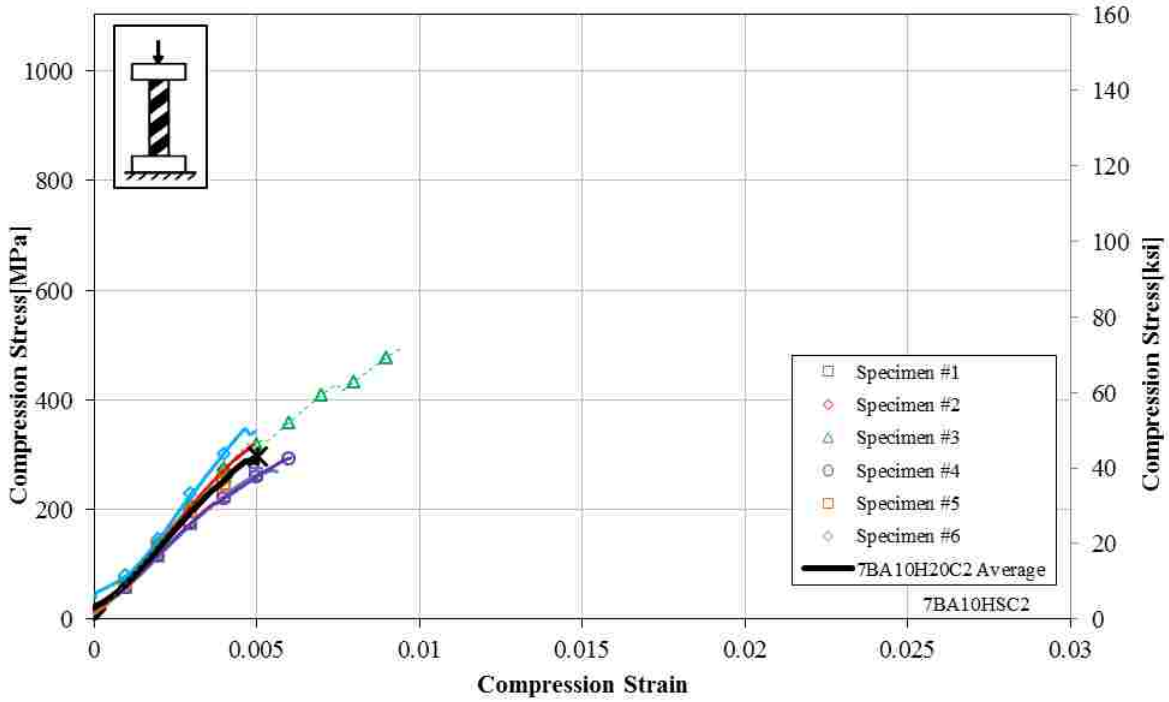

Figure 5.24: Stress-Strain Plot for Half Spiral, 20 J (14.8 ft-lbs.) Impact Specimen, 8 mm (5/16") Diameter, 51 mm (2") Length, (7BA10HSC2)

Table 5.27: Summary Table for Half Spiral, 20 J (14.8 ft-lbs.) Impact Specimen, 8 mm (5/16") Diameter, 51 mm (2") Length, (7BA10HSC2)

Specimen Number (7BA10HSC2)	Cross Sectional Area [mm^2 (in^2)]	Ultimate Compression Strength [MPa (ksi)]	Strain at Max Stress [10^3 με]	Compression Young's Modulus [GPa (10^6 psi)]
1	101.9 (0.158)	272.3 (39.5)	5.5	53.9 (7.8)
2	102.0 (0.158)	318.5 (46.2)	4.9	69.7 (10.1)
3	102.0 (0.158)	493.6 (71.6)*	9.4*	69.9 (10.1)
4	102.8 (0.159)	294.6 (42.7)	6.0	49.7 (7.2)
5	99.8 (0.155)	252.3 (36.6)	4.1	62.5 (9.1)
6	102.2 (0.158)	348.9 (50.6)	4.7	80.6 (11.7)
Average	101.8 (0.158)	297.3 (43.1)	5.0	63.3 (9.2)
Standard Deviation	1.0 (0.002)	38.0 (5.5)	0.7	12.4 (1.8)
	1.0%	12.8%	14.0%	19.5%

* *Specimen did not pass Chauvenet's Criterion, not included in averages.*

Table 5.28: Average Ultimate Compression Strength, 11 mm (7/16") Diameter, 51 mm (2") Length

Specimen Configuration & Impact Energy		Average Max [MPa (ksi)]	Standard Deviation [MPa (ksi)]	[%]
Full Braid	**0 J**	899.5 (130.5)	45.0 (6.5)	5
	10 J	693.0 (100.5)	207.0 (30.0)	30
	20 J	537 (77.9)	110.7 (16.1)	23
Half Braid	**0 J**	897.1 (130.1)	146.0 (21.2)	16
	10 J	627.5 (91.0)	156.0 (22.6)	25
	20 J	378.0 (54.8)	109.4 (15.9)	29
Full Spiral	**0 J**	936.1 (135.8)	101.9 (14.8)	11
	10 J	584.7 (84.8)	42.2 (6.1)	7
	20 J	364.5 (52.9)	53.1 (7.7)	15
Half Spiral	**0 J**	737.5 (107.0)	101.6 (14.7)	14
	10 J	478.9 (69.5)	152.7 (22.2)	32
	20 J	297.3 (43.1)	38.0 (5.5)	13

Table 5.29: Average Strain at Maximum Stress, 11 mm (7/16") Diameter, 51 mm (2") Length

Specimen Configuration & Impact Energy		Average Max [10^3 με]	Standard Deviation [10^3 με]	[%]
Full Braid	**0 J**	16.1	0.5	3
	10 J	12.5	3.7	29
	20 J	10.2	1.8	19
Half Braid	**0 J**	19.0	2.9	15
	10 J	13.8	4.7	34
	20 J	8.73	1.5	18
Full Spiral	**0 J**	17.4	1.5	9
	10 J	11.9	2.5	21
	20 J	7.73	1.13	15
Half Spiral	**0 J**	13.2	2.7	20
	10 J	9.1	3.4	37
	20 J	5.0	0.7	14

Table 5.30: Average Compression Young's Modulus, 11 mm (7/16") Diameter, 51 mm (2") Length

Specimen Configuration & Impact Energy		Average Max [GPa (10^6 psi)]	Standard Deviation [GPa (10^6 psi)]	Standard Deviation [%]
Full Braid	0 J	60.4 (8.8)	0.7 (0.1)	1
	10 J	58.6 (8.5)	2.1 (0.3)	4
	20 J	51.2 (7.4)	4.7 (0.7)	6
Half Braid	0 J	54.1 (7.8)	3.5 (0.5)	7
	10 J	51.5 (7.5)	2.2 (0.3)	4
	20 J	51.7 (7.5)	4.0 (0.6)	8
Full Spiral	0 J	58.9 (8.6)	0.3 (0.1)	1
	10 J	55.6 (8.1)	3.0 (0.4)	6
	20 J	52.4 (7.6)	1.9 (0.3)	4
Half Spiral	0 J	60.0 (8.7)	1.9 (0.3)	3
	10 J	62.2 (9.0)	1.6 (0.2)	3
	20 J	63.3 (9.2)	12.4 (1.8)	20

6 CONFIGURATION AVERAGES

For each group, the average curves were presented in Chapter 5 along with the individual curves for each specimen. In this chapter, the average curves for the 51 mm (2") long configurations are compared. The results are discussed first for the 8 mm (5/16") diameter specimens; and, then for the 11 mm (7/16") diameter specimens. For each diameter, twelve plots were created, emphasizing the influence of different variables. The first plot has all twelve average curves, one for each configuration. The next four plots (full braid, half braid, full spiral, and half spiral) show the influence of impact energy for different sleeve types and configurations. The next three plots (no-impact, low impact, and severe impact) show the influence of sleeve type and coverage for different impact levels. The next two plots (full coverage and half coverage) show the influence of sleeve type and impact energy for different coverage. The final two plots (braid and spiral) show the influence of coverage and impact levels for different sleeve types.

6.1 5/16" Diameter Configuration Averages for 2" Specimens

In this section the results are discussed for the 8 mm (5/16") diameter specimens. Figure 6.1 has all twelve average curves, one for each configuration. Note that the initial moduli are very similar for all specimens, signifying similar stiffness for all geometric configurations and impact levels. Just prior to failure, most configurations experience a decrease in stiffness.

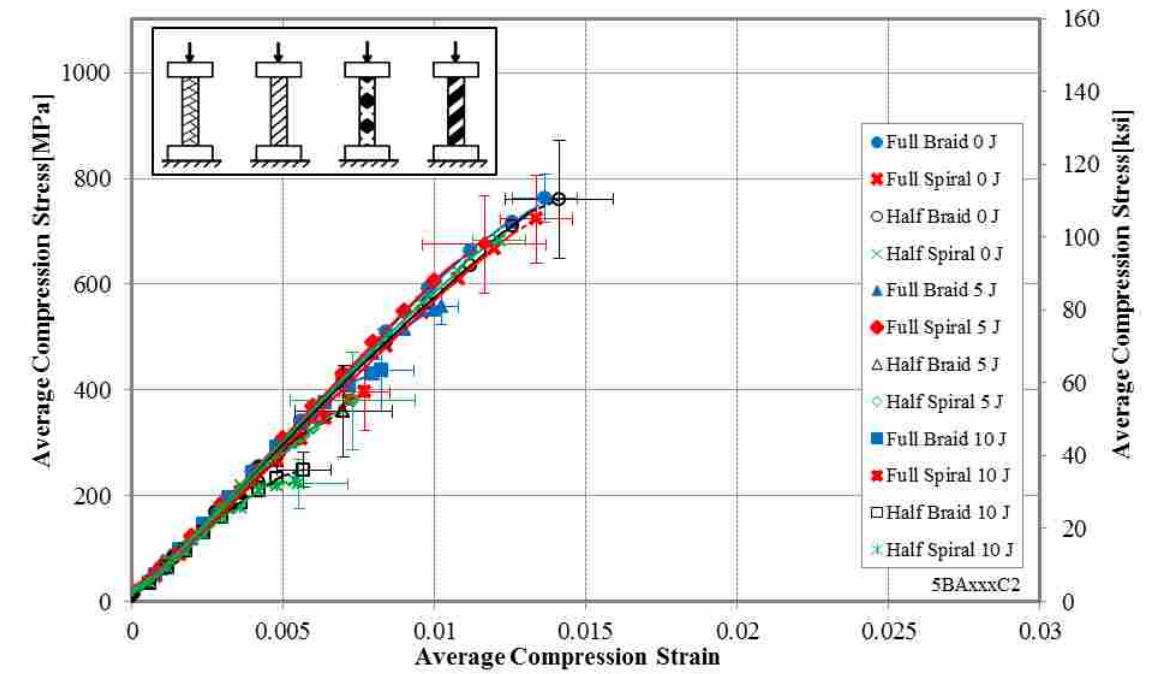

Figure 6.1: Average Stress-Strain Curves for 8 mm (5/16") Specimens

6.1.1 Influence of Impact Energy for Different Sleeve Types and Coverage

The next four plots, Figure 6.2 through 6.5, show the influence of impact energy for different sleeve types and configurations (full braid, half braid, full spiral, and half spiral). A drop in average ultimate strength is apparent with increasing impact energy. Note that there is no significant difference in ultimate compression strength between the no-impact and the 5-J (3.7-ft-lbs.) full spiral configurations.

6.1.2 Influence of Sleeve Type and Coverage for Different Impact Levels

The next three plots, Figures 6.6 through 6.8, show the influence of sleeve type and coverage for different impact levels (no-impact, low impact, and severe impact). Sleeve type and coverage make no significant difference in compression strength for non-impacted specimens as exemplified by Figure 6.6.

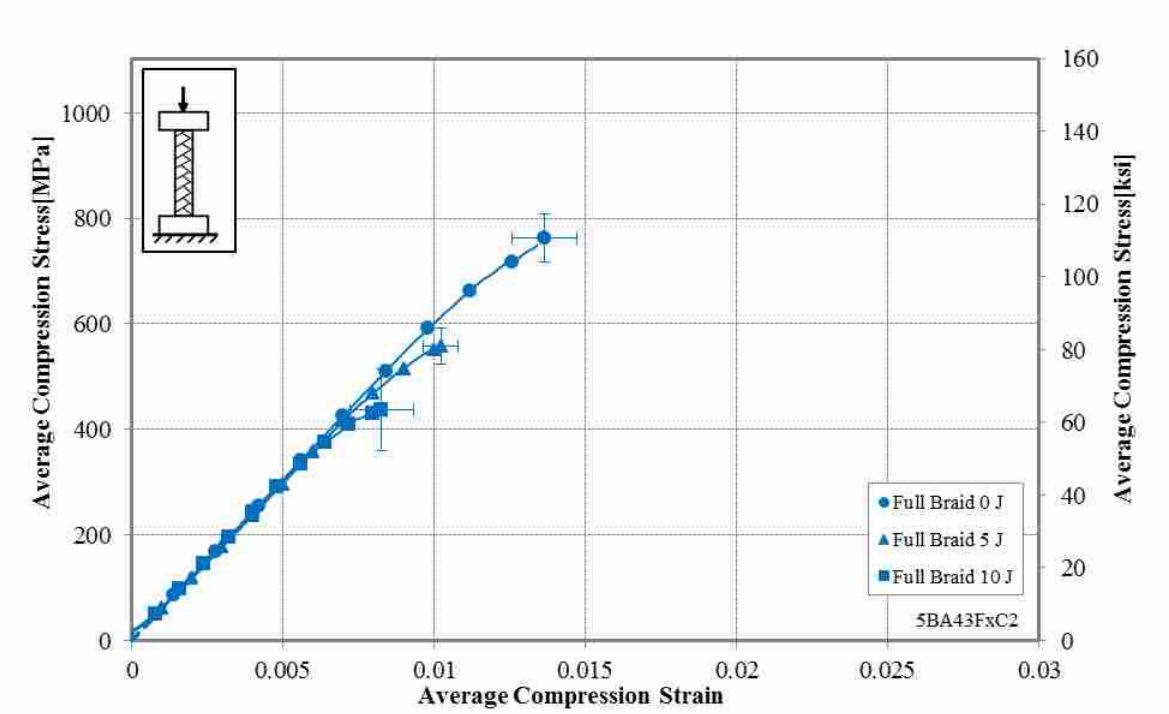

Figure 6.2: Average Stress-Strain Curves for all Full Braid, 8 mm (5/16") Specimens

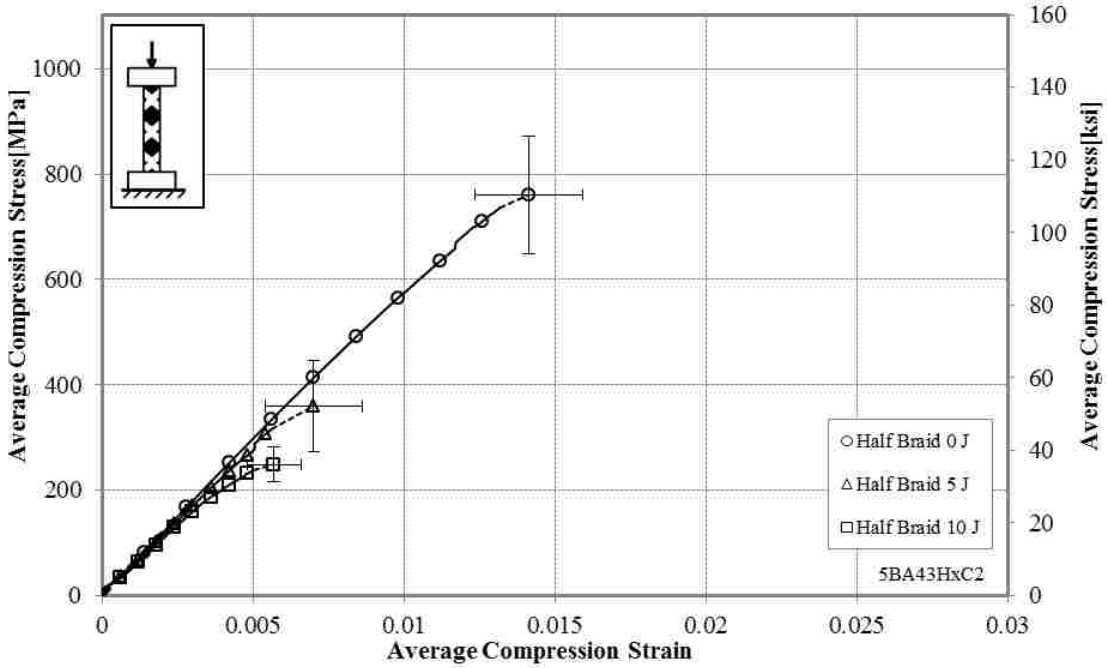

Figure 6.3: Average Stress-Strain Curves for all Half Braid, 8 mm (5/16") Specimens

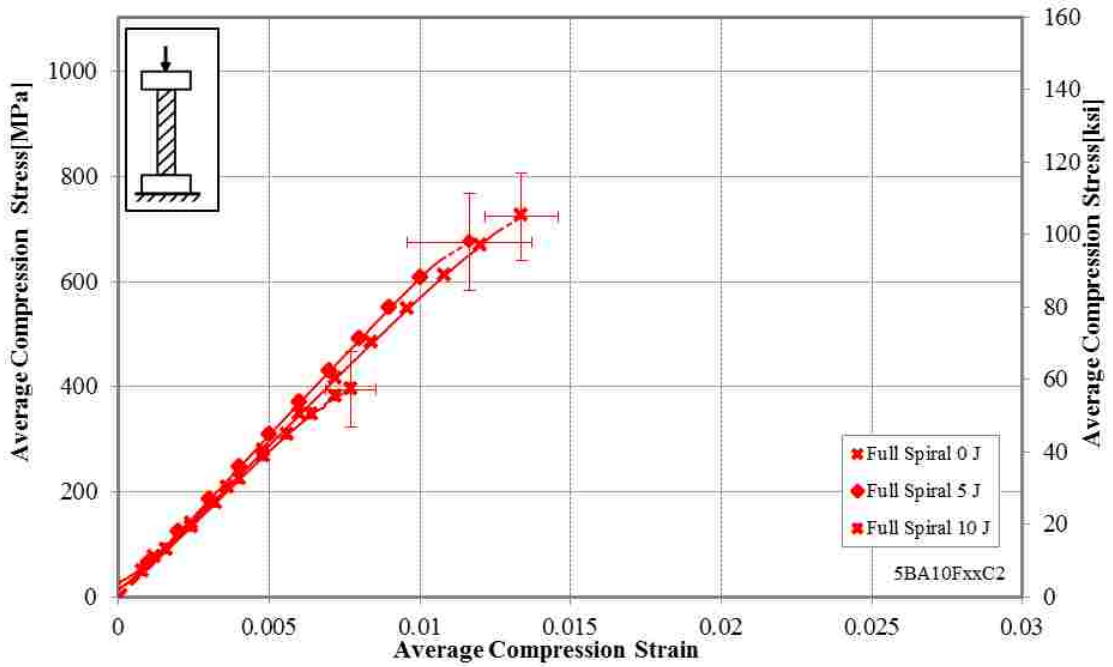

Figure 6.4: Average Stress-Strain Curves for all Full Spiral 8 mm (5/16") Specimens

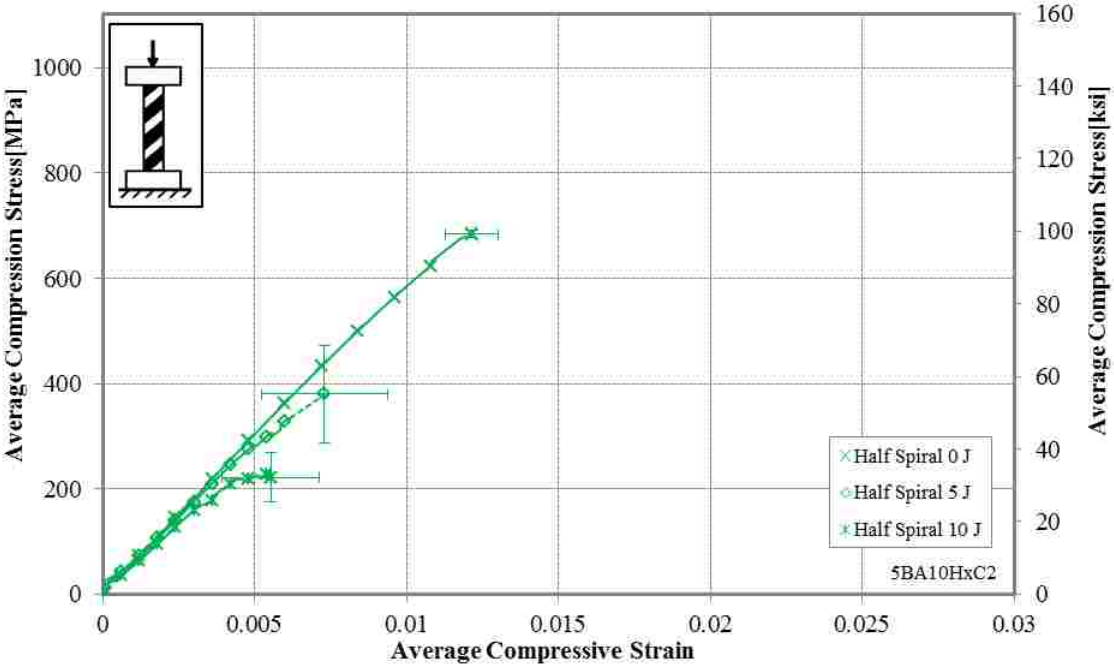

Figure 6.5: Average Stress-Strain Curves for all Half Spiral, 8 mm (5/16") Specimens

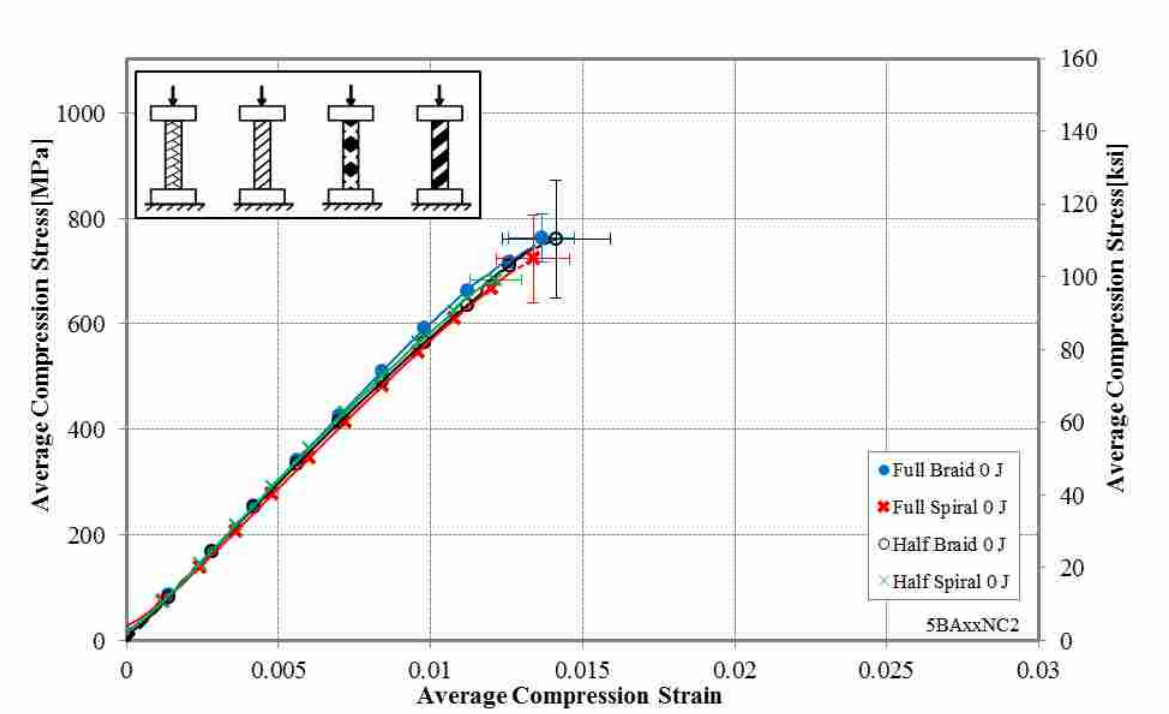

Figure 6.6: Average Stress-Strain Curves for all No-Impact, 8 mm (5/16") Specimens

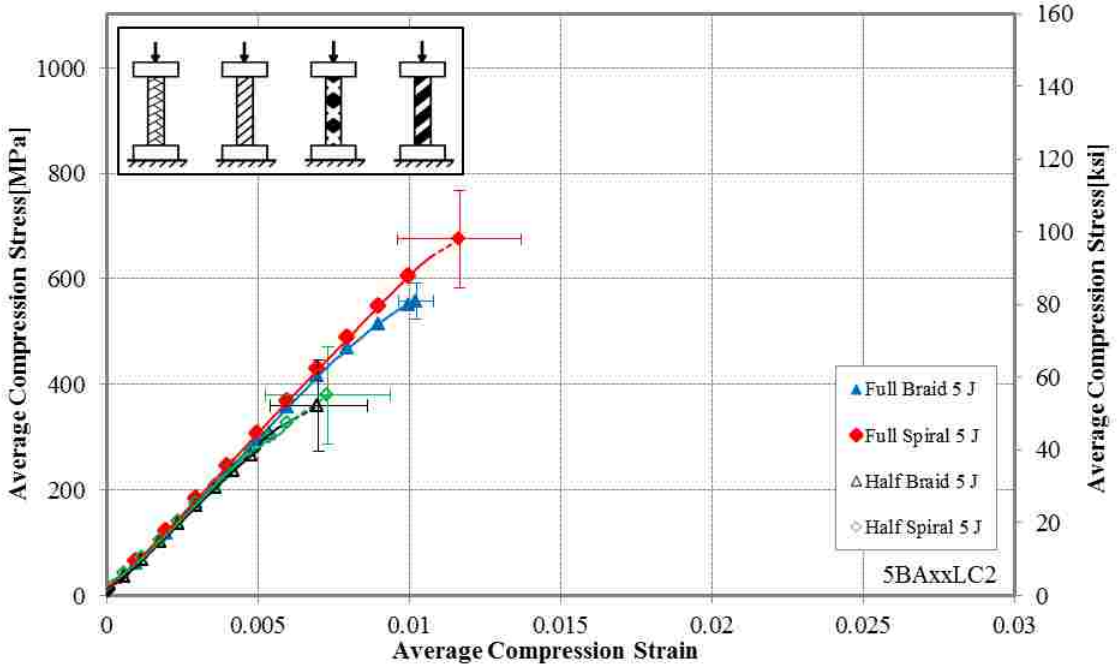

Figure 6.7: Average Stress-Strain Curves for all 5 J (3.7 ft-lbs.) Impact 8 mm (5/16") Specimens

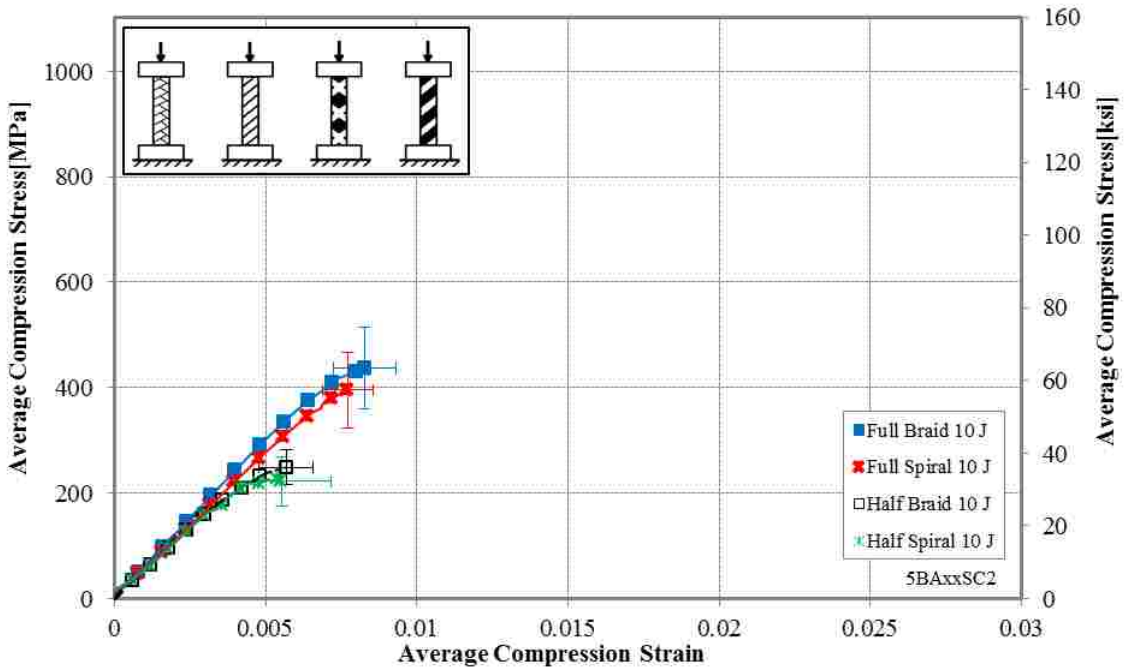

Figure 6.8: Average Stress-Strain Curves for all 10 J (7.4 ft-lbs.) Impact 8 mm (5/16") Specimens

6.1.3 Influence of Sleeve Type and Impact Energy for Different Coverage

The next two plots, Figure 6.9 and Figure 6.10, show the influence of sleeve type and impact energy for different coverage (full coverage and half coverage). When impacted with 5 J (3.7 ft-lbs.), the full spiral is stronger than the full braid.

6.1.4 Influence of Coverage and Impact Levels for Different Sleeve Types

The final two plots, Figure 6.11 and Figure 6.12, show the influence of coverage and impact levels for different sleeve types (braid and spiral).

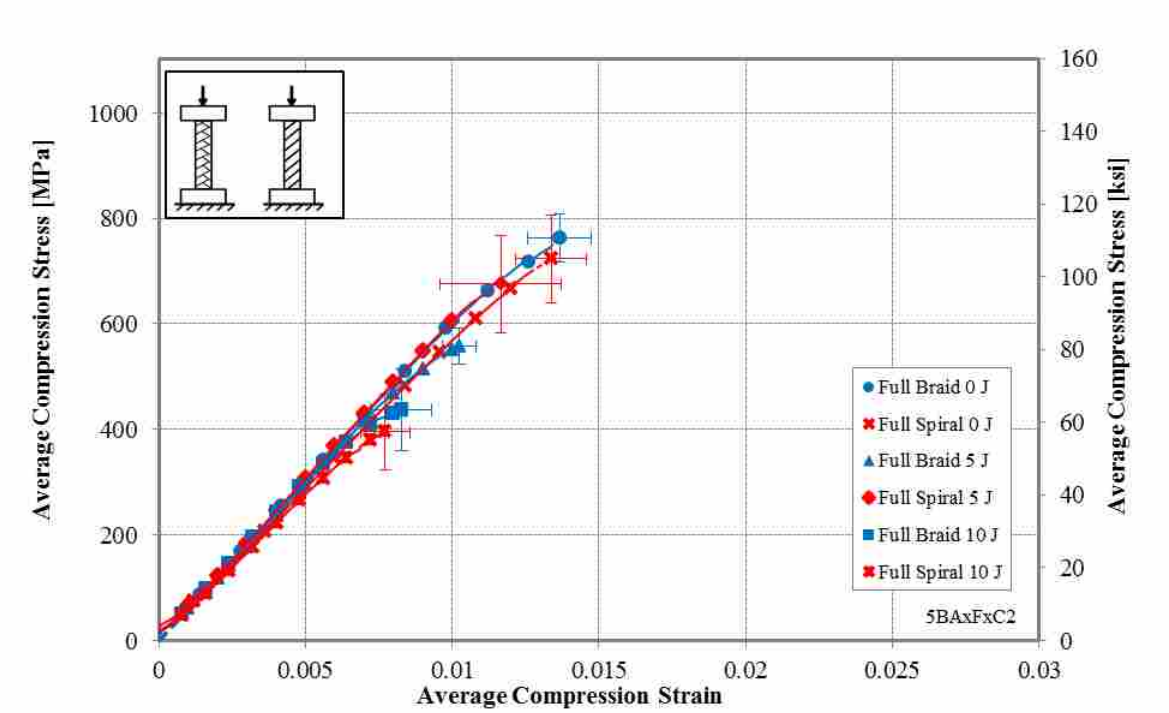

Figure 6.9: Average Stress-Strain Curves for all Full Coverage, 8 mm (5/16") Specimens

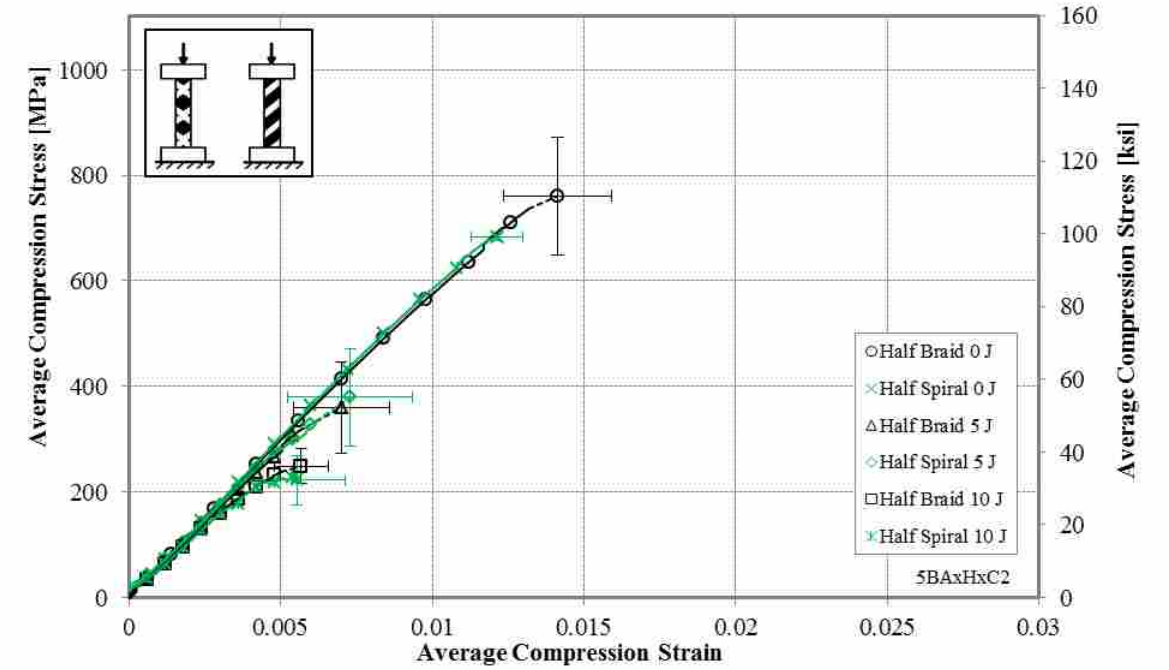

Figure 6.10: Average Stress-Strain Curves for all Half Coverage 8 mm (5/16") Specimens

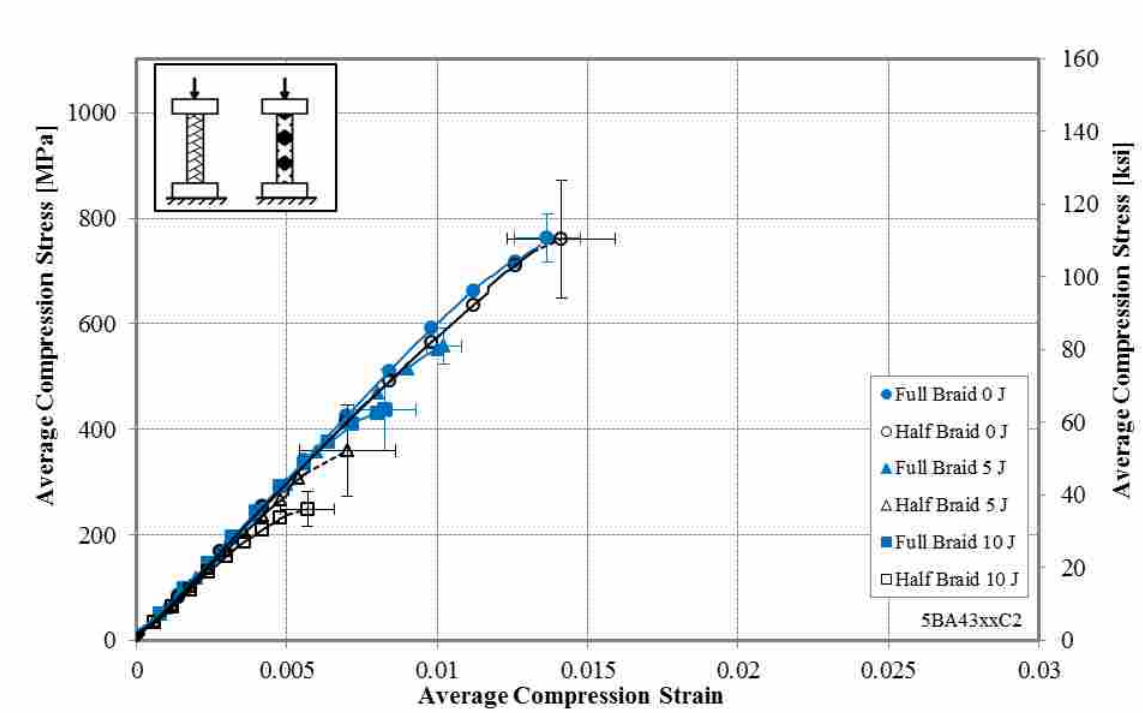

Figure 6.11: Average Stress-Strain Curves for all Braided Sleeve, 8 mm (5/16") Specimens

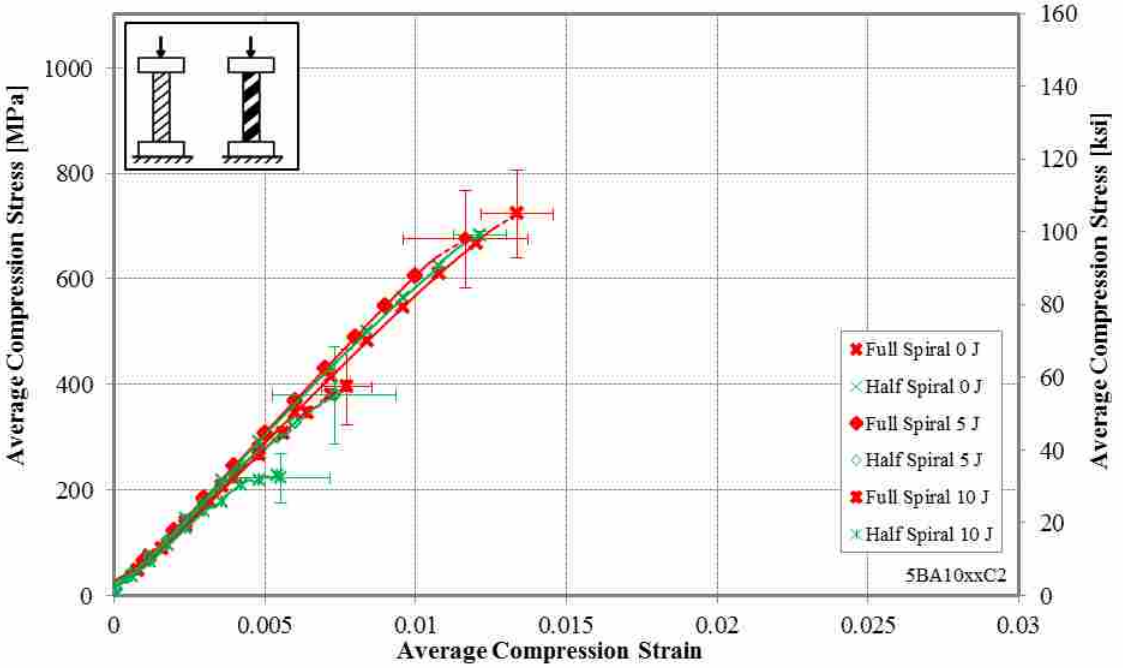

Figure 6.12: Average Stress-Strain Curves for all Spiral Sleeve, 8 mm (5/16") Specimens

6.2 7/16” Diameter Configuration Averages for 2” Specimens

In this section the results are discussed for the 11 mm (7/16”) diameter specimens. Figure 6.13 has all twelve average curves, one for each configuration. Note that the initial moduli are very similar for all specimens, signifying similar stiffness for all geometric configurations and impact levels. Just prior to failure, most configurations experience a decrease in stiffness. The specimens that were not impacted, besides the half spiral, maintain some strength after initial failure exhibiting strains extending beyond 0.025.

6.2.1 Influence of Impact Energy for Different Sleeve Types and Coverage

The next four plots, Figure 6-14 through 6-17, show the influence of impact energy for different sleeve types and configurations (full braid, half braid, full spiral, and half spiral). A drop in average ultimate strength is apparent with increasing impact energy.

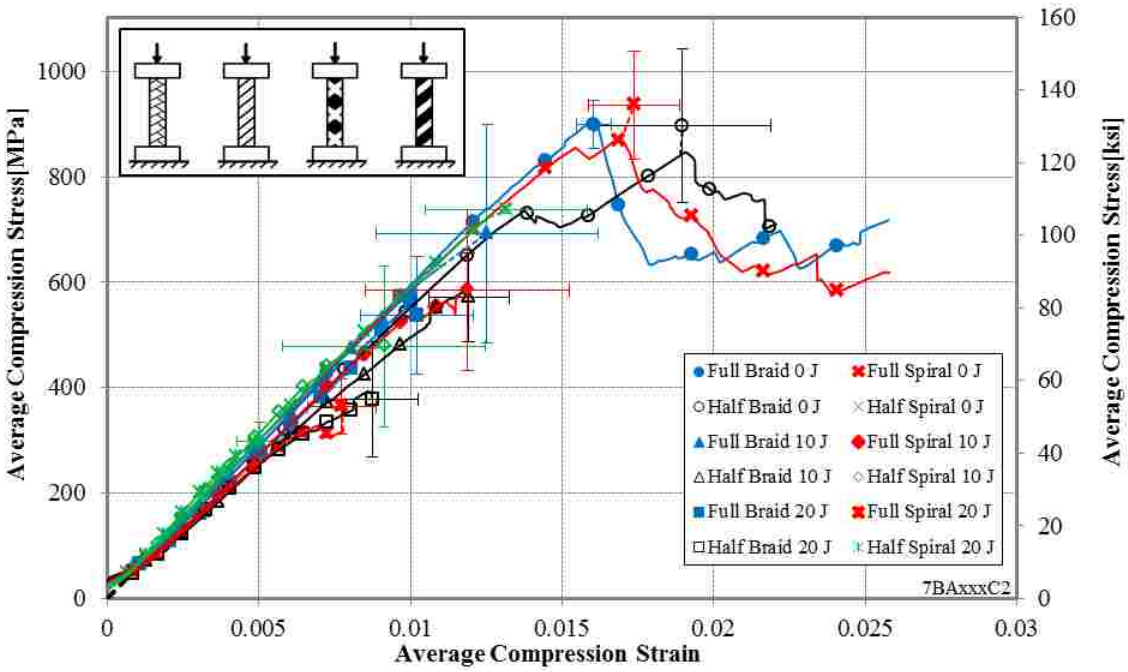

Figure 6.13: Average Stress-Strain Curves for all 11 mm (7/16”) Specimens

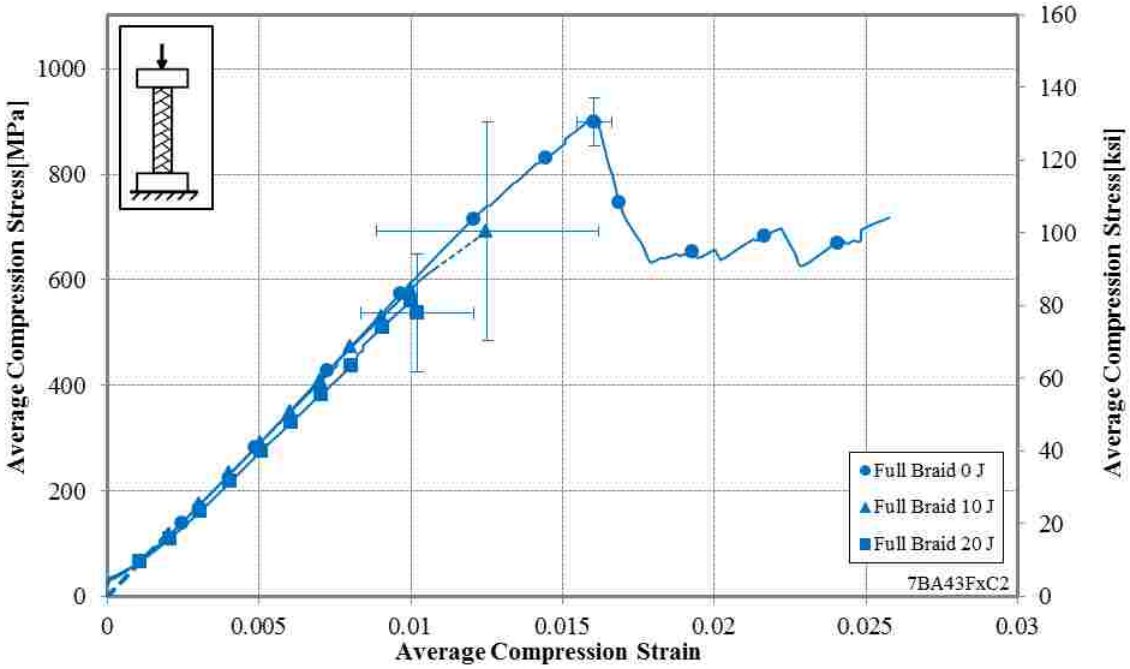

Figure 6.14: Average Stress-Strain Curves for all Full Braid, 11 mm (7/16") Specimens

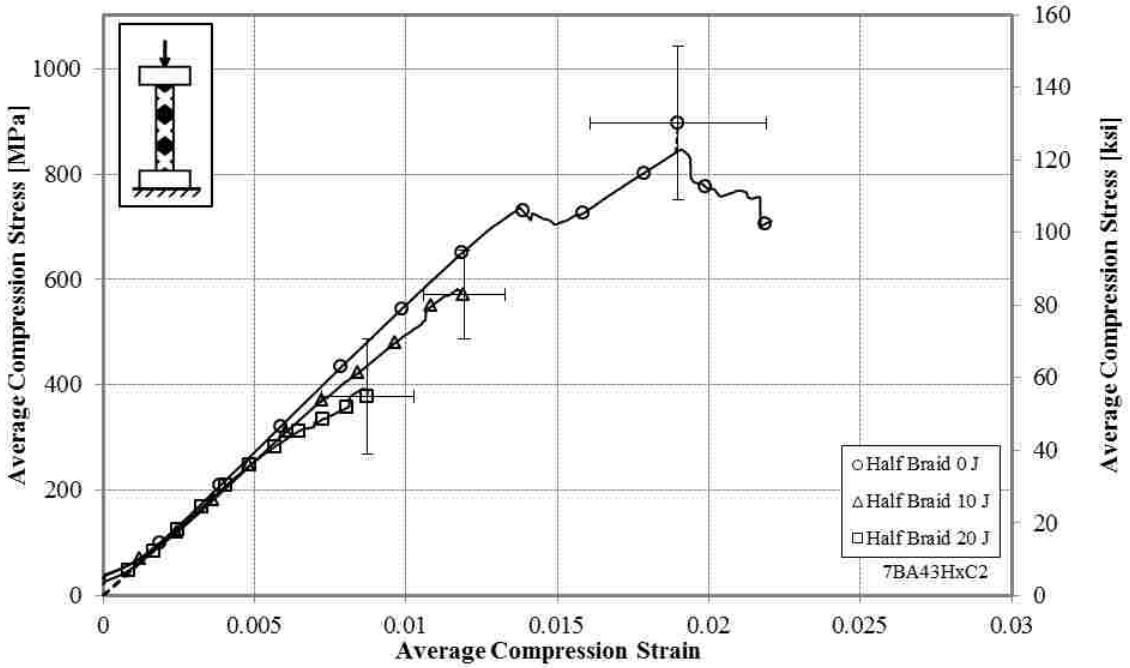

Figure 6.15: Average Stress-Strain Curves for all Half Braid, 11 mm (7/16) Specimens

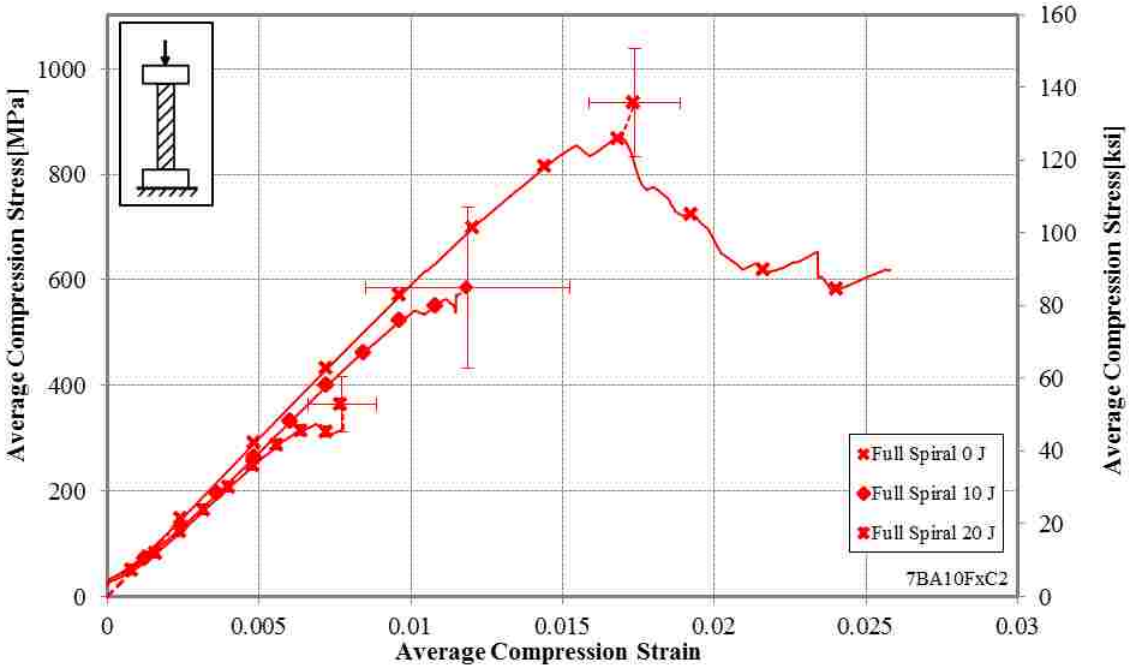

Figure 6.16: Average Stress-Strain Curves for all Full Spiral, 11 mm (7/16") Specimens

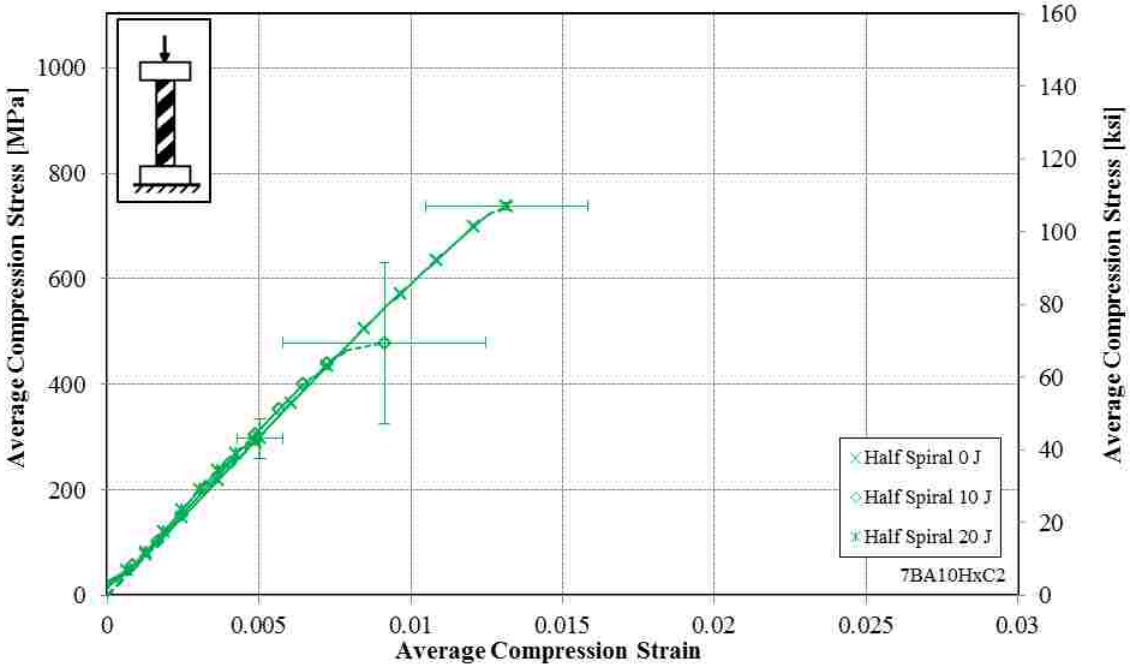

Figure 6.17: Average Stress-Strain Curves for all Full Spiral, 11 mm (7/16") Specimens

6.2.2 Influence of Sleeve Type and Coverage for Different Impact Levels

The next three plots, Figures 6-18 through 6-20, show the influence of sleeve type and coverage for different impact levels (no-impact, low impact, and severe impact). Sleeve type and coverage have no significant difference on compression strength of non-impacted configurations, as exemplified by Figure 6-18. When impacted, full coverage sleeves have greater strength than half coverage sleeves.

6.2.3 Influence of Sleeve Type and Impact Energy for Different Coverage

The next two plots, Figure 6.21 and Figure 6.22, show the influence of sleeve type and impact energy for different coverage (full coverage and half coverage).

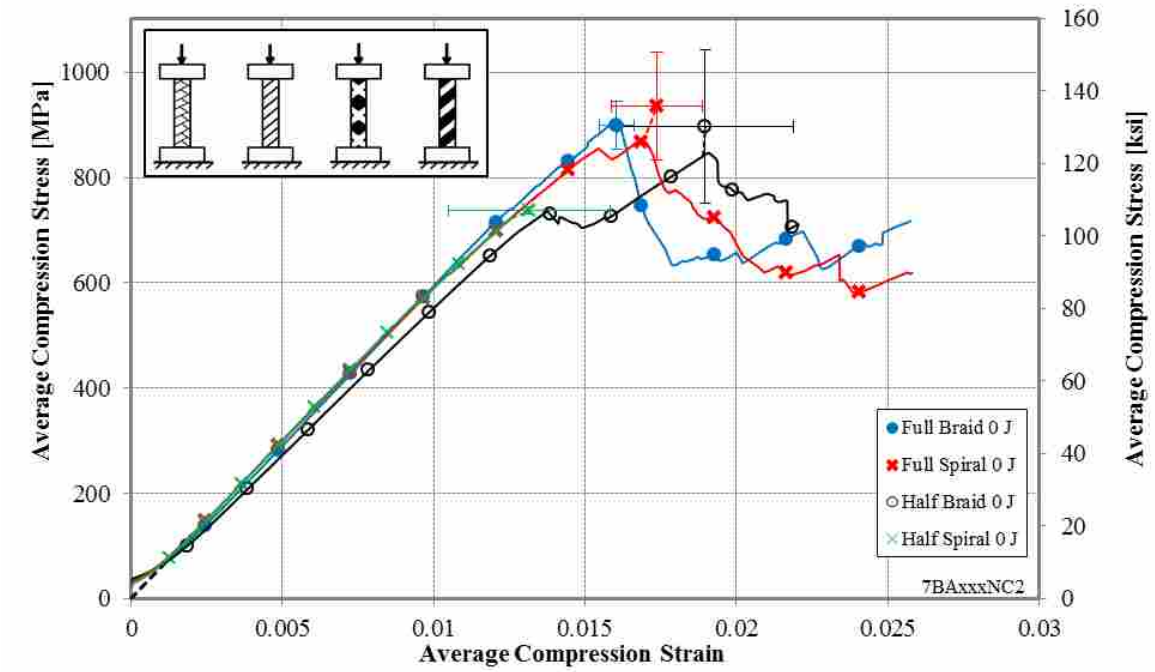

Figure 6.18: Average Stress-Strain Curves for all No-Impact, 11 mm (7/16") Specimens

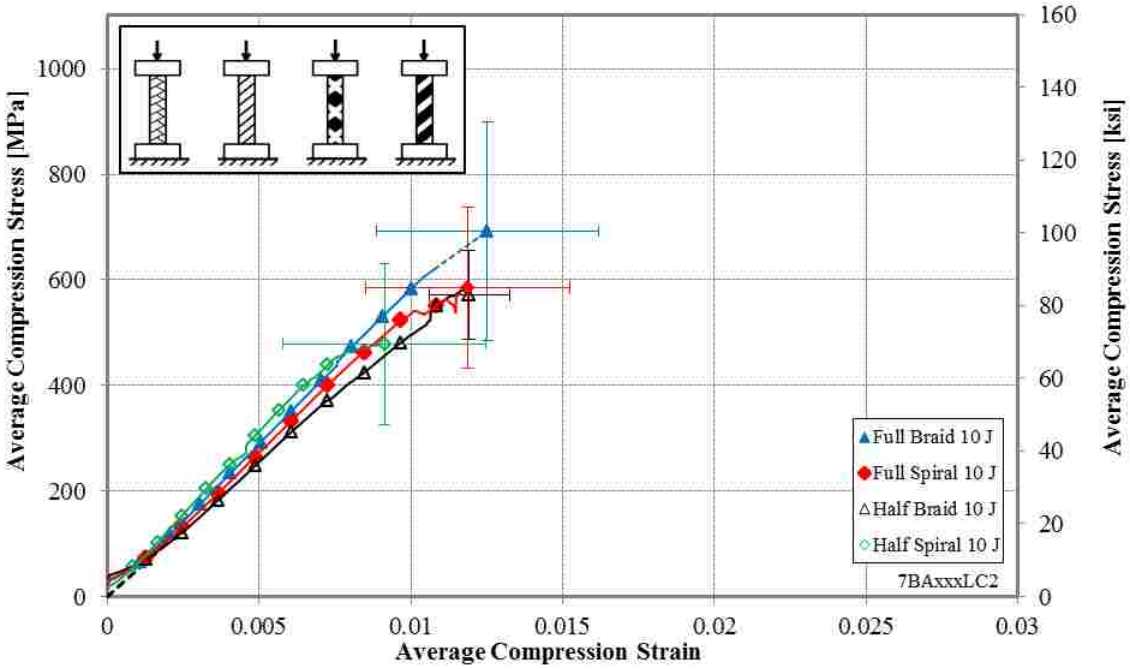

Figure 6.19: Average Stress-Strain Curves for all 10 J (7.4 ft-lbs.) Impact 11 mm (7/16") Specimens

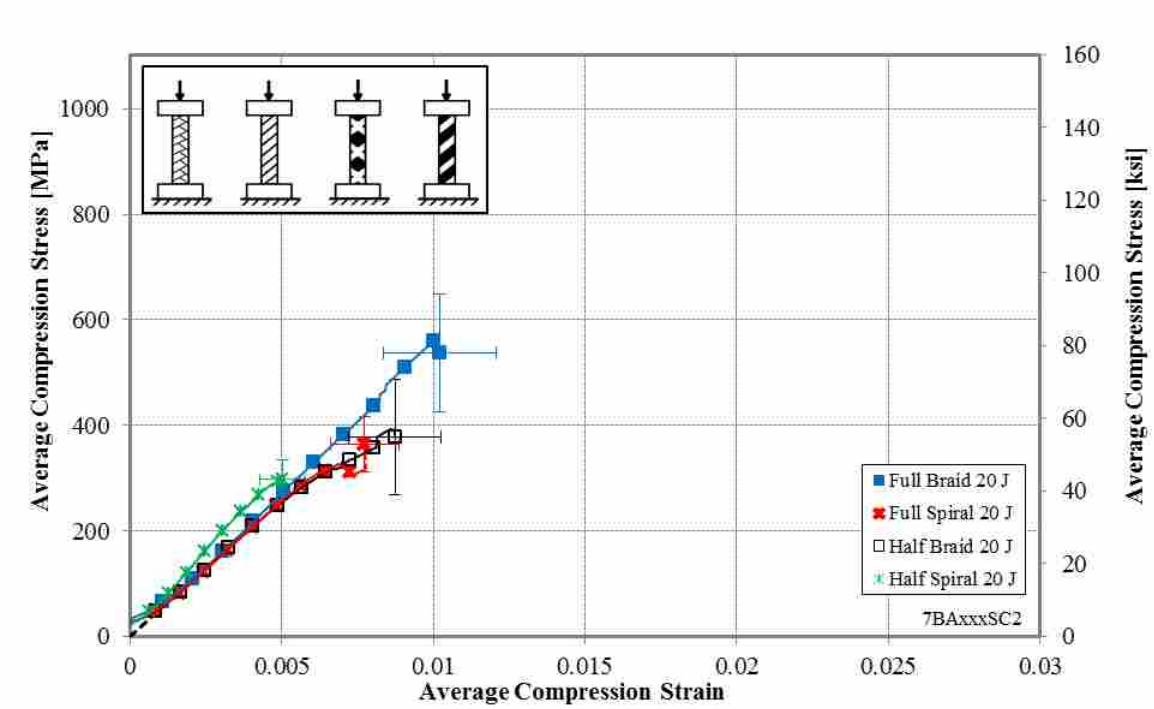

Figure 6.20: Average Stress-Strain Curves for all 20 J (14.8 ft-lbs.) Impact 11 mm (7/16") Specimens

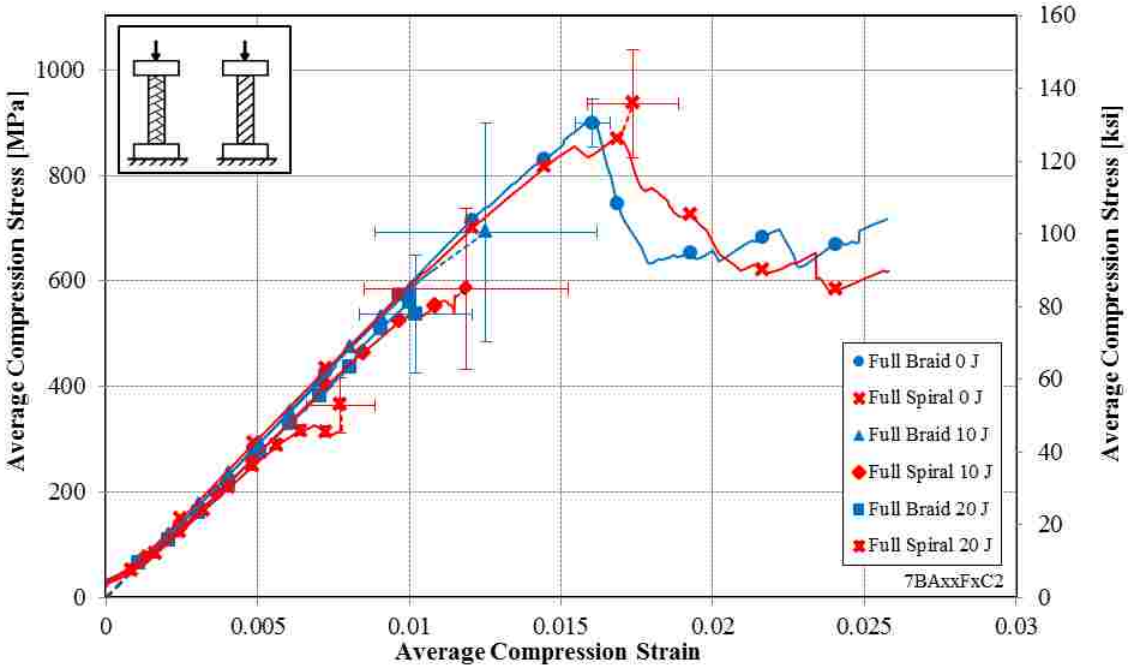

Figure 6.21: Average Stress-Strain Curves for all Full Coverage, 11 mm (7/16") Specimens

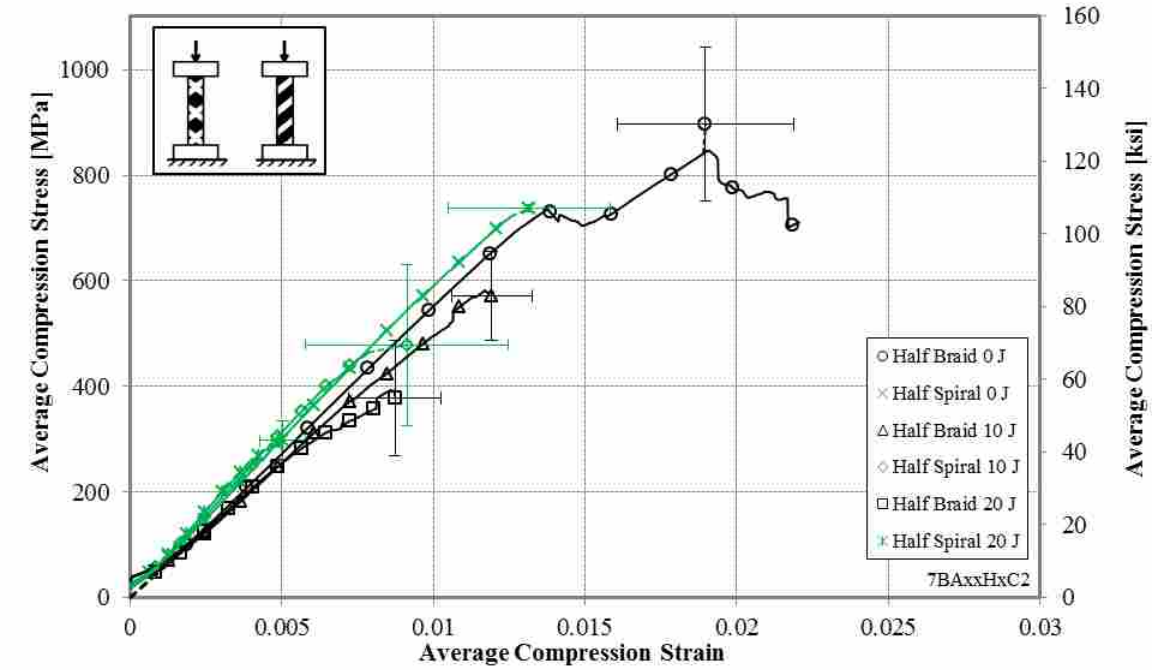

Figure 6.22: Average Stress-Strain Curves for all Half Coverage, 11 mm (7/16") Specimens

6.2.4 Influence of Coverage and Impact Levels for Different Sleeve Types

The final two plots, Figure 6.23 and Figure 6.24, show the influence of coverage and impact levels for different sleeve types (braid and spiral). Average curves for all specimens with a braided sleeve are shown in Figure 6.23. When not impacted there is no significant difference between full and half coverage braided specimens. When impacted at 5 J (3.7 ft-lbs.) or 10 J (7.4 ft-lbs.) the full coverage braid has greater strength than the half coverage braid.

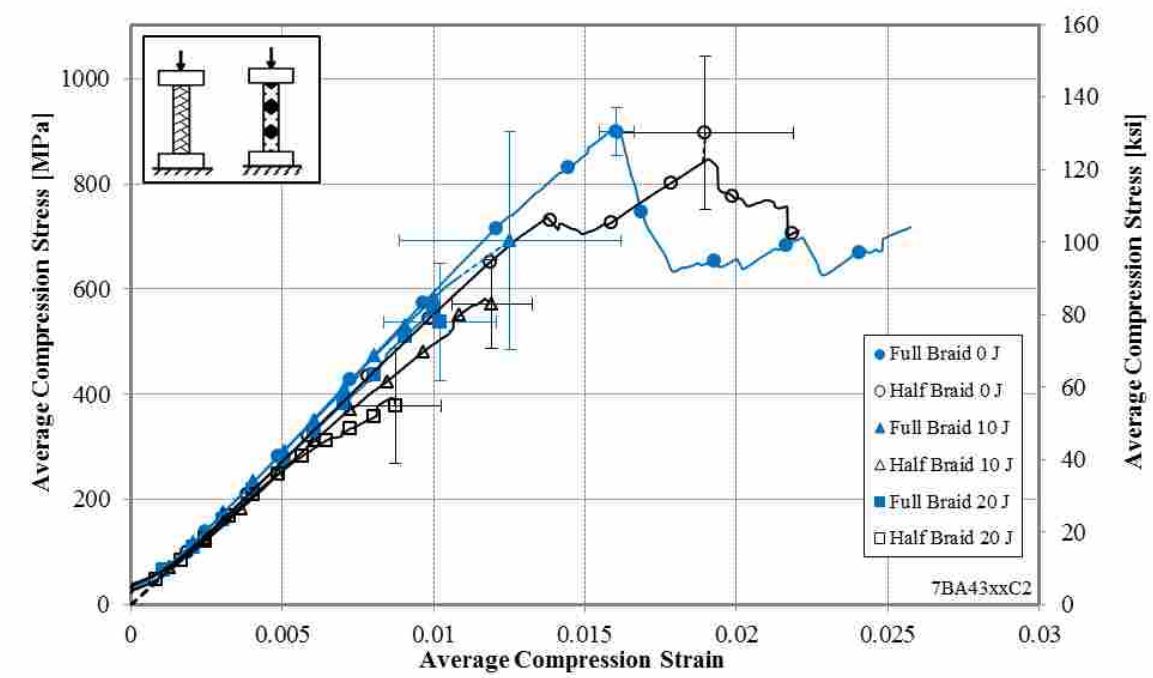

Figure 6.23: Average Stress-Strain Curves for all Braided Sleeves, 11 mm (7/16") Specimens

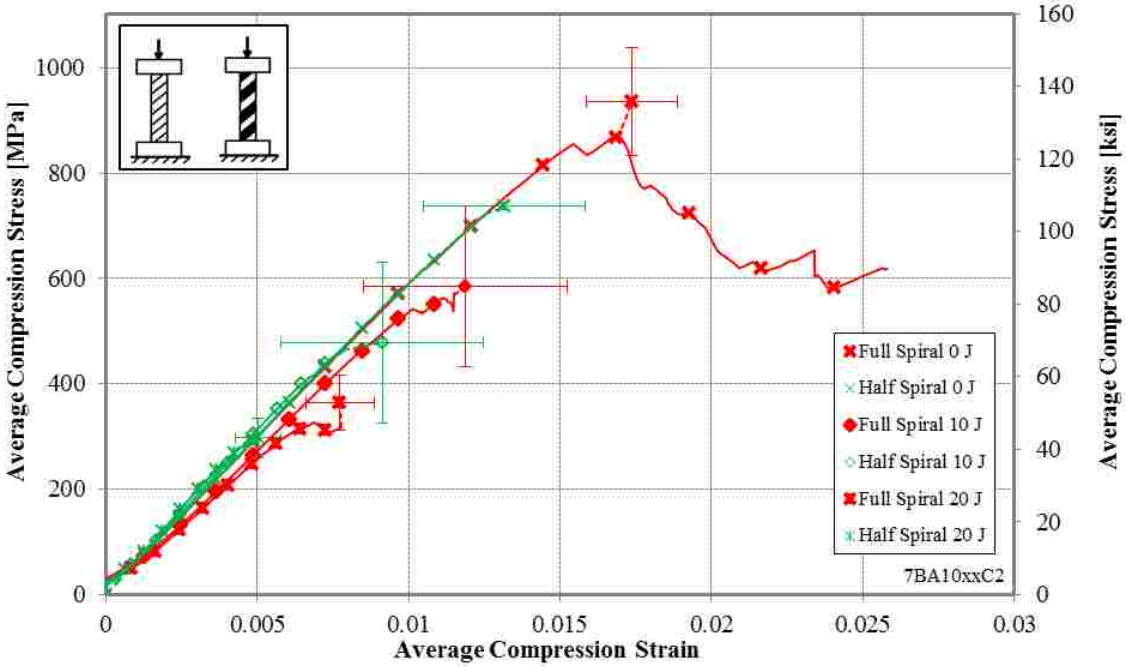

Figure 6.24: Average Stress-Strain Curves for all Spiral Sleeves, 11 mm (7/16") Specimens

7 DISCUSSION OF RESULTS

A discussion of the results for the primary configurations (51 mm (2") length) is presented in this chapter. For both the 8 mm (5/16") and 11 mm (7/16") diameter configurations, two stress-strain plots are presented emphasizing the effect of: 1) sleeve type; and, 2) sleeve coverage. Summary tables of key data from the plots are included.

The stress-strain plots in this chapter were prepared to demonstrate the effect of sleeve type and sleeve coverage on the compression strength after impact. Each plot has six curves, two at each impact level. These curves represent the average of all specimens with the appropriate value for the variable of interest. For example, in Figure 7.1 the individual curves for all non-impacted braided sleeve specimens are averaged together, regardless of full or half coverage. This average curve can be compared to a similarly prepared curve for all spiral sleeve specimens. The average curve continues until the average strain is reached, after which it is truncated and connected to the average maximum stress with a dashed line. Plots with each set of individual curves and the corresponding average curve are in Appendix H.

In the tables, differences in strength between configurations (shown as a percent) are normalized to the first row in the table. The final row of the table shows the overall effect for either sleeve coverage or sleeve type, as specified.

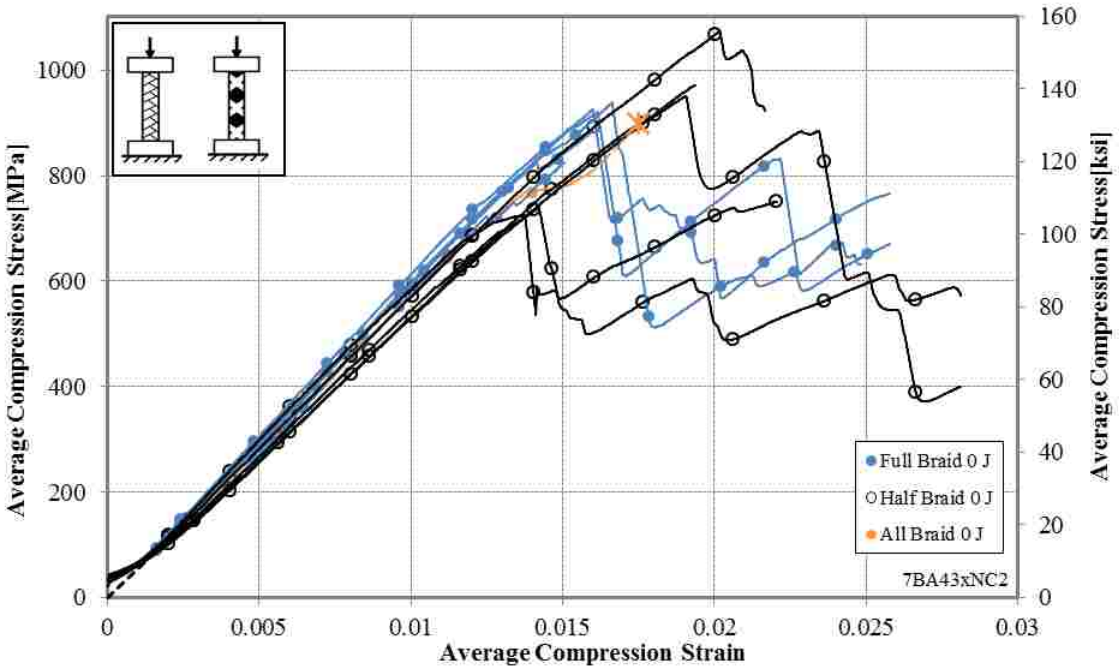

Figure 7.1: Average Stress-Strain Curve for all No-Impact Braided Sleeve Configurations

7.1 5/16" Diameter Analysis for 2" Specimens

This section compares all twelve specimen configurations that have an 8 mm (5/16") diameter. The average curves for the spiral and braided sleeves, for all sleeve coverage's, at each impact level, are shown in Figure 7.2. The bottom row of Table 7.1 provides the difference in strength (shown as a percent) between spiral and braided sleeves, for each impact level. When not impacted, there is an 8% overall difference in strength. At 5 J (3.7 ft-lbs.) there is a 15% overall difference in strength. At 10 J (7.4 ft-lbs.) there is a 9% overall difference in strength. These differences in strength are not significant for composites, which commonly exhibit 10-20% variation. Therefore, the sleeve type does not have a significant effect on the compression strength of the 8 mm (5/16") diameter specimens after impact.

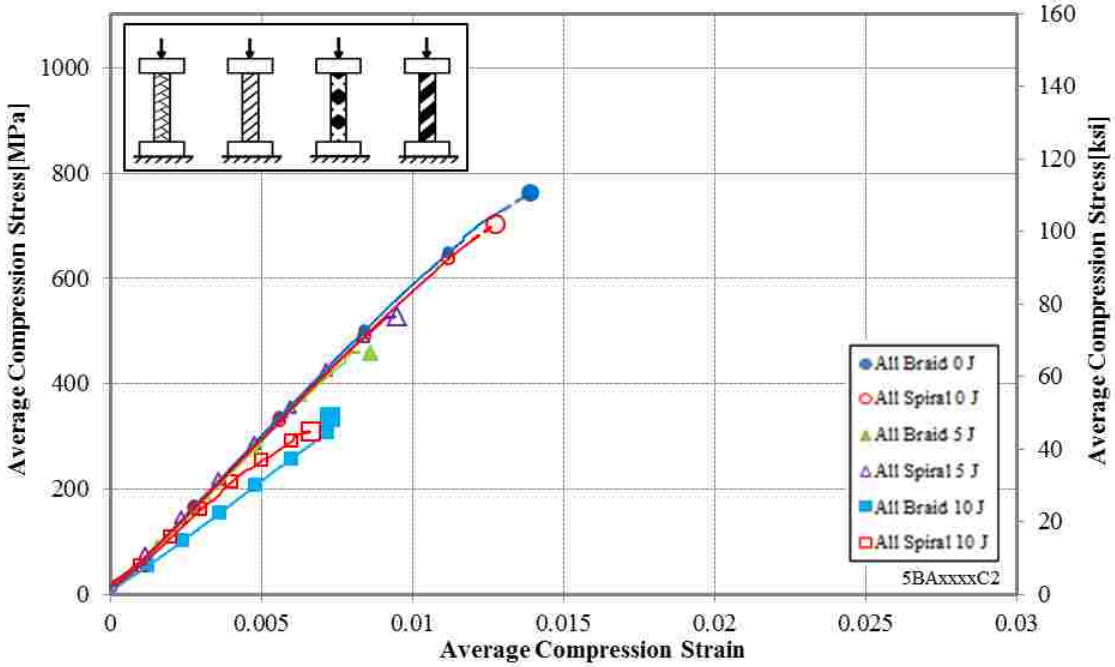

Figure 7.2: Average Stress-Strain Curves for 8 mm (5/16") Diameter Braided and Spiral Sleeve Configurations

Table 7.1: Influence of Braided vs. Spiral Sleeves on the Ultimate Strength of 8 mm (5/16") Diameter Configurations

Configuration Comparison	No-impact	5 J Impact (3 ft-lbs.)	10 J Impact (7.4 ft-lbs.)
Full Braid vs. Half Braid Coverage			
Full Braid Compression Strength [MPa (ksi)]	763 (110.6)	558 (80.9)	437 (63.4)
Half Braid Compression Strength [MPa (ksi)]	761 (110.4)	360 (52.2)	238 (34.6)
Average Braided Sleeve Compression Strength [MPa (ksi)]	**762 (110.5)**	**459 (66.6)**	**338 (49.0)**
Difference [%, relative to full]	**0%**	**-35%**	**-45%**
Full Spiral vs. Half Spiral Coverage			
Full Spiral Compression Strength [MPa (ksi)]	723 (104.9)	675 (97.9)	395 (57.3)
Half Spiral Compression Strength [MPa (ksi)]	684 (99.1)	380 (55.1)	222 (32.2)
Average Spiral Sleeve Compression Strength [MPa (ksi)]	**704 (102.0)**	**528 (76.5)**	**309 (44.8)**
Difference [%, relative to full]	**-6%**	**-44%**	**-44%**
Overall Diff. Between Braided &Spiral Sleeves[%, relative to braid]	**-8%**	**15%**	**-9%**

The average curves for the full and half coverage sleeves, for all sleeve types, at each impact level, are shown in Figure 7.3. The bottom row of Table 7.2 provides the difference in strength (shown as a percent) between full and half coverage sleeves, for each impact level. When not impacted, there is a 3% difference in strength. At 5 J (3.7 ft-lbs.) there is a 40% difference in strength. At 10 J (7.4 ft-lbs.) there is a 45% difference in strength. These differences in strength are significant for composites. Therefore, the amount of sleeve coverage has a significant effect on the compression strength after impact of the 8 mm (5/16") diameter specimens. There is no significant difference between the configurations when not impacted.

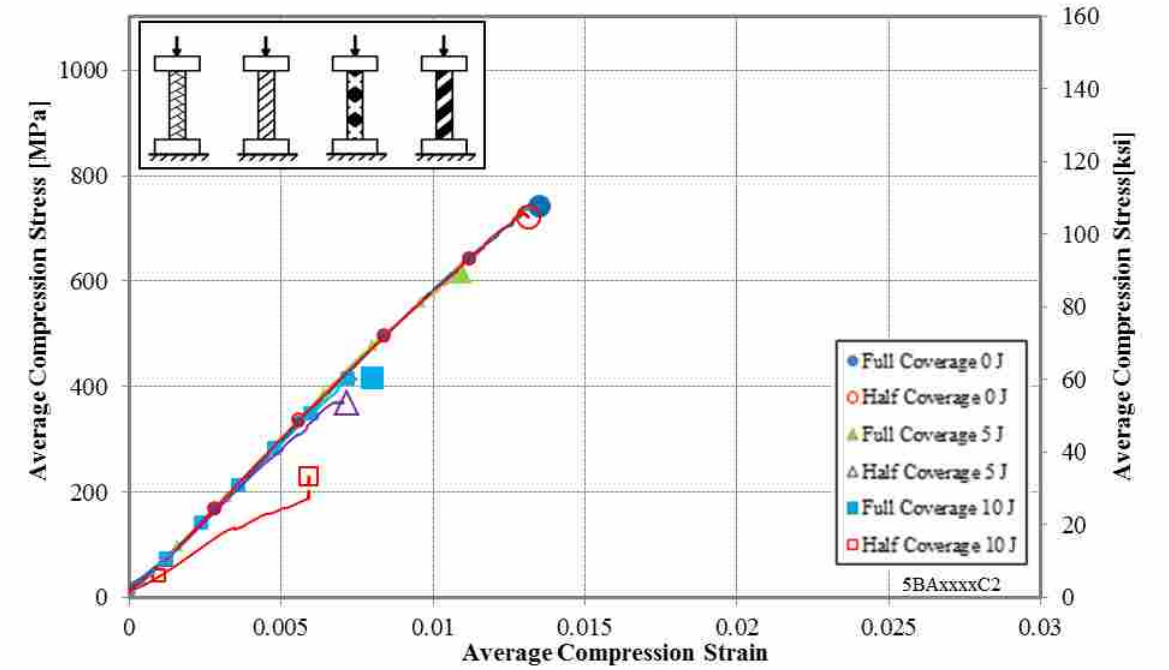

Figure 7.3: Average Stress-Strain Curves for 8 mm (5/16") Diameter Full and Half Coverage Configurations

Table 7.2: Influence of Full vs. Half Coverage on the Ultimate Strength of 8 mm (5/16") Diameter Configurations

Configuration Comparison	No-impact	5 J Impact (3.7 ft-lbs.)	10 J Impact (7.4 ft-lbs.)
Full Braid vs. Full Spiral Coverage			
Full Braid Compression Strength [MPa (ksi)]	763 (111)	558 (81)	437 (63)
Full Spiral Compression Strength [MPa (ksi)]	723 (105)	675 (98)	395 (57)
Average Full Sleeve Compression Strength [MPa (ksi)]	**743 (108)**	**617 (89)**	**416 (60)**
Difference [%, relative to braid]	**-5%**	**21%**	**-10%**
Half Braid vs. Half Spiral Coverage			
Half Braid Compression Strength [MPa (ksi)]	761 (110)	360 (52)	238 (35)
Half Spiral Compression Strength [MPa (ksi)]	684 (99)	380 (55)	222 (32)
Average Half Sleeve Compression Strength [MPa (ksi)]	**723 (105)**	**370 (54)**	**230 (34)**
Difference [%, relative to braid]	**-10%**	**5%**	**-7%**
Overall Difference Between Full & Half Coverage [%, relative to full]	**-3%**	**-40%**	**-45%**

7.2 7/16" Diameter Analysis for 2" Specimens

This section compares all twelve specimen configurations that have an 11 mm (7/16") diameter. The average curves for the spiral and braided sleeves, for all sleeve coverages, at each impact level, are shown in Figure 7.4. The bottom row of Table 7.3 provides the difference in strength (shown as a percent) between spiral and braided sleeves, for each impact level. When not impacted, there is a 7% difference in strength. At 10 J (7.4 ft-lbs.) there is a 16% difference in strength. At 20 J (14.8 ft-lbs.) there is a 23% difference in strength. Only when impacted with 20 J (14.8 ft-lbs.) is the sleeve type significant for the compression strength of the specimen.

The average curves for the full and half coverage sleeves, for all sleeve types, at each impact level, are shown in Figure 7.5. The bottom row of Table 7.4 provides the difference in strength (shown as a percent) between full and half coverage sleeves, for each impact level. When not impacted, there is an 11% difference in strength. At 10 J (7.4 ft-lbs.) there is a 18% difference in strength. At 20 J (14.8 ft-lbs.) there is a 20% difference in strength. These

differences in compression strength after impact are significant for composites. Therefore, the amount of sleeve coverage does have a significant effect on the compression strength after impact of the 11 mm (7/16") diameter specimens. There is no significant difference between the configurations when not impacted.

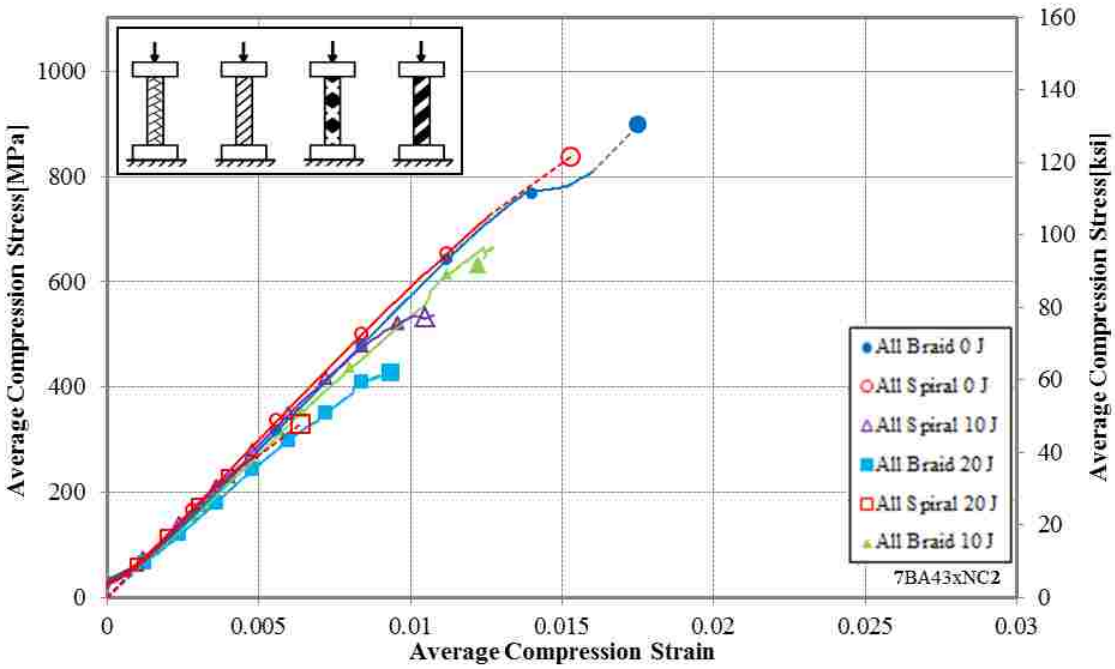

Figure 7.4: Average Stress-Strain Curves for Braided and Spiral Sleeve Configurations, 11 mm (7/16") Diameter

7.3 Comparison of 5/16" and 7/16" Diameters

In this section the 8 mm (5/16") diameter specimens are compared to the 11 mm (7/16") diameter specimens. There are two variables that change between these two groups of geometries: 1) the diameter of the specimen; and, 2) the energy used to impact the specimens. With a diameter increase of 3 mm (1/8"), the area approximately doubles; this variable is normalized by looking at the compression stress rather than the compression load. With regards to the impact energy, the 8 mm (5/16") diameter specimens impacted with 5 J (3.7 ft-lbs.) and

the 11 mm (7/16") diameter specimens impacted with 10 J (7.4 ft-lbs.) are referred to as low impact. The 8 mm (5/16") diameter specimens impacted with 10 J (7.4 ft-lbs.) and the 11 mm (7/16") diameter specimens impacted with 20 J (14.8 ft-lbs.) are referred to as severe impact (see Figure 7.6 and Figure 7.7). The two diameters are also compared at 10 J (7.4 ft-lbs.) impact.

Figure 7.6 compares the 8 mm (5/16") diameter specimens to the 11 mm (7/16") diameter specimens for full and half coverage sleeves. The values for the average compression strength are taken from Tables 7.1-7.4. As seen by the increasing slope of every line, an increased diameter provides greater strength as expected. This is confirmed when looking at the two geometries both impacted with 10 J (7.4 ft-lbs.) as shown with the dashed lines. In both cases, half and full coverage, the larger diameter has greater strength. This difference in strength is attributed to the outer core fibers providing additional protection to the inner core fibers.

Table 7.3: Influence of Braided vs. Spiral Sleeve on the Ultimate Strength of 11 mm (7/16") Diameter Configurations

Configuration Comparison	No-impact	10 J Impact (7.4 ft-lbs.)	20 J Impact (14.8 ft-lbs.)
Full Braid vs. Half Braid Coverage			
Full Braid Compression Strength [MPa (ksi)]	900 (130.5)	693 (100.5)	479 (69.5)
Half Braid Compression Strength [MPa (ksi)]	897 (130.1)	572 (82.9)	378 (54.8)
Average Braided Sleeve Compression Strength [MPa (ksi)]	**899 (260.6)**	**633 (91.7)**	**429 (62.2)**
Difference [%, Relative to Full]	**0%**	**-18%**	**-21%**
Full Spiral vs. Half Spiral Coverage			
Full Spiral Compression Strength [MPa (ksi)]	936 (135.8)	585 (84.8)	365 (52.9)
Half Spiral Compression Strength [MPa (ksi)]	737 (107.0)	479 (69.5)	297 (43.1)
Average Spiral Sleeve Compression Strength [MPa (ksi)]	**837 (121.4)**	**532 (77.2)**	**331 (48.0)**
Difference [%, Relative to Full]	**-21%**	**-18%**	**-18%**
Overall Diff. Between Braided &Spiral Sleeves {%, relative to braid]	**-7%**	**-16%**	**-23%**

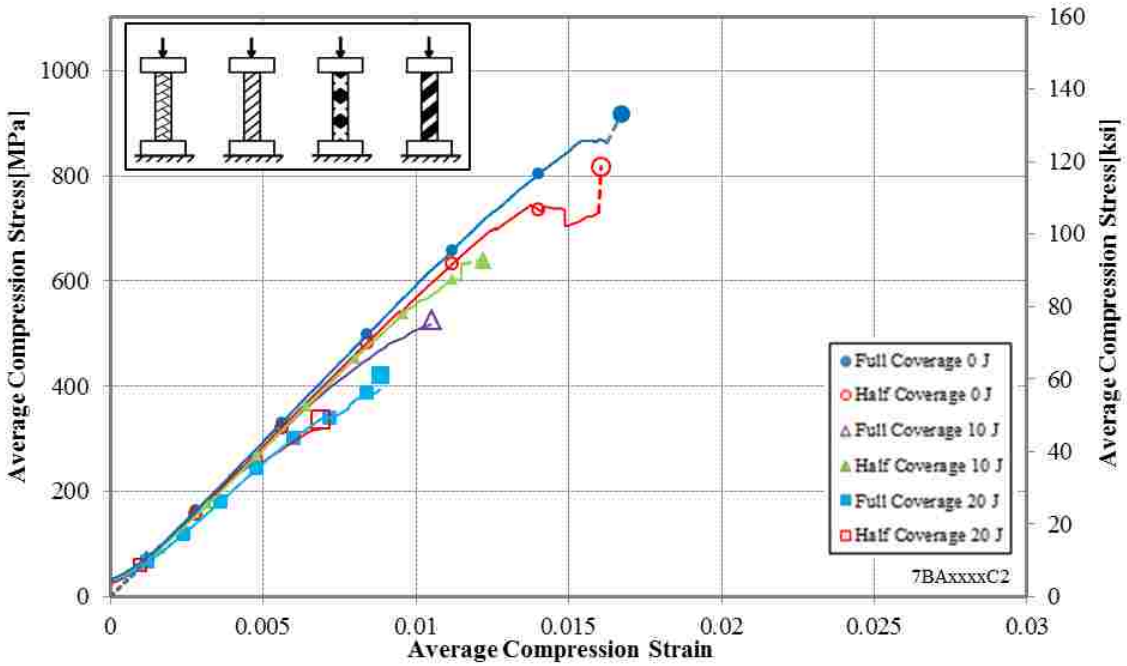

Figure 7.5: Average Stress-Strain Curves for Half and Full Coverage Sleeve Configurations 11 mm (7/16") Diameter

Table 7.4: Influence of Full vs. Half Coverage on the Ultimate Strength of 11 mm (7/16") Diameter Configurations

Configuration Comparison	No-impact	10 J Impact (7.4 ft-lbs.)	20 J Impact (14.8 ft-lbs.)
Full Braid vs. Full Spiral Coverage			
Full Braid Compression Strength [MPa (ksi)]	900 (130.5)	693 (100.5)	479 (69.5)
Full Spiral Compression Strength [MPa (ksi)]	936 (135.8)	585 (84.8)	365 (52.9)
Average Full Sleeve Compression Strength [MPa (ksi)]	**918 (133.2)**	**639 (92.7)**	**422 (61.2)**
Difference [%, Relative to Braid]	**4%**	**-16%**	**-24%**
Half Braid vs. Half Spiral Coverage			
Half Braid Compression Strength [MPa (ksi)]	897 (130.1)	572 (82.9)	378 (54.8)
Half Spiral Compression Strength [MPa (ksi)]	737 (107.0)	479 (69.5)	297 (43.1)
Average Half Sleeve Compression Strength [MPa (ksi)]	**817 (237.1)**	**526 (76.2)**	**337.5 (49.0)**
Difference [%, Relative to Braid]	**-18%**	**-16%**	**-21%**
Overall Difference Between Full & Half Coverage [%, relative to full]	**-11%**	**-18%**	**-20%**

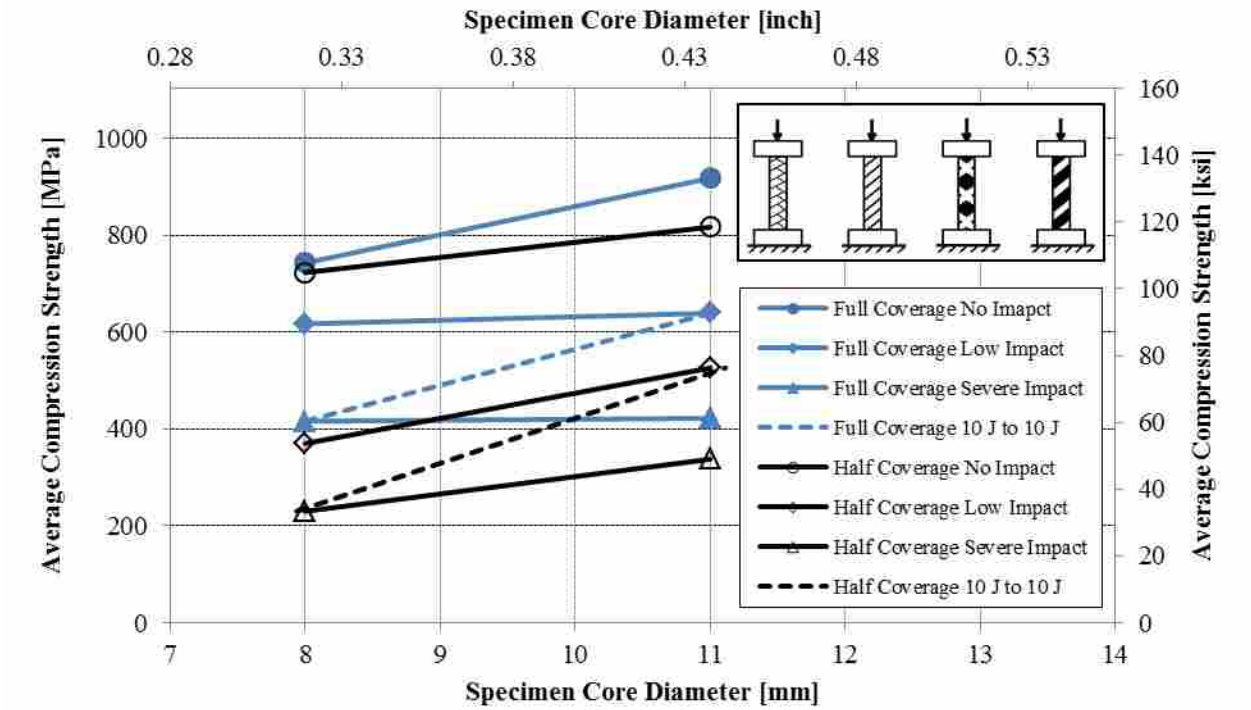

Figure 7.6: Comparison of the 8 mm (5/16") and 11 mm (7/16") Configurations for Full and Half Coverage

Figure 7.7 compares the 8 mm (5/16") and 11 mm (7/16") diameter specimens for all braid and spiral sleeves. The results are similar to the half and full coverage configurations, with the 11 mm (7/16") diameter configurations exhibiting slightly greater damage tolerance than the 8 mm (5/16") diameter configurations.

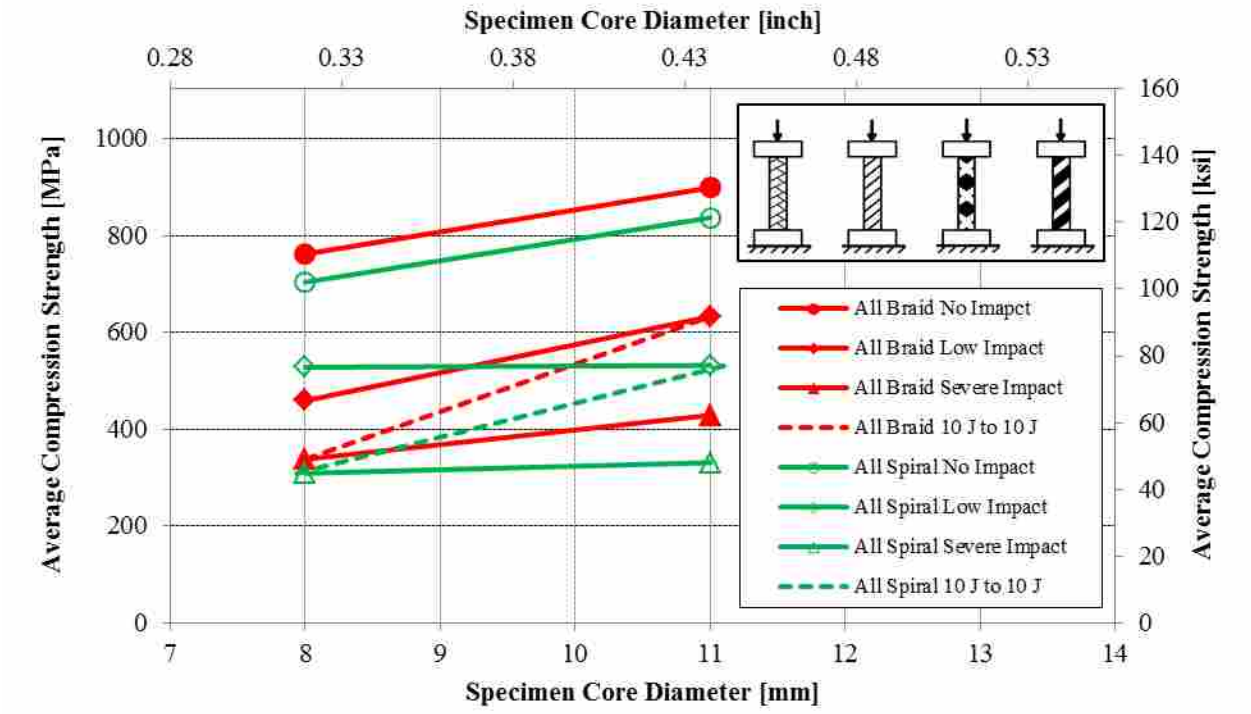

Figure 7.7: Comparison of the 8 mm (5/16") and 11 mm (7/16") Diameter Configurations for Braided and Spiral Sleeves

8 CONCLUSIONS AND RECOMMENDATIONS

This research investigated the effects of an aramid sleeve on the damage tolerance of cylindrical unidirectional basalt/epoxy composites, representing local members of IsoTruss structures. Both braided and spiral sleeves have been shown to successfully consolidate specimens and increase the damage tolerance, particularly, compression strength after impact.

The variables considered in this research include the type of sleeve, the amount of sleeve coverage, the diameter of the specimen, and the level of impact energy. The following sections present: 1) general conclusions; 2) specific conclusions; 3) contributions to the state of the art of IsoTruss technology; and, 4) recommendations for future research.

8.1 General Conclusions

This section provides responses to the question posed in Section 1.3. These responses also provide a general list of major research findings.

1. Either braided or spiral sleeves properly consolidate continuously-manufactured unidirectional basalt/epoxy composites.
2. At lower impact energy levels, braided and spiral sleeves exhibit similar behavior. At higher impact energy levels, a braided sleeve provides more compression strength after impact than a spiral sleeve.

3. Full coverage provides significantly higher compression strength after impact than partial coverage.
4. The 11 mm (7/16”) diameter configurations have slightly greater damage tolerance than the 8 mm (5/16”) diameter configurations
5. Higher impact energy levels decrease the compression strength after impact of unidirectional composites with a consolidating sleeve.

8.2 Specific Conclusions

This section provides specific conclusions and findings for the research.

1. The average non-impacted compression strength of unidirectional basalt/epoxy composites is 800 MPa (116 ksi).
2. When not impacted, the type of sleeve or amount of sleeve coverage does not significantly affect the compression strength of basalt/epoxy configuration.
3. Whether impacted or not, sleeve type does not significantly affect the compression strength after impact of 8 mm (5/16”) diameter configurations.
4. Braided sleeves improve compression strength after 20 J (14.8 ft-lbs.) impact of 11 mm (7/16”) diameter members by 23% compared to spiral sleeves. There is no significant difference between braided and spiral sleeve configurations at other impact energy levels.
5. Full sleeve coverage, 8 mm (5/16”) diameter configurations exhibit 45% higher compression strength after impact than partial coverage.
6. Full sleeve coverage, 11 mm (7/16”) diameter configurations exhibit 20% higher compression strength after impact than partial coverage.

7. The initial stiffness of the members, whether impacted or not, is only minimally degraded by impact.
8. The various sleeve configurations successfully consolidate unidirectional basalt/epoxy composites achieving an average fiber volume of 59% for the composite member.

8.3 Contributions to the State of the Art

The results of this research lead to several advances in understanding the compression strength after impact of basalt/epoxy composites, representative of the members of IsoTruss structures. In particular, this research:

1. Measured the compression strength and compression strength after impact of unidirectional cylindrical basalt/epoxy composites;
2. Quantified the influence of sleeve coverage, sleeve type, and core diameter on the damage tolerance of unidirectional cylindrical basalt/epoxy members;
3. Developed test processes; and,
4. Designed and manufactured fixtures for specimen preparation and testing.

8.4 Recommendations

This section presents recommendations for manufacturing IsoTruss structures and further testing on the damage tolerance of composites.

8.4.1 Manufacturing Recommendations

Recommendations for manufacturing additional test specimens on the latest IsoTruss machine are presented in this section.

1. Ensure materials are of proper quality and remain free of contaminants.
2. Ensure that the pulling forces are symmetric (use counter-weight if needed).
3. Find a way to reduce fraying of fibers passing through the machine wall.
4. Improve the consistency of the bobbin rewind capability and increase the bobbin fiber capacity.
5. Use stronger bearings for the shafts and drive gears in machine wall.

8.4.2 Specimen Preparation and Testing Recommendations

Recommendations for preparing specimens and, for testing specimens are presented in this section.

1. Be extremely careful when cutting specimens. The cutting blades are fragile and expensive, the specimens are very hard, and the blade can snag on the aramid sleeve.
2. Excessive sanding distorts the end caps used for testing. If possible avoid sanding the specimens once set in the end caps to retain a more even end cap surface.
3. The rough nature of the sleeve does not facilitate the use of an extensometer.

8.4.3 Recommended Future Research

Additional areas that need to be investigated for a more comprehensive understating of basalt/epoxy composites, specifically when used in conjunction with IsoTruss technology are presented in this section.

1. Increase the number of test specimens from five to eleven for each configuration to increase reliability of results.
2. The extent of damage incurred in the specimens after impact should be quantified using non-destructive inspection methods (e.g., ultrasound, x-ray). This would enable direct comparison of damage to compressive strength, allowing the results to be extrapolated to different geometries.
3. Explore the behavior of longer specimens that fail in buckling rather than pure compression [34].
4. For this research a Kevlar 49-7100 denier fiber (very large diameter) was used for the sleeve. Sleeves manufactured with a smaller denier aramid tow should be investigated.
5. Evaluate the compression strength after impact for members impacted near or at a node of the IsoTruss structure.

REFERENCES

[1] Agarwal, B., Broutman, L., Chandrashekhara, K., "Analysis and Performance of Fiber Composites Third Edition," John Wiley & Sons Inc., pp. 11-12, 2006.

[2] Strong, A. and D. Jensen., "The Ultimate Composite Structure," *Composites Fabrication*, pp. 22–27, Aug. 2002.

[3] Scoresby, B., "Low Velocity Longitudinal and Radial Impact f IsoTruss™ Grid Structures," M.S. Thesis, Brigham Young University, Provo, Utah, 2003.

[4] McCune, A., "Tension and Compression of Carbon/Epoxy IsoTruss™ Grid Structures," M.S. Thesis, Brigham Young University, Provo, Utah, 2001.

[5] Kesler, S., "Consolidation and Interweaving of Composite Members by a Continuous Manufacturing Process," M.S. Thesis, Brigham Young University, Provo, Utah, 2006.

[6] Winkel, L., "Parametric Investiagation of IsoTruss™ Geometry Using Linear Finite Element Analysis," M.S. Thesis, Brigham Young University, Provo, Utah, 2001.

[7] Hansen, S., "Influence of Consolidation and Interweaving on Compression Behavior of IsoTruss® Structures," M.S. Thesis, Brigham Young University, Provo, Utah, 2004.

[8] Wisnom, M., "Suppression of Splitting and Impact Sensitivity of Unidirectional Carbon-Fibre Composite Rods Using Tensioned Overwind," *Composites Part A: Applied Science and Manufacturing*, Vol. 30, No. 5, pp. 661-665, 1999.

[9] Jao, S., "Energy Absorption of Failing Injection-Molded Rubber-Coated Glass/Nylon Composites," Specialty Conference of Advanced Composites Materials in Civil Engineering Proceeding , Las Vegas, NV, Jan. 31-Feb. 1, 1991, pp. 1-11.

[10] Duguay, A. et al., "Mechanical Properties of Exfoliated Graphite Nonplatelet (XGNP)-filled Impact Modified Polypropylene (IMPP) Nanocomposites," SAMPE 20ll Technical Conference Proceedings: State of the Industry: Advanced Materials, Applications, and Processing technology, Long Beach, CA, May 23-26, 2011. Society for the Advancement of Material and Process engineering, CD-Rom pp. 1-6.

[11] Beard, S. and Chang, F., "Design of Braided Composites for Energy Absorption," Proceedings of the American Society for Composites 15th Technical Conference, College Station, TX, Spetember 25-27, 2000, pp.11-19.

[12] Hamada, H., Coppola, J., Hull, D., "Effect of Surface Treatment on Crushing Behaviour of Glass Cloth/Epoxy Composite Tubes," *Composites*, Vol. 23, No. 2, pp. 93-99, 1992.

[13] Cwik, T. et al., "Investigation of Ballistic Response of CFRP Composites of various Non-Conventional Reinforcement Architectures," *Proceeding of The 18th International Conference on Composite Materials*, Aug. 2011.

[14] Zammit, A., Feih, S., Orifici, A., "2D Numerical Investigation of Pre-Tension on Low Velocity Impact Damage of Sandwich Structures," *Proceeding of The 18th International Conference on Composite Materials*, Aug. 2011.

[15] Kang, W. and Lee, H., "Estimation of residual Strength Distribution of Composite Structure with Impact-Induced Damage," *Proceeding of The 18th International Conference on Composite Materials*, Aug. 2011.

[16] Lee, J., Soutis, C., Kong C., "Prediction of Compression-After-Impact (CAI) Strength of CFRP Laminated Composites," *Proceeding of The 18th International Conference on Composite Materials*, Aug. 2011.

[17] Prichard J. and Hogg P., "The Role of Impact Damage in Post-Impact Compression Testing," *Composites*, Vol. 21, No. 6, pp. 503-511, 1990.

[18] Hosur, M., Chowdhury, F., Jeelani, S., "Low-Velocity Imapct Response and Ultrasonic NDE of Woven Carbon/Nanoclay Nanocomposites," *Journal of Composite Materials*, Vol. 41, No. 18, pp. 2195-2212, 2007.

[19] Cantwell, W. and Morton, J., "The Impact Resistance of Composite Materials - A Review," *Composites*, Vol. 22, No. 5, pp. 347-362, 1991.

[20] Suemasu, H. "The Impact Damage and the Low Compressive Strength of Composite Laminates," *Proceeding of The 18th International Conference on Composite Materials*, Aug. 2011.

[21] Rajaneesh, A., Sridhar, I., Rajendran, S., "Numerical Modeling of Low Velocity Impact response on Metal Foam Cored Sandwich Panels: Effect of Various Facesheet Materials," *Proceeding of The 18th International Conference on Composite Materials*, Aug. 2011.

[22] Woo, K. et al., "High-Velocity Impact Damage Behavior of Graphite-Epoxy Composite Laminates," *Proceeding of The 18th International Conference on Composite Materials*, Aug. 2011.

[23] Yoshimura, A. et al., "damage Simulation of CFRP Laminates Under High Velocity Projectile Impact," *Proceeding of The 18th International Conference on Composite Materials,* Aug. 2011.

[24] Carroll, T., "Predicted Residual Strength of Damaged IsoTruss® Structures," M.S. Thesis, Brigham Young University, Provo, Utah, 2006.

[25] DeFrancisci, G., Chen, Z., Kim, H., "Blunt Impact Damage Formation in Frame and Stringer Stiffened Composite Panels," *Proceeding of The 18th International Conference on Composite Materials,* Aug. 2011.

[26] Soutis, C., "Compression Testing of Pultruded Carbon Fibre-Epoxy Cylindrical Rods." *Journal of Materials Science,* Vol. 34, pp. 3441-3446, 2000.

[27] Kamenny Vek KV 11 Series Data Sheet http://www.basfiber.com/Sites/basfiber/Uploads/BCF%20KV11%20assembled_TDS_eng.202CB9D826F74BC685B3910192BB01FF.pdf

[28] TCR Composites (2007) "UF3325 TCR™ Resin Data Sheet", Revision 10. http://www.tcrcomposites.com/pdfs/resindata/

[29] Dupont, "Section II: Properties of Kevlar®," *Technical Guide Kevlar Aramid Fiber,* http://www2.dupont.com/Kevlar/en_US/assets/downloads/KEVLAR_Technical_Guide.pdf

[30] Jensen, M. and Jensen, D., "Continuous Manufacturing of Cylindrical Composite Lattice Structures*," Proceedings of the International Conference on Textile Composites* (TEXCOMP10), Oct. 26-28, 2010.

[31] Jensen, D., "Using External Robots Instead of Internal Mandrels to Produce Composite Lattice Structures" *Proceedings of the International Conference on Textile Composites (TEXCOMP10),* Oct. 26-28, 2010.

[32] Allen, D., "Influence of Braided Sleeves on the Impact Damage of Cylindrical Unidirectional Elements," *Proceedings of the 18th International Conference on Composite Materials*, Aug. 2011.

[33] Allen, D., "Compression Strength After Impact of Basalt Fiber Members in an Aramid Sleeve," *Proceedings of the SAMPE Tech Conference*, Fort Worth Texas, Oct. 2011.

[34] Embley, M., "Buckling Strength of Damaged Unidirectional Basalt Composite Rods with Braided Sleeves" *Proceedings of the SAMPE Tech Conference,* Fort Worth Texas, Oct. 2011.

APPENDIX A: CURE TEMPERATURE STUDY

The standard manufacturer's cure cycle for UF3330-100 epoxy is one hour at 154°C (310°F) for, proceeded by a temperature ramp up of 2.75°C (5°F) per minute, and a cool down of the same rate. According to TCR Composites the curing time can be reduced in half with each 11° C (20°F) increase in curing temperature, as shown in Table A.1. To find the optimal cure temperature and reduce the time needed to cure the specimens a simple cure study was performed.

Table A.1: Cure Temperature and Corresponding Cure Time

Cure Temperature [°C(°F)]	Cure Time [min]
154 (310)	60
166 (330)	30
177 (350)	15
188 (370)	8
199 (390)	4
210 (410)	2

The specimens were composed of 76 mm (3") long by 8 mm (5/16") diameter core specimens of basalt fibers pre-impregnated with UF3330-100 epoxy, wrapped in a half coverage braided sleeve. The specimens cured at 154°C (310°F), 188°C (370°F), and 210°C (410°F) had a sleeve made from a dry basalt fiber tow. The remaining specimen had an aramid sleeve.

The specimens were tested for compression strength following the procedures outlined above, without impact. The stress-strain curves for each individual specimen along with the

configuration average are shown in Figures A.1 through A.6. The average compression strength, corresponding strain and Young's modulus for each cure temperature are in Table A.2.

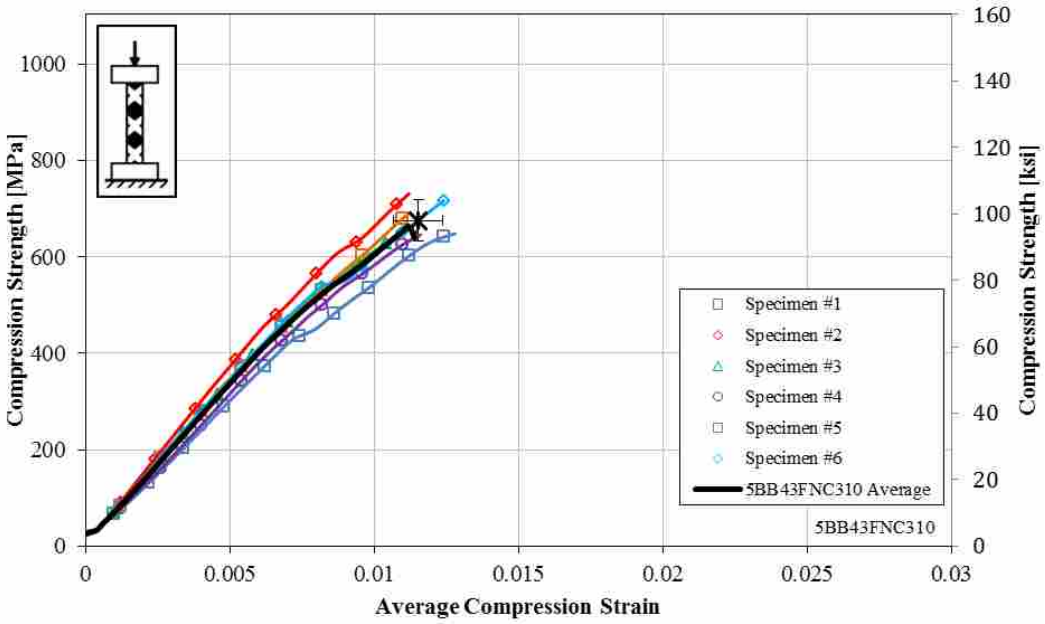

Figure A.1: Stress-Strain Curve for Specimens Cured at 154°C (310°F), with a Basalt Sleeve

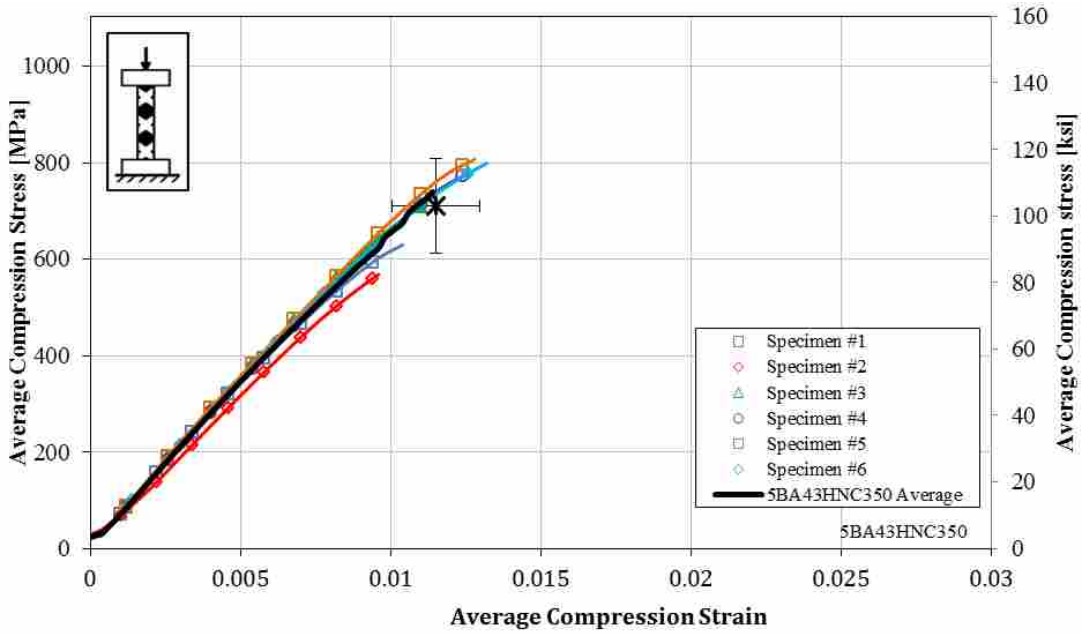

Figure A.2: Stress-Strain Curve for Specimens Cured at 177°C (350°F), with an Aramid Sleeve

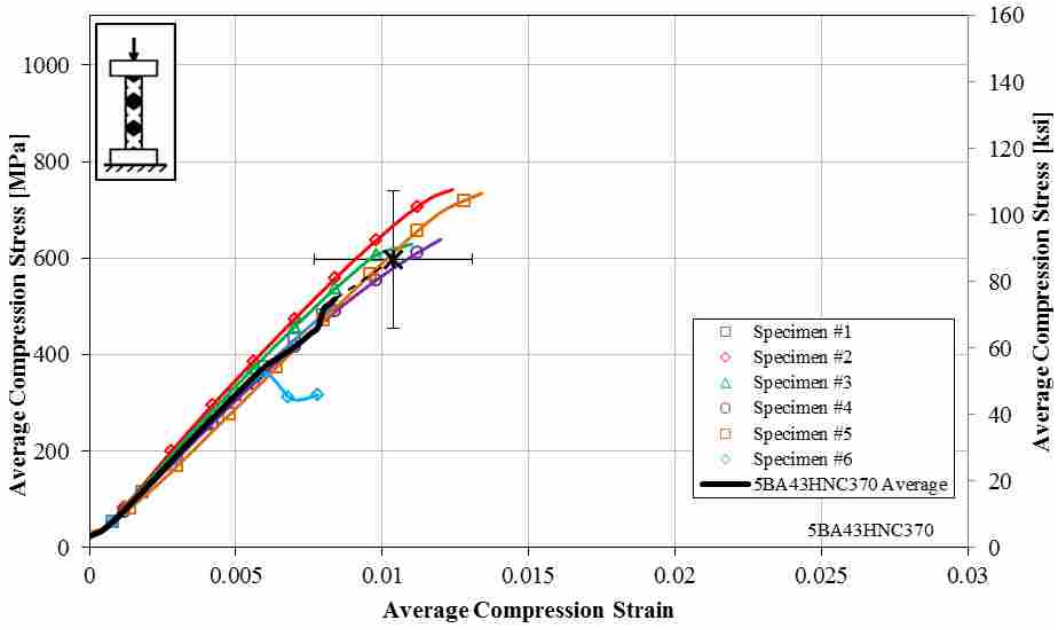

Figure A.3: Stress-Strain Curve for Specimens Cured at 188°C (370°F), with an Aramid Sleeve

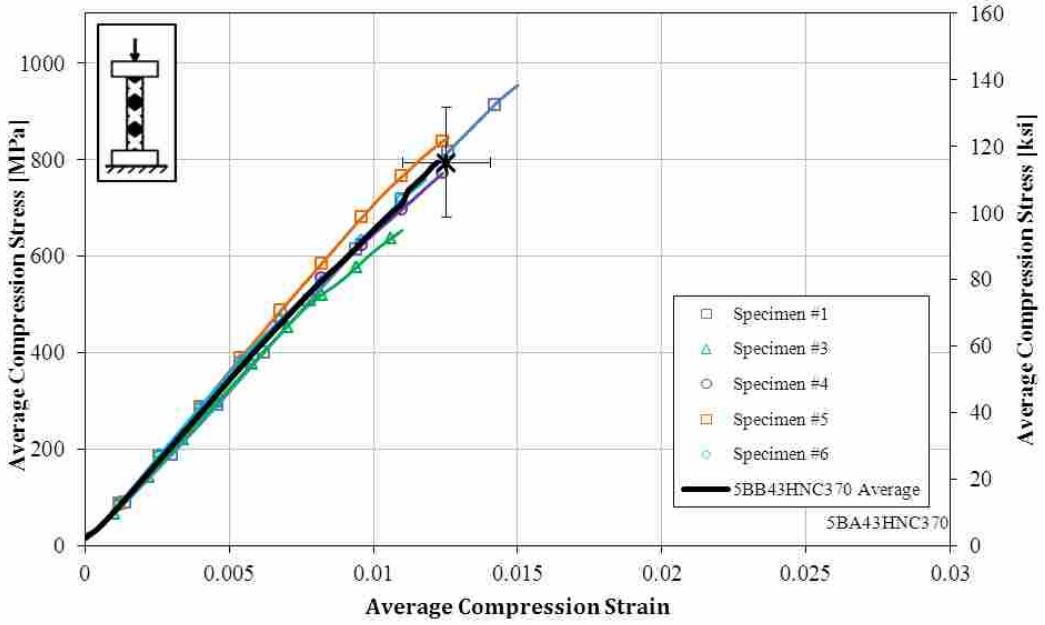

Figure A.4: Stress-Strain Curve for Specimens Cured at 188°C (370°F), with a Basalt Sleeve

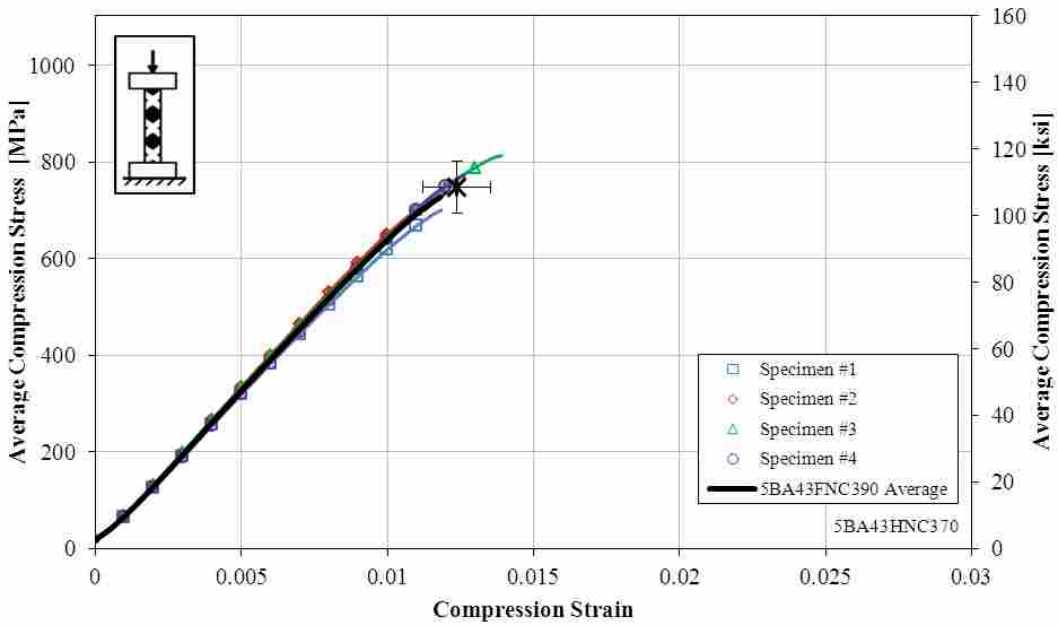

Figure A.5: Stress-Strain Curve for Specimens Cured at 199°C (390°F), with an Aramid Sleeve

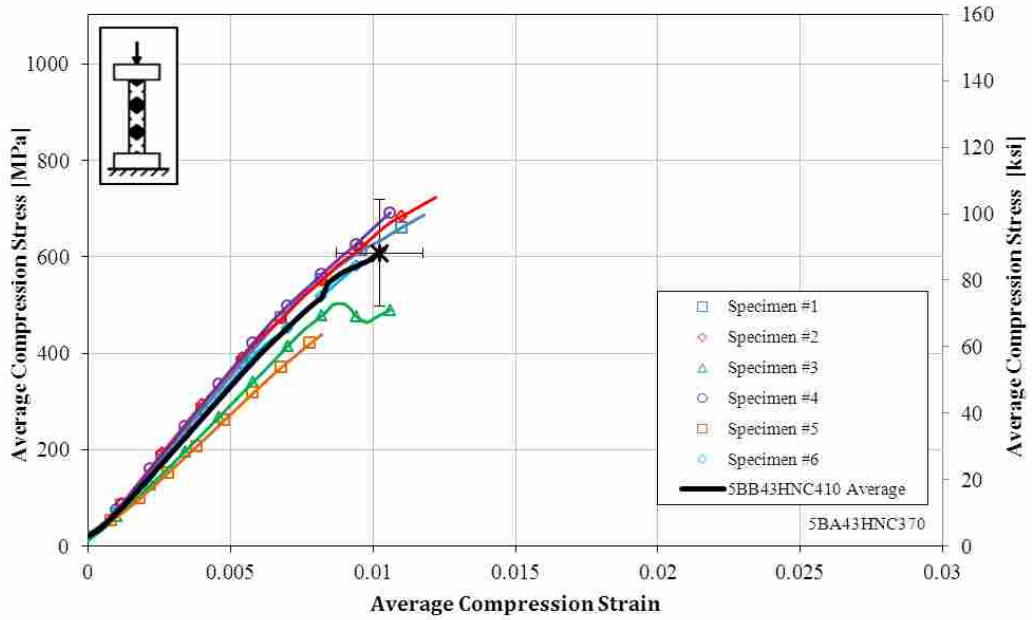

Figure A.6: Stress-Strain Curve for Specimens Cured at 210°C (410°F), with a Basalt Sleeve

Table A.2: Average Compression Strength, Young's Modulus, and Strain at Max Stress

Configuration	Cure Temperature [°C(°F)]	Cure Time [min.]	Ultimate Compression Strength [MPa (ksi)]	Strain at Max Stress [10^3 με]	Compression Young's Modulus [GPa (10^6 psi)]
5BB43HNC310	154 (310)	60	675.4 (98.0)	11.5	67.5 (9.8)
5BA43HNC350	166 (330)	15	710.3 (103.0)	11.5	64.6 (9.4)
5BA43HNC370	177 (350)	8	597.7 (86.7)	10.4	59.8 (9.3)
5BB43HNC370	188 (370)	8	794.4 (115.2)	12.5	67.0 (9.7)
5BA43HNC390	199 (390)	4	675.4 (98.0)	11.5	67.5 (9.8)
5BA43HNC410	210 (410)	2	608.4 (88.2)	10.2	66.2 (9.6)

The compression strength is plotted against the cure temperature in Figure A.7 with a trend line. In Figure A.8, the Young's modulus is plotted against the cure temperature with a trend line. Compression strength peaks near 188°C (370°F). Compression Young's modulus remains fairly constant with an increasing cure temperature. Based on these results, a reduced cure time of 4 minutes (not including ramp up and cool down times) at 199°C (390°F) was chosen for this thesis.

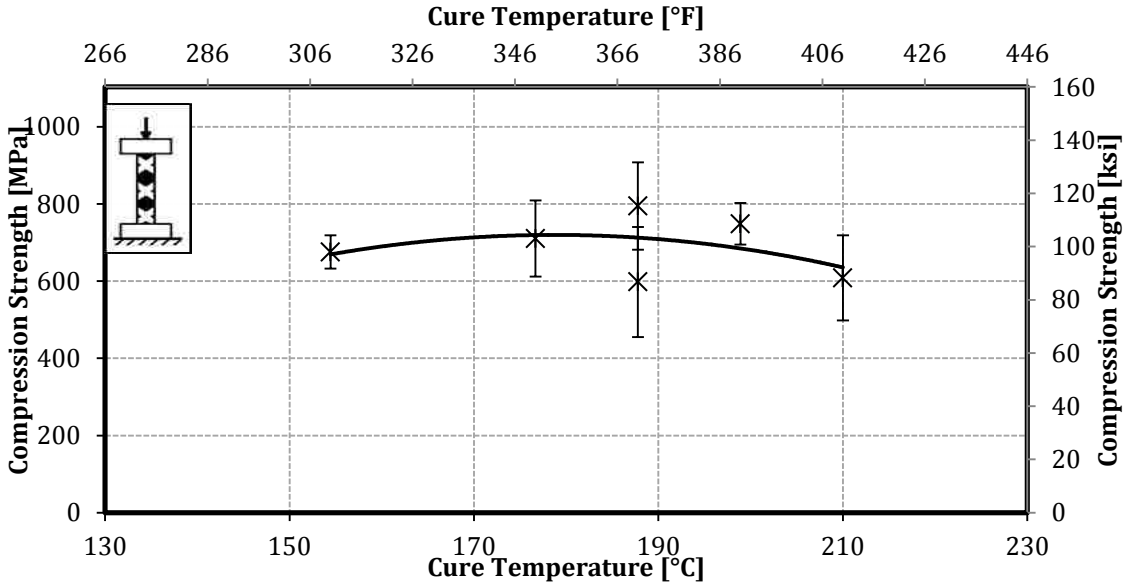

Figure A.7: Compression Strength vs. Cure Temperature

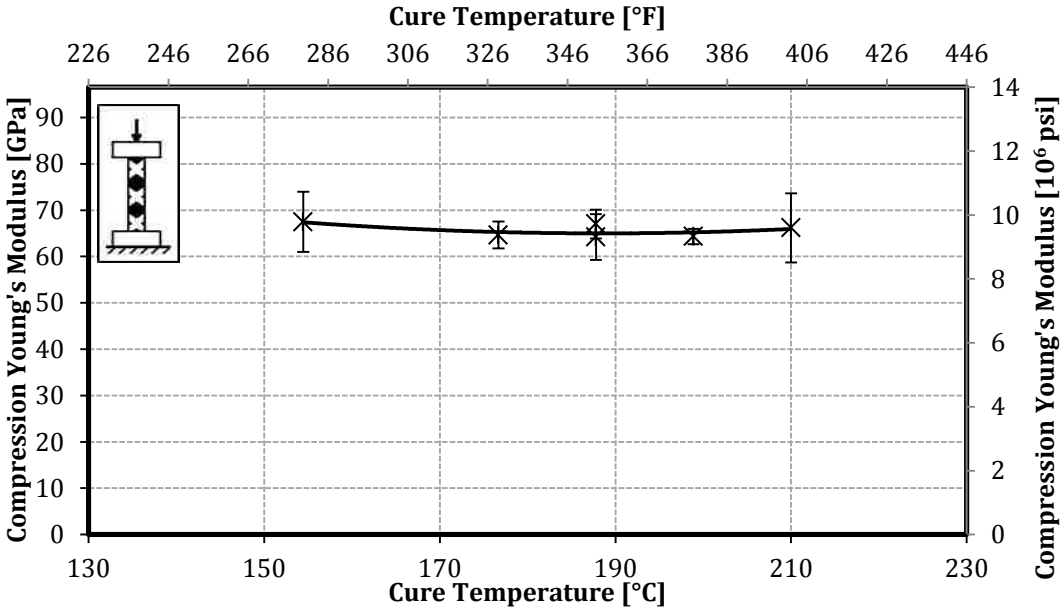

Figure A.8: Compression Young's Modulus vs. Cure Temperature

APPENDIX B: FIBER VOLUME

The results for average fiber volume are summarized in Table B.1. The measurements were obtained by polishing the end of each specimen until clear digital images could be taken following the processes mentioned in the body of the thesis for cross-sectional areas. An average fiber volume percentage of 59% was measured indicating a quality manufacturing process. Figures B.1 through B.4 show typical pictures obtained from the microscope.

Table B.1: Average Fiber Volume Percentage Achieved from Each Sleeve Configuration

Sleeve Configuration	Fiber Volume [%]	Standard Deviation [%]
Full Coverage Braid	58	10
Half Coverage Braid	59	25
Full Coverage Spiral	57	10
Half Coverage Spiral	61	9
Average	59	9

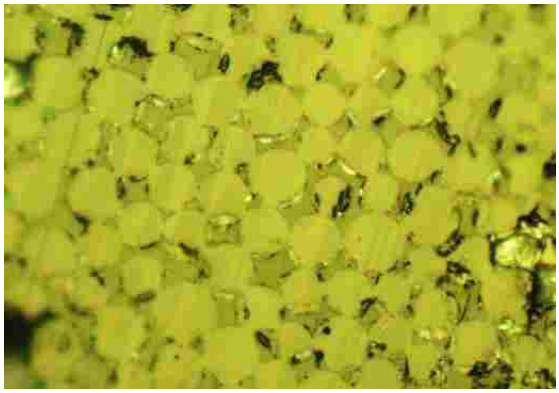

Figure B.1: Typical Cross-Section of Full Coverage Braided Sleeve Specimen

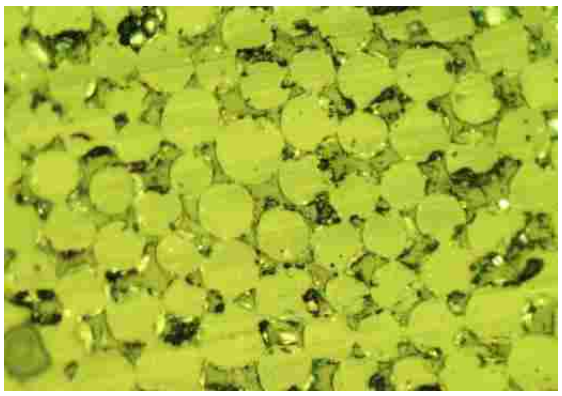

Figure B.2: Typical Cross-Section of Half Coverage Braided Sleeve Specimen

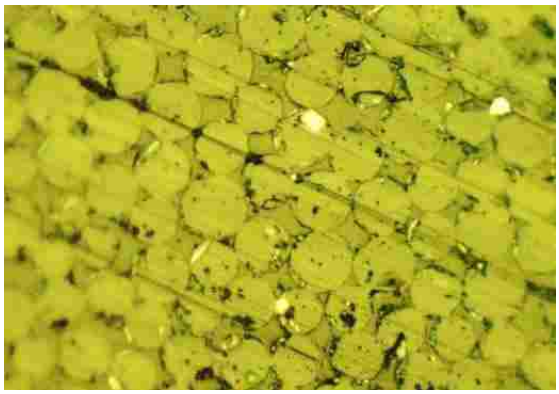

Figure B.3: Typical Cross-Section of Full Coverage Spiral Sleeve Specimen

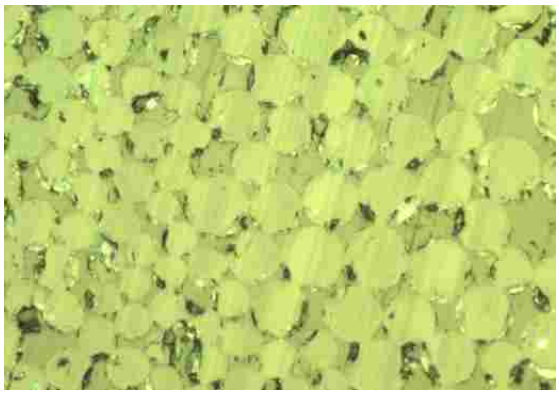

Figure B.4: Typical Cross-Section of Half Coverage Spiral Sleeve Specimen

APPENDIX C: CROSS-SECTIONAL AREA MEASURMENTS

The area measurements for both ends of each specimen and their average are presented in Tables C.1 through C.4.

Table C.1: Cross-Sectional Areas for Braided Sleeve 8 mm (5/16") Specimens

Specimen Configuration		Specimen Number							Average Area	Standard Deviation [%]
		1	2	3	4	5	6	7		
5BA43FSC2										
End 1	[mm^2]	50.0	49.7	49.5	50.6	48.8				
End 2	[mm^2]	49.9	49.1	49.4	50.4	49.2				
Average Area	[mm^2]	**49.9**	**49.4**	**49.5**	**50.5**	**49.0**			**49.7**	**0.6**
Average Area	[in^2]	**0.077**	**0.077**	**0.077**	**0.078**	**0.076**			**0.077**	**0.0**
Standard Deviation	**[%]**	**0.0**	**0.4**	**0.1**	**0.2**	**0.3**				
5BA43FLC2										
End 1	[mm^2]	48.6	48.9	49.8	49.2	49.5	49.3			
End 2	[mm^2]	49.1	48.8	49.1	49.2	49.1	49.9			
Average Area	[mm^2]	**48.9**	**48.9**	**49.5**	**49.2**	**49.3**	**49.6**		**49.2**	**0.3**
Average Area	[in^2]	**0.076**	**0.076**	**0.077**	**0.076**	**0.076**	**0.077**		**0.076**	**0.0**
Standard Deviation	**[%]**	**0.4**	**0.1**	**0.4**	**0.0**	**0.2**	**0.4**			
5BA43FNC2										
End 1	[mm^2]	49.6	49.6	48.7	50.8	49.8				
End 2	[mm^2]	49.5	49.8	48.8	50.6	48.9				
Average Area	[mm^2]	**49.5**	**49.7**	**48.7**	**50.7**	**49.4**			**49.6**	**0.7**
Average Area	[in^2]	**0.077**	**0.077**	**0.076**	**0.079**	**0.077**			**0.077**	**0.0**
Standard Deviation	**[%]**	**0.1**	**0.1**	**0.1**	**0.1**	**0.6**				
5BA43HSC2										
End 1	[mm^2]	54.4	58.2	53.6	52.3	53.7	53.3	53.4		
End 2	[mm^2]	54.4	58.5	53.4	52.0	54.7	51.6	53.5		
Average Area	[mm^2]	**54.4**	**58.4**	**53.5**	**52.2**	**54.2**	**52.4**	**53.5**	**54.1**	**0.8**
Average Area	[in^2]	**0.084**	**0.091**	**0.083**	**0.081**	**0.084**	**0.081**	**0.083**	**0.084**	**0.0**
Standard Deviation	**[%]**	**0.0**	**0.2**	**0.1**	**0.4**	**0.7**	**1.2**	**0.1**		
5BA43HLC2										
End 1	[mm^2]	55.8	53.5	54.4	54.6	54.6				
End 2	[mm^2]	53.7	54.3	54.7	53.0	54.1				
Average Area	[mm^2]	**54.7**	**53.9**	**54.6**	**53.8**	**54.3**			**54.3**	**0.4**
Average Area	[in^2]	**0.085**	**0.084**	**0.085**	**0.083**	**0.084**			**0.084**	**0.0**
Standard Deviation	**[%]**	**1.6**	**0.5**	**0.2**	**1.1**	**0.4**				
5BA43HNC2										
End 1	[mm^2]	54.9	55.0	54.4	55.2	56.3	53.7			
End 2	[mm^2]	53.2	53.3	54.3	54.8	54.5	53.6			
Average Area	[mm^2]	**54.0**	**54.2**	**54.4**	**55.0**	**55.4**	**53.7**		**54.4**	**0.7**
Average Area	[in^2]	**0.084**	**0.084**	**0.084**	**0.085**	**0.086**	**0.083**		**0.084**	**0.0**
Standard Deviation	**[%]**	**1.2**	**1.2**	**0.0**	**0.3**	**1.3**	**0.1**			

Table C.2: Cross-Sectional Areas for Spiral Sleeve 8 mm (5/16") Specimens

Specimen Configuration		Specimen Number							Average Area	Standard Deviation [%]
		1	2	3	4	5	6	7		
5BA10FSC2										
End 1	[mm^2]	50.6	51.6	51.0	51.6	50.8				
End 2	[mm^2]	50.8	51.7	51.0	51.3	50.6				
Average Area	[mm^2]	**50.7**	**51.7**	**51.0**	**51.5**	**50.7**			**51.1**	**0.4**
Average Area	[in^2]	**0.079**	**0.080**	**0.079**	**0.080**	**0.077**			**0.079**	**0.0**
Standard Deviation	**[%]**	**0.1**	**0.0**	**0.0**	**0.2**	**0.1**				
5BA10FLC2										
End 1	[mm^2]	50.3	51.1	51.1	50.8	52.6				
End 2	[mm^2]	51.1	50.4	50.0	50.1	50.1				
Average Area	[mm^2]	**50.7**	**50.7**	**50.5**	**50.5**	**51.3**			**50.8**	**0.4**
Average Area	[in^2]	**0.079**	**0.079**	**0.078**	**0.078**	**0.080**			**0.079**	**0.0**
Standard Deviation	**[%]**	**0.6**	**0.5**	**0.7**	**0.4**	**1.8**				
5BA10FNC2										
End 1	[mm^2]	50.9	51.4	51.0	51.4	51.1	49.7	49.0		
End 2	[mm^2]	51.4	51.4	50.8	51.1	50.7	49.6	49.0		
Average Area	[mm^2]	**51.1**	**51.4**	**50.8**	**51.1**	**50.7**	**49.6**	**49.0**	**50.6**	**1.0**
Average Area	[in^2]	**0.079**	**0.080**	**0.079**	**0.079**	**0.079**	**0.077**	**0.076**	**0.078**	**0.0**
Standard Deviation	**[%]**	**0.4**	**0.0**	**0.1**	**0.3**	**0.2**	**0.1**	**0.0**		
5BA10HSC2										
End 1	[mm^2]	52.4	51.1	52.4	52.2	52.7	51.8	53.1		
End 2	[mm^2]	51.7	52.1	51.4	52.1	51.7	52.4	51.6		
Average Area	[mm^2]	**52.0**	**51.6**	**51.9**	**52.1**	**52.2**	**52.1**	**52.3**	**52.0**	**0.3**
Average Area	[in^2]	**0.081**	**0.080**	**0.080**	**0.081**	**0.081**	**0.081**	**0.081**	**0.081**	**0.0**
Standard Deviation	**[%]**	**0.5**	**0.7**	**0.7**	**0.1**	**0.7**	**0.5**	**1.1**		
5BA10HLC2										
End 1	[mm^2]	51.4	52.1	52.5	52.9	52.1				
End 2	[mm^2]	52.5	51.8	51.0	51.3	51.7				
Average Area	[mm^2]	**51.9**	**52.0**	**51.8**	**52.1**	**51.9**			**51.9**	**0.1**
Average Area	[in^2]	**0.081**	**0.081**	**0.080**	**0.081**	**0.080**			**0.080**	**0.0**
Standard Deviation	**[%]**	**0.7**	**0.2**	**1.1**	**1.2**	**0.3**				
5BA10HNC2										
End 1	[mm^2]	51.0	51.8	52.4	51.6	52.2				
End 2	[mm^2]	52.0	52.0	52.8	51.6	51.7				
Average Area	[mm^2]	**51.5**	**51.9**	**52.6**	**51.6**	**51.9**			**51.9**	**0.4**
Average Area	[in^2]	**0.080**	**.080**	**.082**	**.080**	**.081**			**0.080**	**0.0**
Standard Deviation	**[%]**	**0.8**	**0.1**	**0.3**	**0.0**	**0.4**				

Table C.3: Cross-Sectional Areas for Braided Sleeve 11 mm (7/16") Specimens

Specimen Configuration		Specimen Number						Average Area	Standard Deviation [%]
		1	2	3	4	5	6		
7BA43FSC									
End 1	[mm^2]	92.0	98.3	95.0	98.5	93.7	94.3		
End 2	[mm^2]	93.3	98.7	95.2	98.5	93.8	93.7		
Average Area	[mm^2]	**92.7**	**98.5**	**95.1**	**98.5**	**93.8**	**94.0**	**95.4**	**2.5**
Average Area	[in^2]	**0.144**	**0.453**	**0.147**	**0.153**	**0.145**	**0.146**	**0.148**	**0.0**
Standard Deviation	**[%]**	**0.9**	**0.3**	**0.1**	**0.0**	**0.1**	**0.4**		
7BA43FLC									
End 1	[mm^2]	95.7	94.4	95.3	98.8	98.2			
End 2	[mm^2]	94.6	8408	95.7	101.3	99.2			
Average Area	[mm^2]	**95.1**	**95.1**	**95.5**	**100.1**	**98.7**		**96.9**	**2.3**
Average Area	[in^2]	**0.148**	**0.148**	**0.148**	**0.155**	**0.153**		**0.150**	**0.0**
Standard Deviation	**[%]**	**0.8**	**1.1**	**0.3**	**1.8**	**0.7**			
7BA43FNC									
End 1	[mm^2]	94.3	94.1	94.4	96.0	93.5	94.4		
End 2	[mm^2]	93.9	94.7	94.1	95.5	93.4	94.6		
Average Area	[mm^2]	**94.1**	**94.4**	**94.3**	**95.8**	**93.5**	**94.5**	**94.4**	**0.8**
Average Area	[in^2]	**0.146**	**0.146**	**0.146**	**0.148**	**0.145**	**0.147**	**0.146**	**0.0**
Standard Deviation	**[%]**	**0.3**	**0.5**	**0.2**	**0.4**	**0.0**	**0.1**		
7BA43HSC									
End 1	[mm^2]	99.5	104.8	102.8	101.5	101.1			
End 2	[mm^2]	104.9	104.4	102.4	102.6	102.5			
Average Area	[mm^2]	**102.2**	**104.6**	**102.6**	**102.1**	**101.8**		**102.7**	**1.1**
Average Area	[in^2]	**0.158**	**0.162**	**0.159**	**0.158**	**0.158**		**0.159**	**0.0**
Standard Deviation	**[%]**	**3.8**	**0.3**	**0.3**	**0.8**	**1.0**			
7BA43HLC									
End 1	[mm^2]	103.4	105.2	104.0	105.2	102.9	105.0		
End 2	[mm^2]	102.3	104.4	104.3	105.6	105.0	102.6		
Average Area	[mm^2]	**103.1**	**104.8**	**104.2**	**105.4**	**104.0**	**103.8**	**104.2**	**0.8**
Average Area	[in^2]	**0.160**	**0.162**	**0.162**	**0.163**	**0.161**	**0.161**	**0.162**	**0.0**
Standard Deviation	**[%]**	**1.1**	**0.6**	**0.3**	**0.3**	**1.5**	**1.7**		
7BA43HNC									
End 1	[mm^2]	106.0	104.3	100.8	104.8	104.4	101.7		
End 2	[mm^2]	104.6	105.9	104.3	106.8	105.1	100.8		
Average Area	[mm^2]	**105.3**	**105.1**	**102.5**	**105.8**	**104.8**	**101.2**	**104.1**	**1.8**
Average Area	[in^2]	**0.163**	**0.163**	**0.159**	**0.164**	**0.162**	**0.157**	**0.162**	**0.0**
Standard Deviation	**[%]**	**0.9**	**1.2**	**2.4**	**1.4**	**0.5**	**0.6**		

Table C.4: Cross-Sectional Areas for Spiral Sleeve 11 mm (7/16") Specimens

Specimen Configuration		Specimen Number						Average Area	Standard Deviation [%]
		1	2	3	4	5	6		
7BA10FSC									
End 1	[mm^2]	101.0	99.6	100.3	99.9	97.1			
End 2	[mm^2]	100.6	99.2	98.9	100.8	96.2			
Average Area	[mm^2]	**100.8**	**99.4**	**99.6**	**100.3**	**96.7**		**99.4**	**1.6**
Average Area	[in^2]	**0.156**	**0.154**	**0.154**	**0.156**	**0.150**		**0.154**	**0.0**
Standard Deviation	**[%]**	**0.3**	**0.3**	**1.0**	**0.6**	**0.6**			
7BA10FLC									
End 1	[mm^2]	98.6	98.0	100.3	99.2	95.9	100.4		
End 2	[mm^2]	98.9	101.6	100.4	99.1	96.1	100.6		
Average Area	[mm^2]	**98.8**	**99.8**	**100.4**	**99.1**	**96.1**	**100.6**	**99.1**	**1.6**
Average Area	[in^2]	**0.153**	**0.155**	**0.156**	**0.154**	**0.149**	**0.156**	**0.154**	**0.0**
Standard Deviation	**[%]**	**0.3**	**2.5**	**0.1**	**0.2**	**0.3**	**0.2**		
7BA10FNC									
End 1	[mm^2]	100.4	99.5	99.8	99.3	99.8			
End 2	[mm^2]	101.0	98.9	99.8	100.2	101.3			
Average Area	[mm^2]	**100.7**	**99.2**	**99.8**	**99.8**	**100.6**		**100.0**	**0.4**
Average Area	[in^2]	**0.156**	**0.154**	**0.155**	**0.155**	**0.156**		**0.155**	**0.0**
Standard Deviation	**[%]**	**0.4**	**0.4**	**0.0**	**0.7**	**1.1**			
7BA10HSC									
End 1	[mm^2]	102.0	101.5	105.6	101.8	102.0	102.4		
End 2	[mm^2]	101.8	102.5	101.4	104.8	97.6	102.0		
Average Area	[mm^2]	**101.9**	**102.0**	**102.0**	**102.8**	**99.8**	**102.2**	**101.8**	**1.0**
Average Area	[in^2]	**0.158**	**0.158**	**0.158**	**0.159**	**0.155**	**0.158**	**0.158**	**0.0**
Standard Deviation	**[%]**	**0.1**	**0.7**	**0.9**	**1.4**	**3.1**	**0.3**		
7BA10HLC									
End 1	[mm^2]	102.4	103.8	104.7	101.8	102.0			
End 2	[mm^2]	103.9	103.1	103.4	103.5	104.8			
Average Area	[mm^2]	**103.1**	**103.4**	**104.0**	**102.7**	**103.4**		**103.3**	**0.5**
Average Area	[in^2]	**0.160**	**0.160**	**0.161**	**0.159**	**0.160**		**0.160**	**0.0**
Standard Deviation	**[%]**	**1.0**	**0.5**	**0.9**	**1.2**	**2.0**			
7BA10HNC									
End 1	[mm^2]	106.2	103.1	103.8	106.0	102.1			
End 2	[mm^2]	101.8	103.2	103.1	104.2	104.3			
Average Area	[mm^2]	**104.0**	**103.1**	**103.5**	**105.1**	**103.2**		**103.8**	**0.161**
Average Area	[in^2]	**0.161**	**0.160**	**0.160**	**0.063**	**0.160**		**0.8**	**0.0**
Standard Deviation	**[%]**	**3.1**	**0.1**	**0.5**	**1.3**	**1.6**			

APPENDIX D: SLEEVE COVERAGE MEASUREMENTS

Tables D.1 and D.2 summarize the percent of core surface area covered by the aramid sleeve. These areas were determined at the mid-length of the specimen at 4 evenly spaced points around the circumference. Pictures taken at these points were used to determine the average coverage.

Table D.1: Sleeve Coverage for 8 mm (5/16") Specimens

Specimen Configuration		Specimen Number							Average Coverage	Standard Deviation [%]
		1	2	3	4	5	6	7		
5BA43HSC2										
Side 1	[%]	59.7	74.6	81.4	71.7	76.7			**72.8**	**8**
Side 2	[%]	67.4	80.2	73.9	65.0	79.3			**73.2**	**7**
Side 3	[%]	77.6	77.8	75.7	67.8	66.6			**73.1**	**5**
Side 4	[%]	77.1	64.2	73.7	85.4	83.1			**76.7**	**8**
Average Coverage	[%]	**70.4**	**74.2**	**76.2**	**72.5**	**76.4**			**73.9**	**3**
Standard Deviation	[%]	**9**	**7**	**4**	**9**	**7**				
5BA43HLC2										
Side 1	[%]	68.3	79.8	71.4	85.4	66.0			**74.2**	**8**
Side 2	[%]	87.4	65.8	72.2	86.9	68.4			**76.2**	**10**
Side 3	[%]	78.6	63.7	79.5	64.1	88.4			**74.9**	**11**
Side 4	[%]	71.2	73.4	74.3	59.9	77.6			**71.3**	**7**
Average Coverage	**[%]**	**76.4**	**70.7**	**74.3**	**74.1**	**75.1**			**74.1**	**2**
Standard Deviation	**[%]**	**9**	**7**	**4**	**14**	**10**				
5BA43HNC2										
Side 1	[%]	74.3	85.2	60.7	73.5	86.2	67.8		**74.6**	**10**
Side 2	[%]	86.6	81.5	82.3	81.4	65.7	76.1		**78.9**	**7**
Side 3	[%]	83.8	65.6	87.8	82.9	54.1	86.2		**76.7**	**14**
Side 4	[%]	49.8	61.2	84.8	61.9	82.5	72.8		**68.8**	**14**
Average Coverage	[%]	**73.6**	**73.4**	**78.9**	**74.9**	**72.1**	**75.7**		**74.8**	**2**
Standard Deviation	[%]	**17**	**12**	**12**	**10**	**15**	**8**			
5BA10HSC2										
Side 1	[%]	56.8	48.4	48.6	57.0	55.2	N/A	51.0	**52.8**	**4**
Side 2	[%]	51.0	56.7	64.6	60.2	56.5	N/A	47.5	**56.1**	**6**
Side 3	[%]	40.9	53.2	64.6	65.6	52.4	N/A	64.4	**56.8**	**10**
Side 4	[%]	45.3	58.7	54.0	45.3	50.4	N/A	46.1	**50.0**	**6**
Average Coverage	**[%]**	**48.5**	**54.3**	**57.9**	**57.0**	**53.6**	**N/A**	**52.2**	**53.9**	**3**
Standard Deviation	**[%]**	**7**	**4**	**8**	**9**	**3**	**N/A**	**8**		
5BA10HLC2										
Side 1	[%]	63.0	44.2	58.1	53.2	59.2			**55.5**	**7**
Side 2	[%]	57.6	45.6	42.1	40.6	45.6			**46.3**	**7**
Side 3	[%]	46.3	59.0	50.9	50.9	46.4			**50.7**	**5**
Side 4	[%]	51.5	55.7	64.0	61.3	55.5			**57.6**	**5**
Average Coverage	**[%]**	**54.6**	**51.1**	**53.8**	**51.5**	**51.7**			**52.5**	**2**
Standard Deviation	**[%]**	**7**	**7**	**9**	**9**	**7**				
5BA10HNC2										
Side 1	[%]	50.0	41.1	47.5	42.9	53.4			**47.0**	**5**
Side 2	[%]	49.2	58.9	49.8	58.2	60.2			**55.3**	**5**
Side 3	[%]	59.1	54.9	54.1	60.3	52.2			**56.1**	**3**
Side 4	[%]	56.3	40.2	59.1	39.8	45.8			**48.2**	**9**
Average Coverage	**[%]**	**53.6**	**48.8**	**52.6**	**50.3**	**52.9**			**51.6**	**2**
Standard Deviation	**[%]**	**5**	**10**	**5**	**10**	**6**				

Table D.2: Sleeve Coverage for 11 mm (7/16") Specimens

Specimen Configuration		Specimen Number 1	2	3	4	5	6	Average Coverage	Standard Deviation [%]
7BA43HSC2									
Side 1	[%]	35.6	63.2	48.0	76.7	74.0		**59.5**	**18**
Side 2	[%]	64.6	94.1	41.9	68.5	55.9		**65.0**	**19**
Side 3	[%]	71.1	53.8	50.3	47.6	38.4		**52.2**	**12**
Side 4	[%]	44.1	18.8	79.2	59.6	74.3		**55.2**	**24.5**
Average Coverage	[%]	**53.8**	**57.5**	**54.8**	**63.1**	**60.6**		**58.0**	**4**
Standard Deviation	[%]	**17**	**31**	**17**	**13**	**17**			
7BA43HLC2									
Side 1	[%]	78.7	59.0	48.0	40.6	48.2	54.7	**54.9**	**13**
Side 2	[%]	54.0	65.6	64.0	55.8	68.6	55.9	**60.6**	**6**
Side 3	[%]	57.1	54.5	77.3	80.0	53.5	82.2	**67.4**	**14**
Side 4	[%]	78.4	60.6	63.4	42.7	75.3	42.0	**60.4**	**16**
Average Coverage	**[%]**	**67.1**	**59.9**	**63.2**	**54.8**	**61.4**	**58.7**	**61.3**	**4**
Standard Deviation	**[%]**	**13**	**5**	**12**	**18**	**13**	**17**		
7BA43HNC2									
Side 1	[%]	65.6	77.1	71.2	80.6	60.6	61.1	**69.4**	**8**
Side 2	[%]	49.4	44.5	70.5	80.7	65.1	73.0	**63.9**	**14**
Side 3	[%]	41.4	66.1	77.1	82.2	73.3	72.0	**68.7**	**14**
Side 4	[%]	49.2	24.2	44.6	57.2	87.8	N/A	**52.6**	**23**
Average Coverage	[%]	**51.4**	**52.9**	**65.8**	**75.2**	**71.7**	**68.7**	**64.3**	**9**
Standard Deviation	[%]	**10**	**23**	**14**	**12**	**12**	**7**		
7BA10HSC2									
Side 1	[%]	57.7	70.3	**N/A**	**N/A**	**N/A**		**64.0**	**10**
Side 2	[%]	66.3	58.7	**N/A**	**N/A**	**N/A**		**62.5**	**6**
Side 3	[%]	78.1	45.2	**N/A**	**N/A**	**N/A**		**61.6**	**8**
Side 4	[%]	59.3	62.7	**N/A**	**N/A**	**N/A**		**61.0**	**13**
Average Coverage	**[%]**	**65.3**	**59.2**	**N/A**	**N/A**	**N/A**		**62.3**	**4**
Standard Deviation	**[%]**	**9**	**11**	**N/A**	**N/A**	**N/A**			
7BA10HLC2									
Side 1	[%]	N/A	70.7	65.3	56.6	48.8		**60.4**	**10**
Side 2	[%]	N/A	55.1	57.0	68.5	59.7		**60.1**	**6**
Side 3	[%]	N/A	72.9	57.9	62.5	73.9		**66.8**	**8**
Side 4	[%]	N/A	78.3	70.7	47.4	68.3		**66.2**	**13**
Average Coverage	**[%]**	**N/A**	**69.2**	**62.7**	**58.7**	**62.7**		**63.4**	**4**
Standard Deviation	**[%]**	**N/A**	**10**	**6**	**9**	**11**			
7BA10HNC2									
Side 1	[%]	49.6	70.4	65.0	53.0	75.1		**62.6**	**11**
Side 2	[%]	47.0	77.8	67.1	51.9	65.8		**61.9**	**12**
Side 3	[%]	61.9	91.8	55.7	60.8	63.1		**66.7**	**14**
Side 4	[%]	63.2	70.0	48.2	59.6	75.6		**63.3**	**10**
Average Coverage	**[%]**	**55.4**	**77.5**	**59.0**	**56.3**	**69.9**		**63.6**	**10**
Standard Deviation	**[%]**	**8**	**10**	**9**	**5**	**6**			

APPENDIX E: EXTENSOMETER STUDY

An extensometer was initially used to collect strain data because it is capable of measuring localized strain, whereas the machine strain also accounts for movement in the machine. An MTS 634.12E-24 extensometer was used, as seen in Figure E.1. The extensometer was not providing accurate data and was abandoned after completing preliminary testing. This report describes the concerns with the extensometer, the brainstorming and solutions, and a comparison of the extensometer strain and the machine strain.

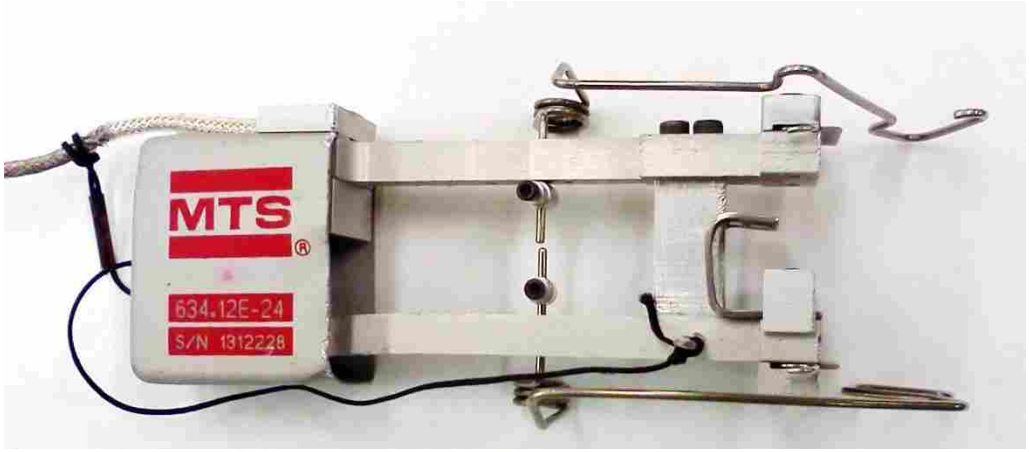

Figure E.1: MTS 634.12E-24 Extensometer Used During Testing

Since the sleeve material was not initially binding well to the core material, the sleeve would balloon out (see Figure E.2) and interrupt the data collection. This implied the specimen quality, and not the extensometer was causing data collection problems.

Figure E.2: Typical Specimen with a Ballooned Sleeve

Manufacturing techniques were improved and higher quality specimens were produced. Even with improved specimens, the data still suggested erroneous results as seen in the typical extensometer stress-strain curve in Figure E.3. Two main concerns include: 1) the large jump in strain; and, 2) the change in strain direction.

The random jumps in strain were removed from the data and the curves that experienced a change in strain direction were truncated. Typical results for one configuration after being altered are shown in Figure E.4. Two of the five specimens have a completely different strain response, yielding a 51% standard deviation.

Many factors could cause the errors observed. First, the extensometer is in relatively poor condition after many years of use in classroom instruction. The data collection cord has begun to fray where it attaches to the extensometer. An additional problem is the pin used to set the distance between the extensometer blades was undersized and allowed some movement. The blades were also dull, not allowing sufficient grip to the specimen. The extensometer was

refurbished, by creating a new pin and sharpening the blades. These fixes improved the results slightly, but overall did not prove successful.

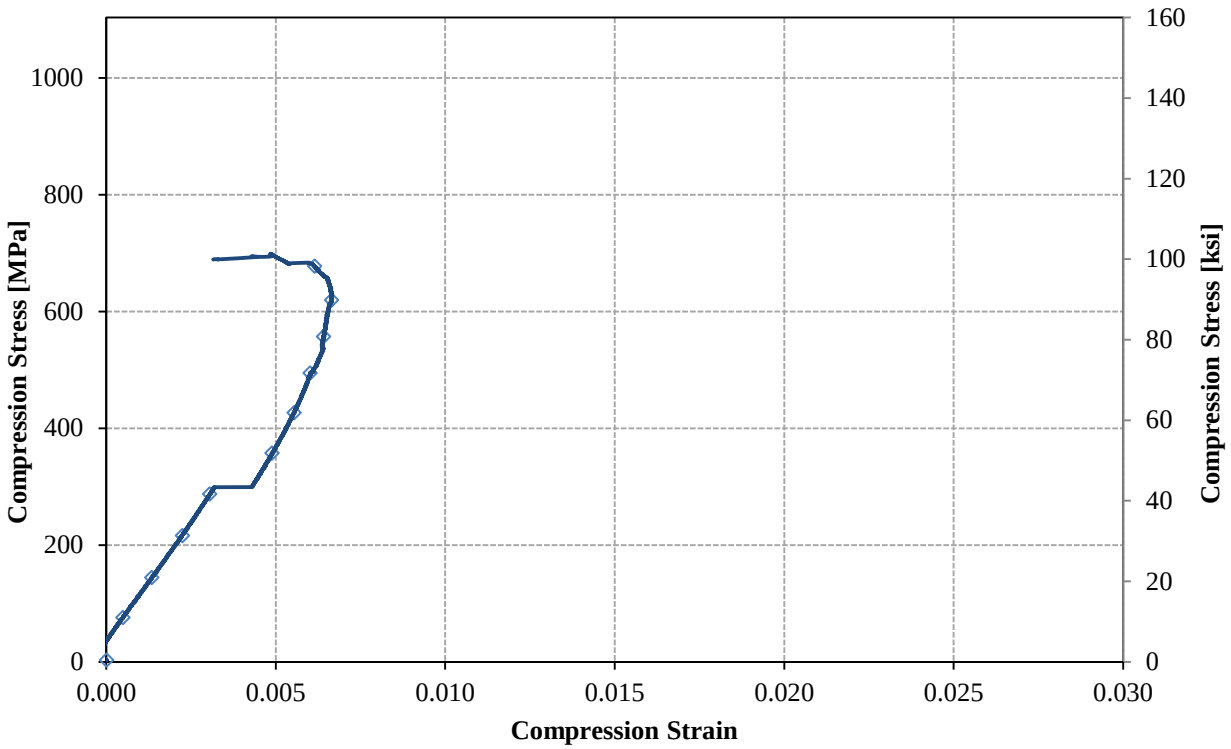

Figure E.3: Typical Unaltered Stress Strain Curve Based on Extensometer Data

Attaching the extensometer properly to the specimen also presented challenges. Initially the extensometer was attached to the specimen by two wire clips as shown in Figure E.5. The concern was that the blades were not sufficiently tight to the specimen, allowing the extensometer to slip during testing. The clips were adjusted to hold the specimen more snuggly and two springs were added as shown in Figure E.6 to increase the force of the specimen against the blades.

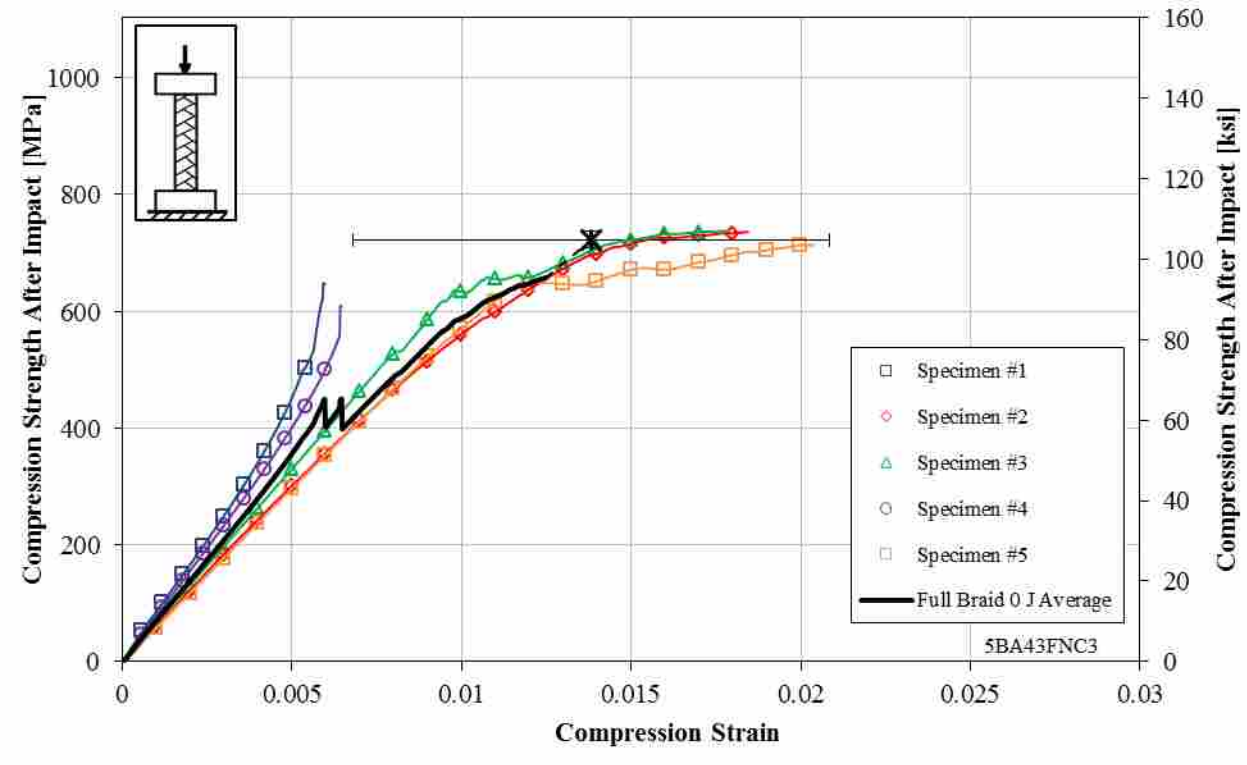

Figure E.4: Typical Curve Shape for Specimens Based on the Extensometer Data

Another concern is that the sleeve of the specimen creates a rough surface as shown in Figure E.7. Extensometer blades set on the peak of the ridges creates an unstable attachment, allowing the blade to slip. When the blades slip apart, this can create the appearance of tensile strain. To avoid this problem close attention was paid during attachment, ensuring that the blades were not set on a ridge. Overall these solutions did slightly improve the test results, but ultimately, did not improve the results enough to restore confidence in the accuracy of the extensometer.

Figure E.5: Extensometer Attached to Specimen with Wire Clips

Figure E.6: Extensometer Attached to Specimen with Wire Clips and Springs

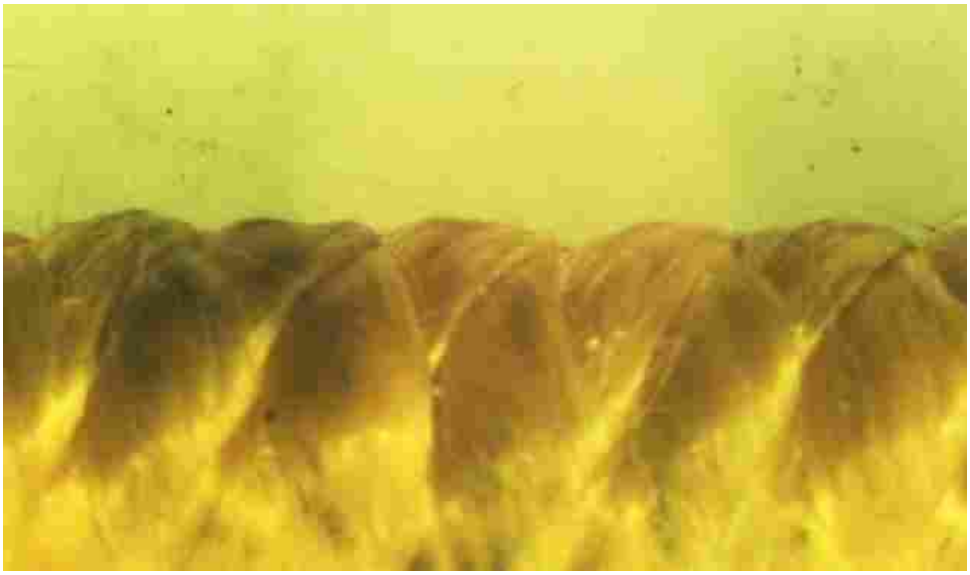

Figure E.7: Typical Ridges on the Rough Specimen Surface (Magnified x7)

To avoid these problems, the extensometer was abandoned and machine displacement data was used to calculate strain in the specimens. This approach came with its share of dilemmas. The most important concern was how accurately the measured displacement represents the actual strain in the specimen. The machine displacement not only includes the displacement of the specimen, but also all the fixturing, pistons, and clamps, referred to as the machine displacement (see Figure E.8). Although the machine is extremely stiff, there is still some effect on the accuracy of the results. An adjustment factor that accounts for the machine displacement was derived, as shown in Figure E.9.

Figure E.8: Total Machine Displacement (See Arrow)

In the derivation, the Young's modulus for the specimens, 64.5 MPa ($9.35X10^6$ psi), was calculated based on non-impacted test specimens. This modulus was based on extensometer data, but was deemed satisfactory when using the initial linear portion of the curve.

The predicted stiffness value (K) for the system was 1.23 MN/cm (700.0 kips/in). As a check on these calculations, a test was performed on the testing machine with no specimen, allowing the test fixtures to press against each other. The resulting load-displacement curve yielded an empirical machine stiffness of 1.34 MN/cm (766.0 kips/inch), close enough to validate the prediction. The empirical value was used as the correction factor for all testing on the Instron compression machine. The majority of 11 mm (7/16") diameter specimens were tested on the 489 kN (110 Kip) MTS compression machine. A corresponding correction factor of 4.18 MN/cm (2391.7 kips/inch) was measured on the MTS.

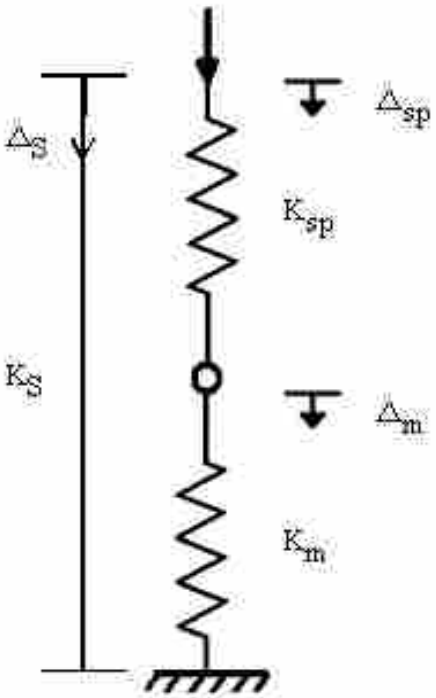

$$\Delta_S = \Delta_m + \Delta_{sp}$$

$$\Delta_m = \Delta_S - \Delta_{sp}$$

$$F = K_m \cdot \Delta_m$$

$$\Delta_S = \frac{F}{K_S}$$

$$\Delta_{sp} = \frac{F}{K_{sp}}$$

$$F = K_m\left(\Delta_S - \Delta_{sp}\right)$$

$$F = K_m\left(\frac{F}{K_S} - \frac{F}{K_{sp}}\right)$$

$$K_m = \frac{F}{\left(\frac{F}{K_S} - \frac{F}{K_{sp}}\right)}$$

$$K_m = \frac{1}{\frac{1}{K_S} - \frac{1}{K_{sp}}}$$

$$K_m = \frac{1}{\frac{K_{sp}}{K_{sp} \cdot K_S} - \frac{K_S}{K_{sp} \cdot K_S}}$$

$$K_m = \frac{K_S \cdot K_{sp}}{K_{sp} - K_S}$$

$$K_S = \frac{E_S \cdot A}{L_S}$$

$$K_{sp} = \frac{E_{sp} \cdot A}{L_{sp}}$$

$$L_S = 3.5 \cdot in$$

$$L_{sp} = 3.5 \cdot in$$

$$K_m = \frac{\frac{E_S \cdot A}{3.5 \cdot in} \cdot \frac{E_{sp} \cdot A}{3.5 \cdot in}}{\left(\frac{E_{sp} \cdot A}{3.5 \cdot in}\right) - \frac{E_S \cdot A}{3.5 \cdot in}}$$

$$K_m = \frac{E_A \cdot E_{sp} \cdot A}{3.5 \cdot \left(E_{sp} - E_S\right)}$$

$$\Delta_m = \frac{F}{K_m}$$

$$\Delta_{sp} = \Delta_S - \Delta_m$$

Figure E.9: Derivation of Displacement within the Machine

The extensometer strain data is compared to the machine strain data for a typical specimen in Figure E.10. The adjusted machine strain curve has the same shape as the unadjusted machine strain curve and the same slope as the extensometer strain data.

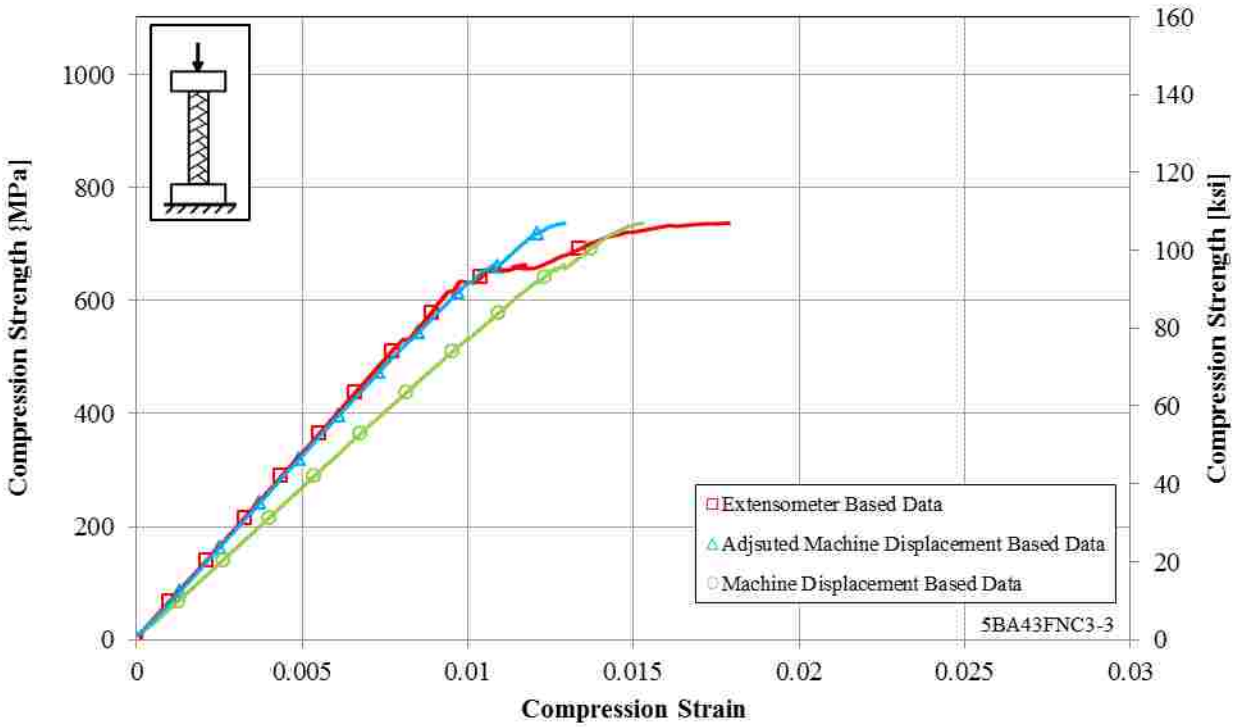

Figure E.10: Stress-Strain Curves for a Single Specimen Based on Extensometer Strain, Machine Strain and Adjusted Machine Strain

For a complete set of specimens, the extensometer strain data is compared to the corresponding machine strain data in Figure E.11. The adjusted machine strain curves are considerably more consistent than the extensometer-based data, implying that the extensometer was not working properly.

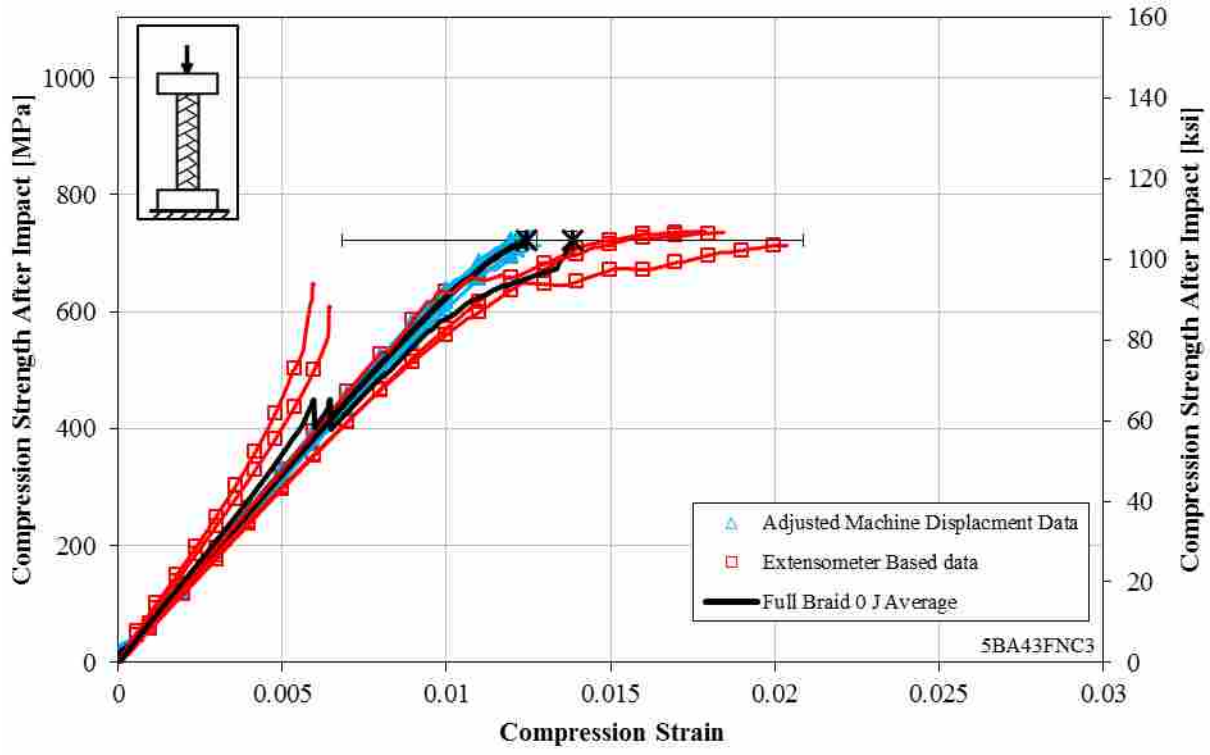

Figure E.11: Stress-Strain Curves Comparing Extensometer Strain to Adjusted Machine Strain

APPENDIX F: POST-FAILURE PICTURES OF SPECIMENS

Pictures of each specimen at the end of the compression tests, while still under load, are shown in Figure F.1 through F.36. Loading was maintained during the photo to accentuate the type and location of failure.

F.1 Preliminary Testing 5/16” Diameter, 3” Length Specimens

Pictures of all specimens with an 8 mm (5/16”) diameter and 76 mm (3”) length while still under load are shown in Figures F.1-F.12.

5BA10FNC3-1

5BA10FNC3-2

5BA10FNC3-3

5BA10FNC3-4

No Photo

5BA10FNC3-5

5BA10FNC3-6

5BA10FNC3-7

5BA10FNC3-8

5BA10FNC3-9

5BA10FNC3-10

Figure F.1: Pictures of Full Coverage Spiral No-Impact Specimens

5BA10FLC3-1

5BA10FLC3-2

5BA10FLC3-3

5BA10FLC3-4

5BA10FLC3-5

Figure F.2: Pictures of Full Coverage Spiral, 5 J (3.7 ft-lbs.) Impact Specimens

5BA10FSC3-1

5BA10FSC3-2

5BA10FSC3-3

5BA10FSC3-4

5BA10FSC3-5

Figure F.3: Pictures of Full Coverage Spiral, 10 J (7.4 ft-lbs.) Impact Specimens

5BA10HNC3-1

5BA10HNC3-2

5BA10HNC3-3

5BA10HNC3-4

5BA10HNC3-5

5BA10HNC3-6

Figure F.4: Pictures of Half Coverage Spiral No-Impact Specimens

5BA10HLC3-1

5BA10HLC3-2

5BA10HLC3-3

5BA10HLC3-4

5BA10HLC3-5

Figure F.5: Pictures of Half Coverage Spiral, 5 J (3.7 ft-lbs.) Impact Specimens

5BA10HSC3-1

5BA10HSC3-2

5BA10HSC3-3

5BA10HSC3-4

5BA10HSC3-5

Figure F.6: Pictures of Half Covearge Spiral, 10 J (7.4 ft-lbs.) Impact Specimens

5BA43FNC3-1

5BA43FNC3-2

5BA43FNC3-3

5BA43FNC3-4

5BA43FNC3-5

Figure F.7: Pictures of Full Coverage Braid No-impact Specimens

5BA43FLC3-1

5BA43FLC3-2

5BA43FLC3-3

5BA43FLC3-4

5BA43FLC3-5

Figure F.8: Pictures of Full Coverage Braid, 5 J (3.7 ft-lbs.) Impact Specimens

5BA43FSC3-1

5BA43FSC3-2

5BA43FSC3-3

5BA43FSC3-4

5BA43FSC3-5

Figure F.9: Pictures of Full Coverage Braid, 10 J (7.4 ft-lbs.) Impact Specimens


5BA43HNC3-1


5BA43HNC3-2


5BA43HNC3-3


5BA43HNC3-4


5BA43HNC3-5


5BA43HNC3-6


5BA43HNC3-7


5BA43HNC3-8


5BA43HNC3-9


5BA43HNC3-10


5BA43HNC3-11


5BA43HNC3-12

Figure F.10: Pictures of Half Coverage Braid No-Impact Specimens


5BA43HLC3-1


5BA43HLC3-2


5BA43HLC3-3


5BA43HLC3-4


5BA43HLC3-5


5BA43HLC3-6


5BA43HLC3-7


5BA43HLC3-8


5BA43HLC3-9


5BA43HLC3-10


5BA43HLC3-11


5BA43HLC3-12

Figure F.11: Pictures of Half Coverage Braid, 5 J (3.7 ft-lbs.) Impact Specimens


5BA43HSC3-1


5BA43HSC3-2


5BA43HSC3-3


5BA43HSC3-4


5BA43HSC3-5


5BA43HSC3-6


5BA43HSC3-7


5BA43HSC3-8

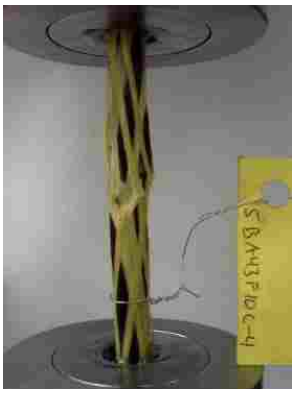
5BA43HSC3-9


5BA43HSC3-10


5BA43HSC3-11

Figure F.12: Pictures of Half Coverage Braid, 10 J (7.4 ft-lbs.) Impact Specimens

F.2 5/16” Diameter, 2” Length Specimens

Pictures of all specimens with an 8 mm (5/16”) diameter and 51 mm (2”) length while still under load are shown in Figures F.13-F.24.


5BA10FNC2-1


5BA10FNC2-2


5BA10FNC2-3


5BA10FNC2-4


5BA10FNC2-5


5BA10FNC2-6

Figure F.13: Pictures of Full Coverage Spiral No-Impact Specimens

5BA10FLC2-1

5BA10FLC2-2

5BA10FLC2-3

5BA10FLC2-4

5BA10FLC2-5

Figure F.14: Pictures of Full Coverage Spiral, 5 J (3.7 ft-lbs.) Impact Specimens

5BA10FSC2-1

5BA10FSC2-2

5BA10FSC2-3

5BA10FSC2-4

5BA10FSC2-5

Figure F.15: Pictures of Full Coverage Spiral, 10 J (7.4 ft-lbs.) Impact Specimens

5BA10HNC2-1

5BA10HNC2-2

5BA10HNC2-3

5BA10HNC2-4

5BA10HNC2-5

Figure F.16: Pictures of Half Coverage Spiral No-Impact Specimens

5BA10HLC2-1

5BA10HLC2-2

5BA10HLC2-3

5BA10HLC2-4

5BA10HLC2-5

Figure F.17: Pictures of Half Coverage Spiral, 5 J (3.7 ft-lbs.) Impact Specimens

5BA10HSC2-1

5BA10HSC2-2

5BA10HSC2-3

5BA10HSC2-4

No Photo

5BA10HSC2-5

5BA10HSC2-6

Figure F.18: Pictures of Half Coverage Spiral, 10 J (7.4 ft-lbs.) Impact Specimens

5BA43FNC2-1

5BA43FNC2-2

5BA43FNC2-3

5BA43FNC2-4

5BA43FNC2-5

Figure F.19: Pictures of Full Coverage Braid No-Impact Specimens

5BA43FLC2-1

5BA43FLC2-2

5BA43FLC2-3

5BA43FLC2-4

5BA43FLC2-5

5BA43FLC2-6

Figure F.20: Pictures of Full Coverage Braid, 5 J (3.7 ft-lbs.) Impact Specimens

5BA43FSC2-1

5BA43FSC2-2

5BA43FSC2-3

5BA43FSC2-4

5BA43FSC2-5

Figure F.21: Pictures of Full Coverage Braid, 10 J (7.4 ft-lbs.) Impact Specimens

5BA43HNC2-1

5BA43HNC2-2

5BA43HNC2-3

5BA43HNC2-4

5BA43HNC2-5

5BA43HNC2-6

Figure F.22: Pictures of Half Coverage Braid No-Impact Specimens

5BA43HLC2-1

5BA43HLC2-2

5BA43HLC2-3

5BA43HLC2-4

5BA43HLC2-5

Figure F.23: Pictures of Half Coverage Braid, 5 J (3.7 ft-lbs.) Impact Specimens


5BA43HSC2-1


5BA43HSC2-2


5BA43HSC2-3


5BA43HSC2-4


5BA43HSC2-5


5BA43HSC2-6


5BA43HSC2-7

Figure F.24: Pictures of Half Coverage Braid, 10 J (7.4 ft-lbs.) Impact Specimens

F.3 7/16” Diameter, 2” Length Specimens

Pictures of all specimens with an 11 mm (7/16”) diameter and 51 mm (2”) length while still under load are shown in Figures F.25-F.36.


7BA10FNC2-1


7BA10FNC2-2


7BA10FNC2-3


7BA10FNC2-4


7BA10FNC2-5

Figure F.25: Pictures of Full Coverage Spiral No-Impact Specimens

7BA10FLC2-1

7BA10FLC2-2

7BA10FLC2-3

7BA10FLC2-4

7BA10FLC2-5

7BA10FLC2-6

Figure F.26: Pictures of Full Coverage Spiral, 10 J (7.4 ft-lbs.) Impact Specimens

7BA10FSC-1

7BA10FSC-2

7BA10FSC-3

7BA10FSC-4

7BA10FSC-5

Figure F.27: Pictures of Full Coverage Spiral, 20 J (14.8 ft-lbs.) Impact Specimens

7BA10HNC-1

7BA10HNC-2

7BA10HNC-3

7BA10HNC-4

7BA10HNC-5

Figure F.28: Pictures of Half Coverage Spiral No-Impact Specimens

7BA10HLC-1

7BA10HLC-2

7BA10HLC-3

7BA10HLC-4

7BA10HLC-5

Figure F.29: Pictures of Half Coverage Spiral, 10 J (7.4 ft-lbs.) Specimens

7BA10HSC-1

7BA10HSC-2

7BA10HSC-3

7BA10HSC-4

7BA10HSC-5

Figure F.30: Pictures of Half Coverage Spiral, 20 J (14.8 ft-lbs.) Impact Specimens


7BA43FNC-1


7BA43FNC-2


7BA43FNC-3


7BA43FNC-4


7BA43FNC-5


7BA43FNC-6

Figure F.31: Pictures of Full Coverage Braid No-Impact Specimens

7BA43FLC-1

7BA43FLC-2

7BA43FLC-3

7BA43FLC-4

7BA43FLC-5

Figure F.32: Pictures of Full Coverage Braid, 10 J (7.4 ft-lbs.) Impact Specimens

7BA43FSC-1

7BA43FSC-2

7BA43FSC-3

7BA43FSC-4

7BA43FSC-5

Figure F.33: Pictures of Full Coverage Braid, 20 J (14.8 ft-lbs.) Impact Specimens

7BA43HNC-1

7BA43HNC-2

7BA43HNC-3

7BA43HNC-4

7BA43HNC-5

Figure F.34: Pictures of Half Coverage Braid No-Impact Specimens

7BA43HLC-1

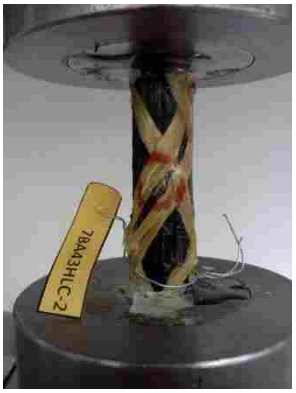

7BA43HLC-2

7BA43HLC-3

7BA43HLC-4

7BA43HLC-5

7BA43HLC-6

Figure F.35: Pictures of Half Coverage Braid, 10 J (7.4 ft-lbs.) Impact Specimens

7BA43HSC-1

7BA43HSC-2

7BA43HSC-3

7BA43HSC-4

7BA43HSC-5

Figure F.36: Pictures of Half Coverage Braid, 20 J (14.8 ft-lbs.) Impact Specimens

APPENDIX G: EXENSOMETER STRAIN-BASED PLOTS FOR 76 MM (3") LENGTH

The figures and tables provided in this section are based on extensometer strain for the 76 mm (3") length specimens. The results were presented at the 18th International Conference on Composite Materials in Korea in August 2011. Table G.1 provides the differences in strength and Figures G.1 and G.2 are the average curves as described in Chapter 7 of this thesis.

Table G.1: Ultimate Strength Comparison of 76 mm (3") Length

Configuration Comparison	Compression Strength [MPa (ksi)]		
	No-Impact	**5-J Impact (3.7 ft-lbs)**	**10-J Impact (7.4 ft-lbs)**
Influence of Sleeve Surface Coverage			
Full Coverage	727 (105)	510 (73.9)	317 (46.0)
Half Coverage	690 (100)	479 (69.5)	232 (33.7)
Difference	-5%	-6%	-27%
Influence of Sleeve Type			
Braided Sleeve	733 (106)	519 (75.2)	266 (38.6)
Spiral Sleeve	696 (101)	471 (68.3)	283 (41.1)
Difference	-5%	-9%	6%

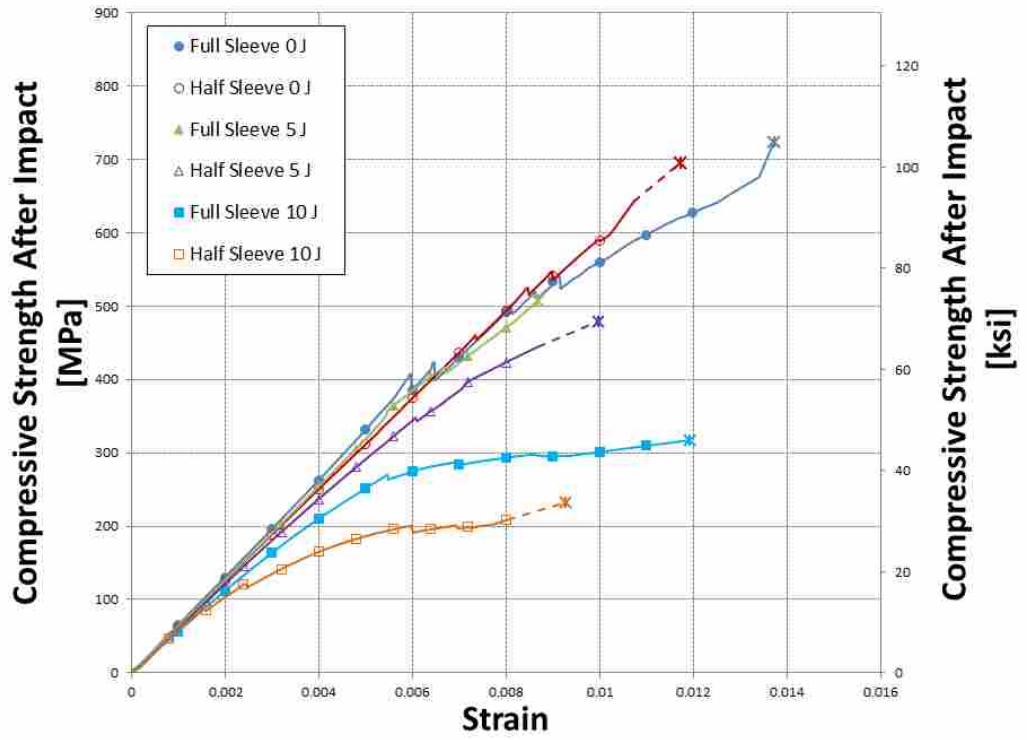

Figure G.1: Average Stress-Strain Curves for Full and Half Coverage Sleeves

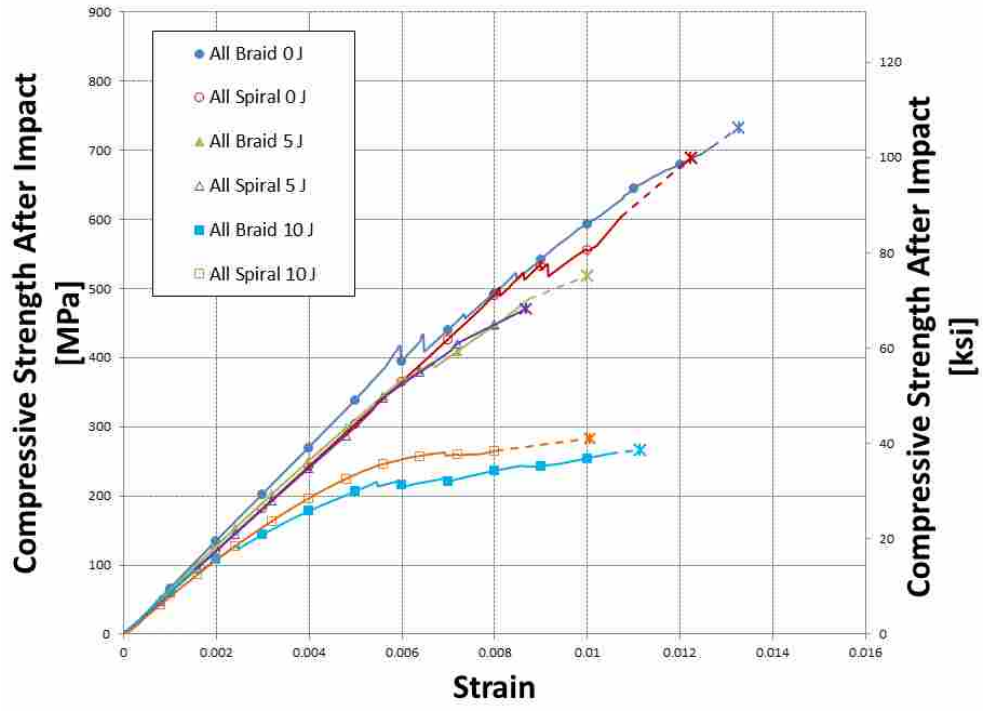

Figure G.2: Average Stress-Strain Curves for Braided and Spiral Sleeves

APPENDIX H: VARIATION OF INDIVIDUAL CURVES FROM AVERAGE CURVES

Plots showing how the average curves were prepared are presented here. The first eleven plots (Figures H.1 through H.11) are for the 11 mm (7/16") diameter 51 mm (2") unsupported length specimens; and the next twelve plots (Figures H.12 through H.23) are for the 8 mm (5/16") diameter specimens with an unsupported length of 51 mm (2").

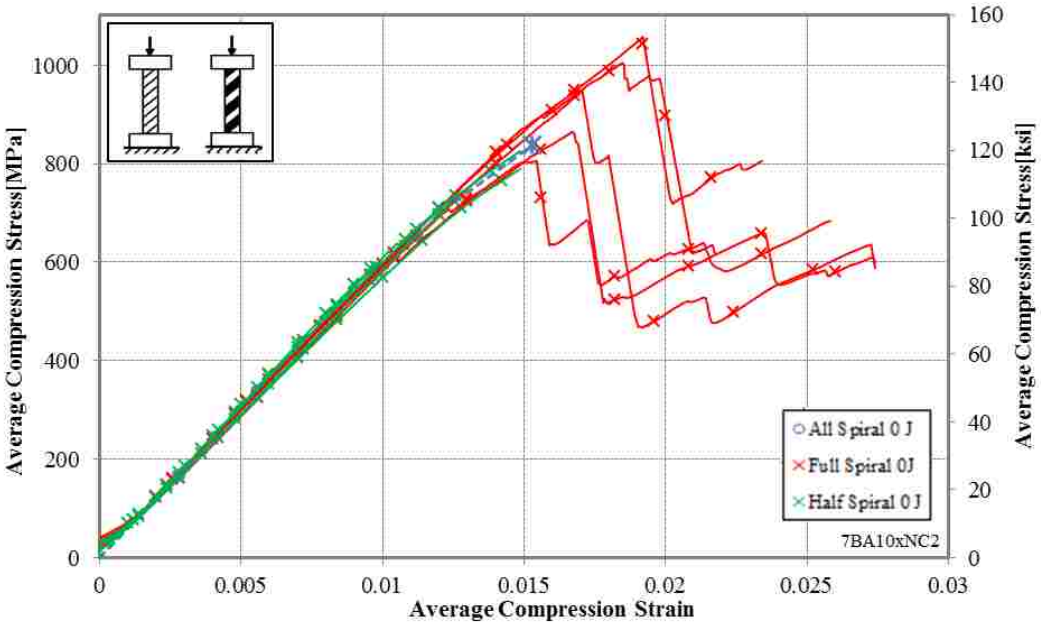

Figure H.1: Average Stress-Strain Curve for No-Impact Spiral Sleeve Coverage

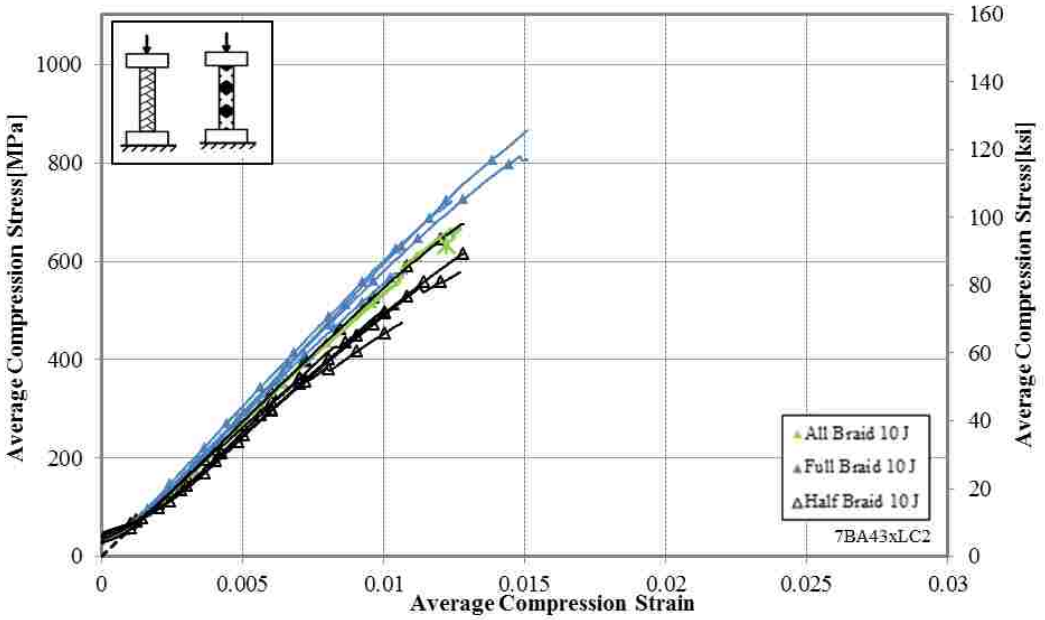

Figure H.2: Average Stress-Strain Curve for 10 J (7.4 ft-lbs.) Impact, Braided Sleeve Coverage

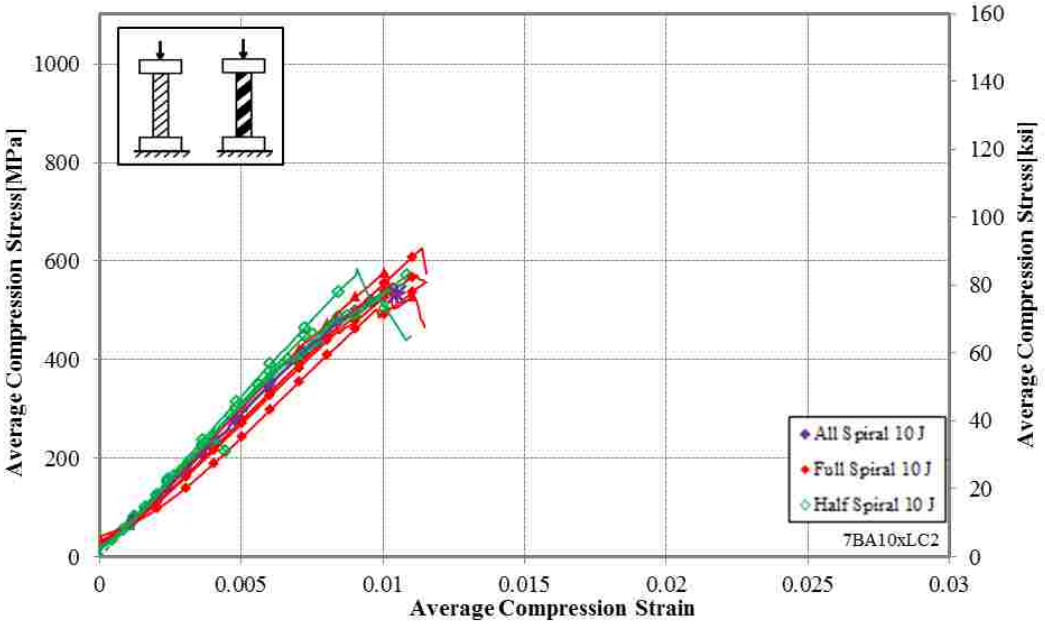

Figure H.3: Average Stress-Strain Curve for all 10 J (7.4 ft-lbs.) Impact, Spiral Sleeve Coverage

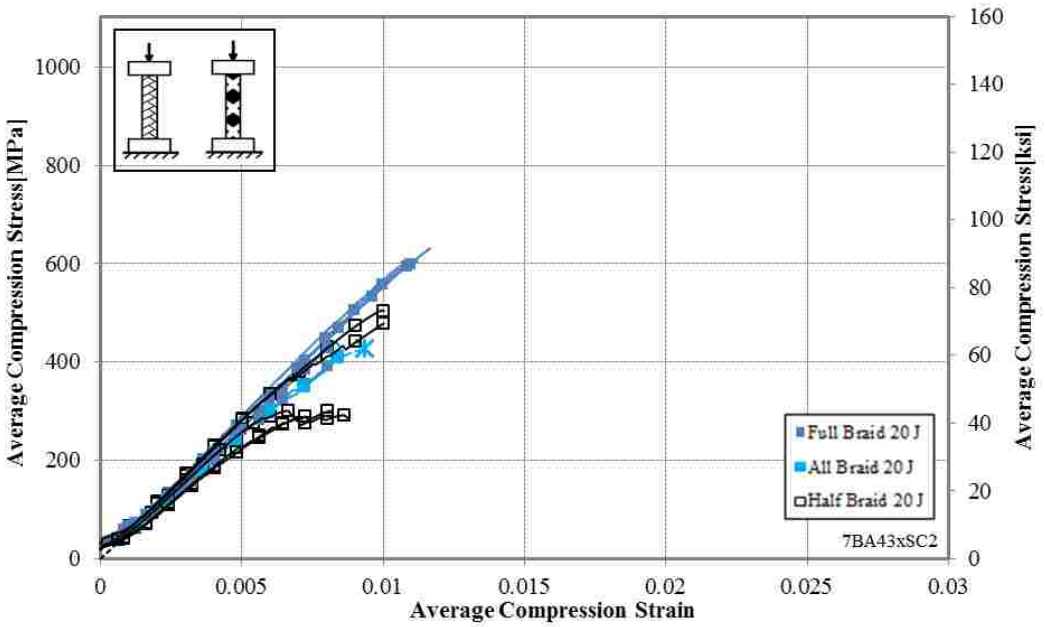

Figure H.4: Average Stress-Strain Curve for 20 J (14.8 ft-lbs.) Impact, Braided Sleeve Coverage

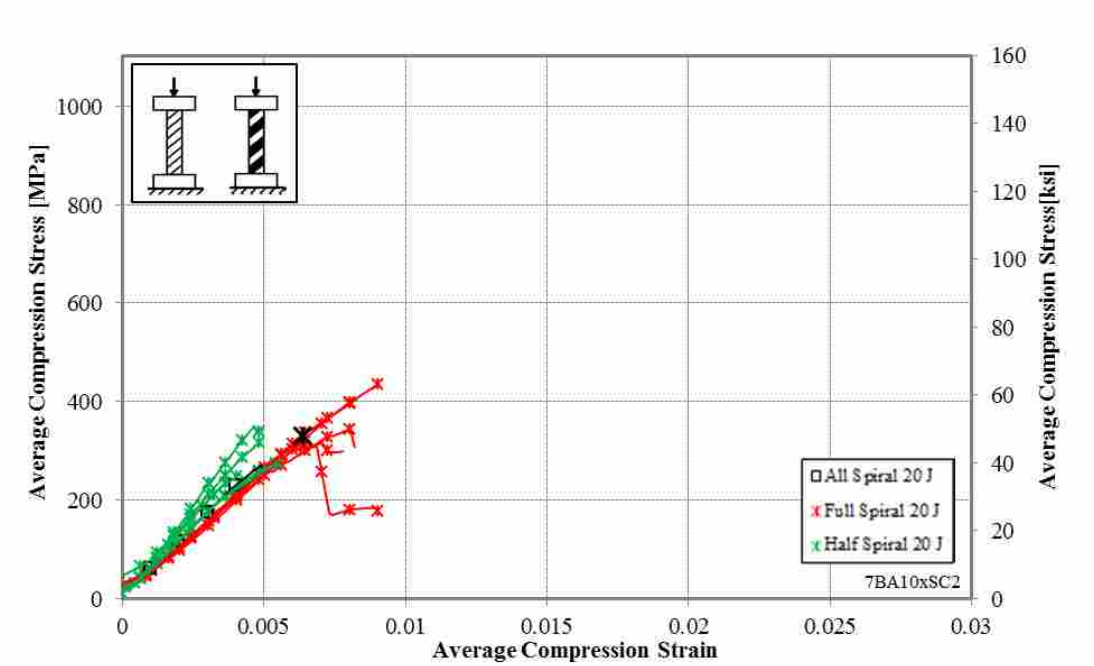

Figure H.5: Average Stress-Strain Curve for 20 J (14.8 ft-lbs.) Impact, Spiral Sleeve Coverage

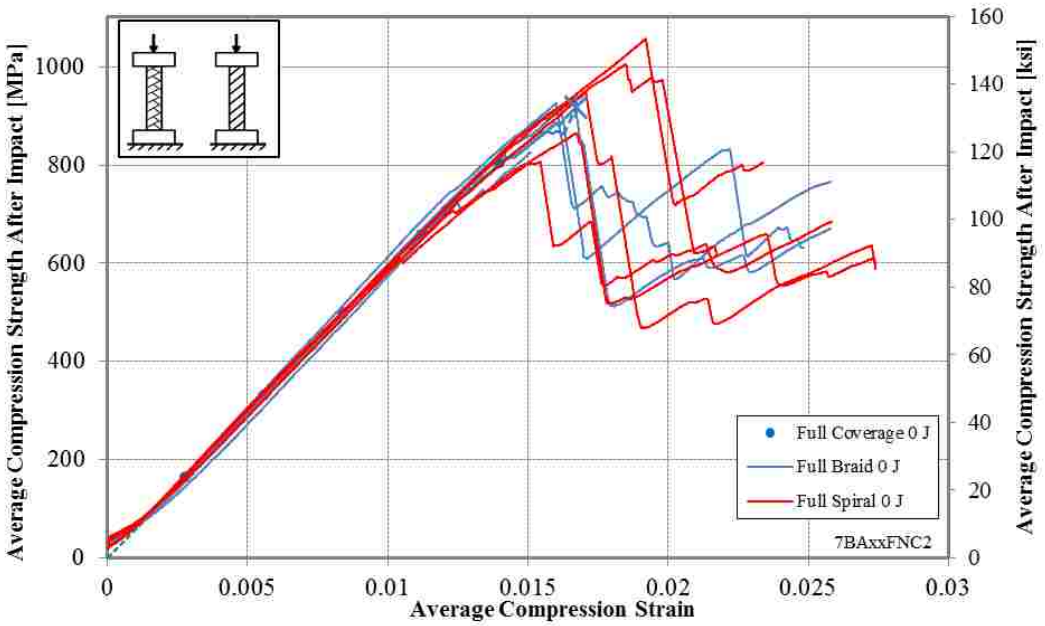

Figure H.6: Average Stress-Strain Curve for No-Impact Full Coverage, 11 mm (7/16") Diameter

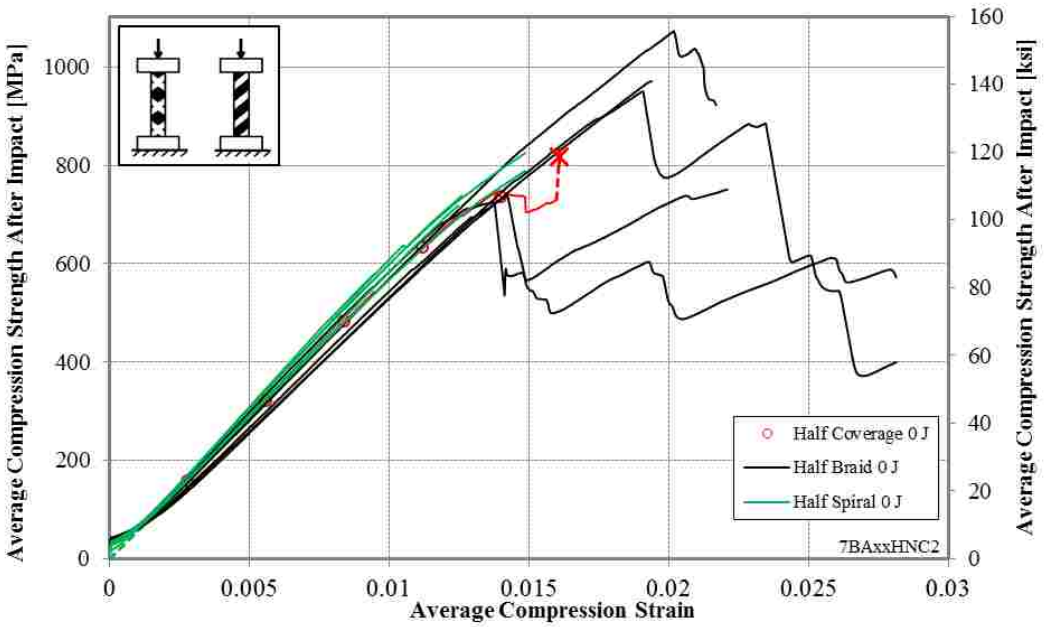

Figure H.7: Average Stress-Strain Curve for No-Impact Half Coverage, 11 mm (7/16") Diameter

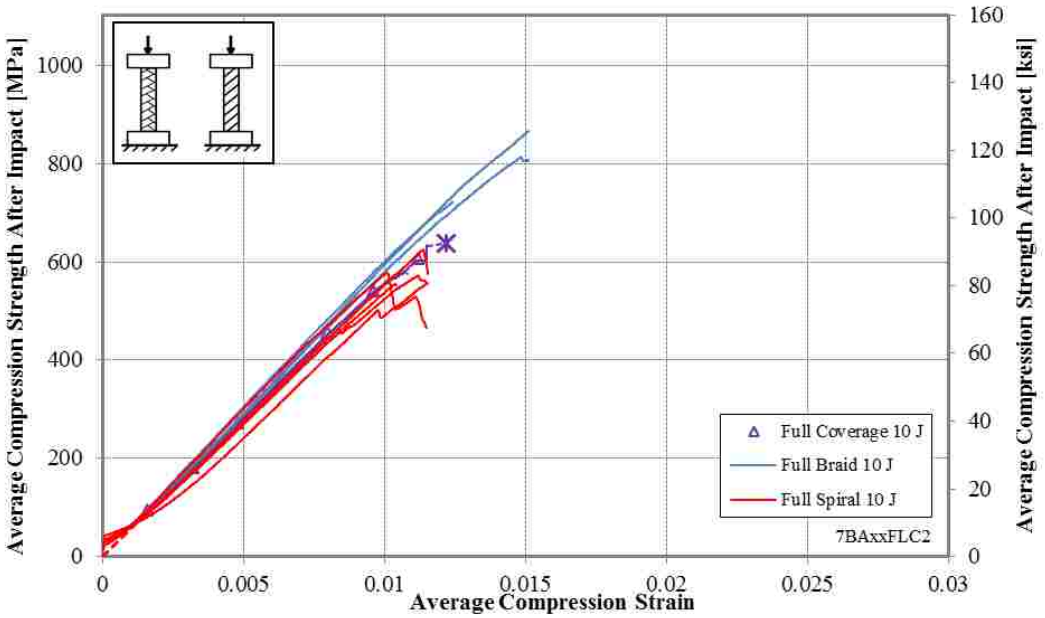

Figure H.8: Average Stress-Strain Curve for 10 J (7.4 ft-lbs.) Full Coverage, 11 mm (7/16") Diameter

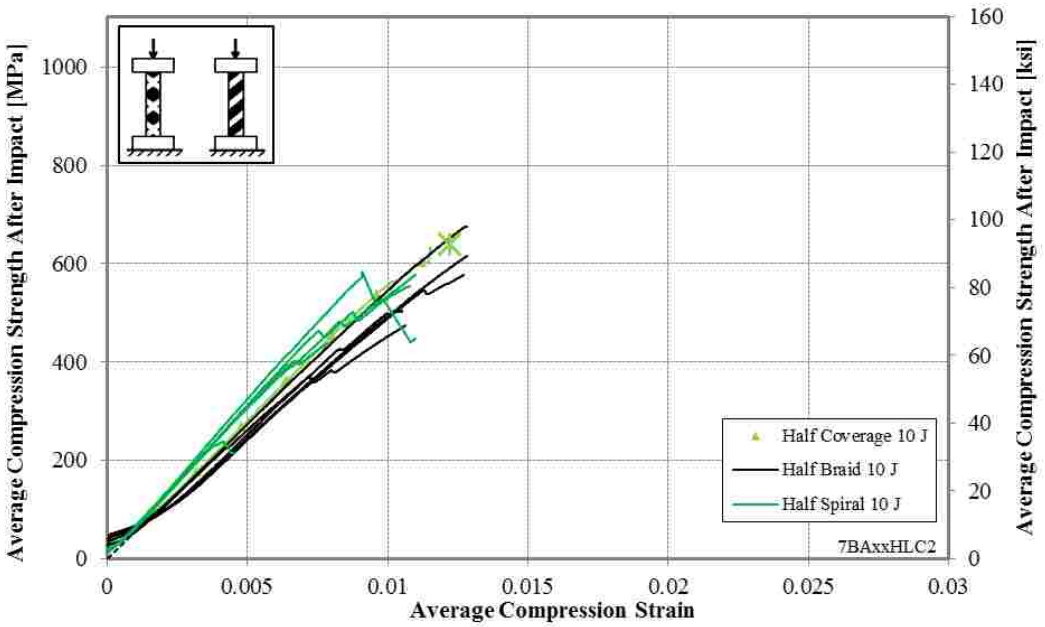

Figure H.9: Average Stress-Strain Curve for 10 J (7.4 ft-lbs.) Half Coverage, 11 mm (7/16") Diameter

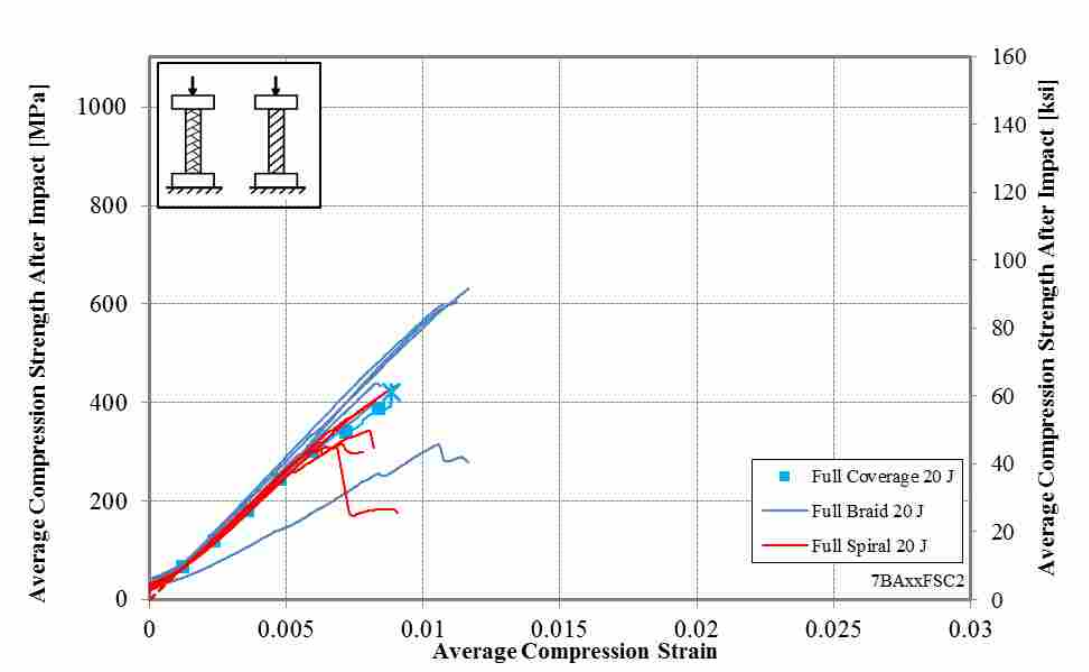

Figure H.10: Average Stress-Strain Curve for 20 J (14.8 ft-lbs.) Full Coverage, 11 mm (7/16") Diameter

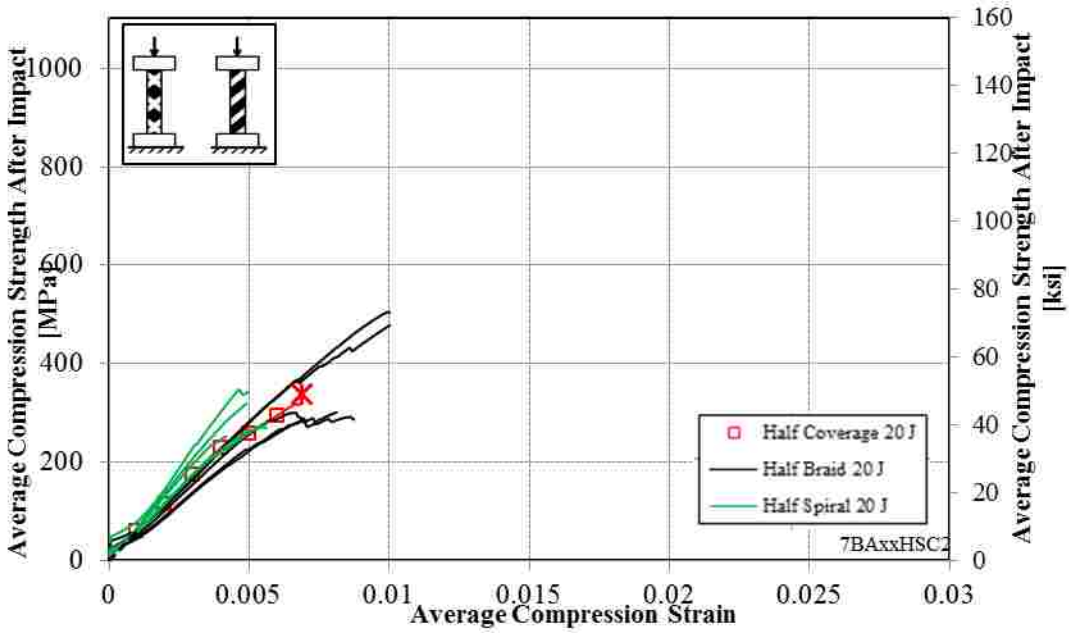

Figure H.11: Average Stress-Strain Curve for 20 J (14.8 ft-lbs.) Half Coverage, 11 mm (7/16") Diameter

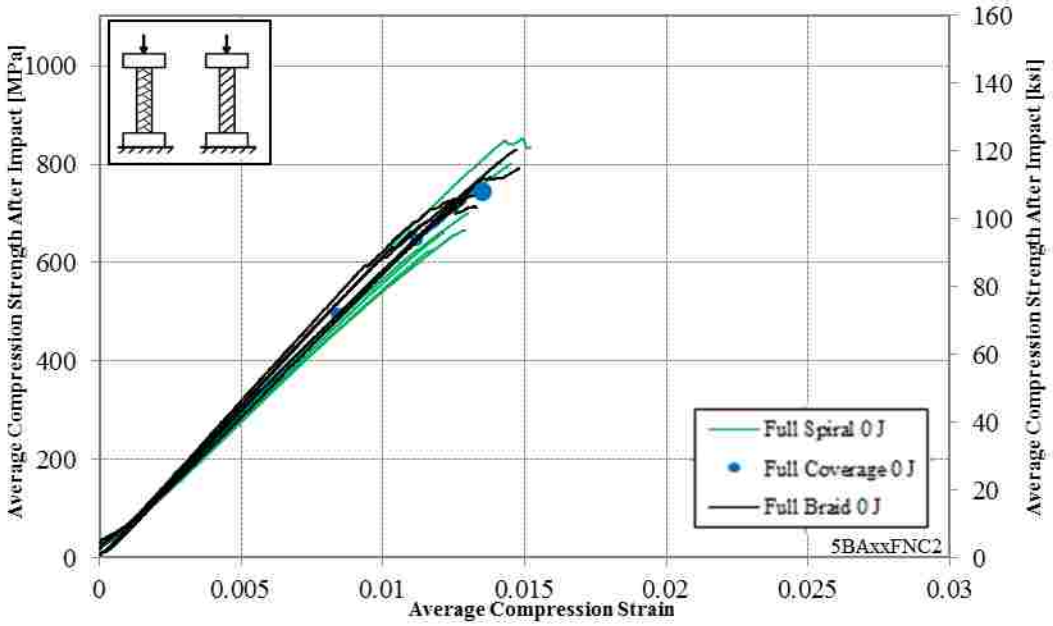

Figure H.12: Average Stress-Strain Curve for No-Impact Full Coverage, 8 mm (5/16") Diameter

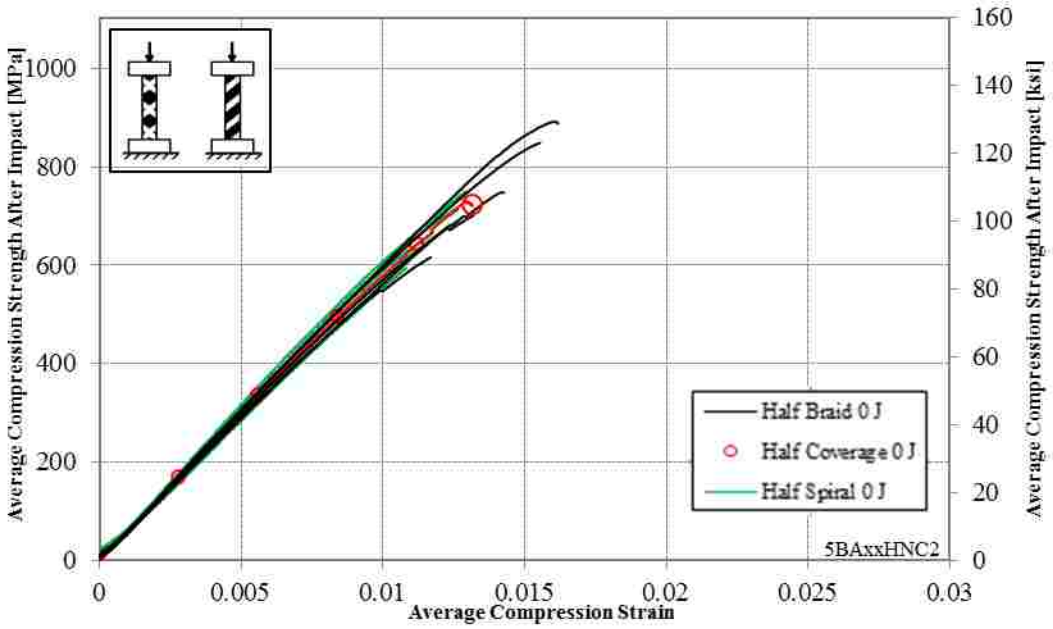

Figure H.13: Average Stress-Strain Curve for No-Impact Half Coverage, 8 mm (5/16") Diameter

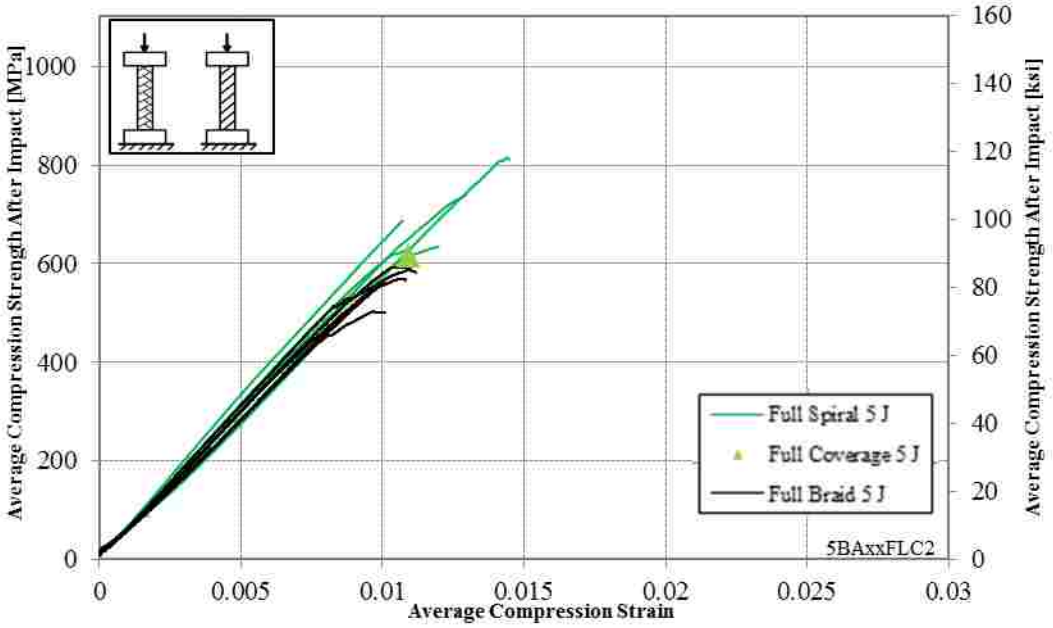

Figure H.14: Average Stress-Strain Curve for 5 J (3.7 ft-lbs.) Full Coverage, 8 mm (5/16") Diameter

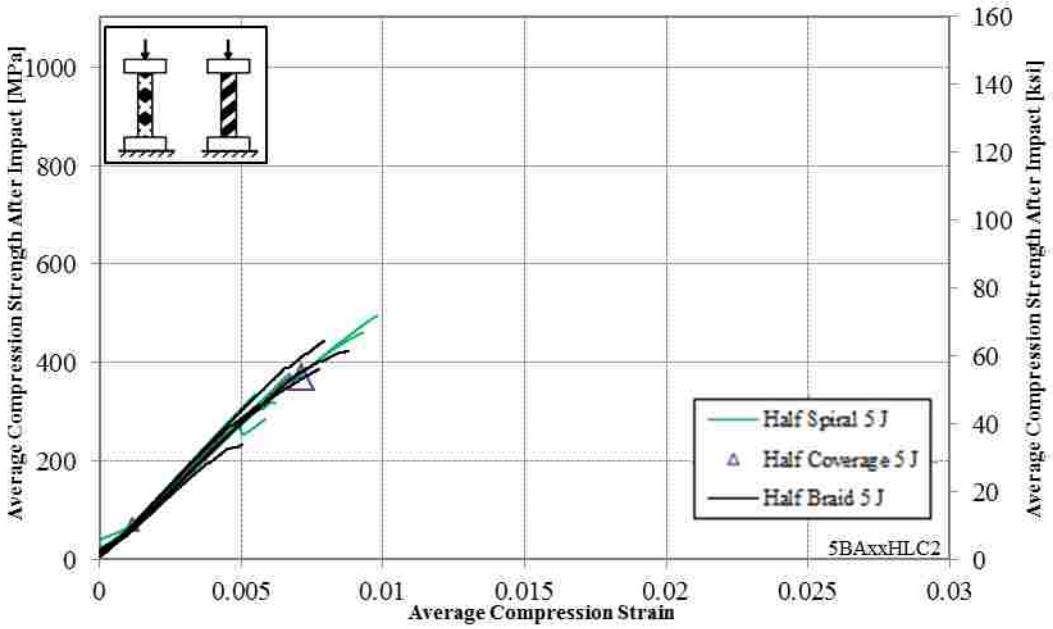

Figure H.15: Average Stress-Strain Curve for 5 J (3.7 ft-lbs.) Half Coverage, 8 mm (5/16") Diameter

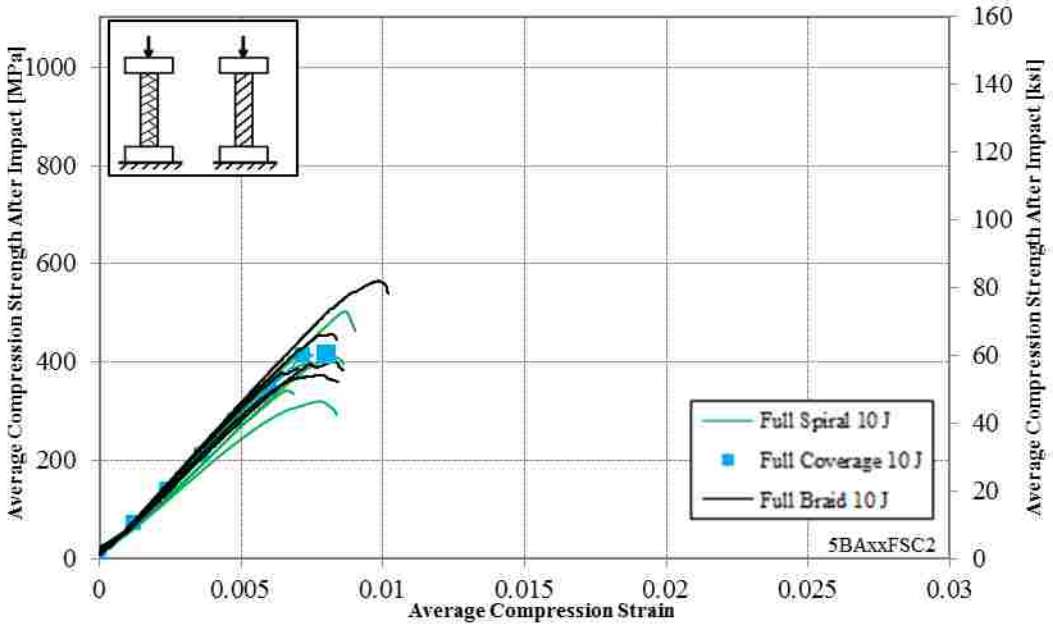

Figure H.16: Average Stress-Strain Curve for 10 J (7.4 ft-lbs.) Full Coverage, 8 mm (5/16") Diameter

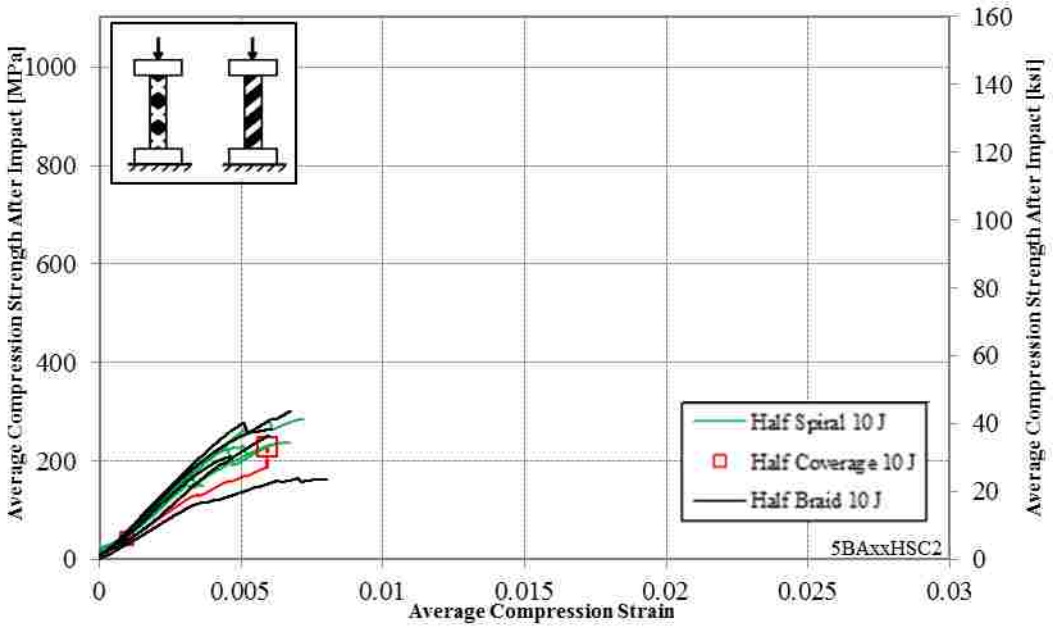

Figure H.17: Average Stress-Strain Curve for 10 J (7.4 ft-lbs.) Half Coverage, 8 mm (5/16") Diameter.

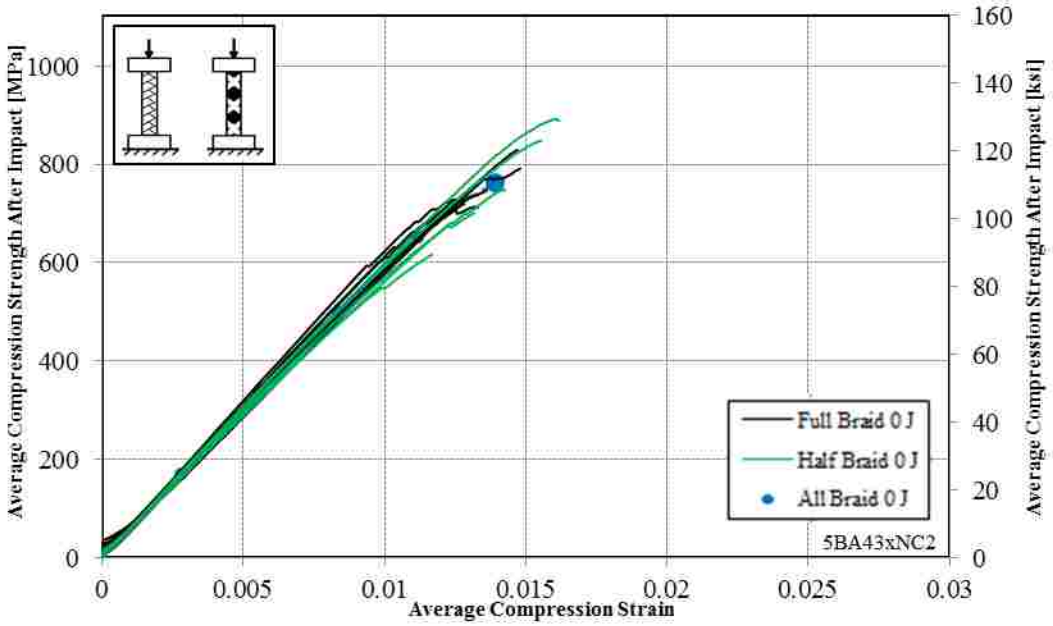

Figure H.18: Average Stress-Strain Curve for No-Impact Braid Type Coverage, 8 mm (5/16") Diameter

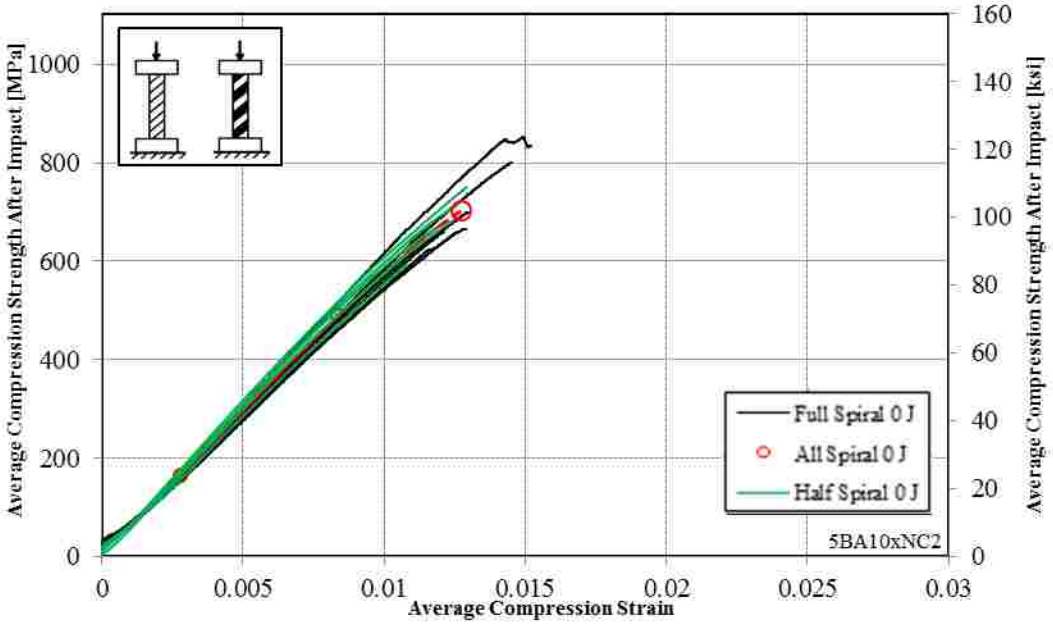

Figure H.19: Average Stress-Strain Curve for No-Impact Spiral Type Coverage, 8 mm (5/16") Diameter

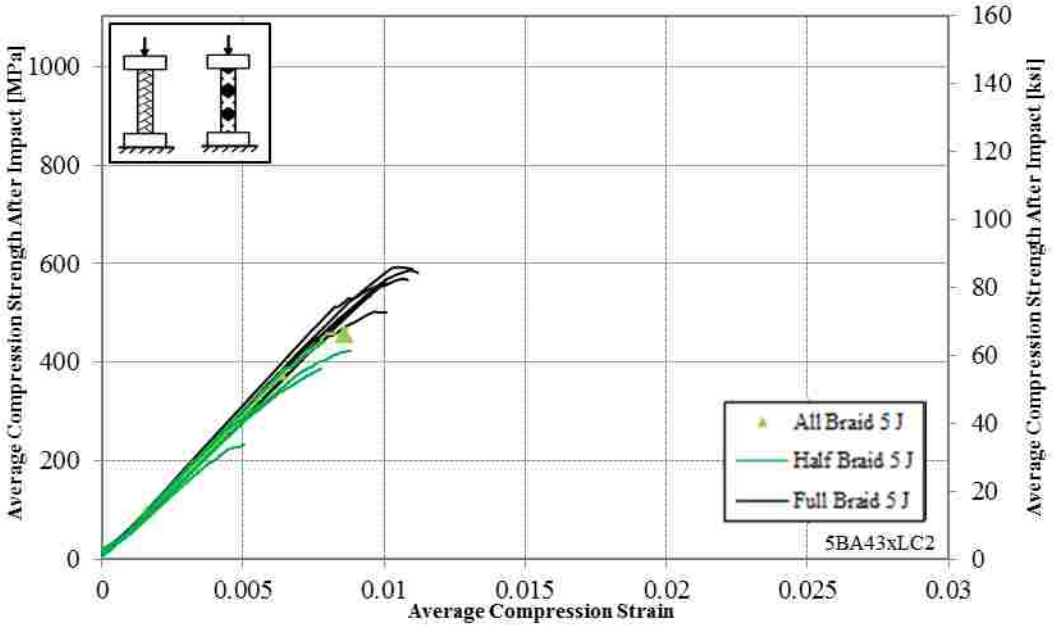

Figure H.20: Average Stress-Strain Curve for 5 J (3.7 ft-lbs.) Braid Type Coverage, 8 mm (5/16") Diameter

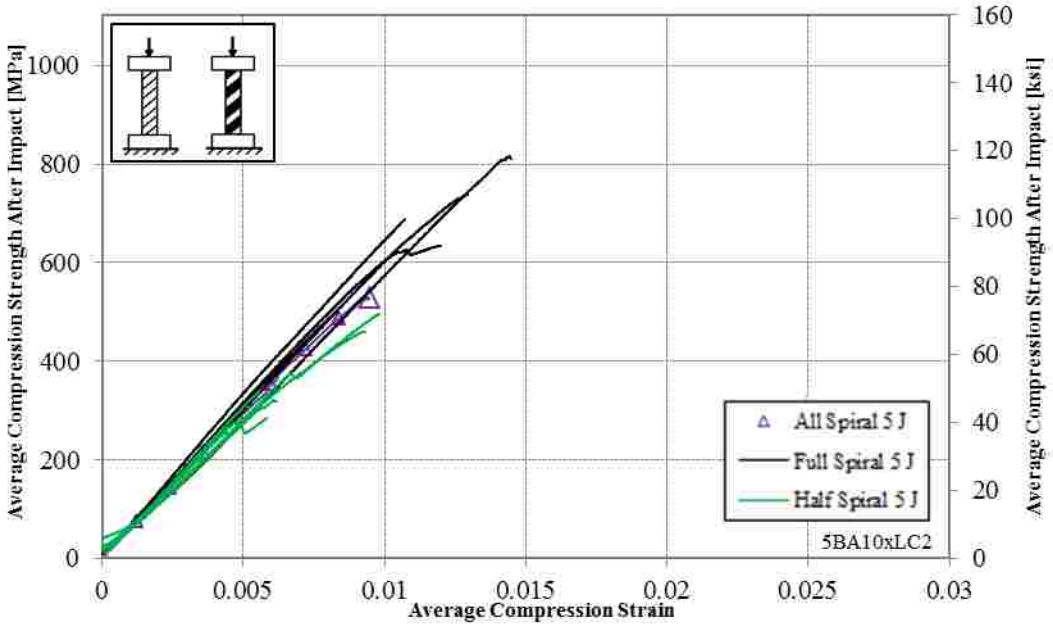

Figure H.21: Average Stress-Strain Curve for 5 J (3.7 ft-lbs.) Spiral Type Coverage, 8 mm (5/16") Diameter

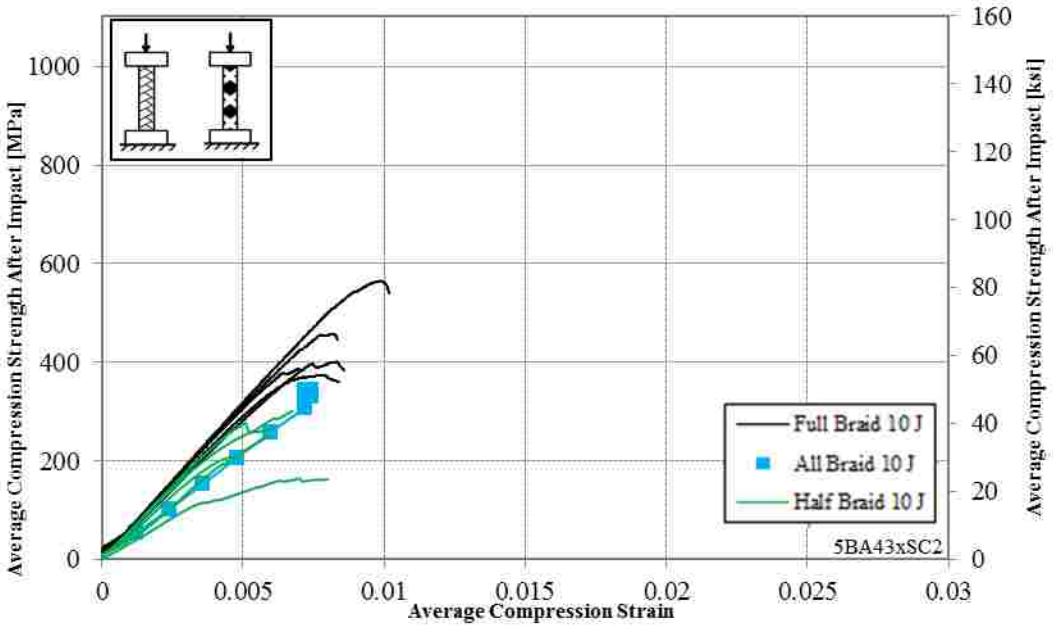

Figure H.22: Average Stress-Strain Curve for 10 J (7.4 ft-lbs.) Braid Type Coverage, 8 mm (5/16") Diameter

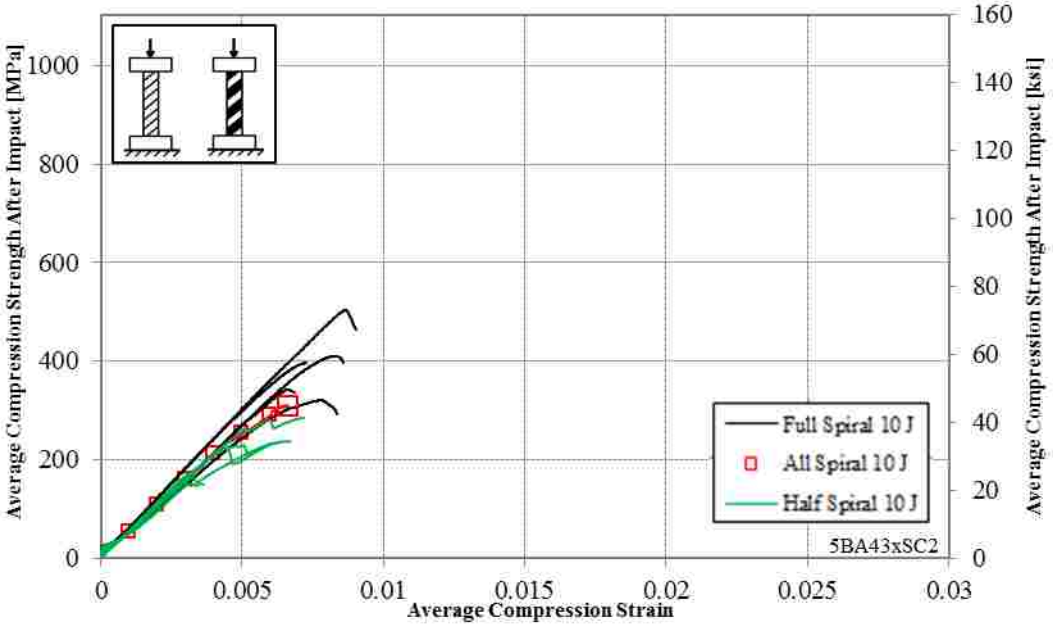

Figure H.23: Average Stress-Strain Curve for 10 J (7.4 ft-lbs.) Spiral Type Coverage, 8 mm (5/16") Diameter